IntechOpen

Aircraft Technology

Edited by Melih Cemal Kuşhan

AIRCRAFT TECHNOLOGY

Edited by **Melih Cemal Kuşhan**

Aircraft Technology
http://dx.doi.org/10.5772/intechopen.70078
Edited by Melih Cemal Kuşhan

Contributors

Joan Cahill, Tiziana C. Callari, Florian Fortmann, Stefan Suck, Denis Javaux, Andreas Hasselberg, Sybert Stroeve, Rosa Arnaldo, Victor Fernando Gomez Comendador, Alvaro Rodriguez Sanz, Javier Alberto Perez Castan, Fang Chen, Hong Liu, Douglas Summerfield, David Raslau, Bruce Johnson, Lawrence Steinkraus, Evren Yasa, Kıvılcım Ersoy, Paolo Gaetani, Alexandru Nicolae Nicolae Tudosie

© The Editor(s) and the Author(s) 2018
The rights of the editor(s) and the author(s) have been asserted in accordance with the Copyright, Designs and Patents Act 1988. All rights to the book as a whole are reserved by INTECHOPEN LIMITED. The book as a whole (compilation) cannot be reproduced, distributed or used for commercial or non-commercial purposes without INTECHOPEN LIMITED's written permission. Enquiries concerning the use of the book should be directed to INTECHOPEN LIMITED rights and permissions department (permissions@intechopen.com).
Violations are liable to prosecution under the governing Copyright Law.

Individual chapters of this publication are distributed under the terms of the Creative Commons Attribution 3.0 Unported License which permits commercial use, distribution and reproduction of the individual chapters, provided the original author(s) and source publication are appropriately acknowledged. If so indicated, certain images may not be included under the Creative Commons license. In such cases users will need to obtain permission from the license holder to reproduce the material. More details and guidelines concerning content reuse and adaptation can be foundat http://www.intechopen.com/copyright-policy.html.

Notice

Statements and opinions expressed in the chapters are these of the individual contributors and not necessarily those of the editors or publisher. No responsibility is accepted for the accuracy of information contained in the published chapters. The publisher assumes no responsibility for any damage or injury to persons or property arising out of the use of any materials, instructions, methods or ideas contained in the book.

First published in London, United Kingdom, 2018 by IntechOpen
eBook (PDF) Published by IntechOpen, 2019
IntechOpen is the global imprint of INTECHOPEN LIMITED, registered in England and Wales, registration number: 11086078, The Shard, 25th floor, 32 London Bridge Street
London, SE19SG – United Kingdom
Printed in Croatia

British Library Cataloguing-in-Publication Data
A catalogue record for this book is available from the British Library

Additional hard and PDF copies can be obtained from orders@intechopen.com

Aircraft Technology
Edited by Melih Cemal Kuşhan

p. cm.

Print ISBN 978-1-78923-644-6

Online ISBN 978-1-78923-645-3

eBook (PDF) ISBN 978-1-83881-454-0

We are IntechOpen, the world's leading publisher of Open Access books

Built by scientists, for scientists

3,700+
Open access books available

115,000+
International authors and editors

119M+
Downloads

151
Countries delivered to

Our authors are among the
Top 1%
most cited scientists

12.2%
Contributors from top 500 universities

CLARIVATE ANALYTICS
BOOK CITATION INDEX
INDEXED

WEB OF SCIENCE™

Selection of our books indexed in the Book Citation Index
in Web of Science™ Core Collection (BKCI)

Interested in publishing with us?
Contact book.department@intechopen.com

Numbers displayed above are based on latest data collected.
For more information visit www.intechopen.com

Meet the editor

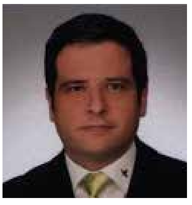

Melih Cemal Kuşhan is an associate professor of Mechanical Engineering at the Eskisehir Osmangazi University. He is the head of the Department of Aviation Science and Technology at the same university. He is a board member of Eskisehir Aviation Cluster, the first aviation cluster in Turkey, which contains the aviation technology companies.
He is the author of more than 50 scientific articles and 75 conference papers. He has also published a book and three book chapters in international books about aviation. His research area focuses on aviation/defence materials, aviation/defence technologies and general aviation. In more than 20 countries, he has been involved in many activities, such as a visiting professor, a project researcher, an invited lecturer and a presenter of scientific papers. He received many international prizes related to his areas of expertise.

Contents

Preface

It is well known that improvements in space and aviation are the leader of today's technology, and the aircraft is the most important product of aviation. Because of this fact, the books on aircraft are always at the center of interest. In most cases, technologies designed for the aerospace industry are rapidly extending into other areas. For example, although composite materials are developed for the aerospace industry, these materials are not often used in aircraft. However, composite materials are utilized significantly in many different sectors, such as automotive, marine, and civil engineering. And materials science in aviation, reliability and efficiency in aircraft technology have a major importance in aircraft design.

In such an important issue, IntechOpen fulfills its mission the best. Until now, many books on airplanes and aircraft technology have been published by IntechOpen, and the public opinion and the academic world have been informed about this important issue.

In this book titled *Aircraft Technology*, which is one of these studies, we have discussed this important topic under three important headings: Flight, Design, and Manufacturing.

The first section is titled "Flight." It has five chapters. Naturally, the most important concept for an aircraft is flight, which includes many concepts from autopilot systems to pilot psychology and flight safety to GPSs.

Design is a very important activity for every part of the process from the idea of a new aircraft to its production and use. Therefore, the second section is titled "Design." In this section, three important chapters related to the design are presented to the world of science by our valuable authors.

The last part of the book is titled "Manufacturing." As is known, manufacturing methods developed in aircraft production have always been privileged; some of these methods are still used only in the space and aviation sector. The additive manufacturing method is also an extremely suitable method to use in the aircraft industry. Therefore, in this section, the additive manufacturing method in the aircraft industry is discussed.

Finally, I would like to point out that we are excited to share our book with valuable aviation public opinion and the world of science. I would like to thank all the staff from IntechOpen, especially Mrs. Kristina Kardum, for their valuable support.

Assoc. Prof. Dr. Melih Cemal Kuşhan
Eskisehir Osmangazi University
Head of Aviation Scince and Technology
Eskisehir, Turkey

Section 1

Flight

Chapter 1

Adaptive Automation and the Third Pilot

Joan Cahill, Tiziana C. Callari, Florian Fortmann, Stefan Suck, Denis Javaux, Andreas Hasselberg and Sybert Stroeve

Additional information is available at the end of the chapter

http://dx.doi.org/10.5772/intechopen.73689

Abstract

Currently, automation does not take into consideration the cognitive and emotional state of the crew. Rather, automation provides assistance based on explicit and static task assignments, with no adaptive capabilities, even though it is capable of providing higher or lower levels of support depending on the crew state and/or complexity of the operational situation. This chapter presents a new adaptive automation concept which offers an innovative 'team' centred approach to solving crew awareness/workload management problems and enhancing flight safety. Partnership underpins the 'Third Pilot' approach. The crew (pilot flying and pilot monitoring), automation and the 'Third Pilot' are in charge together. Overall, partnership is proposed. This replaces existing paradigms involving dynamic changes in control function, where changes can be autonomously controlled by the system. Moreover, a new multimodal cockpit concept is advanced providing enhanced assessment of crew state/workload.

Keywords: adaptive automation, teamwork, workload, human factors, situation awareness, pilot decision making, stakeholder evaluation, cockpit

1. Introduction

Crew task support and information needs vary according to the crew composition, the crews own experience (i.e. familiarity with type, knowledge of the route), the specific flight situation (i.e. traffic and weather), and the crew state (i.e. fatigue, confusion) [1, 2]. With increasing duty time and traffic growth, pilots can benefit from an 'experience aid'. Ideally, the crew and the 'experience aid' (or assistance system) comprise a cooperative system [1, 2]. This cooperative system approach follows the cognitive systems engineering frameworks, as advanced by Hollnagel and Woods [3].

IntechOpen

© 2018 The Author(s). Licensee IntechOpen. This chapter is distributed under the terms of the Creative Commons Attribution License (http://creativecommons.org/licenses/by/3.0), which permits unrestricted use, distribution, and reproduction in any medium, provided the original work is properly cited.

In its current form, automation does not take into consideration the pilot's cognitive and emotional state. Rather, automation provides assistance based on explicit and static task assignments, with no adaptive capabilities, even though it is capable of providing higher or lower levels of support depending on the crew state and/or complexity of the operational situation [1, 2, 4]. It is argued that safety is optimised when human and automated systems adapt both to each other and to the specific operational context. This guarantees fluent and cooperative task achievement—maintaining safety at all times.

This research was undertaken as part of the Applying Pilots' Model for Safer Aircraft (A-PiMod) project, funded by the European Commission (Framework Programmes for Research and Technological Development) [1]. The aim of this project was to demonstrate a new approach/concept (and associated technologies) for an adaptive automation and multimodal cockpit which might mitigate and/or reduce human error. The project commenced in September 2013 and finished in September 2016.

2. Background

2.1. Automation

Currently, Pilots share responsibility for different flight tasks with cockpit systems. As defined by Kaber and Prinzel, adaptable systems are systems which require human delegation of task and 'function authority' to automation during real-time operational performance (i.e. the task distribution is controlled by the user) [5]. This is different to adaptive automation (AA), which allows for dynamic changes in control function allocations between a machine and human operator based on states of the collective human–machine system' [6, 7].

Human factors problems with automation have been cited as contributory factors in many air accidents. This includes: Flight Air France 447 (2009) [8], Flight Spanair 5022 (2008) [9], Flight Helios Airways HCY 522 (2005) [10], Flight China Airlines 140 (1994) [11], and Flight Air Inter 148 (1992) [12]. The air accident reports highlight several human factors issues such as automation surprises, reduced situation awareness, workload problems and over-reliance on automation [1].

2.2. Crew errors

Errors are defined as 'actions or inactions by the flight crew that lead to deviations from organisational or flight crew intentions or expectations' [13]. Unmanaged and/or mismanaged errors frequently lead to undesired aircraft states. Flight crew errors reduce the margins of safety and increase the probability of adverse events [13]. As documented by the International Civil Aviation Organisation [14], human error is a causal factor in between 60%-80% of accidents and serious incidents. It is stated in the 'Flightpath 2050, Europe's Vision for aviation', that 'the occurrence and impact of human error' will be 'significantly reduced through new designs and training processes and through technologies that support decision making' [15].

2.3. Theoretical starting point

In line with a cooperatives systems approach, the question of automation status/communication and its role in the execution of the flight, should to be framed from a team perspective and linked to a risk assessment of the mission and the selection of a course of action. Thus, the theoretical starting point for addressing human factors issues with automation (specifically, teamwork, task distribution, authority, situation awareness, error detection and workload management), is the assessment of the crew/automation/aircraft/environment state in relation to the achievement of the mission level goal (i.e. mission level risk assessment), and the identification of a suitable task distribution at cockpit/agent level, to achieve this [1, 2]. So conceived, automation has a role in relation to (1) real-time risk assessment, (2) the identification of a course of action, (3) the selection and subsequent implementation of a course of action, and (4) the identification of an appropriate task distribution based on the crew state [1, 2].

Further, it is argued that there is relationship between addressing human factors issues with automation (specifically, teamwork, situation awareness, task distribution, authority, error detection and workload management) and improving crew interaction with cockpit systems. The provision of a multimodal concept can support the above. In addition to (1) allowing for flexible interaction with cockpit systems and (2) providing a means to communicate with the crew in relation to crew state and decision support, the multimodal cockpit has a role in relation to (3) supporting the better assessment of crew state/workload (information inputs re crew activity/interactions).

2.4. Methodological background

Stakeholder involvement in programme evaluation has been recognised as one of the most effective approaches to enhancing the use of evaluation findings, and ensuring the validity of the evaluation activities [16]. Stakeholder involvement is defined as the participation of (programme) stakeholders in any phase of an evaluation [17]. Stakeholder involvement can vary with regard to diversity in stakeholder selection for participation, the control of technical evaluation decisions and the depth of stakeholder participation in the programme/project evaluation process [18]. Stakeholders are conceived as invaluable source of knowledge, perspectives, information on context and needs. Drawbacks of stakeholder involvement are also reported. This includes the feasibility of implementing a successful participative study. For example, time, cost, involvement from (disadvantaged) groups and skills required from an evaluator in facilitation and 'good listening' [19].

The involvement of stakeholders to accomplish given tasks by participating in common activities has been central to 'Community of Practice' concepts [20]. 'Community of Practice' members engage in a set of relationships over time around some particular area of technical knowledge or skill associated with the given tasks. This allows the members of a specific 'Community of Practice' to generate a sense of joint enterprise and identity by sharing a practice—doing things together, developing a sense of place, common goals. In Wenger's analysis, three characteristics are crucial to define a 'Community of Practice': (1) the 'domain'—which specifies the identity of COPs with the specific competence and commitment the stakeholders engage; (2) the 'community'—stakeholders build their relationship interacting in joint activities, sharing information and common objectives and learning from each other; and (3) the 'practice'—stakeholders share a repertoire of resources (experiences, stories, tools, ways of addressing recurring problems) which help forming the practice with time and sustained interaction [20].

3. Research design

3.1. Objective

The aim of the A-PiMod project was to demonstrate a new adaptive automation concept (and associated technologies) enabled by a hybrid of three elements: (1) multimodal pilot interaction, (2) operator modelling and (3) real-time risk assessment. It is anticipated that the introduction of this new automation concept will reduce human error—making substantial progress in relation to aim of reducing the accident rate by 80%. **Table 1** below provides a description of the high level project goals

3.2. Overview

The overall design/evaluation methodology combines formal HMI design/evaluation activities (i.e. interviews and simulator evaluation), informal HMI design/evaluation approaches (i.e. participatory design activities), along with an integrated stakeholder approach to evaluation [4]. Overall, 23 COP sessions and two phases of simulator evaluation have been undertaken. The first phase of simulator evaluation involved eight participants, while the second phase involved 12 participants. This has been reported in more detail in [1, 2].

3.3. Community of practice

The concept of 'Community of Practice' as proposed by Wenger [20] underpins the A-PiMod 'Community of Practice' approach. The A-PiMod 'Community of Practice' involved stakeholders who shared technical knowledge and skills associated with relevant functions in the Air Traffic Management (ATM system), and broader aviation related domain. Overall the role of participants in the A-PiMod 'Community of Practice' concept was characterised as a 'participatory' approach. Members engaged in a range of validation/evaluation activities on a continuous/regular basis, through the run-time of the project.

The panel of stakeholders in A-PiMod included both 'primary users' (i.e. internal stakeholders representative of each project partner), and 'all legitimate groups' (i.e. external stakeholder

No	A-PiMod high level project goals
1	To reduce accident rate by 80%
2	To achieve a substantial improvement in the elimination of and recovery from human error
3	To mitigate the consequences of survivable accidents
4	To support smart pilot assistance

Table 1. A-PiMod high level project goals.

representative of the aviation-related industry and Flight operational system). Stakeholder participation involved consultative interaction along with engagement in technical research tasks.

Figure 1 below depicts the composition of the community of practice – with attention to the levels of expertise of both internal and external stakeholders. Internal stakeholders are represented in blue. External stakeholders are represented in amaranth. The overlapping levels of expertise are indicated by the red dotted line.

3.4. Simulator evaluation

Two sets of simulator evaluation were undertaken. In both cases, the evaluation involved a mixed-method approach with the administration of semi structured interviews, simulator observations, collaborative workshop sessions and questionnaires. Each set of evaluations involved two crew members and elapsed over 2 days. Overall, a scenario-based evaluation approach was adopted. Simulator evaluation involved the use of the DLR simulator—the GECO system.

In day 1, participants were first briefed about the overall procedures, consent was obtained, and profile information was elicited. Then participants undertook a semi-structured interview regarding the current state of automation and HF still-open issues. After this both participants obtained training, in relation to interacting with the new adaptive automation multimodal concept/technologies in the simulator. The training was delivered with the support of slides, software training tools, and some hands-on training in the simulator (i.e. using

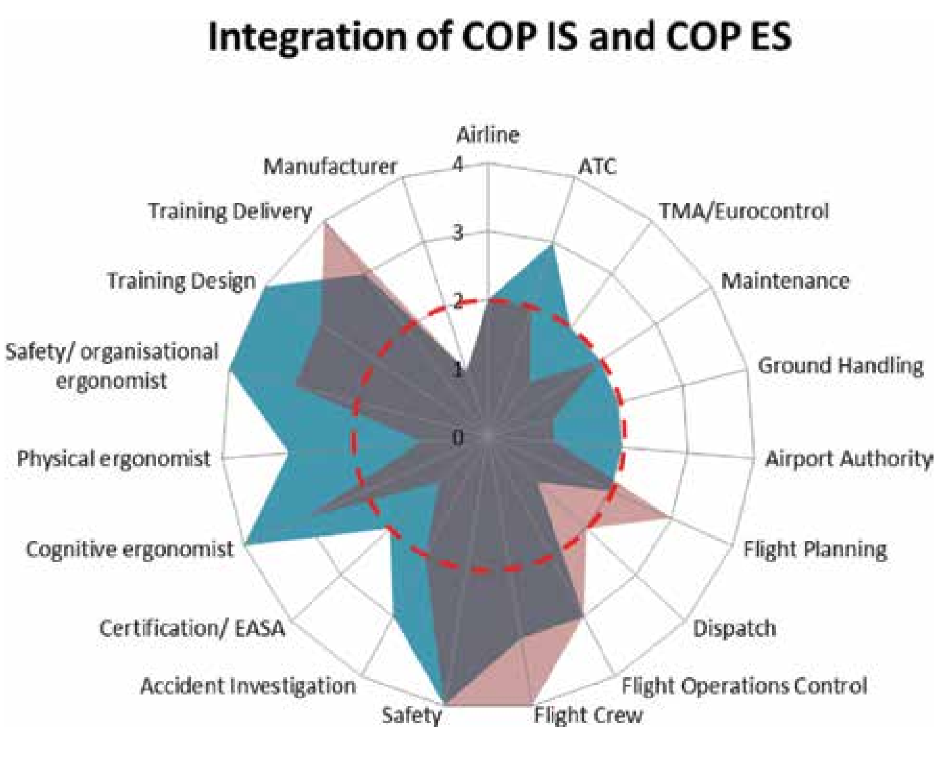

Figure 1. A-PiMod Community of Practice: Stakeholder Competency and Knowledge (Source: Cahill et al. [2]).

the A-PiMod user interface displays such as the MC-M Display and the MultiModal ND). Then, hands-on training in relation to using the GECO simulator was provided. After this training session, participants undertook the specific simulator evaluation session, addressing the adaptive automation and multimodal concept/technologies. After the simulator sessions, participants were asked to complete a questionnaire evaluating the adaptive automation and multimodal concept and technologies. Further, a specific simulator session was undertaken with a focus on the interaction with the MultiModal ND. This involved a collaborative session to evaluate the operational and safety aspects pertaining to the multimodal cockpit.

In day 2, participants were asked to evaluate the adaptive automation and multimodal concept and technologies. This involved individual post evaluation individual semi-structured interviews. Then a collaborative workshop session was undertaken. This focussed on three distinctive scenarios (i.e. (1) supporting routine operations, (2) avoidance of conflict of taxi/way or apron, (3) Incapacitation (VETO)) and to what extent A-PiMod could support the Pilots in relation to workload management, error identification, situation awareness, teamwork, and how this would have an impact on the error reduction. After this, the participants completed an individual questionnaire related to benefits analysis.

3.5. Assessment of benefits/safety impact

In order to assess the potential safety impact of the new automation concept (and allied multimodal cockpit), a systematic approach was applied. This involved the elicitation of structured feedback from pilots and experts, using the Total Aviation Risk model [21]. Specifically, structured feedback was captured in relation to potential change factors for base events in this risk model [21]. The total aviation system risk model contains 425 base events and 51 end states. The particular structure of an event sequence diagram and its connected fault trees depends on the scenario considered. The probability change factors of all impressionable base events are determined in the safety assessment on the basis of information gathered in multiple workshops with members of the Community of Practice (COP). In the workshops the participants discussed the kinds of mechanisms facilitated by the innovative concept which may increase or decrease the probability of a particular base event in a scenario. The specific details of the quantification of safety impact have been reported in another paper [22].

4. Proposed adaptive automation concept

Overall, the objective is to provide assistance to the flight crew when and if required. Automation acts as a third crew member providing information and task support to crew –safeguarding the mission level goal [1, 2].

The third pilot approach involves providing (1) decision/information support, and (2) workload support. This follows from the hypothesis that information underpins good decisions, which in turn results in safe aircraft states. Further, it follows the philosophy that if there in increase in workload, certain functions should be shifted to automation, to reduce the cognitive/physical burden on the crew.

The overall approach involves continuously monitoring the operational situation and the allied crew/automation state, to determine the best distribution of task activity between the crew and automation [1, 4]. It is anticipated that this will ensure the safe completion of the flight. If there is an increase in workload, certain functions will be shifted to automation, to reduce the cognitive/physical burden on the crew. Also, automation is used to support information management tasks (i.e. information gathering and information assessment). This in turn has an impact on safety. Real-time feedback is provided to the Flight Crew via a cockpit user interface (i.e. HMMI Interaction Manager), so that the crew at all times understand the status of (1) the operational situation, and (2) the joint crew automation system. This ensures full situation awareness, which in turn impacts on mission safety. All of the above ensures that the aircraft remains in a safe state. This in turn has consequences at a process level (i.e. both single and multiple flight levels).

The team comprises the Flight Crew (namely the Pilot Flying and the Pilot Monitoring), the 'Third Pilot' and automation. Accordingly, the third pilot is conceived as a virtual team-member [1, 2, 4]. All team members co-operate in relation to making and executing mission level decisions. Mission level decisions are enacted at the mission level and translated into new cockpit level tasks that have to be distributed between the crew and automation, and then performed by them. The system continuously monitors the operational situation and the allied crew/automation/aircraft state, to determine the tasks the team has to perform together, and how to best distribute them between the crew and automation.

The new cockpit technology (i.e. automation and associated systems) allows us to answer the following questions:

- Is the joint crew/automation system in a safe state?
- Is there a potential for a safety critical aircraft state (i.e. now and/or the near future)?
- Do the crew (Pilot Flying and Pilot Monitoring) require support in terms of increased levels of automation?
- Do we need to adjust the level of automation?
- Do the crew require information/decision support?

A-PiMod flags potential risks—providing operational guidance in relation to managing those risks. Pilots have final control, but are responsible and accountable for their decisions and actions [1]. The crew are responsible for assessing the risk status of situation and the appropriate course of action. As such, the crew are not required to follow the decision support provided by the third pilot. This decision support is an aid, not a requirement. The crew can over-ride system proposals/decisions, except in certain critical situations (i.e. incapacitation).

A-PiMod adopts a team centred approach as opposed to a crew centred approach. Specifically, is assists the Flight Crew in relation to information and workload management (i.e. intervention if over and/or under loaded). Automation is conceived as an extension of the pilot's ability to carry out an action(s). Automation provides decision and information support. In principle, we are focussing on the outcome. That is, we are considering what is best for the safe and efficient completion of the mission, as opposed to adapting to human needs. As indicated in the architecture concept (see below), if the Pilot Flying/Pilot Monitoring is overloaded and this threatens the completion of the mission, the task distribution is adapted at the agent level [1, 2].

As reported previously, we propose partnership as opposed to dynamic changes in control function (such that changes can be managed autonomously by the system) [1]. The A-PiMod architecture describes the means for the adaptive completion of Mission Level tasks and their distribution between the crew and automation. This includes the real-time analyses of both the pilot's state (situation awareness and workload) and mission risks [1]. Apimod will permanently assess what has to be done by the cockpit (mission and its context = > cockpit level tasks), distributing it between the crew and automation, and assessing if these agents are correctly performing the tasks they have been assigned (i.e. recover from a stall, avoid ground obstacles, etc.). Task distribution is the product of a situation management process [1]. Here, the pilot flying and pilot monitoring, along with other automated processes cooperate to assess the situation, its risks, what has to be done (cockpit level tasks) and the associated risks [1]. This results in a task distribution.

As described in the architecture concept, in situations where the flight crew are overburdened, task distribution is adapted at the agent level [1]. Automation adapts to crew states and capabilities, so that all required cockpit-level tasks are performed [1]. It is this architecture that guarantees the safe completion of the flight.

The proposed automation concept addresses the key decision requirements as defined in the safety case [1, 2, 4]. For more information, please see **Table 2** below.

No	Decision requirement	How supported by automation
1	Authority	Boundaries for automation set in relation to role of Pilot and associated decision authority
2	Information	Supports information acquisition and analysis
3	Time	Automation provide real time updates as to status of situation (both current and future) so have time to anticipate potential future problems and how might manage them
4	Judgement	Automation provides decision assistance – providing feedback on potential course of actions and risk associated with each.
		Automation can gather decision support information from actors outside the cockpit – if collaborative/consultative decision
5	Teamwork	Human agents/crew and automation are conceived as a team
		Better collaboration between team members – enhance situation awareness and increase safety
		Cockpit as a cooperative system
		Support teamwork in terms of information sharing: (1) information sharing between crew and automation, and (2) information sharing between cockpit and agents outside the cockpit
6	Feedback	Automation provides feedback (updated information picture) in relation to the outcome of decisions taken and next steps

Table 2. Automation provides support for decisions.

Underpinning the Third Pilot concept is the A-PiMod multimodal cockpit concept [1, 2]. The multimodal cockpit (1) allows for monitoring of crew interactions with cockpit systems, (2) supports crew communication with automation (i.e. via the MCM Display) and (3), enables voice and touch interaction with cockpit displays [1, 2].

5. Proposed technical architecture

The A-PiMod architecture allows for (1) adapting the mission based on current circumstances and (2) the subsequent organisation of the cockpit (task distribution between the crew and automation) and (3) the circulation of information between the crew and cockpit systems (including automation) to the current and future situation(s) [23]. The starting point in the architecture is to adapt the mission permanently, and to translate a given mission configuration (e.g. decision to divert to closest airport) into tasks that have to be executed by the 'team'. The tasks are then distributed between the team members (crew and automation) based on their current states and capabilities.

Figure 2 below depicts the A-PiMod architecture. This is based on a three layer hierarchy of tasks [23].

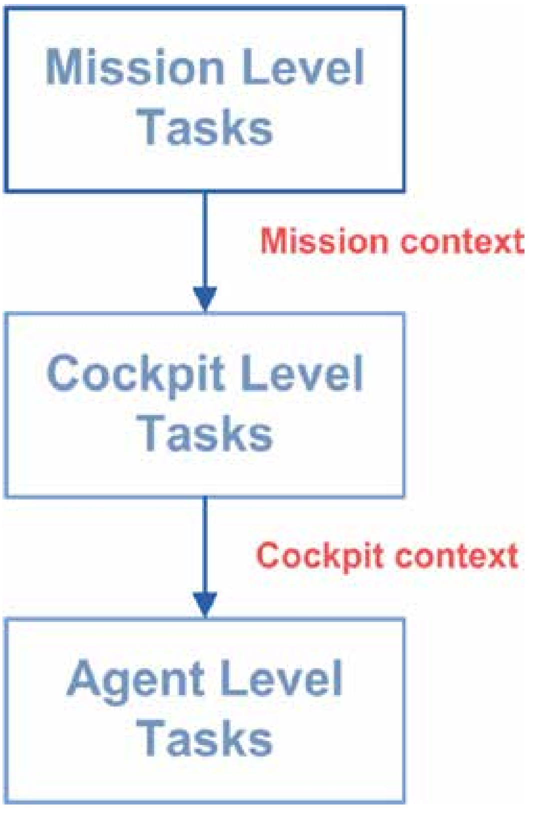

Figure 2. Task Hierarchy.

The architecture is a 'control' architecture; it's about the distributed control of a given object. In this example, this refers to the overall aircraft state including navigation and trajectory. Tasks at a given level are translated into the tasks of the level below based on the context of their execution [23]. At the mission level, the context of execution includes (1) the state of the aircraft and (2) the traffic and environmental context in which the aircraft is flying (i.e. weather, ATC, traffic). At the cockpit level, context refers to (1) the status of the cockpit agents (namely pilots and automation) and (2) cockpit equipment (i.e. displays).

As detailed in **Table 3** below, this control architecture is elaborated in relation to three levels. This includes the mission level, the cockpit level and the agent level. These levels are hierarchical—each level is a decomposition of the level above. All actions occur at the agent level. The upper levels are about deciding what tasks the different agents perform, based on the current contexts, at the mission and cockpit levels.

The key level is the cockpit level. We are trying to see what the cockpit as a whole (i.e., all of its agents—be they human or machine) has to do at a given point to achieve the Mission Level Tasks (in the current situation). Then, what the cockpit as a whole has to do is distributed between the agents available in the cockpit.

It should be noted that the broader ATM system level is not explicitly referred to in the architecture. This is because the other aircraft are not under the control of the architecture. They are part of the context in which the architecture is flying (i.e. achieving its control tasks).

As indicated in **Figure 3** below, several technical components have been specified, linking to the overall architecture concept.

As outlined in **Table 4** below, the A-PiMod architecture consists of seven components and two separate software systems [22].

A key feature of the architecture is the distinction between components and modules:

- A component is a functional unit that performs specific tasks (e.g. risk assessment at the mission level). In the A-PiMod architecture a component is always a small cooperative system made of the crew +1 module.
- A module is a software system that acts with the crew as a team in this specific functional unit. The module provides assistance to the crew in the performing the component's tasks

Level	Description
Definition of mission level tasks	Single flight level—mission phase/sub-phase, context, A/C state—the context the aircraft is in
Definition of cockpit level tasks	Tasks that need to be performed by all (i.e. crew and automation) to achieve mission goals given specific context elaborated
Definition of agent level tasks	Actions undertaken by crew or automation to achieve mission goals in specific context

Table 3. Architecture levels.

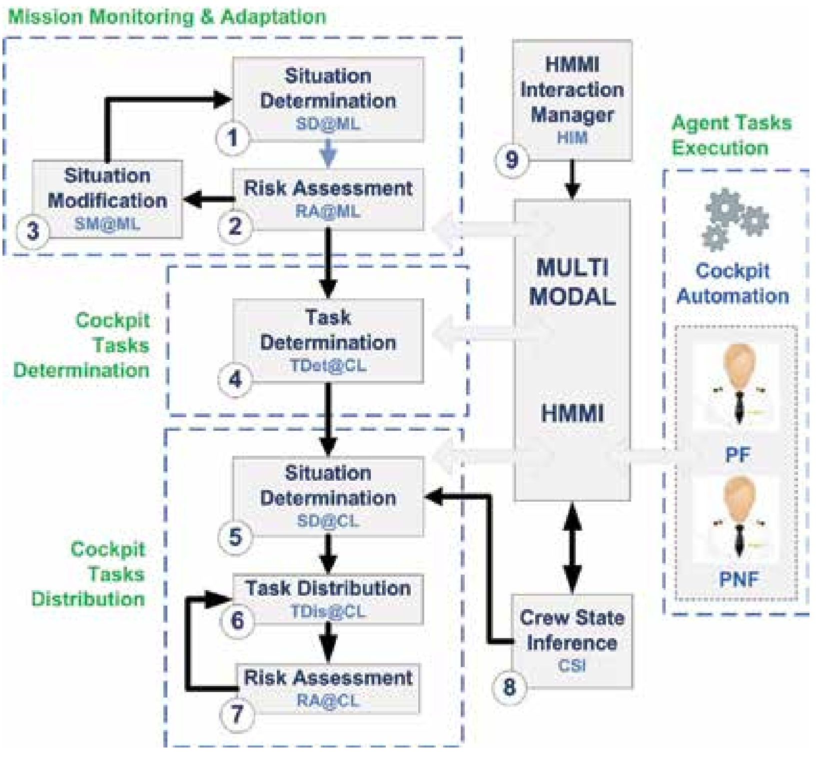

Figure 3. A-PiMod Architecture (Source: Cahill et al. [2]).

Component	1.	Situation determination @Mission Level
	2.	Risk assessment @Mission Level
	3.	Situation modification@ Mission Level
	4.	Task determination @Cockpit Level
	5.	Situation determination @Cockpit Level
	6.	Task distribution @Cockpit level
	7.	Risk assessment @ Cockpit Level
Separate Software Systems	1.	Crew state inference
	2.	HMMI interaction manager

Table 4. A-Pimod architecture.

Thus regarding risk assessment at the mission level, it will always be performed together by the crew and the dedicated module, acting as a small team for that purpose. Both the crew and the module have the common goal to achieve the function assigned to the component. This is what brings great flexibility to the architecture. It allows each component to be executed exclusively by the crew ('manual' mode), e.g. the crew solely assess the risks, by the module ('automated' mode), e.g. the module solely assess the risks and the crew has no say in that evaluation, or by both the crew and module ('mixed' mode), e.g. the module produces a risk assessment and the crew acknowledge or reject it. This is true for all seven components in the architecture. Each is made of the crew and a dedicated module. Given the crew can participate to all seven components, the crew superposes the seven functions associated with the individual components, and this is exactly what human pilots do. They perform all these operations permanently, without being aware of that dissociation between seven elementary functions. They are thus part of the situation assessed by the Situation Determination/Modification @Mission Level component. All these tasks are permanently revised, distributed and executed, based on the context.

In addition, visual analysis of pilots' behaviour is recorded to infer human operator's (pilot's) mental state, stress level, and general workload. The following instruments/technologies are used to obtain information about the pilot's behaviour:

- Eye tracking
- Gesture recognition
- Head pose

6. Pilot interaction in the cockpit and associated user interfaces(s)

6.1. Overview

Crew interaction with cockpit systems is simple and user friendly. In addition to traditional controls, pilots interact with the system using voice and touch. This interaction is tracked by the system (i.e. what tasks performing, level of fatigue, involvement in activity). This form of tracking is referred to as 'crew state monitoring' [1]. Crew feedback is provided via a new cockpit user interface (Mission and Cockpit Level Management Display—MCMD). This provides information about (1) the risk status of the operational situation (this includes an assessment of the status of joint crew/automation system) and (2) what to do (including the provision of best options/alternatives based on different 'technical' contributing factors such as fuel remaining, the weather status at alternate airports and so forth) [1, 2]. As noted previously, the crew can over-ride system proposals/decisions, except in certain critical situations such as crew incapacitation.

6.2. The A-PiMod MC-M display

The A-PiMod Mission and Cockpit Management Display (MC-M Display) enables communication between the Flight Crew and the new adaptive automation technologies [1]. The MC-M Display supports both mission and cockpit management tasks. As depicted in **Figure 4** below, the proposed MCMD features two related sub-displays—the mission and cockpit level

http://dx.doi.org/10.5772/intechopen.73689

Figure 4. The MC-M Display (Source: Cahill et al. [1]).

displays [21]. In the cockpit level display, one can see the tasks assigned to the crew and to automation. The software allows the crew to change that distribution—both manually (crew) or automatically (automation). In keeping with concepts of authority/pilot control, all task distribution changes have to be approved by the crew before becoming active.

6.3. Multimodal interaction

During the A-PiMod project a multimodal system prototype was developed to explore possibilities of multimodal interaction in context of flight deck. From the perspective of human-machine interaction, the flight deck interfaces should be able to accommodate large number of diverse tasks while maintaining high level of efficiency, usability and uncompromised safety. In A-PiMod multimodal interaction was demonstrated through the Multi-Modal Navigation Display (ND) [1, 2].

A number of other systems are linked to the crew state estimation and crew task determination components, for the purpose of inferring (1) the pilot's mental state, stress level and general workload, and (2) predicting potential errors, missed events and/or overlooked information. This includes eye tracking, gesture recognition and head pose tracking technology [1].

7. Crew state monitoring

Crew state monitoring (that is, focussing the Pilots attention on their state along with that of their crew member—and on the current and future state of the aircraft) is an important function of the third pilot. If fatigued, pilots may either forget or omit to review all the safe options. The 3rd crew member (automation) will consider all safe options and prompt the crew in regard to possible options, to ensure that a safe decision is made. In this context, a key challenge is how to get the two human crew members to share their 'current state' with the 3rd crew member [1]. Such an exchange should be meaningful and informative but not self-incriminating in any post hoc analysis [1]. Normal human interactions can easily accommodate this. For example, such information might be imparted as part of pre-flight social interactions/conversation. However, this is hard to replicate in relation to human/machine (i.e. third pilot) interaction

The assessment of crew state goes beyond issues of workload. It concerns many factors including crew experience, flight hours, crew familiarity with the proposed route and departure/landing airports, training background and so forth. The crew state might be assessed as less optimal in situations when the two crew members are unfamiliar with the route. From an operational/Pilots perspective, the starting point for crew state monitoring is the crew briefing/flight planning. Depending on the crew situation, this might occur a week before the flight and/or at the time of the pre-flight, flight planning and briefing task. In addition, knowledge of the joint crew status is and any issues linked to this is required [1, 2]. Potentially, the crew might need to report their status/state before the flight commences [1, 2]

The means/basis by which crew state information (i.e. eye tracking data, gesture data, voice, and touch data) is used to assess the crew state needs to be carefully considered. The assessment of this data depends on what we already know about the crew (for example, location in roster and expected level of fatigue). For example, if the crew are not looking at the correct area of the screen, and/or are blinking their eyes a lot, it may not be a problem. In this case, the crew might be very familiar with the route and may be more or less fatigued (i.e. location in roster—first day or last day). However the system might interpret this behaviour differently if the crew are unfamiliar with the route, and on the last day of their roster (i.e. expect higher level of fatigue)

If A-PiMod is to become a trusted (and relied upon) 3rd crew member, it needs to interact with the crew in a manner consistent with 'normal' human-human interaction [1]. Potentially, to be fully integrated in the 'team', it needs to engage in some form of 'social' interaction, and not only technical interactions [1, 2]. This latter issue has not been explored in A-PiMod and requires further consideration

How emphatic a team member is automation? When and how can it articulate its concerns, and potentially, over-ride the crew member's decisions? In most (but not all situations), the cockpit crew have the final authority and can veto automation. This approach reflects an 'adaptable systems' logic. However, there may be situations (identified by the crew monitoring technology) where it is necessary for automation to 'take charge' to ensure flight safety (for example, situations of crew incapacity). Accordingly, three different levels of crew state monitoring can be defined. For example, (1) passive support, (2) active support and (3) intervention/

over-ride [1]. In this sense, A-PiMod represents an adaptive automation approach. Arguably, a fully adaptive automation approach requires modelling and assessment of both the crew and aircraft state [1, 2]. The A-PiMod system represents a significant advancement in relation to the modelling of crew state (i.e. touch, voice, gesture, use of multimodal displays and so forth). However, aircraft state modelling potentially necessitates integration with aircraft systems and wider ATM and ground systems. This has not been demonstrated in the A-PiMod project

8. Innovation

It is proposed that the Third Pilot/A-PiMod system (1) reflects a mix of the logic associated with adaptable systems and adaptive automation, while (2) also providing something new (i.e. multimodal cockpit concept).

In relation to (1), we are

- Providing a framework for crew-automation cooperation for all activities occurring in the cockpit involved in the completion of a flight
- Extending concepts of assistance (as defined by adaptable systems), where the crew are in conceived to be in control all of the time
- Utilising certain features of adaptive automation—that is, providing task support to the crew following an assessment of crew state (i.e. inferences about crew situation awareness and workload)

In general, this new automation concept is predicated on concepts of partnership. The crew and automation are in charge together. As reported previously, in principle, the crew are in charge (concepts of professionalism and responsibility). However, there will always be particular safety critical situations when automation can take charge (i.e. fully adaptive).

In terms of (2), a new multimodal cockpit concept has been advanced. This enables improved assessment of the crew state/workload and provides a means to provide task and decision support information to the crew. Further, it allows for touch and voice interaction with cockpit systems. Evidently, the application of multimodal in the cockpit is not new. However, the application of crew interaction data (i.e. crew voice and touch interaction in the cockpit), as an input to crew state monitoring is innovative.

The third pilot has different modes of operation. This includes (1) passive monitoring, (2) active monitoring and (3) over-ride. It is anticipated that (1) and (2) will be the most typical operational modes. That is, providing task and decision support to pilots based on an understanding/assessment of the crew state and specific workload requirements at a given point in time. In certain non-routine situations (3) will be required (i.e. fully adaptive). The partnership/third pilot concept is defined in relation to the combination of these three modes of operation. In the future, mode (3) might be become routine, whiles modes (1) and (2) might become less routine. Either way, the advancement of this concept will require considerable effort in relation to both development and certification [1].

9. Assessment of benefits and safety quantification

9.1. Assessment of benefits/impact

The expected benefits/impact were validated through extensive field research including 27 COP sessions, Validation Cycle 1 (VC1), Validation Cycle 2 (VC2) and evaluation with stakeholders at a demonstration day event [1, 2]. Overall, validation activities indicate that the 'Third Crew Member' may yield many operational and safety benefits. As defined in **Table 5** below, these benefits can be grouped at different levels (i.e. cockpit, task, process and ATM System).

It is anticipated that this third pilot approach will enhance flight safety, especially in abnormal situations. The third pilot will not remove human error. Rather, it will reduce it. This is largely attributable to improvements in error detection and error management. A cockpit that is designed

No	Benefit	Benefit level
1	Improved access to information—faster access	Cockpit
2	Improved mechanisms to interact with information (i.e. voice, touch and gesture)	
3	Provide variability in way of the automation control selection (i.e. via voice, touch and gesture)	
4	Better interaction between automation and Pilots—clear communication lines, clear understanding of who does what and, when/how transfer work between both	
6	Flexible and natural interaction with cockpit systems (MM)	Task
7	Decision support—how to proceed in safety critical situation and/or normal situation	
8	Provide task support to crew in relation to assessing the situation and deciding on a course of action	
9	Reduce workload in complex/high risk situations	
10	Pilots always know 'what is going on' (i.e. reliable situation awareness)	
11	Complementary ways in which to interact with information (i.e. MM interaction)	
12	Reduction in workload	
13	Improvement in information management—support information acquisition and information analysis	
14	Improvement in situation awareness	
15	Improvement in situation assessment	
16	Provision of new information (i.e. status of operation, status of automation and routing advice)	
17	Improvements in the elimination of and recovery from human error	
18	Support for error identification and broader TEM	
19	Error reduction	
20	Error mitigation	
21	Error avoidance—avoidance of safety critical situations	
22	Better interaction between automation and Pilots—clear communication lines, clear understanding of who does what and, when/how transfer work between both	

No	Benefit	Benefit level
23	Completion of mission in accordance with the flight plan	Process
24	Safe landing	
25	Reduction in accident rate	
26	Help mitigate the consequences of survivable accidents	
27	Indirect support—flight punctuality	
28	Indirect support—management of delays	
29	Indirect support—more efficient flights (and allied impact on fuel consumption)	
30	Reduction in accident rate	System/ATM
31	Indirect support—flight punctuality	
32	Indirect support—management of delays	
33	Potential link to SESAR SWIM concept (i.e. sharing information across ATM network)	
34	Potential to extend to support single crew operations	

Table 5. Operational and Safety Benefits.

with the A-PiMod approach in mind will extend automation capabilities in an adaptive way, to the extent necessary to support a safer flight. Potentially, such an adaptive automation approach might prevent many accidents. In this regard, we might consider the AF 447 accident [8]. As indicated in the accident analysis research with COP members and VC2 participants, all 19 participants indicated that A-PiMod would have played a significant role in preventing this accident.

9.2. Safety quantification

As reported previously, it is expected that the A-PiMod concept might lead to a reduction in the probability of fatal accidents by 43% [1, 21].

The assessment of safety impact concerns what has been advanced from a conceptual perspective (i.e. A-PiMod concept), as opposed to the technological progress (set of tools developed in the A-PiMod project, which reflects a particular implementation of the concept) [1, 21]. It is these set of tools that were validated in simulator evaluations [1, 2, 4]. These tools can be viewed as a first technical instantiation of the A-PiMod system. The sophistication, scope and integration of the tools can be improved in future research and development [22]. Once implemented, the expected impact might be further assessed.

10. Conclusions

In the perfect world, A-PIMOD would provide an airline with the most experienced team (crew and automation), capable of dealing with any situation (routine, non-routine, safety critical), where skill level is constant, across all weather/routes/airports/time zones. The third Pilot helps avoid dramas. The Third Pilot/A-PiMod will not eliminate human error. Rather, it will reduce error (human error is a reality and errors will always happen), and help manage them if they occur. In this way, the third pilot approach can be conceptualised in relation to 'Smart Pilot Assistance'.

A-PiMod will enable the automation system to account for pilots' emotional and cognitive states. For example, normal, tired, stressed, overloaded and incapacitated. Together with a thoroughly designed adaptive multimodal cockpit, this new technology will significantly improve the safety of flight, especially in abnormal situations and during situations of crisis management.

It should be noted that the assessment of safety impact has been undertaken for the A-PiMod concept, rather than for its particular implementation as achieved in the A-PiMod project. The A-PiMod concept is an advanced adaptive automation concept for a multi-modal cockpit, wherein the automation is seen as a third pilot, and crew and automation continuously adapt to each other and the context, such that safety is maintained. In the course of the A-PiMod project a particular implementation of the concept was achieved by development of a set of tools, and these tools were used in validation experiments (i.e. validation cycle 1 and validation cycle 2), in a flight simulator context. This set of tools can be viewed as a first technical instantiation of the A-PiMod system, and the sophistication, scope and integration of the tools can be improved in future research and development.

Acknowledgements

The research received funding from the European Commission's Seventh Framework Programme (FP7/2007-2013) under grant agreement N. 605141—Applying Pilot Models for Safety Aircraft (A-PiMod) Project. We would like to thank member of the A-PiMod Project Team for their collaboration in this research. Further, we would like to thanks our COP members (particularly, Paul Cullen, William Butler, Martin Duffy and Stephen Duffy) for their invaluable input. Critically, the emerging adaptive automation concept is predicated on extensive feedback in relation to flight crew experience with automation (and associated problems).

Author details

Joan Cahill[1]*, Tiziana C. Callari[1], Florian Fortmann[2], Stefan Suck[2], Denis Javaux[3], Andreas Hasselberg[4] and Sybert Stroeve[5]

*Address all correspondence to: cahilljo@tcd.ie

1 Trinity College Dublin (TCD), Dublin, Ireland

2 OFFIS, Oldenburg, Germany

3 Symbio Concepts and Products, Bassenge, Belgium

4 Deutsches Zentrum für Luft- und Raumfahrt (DLR), Braunschweig, Germany

5 Netherlands Aerospace Centre NLR (NLR), Amsterdam, The Netherlands

References

[1] Cahill J, TC Callari, F Fortmann, S Suck, D Javaux, A Hasselberg, SH Stoeve, BA van Doorn. Automation and the third pilot: Managing teamwork and workload in an airline cockpit. Human Mental Workload: Models and Applications: Proceedings of the First Symposium on HWorkloads, Dublin, June 2017; 2017. http://www.springer.com/kr/book/9783319610603. Longo, Luca, Leva, M. Chiara (Eds.) pp. 161-174. ISBN 978-3-319-61060-3

[2] Cahill J, Callari TC, Fortmann F, Javaux D, Hasselberg A. A-PiMod: A new approach to solving human factors problems with automation. In: Harris D, editor. Engineering Psychology and Cognitive Ergonomics. EPCE 2016. Lecture Notes in Computer Science. Vol. 9736. Cham: Springer; 2016

[3] Hollnagel E, Woods D. Joint Cognitive Systems: Foundations of Cognitive Systems Engineering. Boca Raton, Florida, USA: CRC Press; 2005, 2005

[4] Cahill J, Callari TC. A novel human machine interaction (HMI) design/evaluation approach supporting the advancement of improved automation concepts to enhance flight safety. In: de Waard D, Sauer J, Röttger S, Kluge A, Manzey D, Weikert C, Toffetti A, Wiczorek R, Brookhuis K, Hoonhout H, editors. Proceeding of the Ergonomics Society Europe Chapter 2014. Annual Conference "Human Factors in high reliability industries" Lisbon, Portugal; 2015. Available from http://www.hfes-europe.org/human-factors-high-reliability-industries-2/

[5] Kaber DB, Prinzel LJ. Adaptive and Adaptable Automation Design: A Critical Review of the Literature and Recommendations for Future Research; 2006. NASA/TM-2006-214504

[6] Hilburn BJ, Byrne E, Parasuraman R. The effect of adaptive air traffic control (ATC) decision aiding on controller mental workload. In: Mouloua M, Koonce JM, editors. Human-Automation Interaction: Research and Practice. Mahwah, NJ: Lawrence Erlbaum Associates, Inc; 1997. pp. 84-91

[7] Kaber DB, Riley JM. Adaptive automation of a dynamic control task based on secondary task workload measurement. International Journal of Cognitive Ergonomics. 1999;**3**:169-187

[8] Flight AF 447 (2009, June 1). Final Report on the accident on 1st June 2009 to the Airbus A330-203 registered F-GZCP operated by Air France flight AF 447 Rio de Janeiro (Published July 2012). Retrieved from Bureau d'Enquêtes et d'Analyses pour la sécurité de l'aviation civile (BEA). http://www.bea.aero/docspa/2009/f-cp090601.en/pdf/f-cp090601.en.pdf

[9] Flight Spainair 5022 (2008, August 20). Final Report on the accident on 20th August 2008 involving a McDonnell Douglas DC-9-82 (MD-82) registration EC-HFP operated by Spainair at Madrid-Barajas Airport (Published October 8, 2008). Retrieved from Comisión Investigación de Accidentes e Incidentes de Aviación Civil (CIAIAC). http://www.fomento.es/NR/rdonlyres/EC47A855-B098-409E-B4C8-9A6DD0D0969F/107087/2008_032_A_ENG.pdf

[10] Flight Helios Airways HCY522. Final Report on the accident on 14th August 2005 involving a Boeing 737-31S registration 5B-DBY operated by Helios Airways at Grammatiko, Hellas (Published November 2006). Retrieved from Air Accident Investigation and Aviation Safety Board (AAIASB); 2005, August 14. http://www.moi.gov.cy/moi/pio/pio.nsf/All/F15FBD7320037284C2257204002B6243/$file/FINAL%20REPORT%205B-DBY.pdf

[11] Flight China Airlines 140. Final Report on the accident on 26th April 1994 involving an Airbus Industrie A300B4-662R registration B1816 operated by China Airlines at Nagoya Airport (Published July 19, 1996). 1994, April 26. Retrieved from Aircraft Accident Investiga-tion Commission. http://www.skybrary.aero/bookshelf/books/808.pdf

[12] Flight Air Inter 148. Final Report on the accident on 20th January 1992 involving an Airbus A320 registration F-GGED operated by Air Inter Airlines in Vosges Mountains (near Mont Sainte-Odile). Retrieved from Bureau d'Enquêtes et d'Analyses pour la sécurité de l'aviation civile (BEA). 1992, January 20. http://www.bea.aero/docspa/1992/f-ed920120/htm/f-ed920120.html

[13] SKYbrary Aviation Safety. 2017. Retrieved From: https://www.skybrary.aero/index.php/Human_Error_Types

[14] International Civil Aviation Organisation. Annex 13: Aircraft Accident and Incident Investigation; 2010

[15] European Commission. Flightpath 2050, Europe's Vision for aviation. Luxembourg: Publications Office of the European Union; 2011

[16] Brandon PR, Fukunaga L. A review of the findings of empirical studies of stakeholder involvement in program evaluations. American Journal of Evaluation. 2014;**35**:26-44. DOI: 10.1177/1098214013503699

[17] O'Sullivan RG. Collaborative evaluation within a framework of stakeholder-oriented evaluation approaches. Evaluation and Program Planning. 2012;**35**:518-522

[18] Cousins JB, Whitmore E, Shulha L. Arguments for a common set of principles for collaborative inquiry in evaluation. American Journal of Evaluation. 2013;**34**(1):7-22

[19] Fitzpatrick J, Sanders J, Worthen B. Program Evaluation: Alternative Approaches and Practical Guidelines. 4th ed. New York: Pearson; 2010

[20] Wenger E. Communities of Practice: Learning, Meaning, and Identity. Cambridge: Cambridge university press; 1998

[21] Ale BJM, Bellamy LJ, Cooke RM, Goossens LHJ, Hale AR, Roelen ALC, et al. Towards a causal model for air transport safety—an ongoing research project. Safety Science. 2006;**44**:657-673

[22] Stroeve S, Van Doorn BA, Cahill J. A safety impact quantification approach for early stage innovative aviation concepts: Application to a third pilot adaptive automation concept. Paper presented at SESAR Innovation Days, Delft, November 2016; 2016

[23] Javaux D, Fortmann F, Möhlenbrink C. Adaptive Human-Automation Cooperation: A General Architecture for the Cockpit and its Application in the A-PiMod Project. Proceedings of the 7th International Conference on Advanced Cognitive Technologies and Applications (COGNITIVE 2015). International Academy, Research, and Industry Associa-tion (IARIA). 2015. ISBN: 978-1-61208-390-2

Chapter 2

Aviation 4.0: More Safety through Automation and Digitization

Rosa Arnaldo Valdés,
Víctor Fernando Gómez Comendador,
Alvaro Rodriguez Sanz and Javier Perez Castán

Additional information is available at the end of the chapter

http://dx.doi.org/10.5772/intechopen.73688

Abstract

The world is talking about the Industry 4.0 or the fourth industrial revolution, that is, the current trend of higher level of automation, digitalization and data exchange in manufacturing technologies. It includes cyber-physical systems, Internet of Things and cloud computing among other technological assets. With more than 5000 sensors, which generate up to 10 GB of data per second, modern aircraft engines are an exponent of what digitalization and the Internet of Aircraft Things could furnish, as part of the upcoming Industry 4.0 revolution, in the aviation industry. This new era has the potential to improve air transport key performance areas. Particularly, in an industry where safety levels are so high and the margins for improvement are extremely tight, this upcoming era might imply a shift in safety improvement. In an attempt to define Aviation 4.0, this chapter discusses the stages of aviation development from basic VFR flight rules at Aviation 1.0 up to Aviation 4.0 where cyber-physical systems are designed to assist humans' unkind or hazardous work, to take decisions and to complete tasks autonomously. It illustrates the current and future cases of application of Aviation 4.0 to increase the aviation safety, while outlines how they might increase aviation safety levels.

Keywords: industry 4.0, aviation 4.0, digitization, IOT, big data, cyber-physical

1. Introduction

The manufacturing industry is going through remarkable changes. The fourth revolution, driven by the Internet of Things (IoT), is here. It is creating intelligent networks, connecting

IntechOpen

© 2018 The Author(s). Licensee IntechOpen. This chapter is distributed under the terms of the Creative Commons Attribution License (http://creativecommons.org/licenses/by/3.0), which permits unrestricted use, distribution, and reproduction in any medium, provided the original work is properly cited.

machines, work, and systems that can independently interchange data and commands, initiate actions and control each other autonomously [1]. Experts estimate that 85% of enterprises will implement Industry 4.0 solutions in all important business divisions in 5 years. By 2020, it will be equivalent to an annual expenditure of €140 billion only at European level [2].

However, what is the Industry 4.0? This is the question that the industry world is talking about. Industry 4.0 [3] is sometimes referred to as the fourth industrial revolution, after the steam-powered mechanical machines, the electrically powered mass production and the electronically/IT-powered automated manufacturing. It focuses on the establishment of intelligent products and smart production processes as well as on vertically and horizontally integrated manufacturing systems [4]. Smart products are distinctively distinguishable, may be situated at any moment in time, and record past and current information or status as well as alternative ways to attain their target. Smart production processes [5] are intelligent production processes in which the various steps in the lifecycle are integrated with each other, starting with the design phase and ending with the retirement phase. The four stages of the industrial revolution are illustrated in **Figure 1**.

The concept is renamed locally according to the different initiatives going on in various geographical areas and industry branches. A few of them are:

- Internet of Things (IoT) [6] refers to the world in which all everyday objects and devices are completely interconnected for seamless interoperability;
- Industrial Internet of Things (IIoT) [7] is what you get when applying the concepts of IoT to an industrial setting, for example, in production;
- Smart Manufacturing is a term mainly used in the USA, and China2020 is a term mainly used in China [8];
- Factory of the Future is a large research initiative supported by the EU, in which new technologies (such as IoT) should be applied to factories;
- Industrial Internet (General Electric), Connected Enterprise (Cisco), and so on;
- Industrial Digitalization is a term used in Sweden, which stresses the impact and potentials of digitalization in both manufacturing and process industries.

The difference between these initiatives does not lie in the goals, but rather in the selection of enabling technical solutions (e.g., wireless or not, use of Internet or proprietary networks, point-to-point communication or not, cloud-based or not, etc.).

As far as aviation is concerned, the main applications of the Industry 4.0 concept so far are related to the aerospace manufacturing processes. Barbosa [9] provided a contextual outline of how robotics, additive manufacturing, augmented reality, IoT and simulation are currently applied at the aeronautics manufacturing industry. He illustrated some novelties in the aerospace industry related to Industry 4.0 and its day-to-day benefits.

Even if there is still a long way to go before the first fully automated airplane is produced, application of robots at Airbus and Boeing will make monthly production rates above 30 units

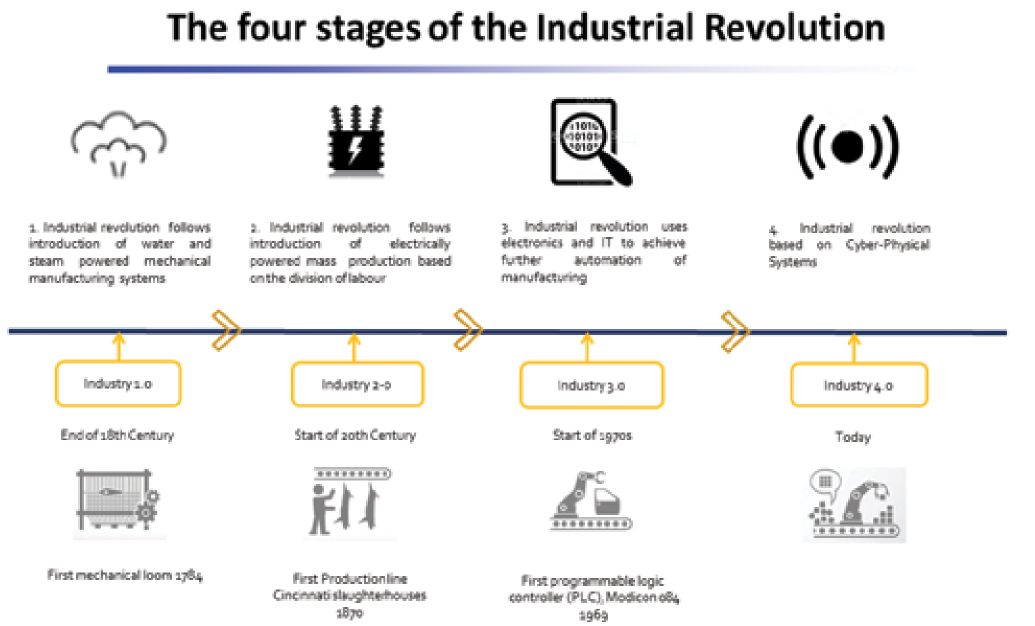

(*Source DFKI Boss, 2011*).

Figure 1. The four stages of the industrial revolution.

possible for some aircraft types. A new Airbus spin-off company, InFactory Solutions, is developing the corporation vision of the "Factory of the Future," with products and services for connected manufacturing under a fully connected and digital production environment. [10]

At the same time, some authors have pointed out the impact of Industry 4.0 key enabling technologies on how safety is managed at the production sites. Big data analytics can provide precise data for operational control, and IoT might improve equipment safety through a better maintenance [11–13].

However, the potential of Industry 4.0 key enabling technologies to increase the extremely tight safety levels in aviation operation has not yet been addressed. This chapter discusses how the upcoming Aviation 4.0 era (Industry 4.0 for aviation) might imply a paradigm shift opportunity in safety improvement. It analyzes, from an evolutionary perspective, the stages of aviation development, from basic VFR flight rules at the Aviation 1.0, up to Aviation 4.0 stage where cyber-physical systems will be designed to assist humans' physically strenuous, unpleasant or dangerous work, to take decisions and to complete tasks autonomously. It also illustrates case studies of the application of the Aviation 4.0 concept to increase aviation safety.

2. The concept of aviation 4.0

Just as we can establish four stages in the industrial revolution, we can establish four stages in the evolution of commercial aviation. These four stages are closely related to the adoption of higher levels of automation on board aircraft; and controversially, they do not correspond to a deliberate attempt of improving aviation safety in a steady way, but rather to a continuous adaptation to the challenges imposed by its environment following a trial-and-response approach. The four stages in commercial aviation revolution, from Aviation 1.0 to Aviation 4.0 are summarized in **Table 1**.

The first evolutionary stage, Aviation 1.0, corresponded to the beginning of the commercial aviation were flight evolved under visual flight rules, following visuals clues and signals and there was hardly any instrumental aid to help pilots to fly. This era was dominated by the technological challenges posed by how to build and fly an aircraft. Very simple instruments constituted the so-called first steps toward "*virtualization of the environment*"; and provided basic indications required for the flight: first, anemometers and altimeters to indicate airspeed and altitude; pneumatic and electric gyroscopes to measure attitude and stabilize an artificial horizon; basic mechanical autopilots to keep a straight flight; servos and devices to perceive forces on aerodynamic surfaces (artificial feel load, Mach trim compensator), and so on. Mechanic inventions were progressively incorporated to flight controls in parallel with electric basic instruments to help pilots.

The second stage, Aviation 2.0 was dominated by the replacement of old mechanism by electric devices. Technological advances were driven by two important challenges imposed by the continuous and steady growth of aviation, with a higher number of aircraft operating in the same environment, under all weather conditions: (i) how to fly an aircraft under adverse meteorological conditions? and (ii) how to control multiple aircraft flying in dense traffic in the same airspace?

New instruments such as the VOR (very high-frequency omnidirectional range) and ILS (instrument landing system) allows the pilots to follow safely tracks and approach paths. On board

Stage of aviation development	Characteristics	Characteristics of signal processing	Main challenges
Aviation 1.0: VFR	Airspace	Visual signals	How to build and fly an aircraft?
Aviation 2.0: IFR	Frequency Space	Technical analog signals	How to fly an aircraft under adverse met conditions? How to control multiple aircraft flying in dense traffic in the same airspace?
Aviation 3.0: Assistance Systems; Safety Nets	Data Space (Digitization; Informatization)	Digital data processing; Digital data communication	To support the people with the help of aggregated, visualized, understandable information to make informed decisions; SWIM
Aviation 4.0: AFR, RPAS, Decentralized decisions by systems	Cyber Space (Automation; Artificial Intelligence)	Cyber-physical systems	Cyber-physical systems to assist humans' physically strenuous, unpleasant or dangerous work. Cyber-physical systems to take decisions and to complete tasks autonomously

Table 1. The four stages in commercial aviation revolution: From aviation 1.0 to aviation 4.0 [17].

innovations, such as electric autopilots, auto-throttle, flight directors, airborne weather radars, navigation instruments, inertial platforms, and so on, resulted in high safety enhancements. This evolution comes with a rise of information to be managed by the pilot, who might be confronted with more than 600 devices and indicators to be monitored and controlled in the cockpit.

Aviation 3.0, the third stage in the revolution of commercial aviation involved the massive incorporation of electronics in the cockpit, driven by the availability of reliable and usable digital data processing and data communication technology that invaded the market and society. At the beginning of this revolution, electronics significantly helped to diminish the clutter of instruments and replace the old indicators with integrated colored displays, cathode ray tube (CRT) and liquid crystal display (LCD), capable of providing a synthetic and analytic view of multiple parameters in a limited area of the cockpit. Technological solutions were progressively designed to support the operators (pilots and controllers) informed decisions, with the help of aggregated, visualized, understandable information. Operations onboard and outside of the aircraft shifted from tactical to strategic, and assistance systems and safety nets became crucial elements to increase the level of safety in commercial aviation.

The amount of information available in the system raised exponentially while became no longer immediately accessible and visible to the operator, who was forced to evolve his/her role from an active role (flying or controlling tasks) toward a monitoring role. This third revolution in aviation brings the emergence of the notion of the "electronic echo-systems." As an example, an A-320 incorporated around 190 computers, placed all through the fuselage, which interacts with them without the pilot being aware. The complexity of the "electronic echo-systems" is an epistemological obstacle for pilots and controllers, which might adversely affect the safety of the operation as far as they become sometimes "out of the loop."

Modern advanced aerospace systems will be characterized by a tight combination between onboard cyber systems (e.g., processing, communication) and physical elements (e.g., platform structure, sensing, actuation and environment), defined by researchers as "engineered systems that are built from and depend upon the synergy of computational and physical components" [14, 15]. Therefore, Aviation 4.0 is concerned with the design of cyber-physical Systems (CPS) that are able to assist humans' demanding work by helping them to take decisions and to complete tasks autonomously, and with its integration of cyber-physical components in future aviation information systems [16].

Cyber-physical systems will make the Aviation 4.0 airframe a digital and smart airplane. The amount and diversity of operational data that can be collected onboard of the aircraft and by ground operations will raise exponentially. In Aviation 4.0, supervisory control in the manufacturing processes and big data acquisition and processing networks make possible automation and integration with IT systems. Airplane operations relay on a grand scale on the employment of CPS. Future Air Traffic Management systems are conceived as a cyber-physical system-of-systems (CPSS) that demand tight amalgamation to provide the required capacity, efficiency, safety and security system performance. In this scheme, examples of cyber components are aircraft digital communications, weather/traffic forecast, flight planning/optimization algorithms, situation awareness and decision support software, and so on, while example of physical components are mobile aircraft; dynamic airspace traffic, weather, pollution, noise; pilots, air traffic controllers, airlines crew, and so on.

Even today, with only a limited deployment of airborne cyber-physical systems, the available information is immense: maintenance messages/fault codes, quick access recorder (QAR) of flight and system parameters; maintenance action logs/test results/shop data; real-time data and real-time information management for decision-making, and so on. The great technological parallel developments in data analytics will support active reaction to these enhanced aircraft operations. To illustrate the diversity and the volume of data that the total deployment of aviation will imply 4.0, let us consider that the modern engines (such as the Pratt & Whitney's Geared Turbo Fan GTF engine) can have up to 5000 sensors generating up to 10 GB of data per second. A single twin-engine aircraft with an average 12-h flight time can produce up to 844 TB of data, 20% more data than Facebook daily accumulated data. While an Airbus A320 transmits about 15,000 parameters per flight, the figure is 250,000 for the A380 and 400,000 for the A350. It seems, therefore, that the data generated by the aerospace industry alone could soon surpass the magnitude of the consumer Internet. However, the wave of data is "useless" without targeted analysis.

This revolution is not exempted of defies. Challenges related to information assurance and cyber security include the certification of cyber security requirements for e-Enabled airplanes; the development of anti-tamper avionics hardware and software and the collaboration of industry and governments to address the cyber threat to aviation. There are also very important technological challenges for airplane operations, which are as follows:

- worldwide aeronautical networks interoperability, including signal processing and wireless performance as well as the aircraft interfaces to the Internet;
- verification and validation of the onboard software, how to secure end-to-end entire SW supply processes, the understanding of cyber-physical life-cycle scale;
- improvement of airplane health, control and prognostics by exploiting sensor networks and data fusion, information management and data analytics and, critical real-time data sharing, appropriate end-to-end information exchange, distributed decision-making; and finally
- human-automation interface issues such as visualization, keeping human-in-the-loop and connection between aircraft controls and air traffic systems.

Industry 4.0 technologies (automation, IOT, artificial intelligence, cognitive computing, big data analytics, digitization, etc.) have the potential to generate a paradigm shift in the aviation industry, generating new mechanisms to make it not only more efficient but also safer. Unexplored concepts and approaches to safety start to being discovered by companies and researchers in an attempt to approach safety from different perspectives with the new tools that Aviation 4.0 makes available.

In the following sections, we revise up to six case studies that illustrate the application of Aviation 4.0 concept to significantly increase the safety levels in aviation.

1. Automatic flying in predefined situations in a rule-based way.
2. Developing a robust aircraft predictive maintenance.

3. Cockpit safety cognitive computing aid systems.
4. Real-time weather information update.
5. Improved search and rescue services especially in the oceanic or remote area.
6. Real-time human performance monitoring and alerting based on nonintrusive physiological sensors/signals and contextual information.

3. Automatic flying in predefined situations in a rule-based way

Recent aviation history is splashed with occurrences that have led researches to consider the concept of AFR "Automatic/Autonomous Flight Rules," which implies "Automatic flying in predefined situations in a rule-based way".

On 1 July 2002 at 23:35, flights DHL Flight 611 and Bashkirian Airlines Flight 2937 collided at 36,000 feet over the German town of Überlingen. The investigation identified the deficiencies in the air traffic control service and the error of one of the crew to follow the indications of the onboard aircraft collision avoidance system (traffic collision avoidance system—TCAS) in the origin of the accident. The TCAS was able to effectively anticipate the collision and generate proper and correct alarms to alert the crews and generate evasion trajectories to be followed by each crew. TCAS resolution maneuvers were correctly generated. If both crews had acted accordingly, following the "rules" and the TCAS resolution indications, the accident would have been avoided.

On 24 March 2015, the flight German Wings Flight 4 U 9525 crashed in the French Alps. The aircraft followed a descent trajectory guide by the pilot, who had set the autopilot to descend to 100 ft. (30 m) and augmented the descending speed of the aircraft. One minute before the aircraft hit the ground, the system that alerts of dangerous proximity of the aircraft to the terrain (enhanced ground proximity warning system—EGPWS) generated correct and proper warnings indicating to the pilot to ascend to avoid collision with the ground.

On both situations, the aircraft systems correctly detected the dangerous situation and "warnings" were generated properly, although not appropriately followed by the crew. Both cases would have been avoided if the warnings have been automatically followed when the crew was not taking appropriate action in due time.

These support the idea to develop "rules of flight" where the Aviation 4.0 cyber-physical (expert or AI) aircraft system will follow the warnings automatically, in case the crew is not taking appropriate action in due time.

Other recent occurrences raise the question about the capabilities of Aviation 4.0 to prevent or avoid particular accidents. Malaysian Airlines Flight MH370 left the cleared flight path and disappears from radar screen without any communication with ATC. Could an Aviation 4.0 FMS prevent from deviating from the filed flight plan in that massive way (without having activated/provided a feasible "alternate" routing)? In a more general approach, could an Aviation 4.0 FMS prevent from flying into a no-fly-zone (NFZ) or a restricted area?

Figure 2. Automatic flying in predefined situations.

Aviation 4.0, using the potential of automatic flying in predefined situations, as illustrated in **Figure 2**, and in a rule-based way, could help to overcome today's safety and security gaps, although key R&D work (Aviation 4.0 Research Agenda) is still needed to get it done, such as the:

- Identification and definition of automatic/autonomous flight rules.
- Predefinition of situations, where automatic (autonomous) flying to be activated and to be deactivated after the situation has improved.
- Standardization of "sensor" signals (data inputs) needed to determine, whether an in-flight situation is out of an acceptable "envelope."
- Safety Analysis for Aviation 4.0.
- Resolution of regulatory and liability issues.

Many puzzle stones needed are already available and in operational use, and developments and experiences from other domains can be taken on board. Missing links are topics for a future research agenda; however, no unsolvable issues identified so far. On the one hand, engineering and operational skills and experience are needed; on the other hand, skills and experience in (social) change management are not negligible.

4. Developing a robust predictive aircraft maintenance

Although most commercial jets still operate engines with limited sensing capability (around 250 sensors), the last onboard maintenance systems manage to enable structure preventive maintenance services. Typically A380 preventive maintenance system is able to generate a list of "pending items to fix" to prevent the next failures causing MMEL issues affecting aircraft dispatch. Ground statistical analysis of fleet historical aircraft maintenance messages and aircraft condition monitoring are used to start preventive maintenance actions upon preventive conditions. Nevertheless, these systems are not able to provide information about the real-time remaining tolerance margin before the occurrence of the next impacting MMEL item, in terms of additional remaining failures of line replaceable units, failure combination and quantified risk.

However, with the advent of Aviation 4.0, the challenge of achieving a real-time effective predictive maintenance capability is becoming a new market for the aeronautical industry. The A350 is able to record in-flight 400.000 parameters, what combine with big data analytics have the potential to comprehend the comportment of the aircraft deeply enough to conduct the maintenance interventions before failures occur. To exploit this market, Airbus and Rolls-Royce have already established a partnership to offer a global expertise in predictive maintenance on A350.

Predictive maintenance has the potential to avoid accidents and extend the aircraft's lifetime by the anticipation of problems before they worsen and spread, and even by programing maintenance of replacement just before the failures or problems occur.

The advantages of Aviation 4.0 IoT aircraft extend to fuel costs and efficiency. Real-time analysis of an airplane engine's sensors can detect and correct the operating inefficiencies that translate to increased fuel consumption.

The potential of predictive maintenance combined with synchronized logistics will have the potential to improve turnaround times, diminish maintenance interventions and the time and number of inactive aircraft in hangars while waiting for parts and service. Real-time reception of the onboard data will allow ground maintenance teams to have parts and technicians ready before the plane lands, so the technical interventions might be done in the minimum time, reducing affections to the flight schedule.

If additionally combined with augmented work technologies, the maintenance work could be transformed into an enhanced troubleshooting environment where technicians might have in a single view of all necessary maintenance information pertinent to the problem. This will reduce the occurrence of human errors during maintenance interventions, impacting positively the probability of accidents due to maintenance errors as well as improving both efficiency and economics.

This information is useful for maintenance purposes after the flight has landed, and the data are downloaded and evaluated. What if centralized maintenance and aircraft condition monitoring data were received in real-time by maintenance personnel on the ground? Or combined in real-time with data analytics, centralized maintenance and logistics information? Or used to integrate aircraft preventive diagnosis with information coming from prognostics?

Data received in real-time by personnel in charge of the maintenance while they are on the ground waiting for the flights will allow the maintenance teams to anticipate any problems before the flight lands, and it will allow technicians to have the parts and specialist ready for a quick intervention. Data analytics and interconnected smart sensors will allow to combine predictive maintenance with synchronized logistics system and reducing not only the risk of in-flight failure but also the cost of aircraft awaiting parts and service.

Maintenance technicians are alerted of a maintenance problem from ACARS messages, voice messages, the aircraft crew logbook and/or conversation with the flight crew. But until now, the troubleshooting information needed to combat the problem has not been centralized, and is not easily accessed while the technicians are on the ramp working on a plane. Technologies

Figure 3. Predictive and augmented maintenance.

like Google Glasses have the potential to recreate complex diagrams and technical information in a 3D-augmented reality environment that boosts the perception of the technicians about the problem and its possible solutions. Maintenance teams might benefit from augmented work technologies to enhance the maintenance and service. An enriched troubleshooting environment with an integrated view of all necessary maintenance information pertinent to the problem might become a fourth dimension that enables remote assistance and guidance as well as real-time access to the most complete documentation while on the job. Predictive and augmented maintenance applications are illustrated in **Figure 3**.

5. Cockpit safety cognitive computing aid systems

Cognitive computing is the capability of the computational systems to emulate the behavior of the human brain, that is:

- Manage and stock huge volumes of data and information in a wide variety of formats (pictures, sound, text, symbols, alphanumeric characters, conversations, etc.);
- Find optimal solutions and process situations that are never experienced before;

- Process information and inputs without requiring data to be organized or compliant with a predefined and close structure or format;
- Organize data and information to find patterns and obtaining hindsight from the information;
- Integrate and combine new data with previous past knowledge and experiences, making sense of such mixture;
- Learn from experience, retaining prior questions and contexts;
- Make decisions and provide intelligent answers to questions based on inferences from the information received;
- Refine and update of decision and answers from a continuous information gathering and processing.

Applications of cognitive computing in aviation safety are illustrated in **Figure 4**. A good exponent of a cognitive computing system is IBM's Watson. Watson is able to process questions expressed in natural human language, and gather and analyze unstructured information and assistance operators make enhanced sensitive choices. Information feed into Watson does not need to match any inflexible parsing. Watson learns from previous experience, prior information and questions, and the context where those questions were made. Moreover, the system is able to argument the evidence it relies on and therefore, the explanations behind its recommendations. All these capabilities for interpreting, evaluating and recommending solutions convert Watson (or other similar cognitive computing systems) into a key enabler for aviation safety improvement.

Airbus Group is working on the development of a Watson Cockpit Mentor, that is, studying how to use Watson technology to help guide pilots through crisis and reducing the information overload pilots during an emergency. In the case of a flight emergence, the system will be able

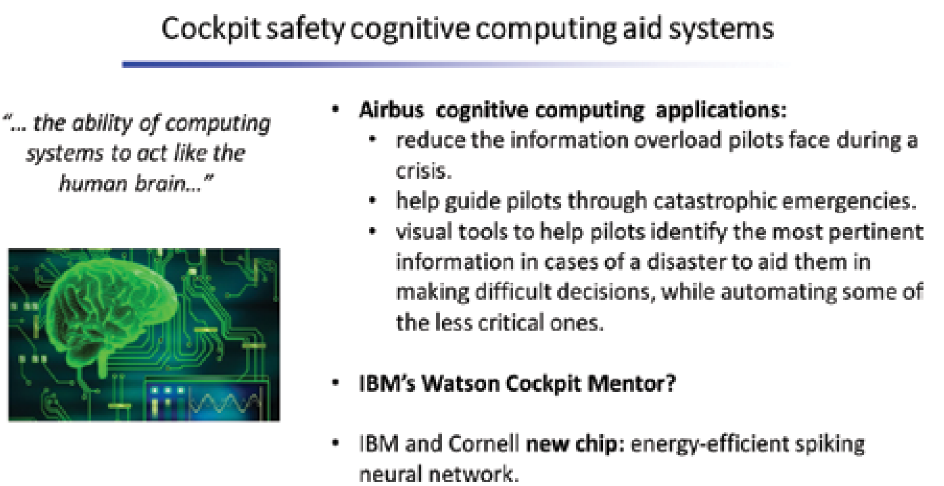

Figure 4. Aviation safety cognitive computing applications.

to interpret not only the information about the status and performance of the aircraft systems but also the pilot description of the problem in simple spoken natural language and the relevant technical materials and documents. Watson crew assistance will interpret the problem and all the information logically will discern critical information on the cabin relevant to the problem solution and make recommendations to the pilot. Those recommendations might concern a modification of the operation of the aircraft to mitigate the problem, a guide in the troubleshooting of the problem, and so on. The system might take care automatic control of less critical decisions and flight task, relieve the crew of nonessential emergency-related activities and therefore, allow the pilot to concentrate on these resources on the resolution of the emergence.

As much as this project might look like science fiction, it is actually one of the collaborative activities between Airbus and IBM. Airbus is also developing cognitive computing applications in other fields of the aircraft operation such as fuel efficiency, maintenance capabilities and operational optimization of the aircraft.

6. Improved search and rescue services especially in oceanic or remote area

Some recent accidents have involved aircraft disappearing, sometimes over the oceans without notice or communications, and very expensive and sometimes unfruitful rest recovery campaigns. The last unfortunate MF370 event has reinforced the efforts of the aeronautical community to develop the concept operations for the Global Aeronautical Distress and Safety System (GADSS). This system will track the aircraft everywhere and under all conditions, it will locate the aircraft when in distress, and it will ensure the timely recovery of Flight and Cockpit Voice Data.

The requirements for these systems are established for normal tracking conditions and for the location of an airplane in distress conditions. It has been establishing an aircraft-tracking time interval of 15 min whenever air traffic services obtain an aircraft's position information at greater than 15 min intervals for airplanes with a seating capacity greater than 19.

Requirements for the location of an airplane in distress (a state that if uncorrected could result in an accident) establish airplane to autonomously transmit information from which a position can be determined at least once every minute. This will provide a high probability of locating an accident site to within a 6 NM radius. This transmission can be activated:

- automatically based on flight behavior and triggered by abnormal or specific events;
- manually from the air crew; and
- manually from the ground.

These requirements will be applicable to new airplanes with take-off weight greater than 27,000 kg from 1 January 2021. The provisions relating to one-minute distress tracking are performance-based, not technology-specific, which means that airlines and aircraft manufacturers

http://dx.doi.org/10.5772/intechopen.73688

Figure 5. Aviation 4.0 distress tracking systems.

may consider all available and emerging technologies which can deliver the one-minute location tracking requirement specified. Main characteristics of Aviation 4.0 distress tracking systems are summarized in **Figure 5**.

There is a range of already installed aircraft technologies/services that can be used for this purpose in the near-term (ADS-C, DS-B, stand-alone sitcom, ACARS, etc.). Mid-term solutions imply space-based ADS-B solutions based upon LEO polar satellite systems, expected to be available around 2018. Long-term solutions envisage automatic deployable flight recorders or real-time data streaming.

The advantages of aviation 4.0 IoT aircraft will allow real-time analysis of an airplane performance and operation, detecting deviations of normal behavior, not standard operating conditions and not desired aircraft states as well as precursors of dangerous conditions that might lead to an accident. IoT would help to connect the missing dots, proper alarm generation, proper tracking, administration, intercommunication among the stakeholders.

7. Real-time human performance monitoring/alerting

The ecosphere of wearable devices is probably one of the newest, more attractive and at the same time, challenging area of the Internet of Things (IoT). Its applications might vary widely and in particular, the possibilities in the field of aviation are just beginning to be explored. The design, production and integration of wearable devices in aviation operations are on the IoT cutting edge. Requesting to be the first airline to incorporate wearable technology in its operation, EasyJet has designed and produced advanced uniforms that integrate wearable

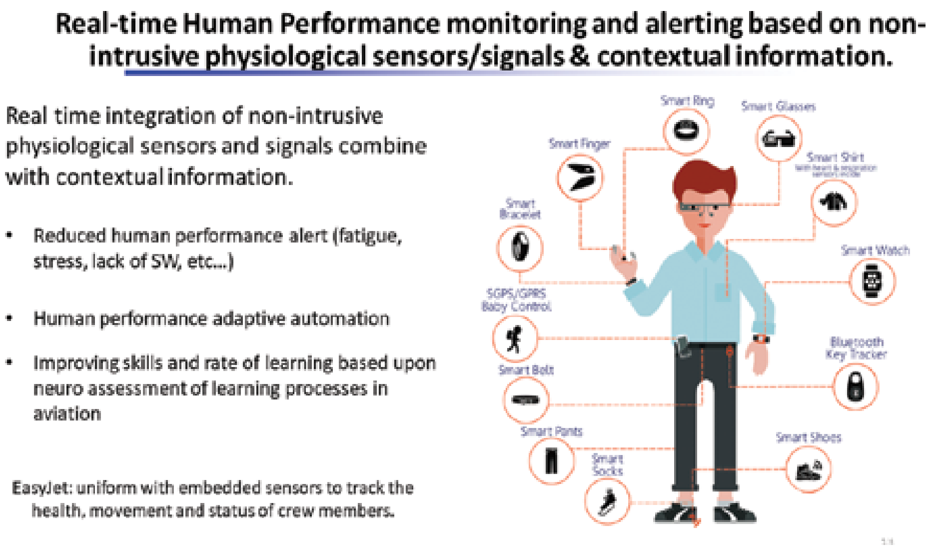

Figure 6. Real-time human performance monitoring and alerting based on nonintrusive physiological sensors/signals and contextual information.

technology for the in-crew and ground staff, with an aim to increase safety in the operation. Air New Zealand uses wearable devices to track unaccompanied children on short- and long-distance flights.

This technology allows sensing, storing, interpreting and communicating information about the wearer's body or surroundings by using reliable, not expensive and nonintrusive sensors and devices. Real-time human performance monitoring and alerting based on nonintrusive physiological sensors, signals and contextual information are illustrated in **Figure 6**.

Real-time integration of nonintrusive physiological sensors and signals combined with contextual information offers a great potential to tackle problems related to one of the aviation safety corner stones, human factors. This technology could help to:

- detect and alert the reduced human performance situations (fatigue, stress, lack of SW, etc.);
- develop better and more reliable human performance adaptive automation; and
- improve skills and rate of learning based upon neuro assessment of learning processes in aviation, and so on.

8. Conclusions

The manufacturing industry is going through amazing fourth evolution driven by technological breakthroughs such as the Internet of Things (IoT), intelligent networks, connecting machines, work and systems, that can independently interchange data and commands, initiate actions and control each other autonomously. New manufacturing focuses on intelligent products and smart production processes as well as on vertically and horizontally integrated manufacturing systems.

Even if renamed locally according to different initiatives going on in various geographical areas and industry branches, the concept is universal. Experts estimate that 85% of enterprises will implement Industry 4.0 solutions in all important business divisions in 5 years. By 2020, it will be equivalent to an annual expenditure of €140 billion only at European level.

As far as the aviation is concerned, the main applications of the Industry 4.0 concept so far are related to the aerospace manufacturing processes such as robotics, additive manufacturing, augmented reality, IoT and simulation. However, the potential of Industry 4.0 key enabling technologies to increase the extremely tight safety levels in aviation operation has not yet been addressed, besides for the consideration on how safety is managed at the production sites. This chapter discusses the potential of Industry 4.0 key enabling technologies to increase the extremely tight safety levels in commercial aviation, and how the upcoming Aviation 4.0 (Industry 4.0 for aviation) might imply a paradigm shift opportunity in safety improvement.

This chapter analyzes, from an evolutionary perspective, the stages of aviation development, from basic VFR flight rules at the Aviation 1.0 up to Aviation 4.0 stage where cyber-physical systems will be designed to assist humans' physically strenuous, unpleasant or dangerous work, to take decisions and to complete tasks autonomously.

The authors establish four stages in the evolution of commercial aviation, which are similar to the four stages in the industrial revolution. These four stages are closely related to the adoption of higher levels of automation on board aircraft. The first evolutionary stage, Aviation 1.0, corresponded to the beginning of the commercial aviation were flight evolved under visual flight rules, following visuals clues and signals, and there was hardly any instrumental aid to help pilots to fly. The second stage, Aviation 2.0 was dominated by the replacement of old mechanism by electric devices. Aviation 3.0, the third stage in the revolution of commercial aviation involved the massive incorporation of electronics in the cockpit. Finally, Aviation 4.0 is concerned with the design of cyber-physical systems (CPS) that are able to assist humans' demanding work by helping them to take decisions and to complete tasks autonomously, and with its integration of cyber-physical components in Future Aviation Information Systems. Cyber-physical systems will make the Aviation 4.0 airframe a digital and smart airplane.

Aviation 4.0 technologies (automation, IOT, artificial intelligence, cognitive computing, big data analytics, digitization, etc) have the potential to generate a paradigm shift in the aviation industry, generating new mechanisms to make it not only more efficient but also safer. Unexplored concepts and approaches to safety start to being discovered by companies and researchers to approach safety from different perspectives with the new tools that Aviation 4.0 makes available. The authors have finally illustrated six case studies of the application of the Aviation 4.0 concept to increase the aviation safety, which is a reality nowadays:

- Automatic flying in predefined situations in a rule-based way.
- Developing a robust aircraft predictive maintenance.
- Cockpit safety cognitive computing aid systems.

- Real-time weather information update.
- Improved search and rescue services especially in the oceanic or remote area.
- Real-time human performance monitoring and alerting based on nonintrusive physiological sensors/signals and contextual information.

However, this revolution is not exempted of defies. Challenges related to information assurance and cyber security include the certification of cyber security requirements for e-Enabled airplanes; the development of anti-tamper avionics hardware and software and the collaboration of industry and governments to address the cyber threat to aviation. There are also very important technological challenges for airplane operations, which are as follows:

- worldwide aeronautical networks interoperability, including signal processing and wireless performance as well as the aircraft interfaces to the Internet;
- verification and validation of the onboard software, how to secure end-to-end entire SW supply processes, the understanding of cyber-physical life-cycle scale;
- improvement of airplane health, control and prognostics by exploiting sensor networks and data fusion, information management and data analytics and, critical real-time data sharing, appropriate end-to-end information exchange, distributed decision-making; and finally
- human-automation interface issues such as visualization, keeping human-in-the-loop and connection between aircraft controls and air traffic systems.

Author details

Rosa Arnaldo Valdés*, Víctor Fernando Gómez Comendador, Alvaro Rodriguez Sanz and Javier Perez Castán

*Address all correspondence to: rosamaria.arnaldo@upm.es

Universidad Politécnica de Madrid, Spain

References

[1] Chen T, Stai H-R. Ubiquitous manufacturing: Current practices, challenges and opportunities. Robotics and computer-integrated manufacturing. 2017;**45**:126-132

[2] Industry 4.0. Challenges and Solutions for the Digital Transformation and Use of Exponential Technologies. Deloitte; 2016

[3] Anonymous. Maintenance in the sense of industry 4.0. KGK-KAUTSCHUK GUMMI KUNSTSTOFFE. 2017;**4**:12-14

[4] Johnsson C. Introduction to Industry 4.0; White Paper LTH. Sweden: LTH, Lund University; 2016

[5] Moreno A, Velez G, Ardanza A. Virtualisation process of a sheet metal punching machine within the industry 4.0 vision. International Journal of Interactive Design and Manufacturing - IJIDEM. 2017;**11**(1):365-373

[6] Notlagh NH, Taleb T, Arouk O. Low-altitude unmanned aerial vehicles-based internet of things services: Comprehensive survey and future perspectives. IEEE Internet of Things Journal;**3**(6):889-922

[7] Wong EY, Wong W. The development of reusable luggage tag with the internet of things for mobile tracking and environmental sustainability. Sustainability. 2017;**91**:1-12

[8] Niehoff S, Siems T, et al. Sustainability aspects of a digitalized industry: A comparative study from China and Germany. International Journal of Precision Engineering and Manufacturing-Green Technology. 2017;**4**(2):227-234

[9] Franco Barbosa G. Aviation manufacturing towards to industry 4.0: A review. In: 4th International Conference and Exhibition on Mechanical & Aerospace Engineering; 2016; Florida. 2016

[10] Zheng W, Wang J, Shen YEbZM, Xing L, Li Z, et al. Research on Design of Aircraft Autonomous Support System Based on IoT. In: Zuo MJ, Xing L, Li Z, et al., editors. Research on Design of Aircraft Autonomous Support System Based on IoT. Chengdu: 2016

[11] Comitz P, Kersch A. Aviation analytics and the Internet of Things. In: IEEE, editor. Integrated Communications Navigation and Surveillance (ICNS); Vermont: 2016

[12] Shah M. Big Data and The Internet of Things. In: Japkowicz and Stefanowski, editors. Big Data Analysis: New algorithms for a new society, Springer Series on Studies in Big Data. 2015

[13] Troiano A, Pasero E. A runway surface monitor using internet of things. Journal of Electrical Engineering-Elektrotechnicky Casopis. 2014;**65**(3)

[14] NSF. Cyber-Physical Systems [Internet]. [Updated: September 17, 2017]. Available from: https://www.nsf.gov/news/special_reports/cyber-physical/

[15] Tomlin CPGSS. Conflict resolution for air traffic management: A study in multiagent hybrid systems. IEEE Transactions Automatic Control. 1998

[16] Mosterman PJ, Zander J. Cyber-physical systems challenges: A needs analysis for collaborating embedded software systems. Software and Systems Modeling. 2016;**15**(1):5-16

[17] Waldinger P. Aviation 4.0. In: Association for the Scientific Development of ATM in Europe, Series of Research Tournaments. Association for the Scientific Development of ATM in Europe: Delft; 2016

Chapter 3

Physiologic Challenges to Pilots of Modern High Performance Aircraft

Douglas Summerfield, David Raslau,
Bruce Johnson and Lawrence Steinkraus

Additional information is available at the end of the chapter

http://dx.doi.org/10.5772/intechopen.75982

Abstract

Fourth generation aircraft, such as the McDonnell Douglas F-15 "Eagle," and the fifth generation platforms that followed, including the Lockheed Martin F-22 "Raptor," pose unique physiological challenges to arguably the most important "system" on the aircraft, the human. Advances in aeronautical engineering have enabled next-generation aircraft to operate well beyond the natural limits of human endurance. Although the demand for unmanned systems is increasing exponentially, continued use of manned aircraft is still desirable within civilian and military operations for various safety and security reasons. With the continued presence of pilots in cockpits, future aircraft designers will require a basic understanding of the unique physiological factors affecting human performance in this domain. Given knowledge of human limitations, strategies for real-time on board monitoring of the "human system" may be employed to increase the safety of the pilot and aircraft.

Keywords: fifth generation aircraft, aerospace medicine, acceleration atelectasis, future of manned flight, human cockpit monitoring

1. Introduction

Aerospace Medicine is a sub-specialty within the broader Occupational Medicine discipline, requiring licensed physicians to complete specialized training to ensure and enhance the health, safety, and performance of individuals exposed to air and space operational settings. Unique hazards in these environments include exposure to microgravity conditions, various radiation sources, multi-axial G-forces, and hypoxic conditions, among others. Aerospace medicine practitioners often further specialize in niche aspects of aerospace medicine, applying

IntechOpen

© 2018 The Author(s). Licensee IntechOpen. This chapter is distributed under the terms of the Creative Commons Attribution License (http://creativecommons.org/licenses/by/3.0), which permits unrestricted use, distribution, and reproduction in any medium, provided the original work is properly cited.

human performance enhancement (HPE) and human systems integration (HSI) tenets to both hyperbaric environments (dive medicine) and hypobaric disciplines (space medicine, high-altitude wilderness medicine). Additionally, some specialize in human dynamics; focusing on highly integrated "man-machine" challenges such as high-performance aircraft and ejection seat emergency escape technologies [1]. As human factors specialists, Aerospace Medicine specialists are ideally suited to participate in the development of new life-support systems in modern aircraft. Unfortunately in recent times, there appears to be a decrease in the medical role during initial design and testing, leaving medical specialists scrambling to make sense of new physiologic ailments after an aircraft has become operational. This has not always been the case. This chapter will address emerging challenges to human health in modern "next generation" fighters as well as ways in which engineers and aerospace medicine professionals may address them.

1.1. Brief history of aerospace medicine

Scientific interest in the effects of human and animal exposure to high-altitude environments can be traced to the observations of Father Jose de Acosta in the late 1590s, more than 300 years before the Wright brothers first flew their *Flyer* among the dunes at Kitty Hawk, North Carolina. Evaluating the Andes high-altitude mountainous environment, Father Acosta surmised the thin "element of air" was causing animals and humans to become ill [2]. Decades later, in 1643, Evangelista Torricelli created the first experimental vacuum. In honor of his accomplishments physical units of pressure were named after him and are known as torrs [3]. Later, Robert Boyle of "Boyle's Law" fame, described the first case of decompression sickness when he observed bubble formation in the eyes of a viper exposed to vacuum environments [4].

Research on the physiologic responses specific to flight took place among early balloonists. On September 19, 1783, brothers Joseph and Etienne Montgolfier sent aloft a duck, a rooster, and a sheep to elucidate hypoxia-like effects on mammals [5]. Unfortunately, shortly thereafter in 1783, researcher Jacques Charles, of Charles' Law fame, endured the first aviation mishap. While piloting a balloon, his passenger unexpectedly exited the basket, thus lightening the balloon and triggering a rapid ascent to an approximate altitude of 10,000′ MSL, causing Charles to experience ear and sinus pain [6]. Even one of the United States' founding fathers, Benjamin Franklin, took an early interest in high altitude research when he asked early balloonist Dr. John Jeffries to take his pulse during a flight. Jeffries noted that his pulse increased from 84 beats per minute (bpm) at sea level, to 92 bpm at an altitude of 5812′ MSL [7].

Regrettably, the first fatalities in aviation occurred on June 15, 1785 when Pierre de Rozier and Pierre Romain unsuccessfully attempted to pilot a balloon across the English Channel. Thirty minutes after takeoff their balloon caught fire, killing both of them. Interestingly, this event also witnessed the first ground casualty, although not as a direct result of impact; De Rozier's fiancée, who witnessed the event, subsequently collapsed and died. Other notable medical incidents occurred during early balloon flights including the first in-flight emergency (IFE) when, on March 7, 1809, John Pierre Blanchard experienced a cardiac arrest, otherwise known as a "heart attack," while piloting his balloon. During the episode, he fell from his balloon from a height of approximately 50′, dying a year later from his related injuries [7].

One of the early grandfathers of Aviation Medicine was French physiologist Paul Bert. He trained in engineering, law, physiology, and medicine. His work included experiments demonstrating oxygen toxicity on animals as well as the therapeutic nature of oxygen in relieving symptoms found in balloonists at altitude. In 1878 he wrote *La Pression Barometrique, Recherches de Physiologie Experimentale,* which was so comprehensive it was later translated into English and used by early aerospace physicians during World War II [4, 8].

The Wright Brothers, with their successful flight on December 17, 1903, ushered in the age of powered heavier-than-air flight. Within 5 years, on September 17, 1908, the first passenger died in an aircraft accident. Orville Wright was demonstrating the latest model of the Wright Flyer to the US Army when the right propeller broke in flight leading to a stall and crash. The passenger on that flight was Army Lieutenant Thomas Selfridge who suffered a skull fracture. Despite attempts at early neurosurgery, Lt Selfridge died 3 h later. Orville himself suffered four broken ribs, a broken thigh, and a dislocated hip. It was felt that Lt Selfridge may have survived had he been wearing head protection and as a direct result of this accident, one of the first human safety measures in aviation was employed: the use of a helmet [9]. Later, after all six of the Wright model C aircraft, which the army had purchased, crashed, further engineering safety measures were taken by the US Army. An investigation board felt that “pusher” type aircraft were more unstable and a crash would result in the engine, which was situated behind the pilot, coming forward and crushing the aviator. Subsequent US military aircraft of the era had engines in the “tractor” configuration [10].

Aside from aircraft design, advances in pilot selection began to make aviation safer. Pre-war aviators often were those found to be unfit for the infantry. Even early in World War 1 “soldiers disqualified for further combat because of battle fatigue, shell shock … became pilots.” The end result was up to 42% of aircraft losses and deaths may be caused by “human factors” [11].

In this setting Dr. Theodore Lyster appeared. Dr. Lyster is considered by many to be the “Father of Aviation Medicine.” An American Army doctor, he arrived in Europe in December of 1917 and spent 3 months studying pilots and conditions affecting their performance. He then returned to the United States and established the Air Service Medical Research Lab on Long Island which had a hypobaric chamber. He developed new medical standards for the US Army Air Corps. In addition it was Dr. Lyster who first introduced the term “flight surgeons” when describing physicians who specialize in caring for aviators, and he was instrumental in ensuring that flight surgeons were part of each flying unit and would deploy with their squadrons rather than being assigned to a separate larger medical command [12]. This practice is still in place today in the United States military where an assigned flight surgeon is an integral part of each squadron.

Despite these new standards set by Dr. Lyster, it seemed as if the medical and aviation communities were in a perpetual battle between standards that were too rigid and aviators who excelled despite physical defects which would have otherwise grounded them. One famous civilian who personified this was Wiley Post who lost his eye in an oil rig accident early in his aviation career. He subsequently went on to become the first pilot to solo around the world, discover the jet stream, and he created the first practical pressurized suit for high altitude flying [13].

Additional examples of highly skilled pilots who did not meet the current medical standards are found in World War 1. One of the most famous American units to fight in the war was the Lafayette Escadrille. These flyers, several of whom obtained the unofficial title of "Ace" after downing five enemy aircraft, were hard worn by their combat service. Many of the members could not meet the Army Air Corps medical standards. Raul Lufbery, the triple Ace, was "over-age, had rheumatism, and could not walk a straight line backwards." Others had poor vision, color blindness, and injured extremities. Eventually these pilots would be granted special approval so their valuable experience would not be lost in a fledgling service so in need of experienced veterans [14].

The controversy continued into World War 2, where one can find any number of stories of aviators "cheating" at their eye exam. This includes Robert Morgan who would later pilot the "Memphis Belle," one of the first B-17s to famously complete all its required missions with its crew intact [15]. After the war Chuck Yeager broke the sound barrier with broken ribs after he fell from his horse, a condition which would have surely temporarily grounded him had he disclosed it to his flight surgeon [16].

In recent years, there has been a shift in the medical community from a restrictive approach, to the perspective of "how do we keep aircrew in the cockpit." An example of this is seen in how NASA decided to return to space the well-known astronaut Story Musgrave after he underwent cataract surgery [17]. A further example is the United States Air Force's lifting of restrictions on pilots who have had laser corrective eye surgery, or the fact that the Federal Aviation Administration (FAA) grants Special Issuances which by 2014 constituted 6% [18] of all certificates. It is with this mindset that the rest of the chapter is devoted, that of keeping the pilot in the cockpit even when technological advances push the limits of human endurance.

1.2. Current training and educational programs of aerospace medical personal

In the United States there is a wide array of education and training among the physicians who work in the realm of aerospace medicine. There are two primary tracks, military and civilian, with each track consisting of a "basic" and "advanced" level. The advanced levels of each track graduate medical specialists competent to become board certified in Aerospace Medicine under the purview of the American Board of Preventive Medicine.

In the military, physicians are referred to as flight surgeons. "Basic" flight surgeons attend their service's specific primary courses, after which they are considered flight rated officers in the U.S. Military. Military flight surgeons have graduated medical school and have completed 1 year of post-graduate training, typically referred to as an intern year. Each branch of the military has different course requirements and duration to obtain "basic" flight surgeon status. The Air Force program consists of three courses of several weeks' duration which include classroom training as well as civilian and military flight experiences. Students are exposed to hypobaric conditions using altitude chambers and those who fly with fighter aircraft are tested in centrifuges. Basic Army flight surgeon training is similar with an emphasis placed on rotary wing aircraft and Blackhawk helicopter simulations. The Navy program is substantially longer and includes phases in which Naval flight surgeon candidates take basic ground school side by side with student Naval and Marine aviators, as well as significantly more "stick time" in both rotary and fixed wing aircraft. Regardless of the branch, all military flight surgeons are expected to fly with their assigned aircraft. In this way trust is built between the flight surgeon and his/her aviator patients, and the rigors of flight can be experienced firsthand, something which cannot be gained from medical books or classroom didactics (**Figure 1**). Physicians in the civilian sector who certify civilian pilots under Federal Aviation Administration (FAA) guidelines are referred to as Aviation Medical Examiners (AMEs). These are physicians trained and designated by the FAA to certify pilots' medical certificates. Physicians can be trained in any specialty with the requirement that they attend a 1-week course with refresher training every 36 months [19].

Advanced training in Aerospace Medicine leading to board certification is significantly longer than civilian or military basic courses and lasts 2–3 years depending on the program. These programs include the Air Force program located at Wright-Patterson Air Force Base, the Army program at Ft. Rucker in Alabama, and the Navy program located at Pensacola, FL. The civilian programs are located at the University of Texas-Medical Branch in Galveston, TX, and the Mayo Clinic in Rochester, MN [20]. All programs require completion of an MD or DO degree and at least 1 year (internship) in clinical care. In addition, most programs require students to obtain a Masters in Public Health during their time spent in training. Although there is naturally some overlap in topics covered, the programs then diverge in their education to focus on the specific needs of the respective military or civilian populations.

Military training focuses on a typically younger, healthier population that works with high-performing aircraft in challenging training and combat situations. Therefore a variety of training is needed including learning the flight environment, broad clinical experience, and even accident investigation. In addition, aerospace trained physicians in the military will also

Figure 1. United States military flight surgeons are mandated to experience the rigors of flight to better understand the physiologic demands placed on their aircrew patients. The rise of single-seat only aircraft are challenging the abilities of these medical professionals to diagnose and treat new ailments seen in modern fighter-type aircraft.

take care of family members of the aircrew, which expands the requisite medical knowledge needed for competent care.

The civilian programs focus on care for the civilian aerospace communities (commercial and private pilots, Air Traffic Control, etc.) and, more rarely, space crew and passengers. As mentioned previously, there has been a shift in medical evaluations from a restrictive approach to developing standards for safe return to flight after adequate medical evaluation and treatment. Therefore, there is a strong emphasis on clinical experience and working closely with the Civil Aerospace Medical Institute (CAMI) division of the FAA. In the case of space crew members or passengers, training is coordinated with NASA, private agencies, and the FAA.

With increasing numbers of single-seat aircraft it is becoming harder for flight surgeons to actively participate in this unique environment (**Figure 2**). Fifth generations aircraft such as the F-35 and F-22 are all strictly single seat aircraft. When these modern aircraft have been associated with unusual and unexpected health concerns for their pilots, it has been more challenging for flight surgeons to diagnose and treat these problems since they cannot experience these conditions for themselves. A small cadre of military pilot-physicians exists, and they have been useful in human-machine risk assessment and mitigation approaches, but most flight surgeons serving high performance aircraft operations are limited in their ability to directly observe flight operations, and this has hampered investigations.

Figure 2. Advanced training in Aerospace Medicine may include further hands on exposure in high performance aircraft. Here, a United States Air Force Resident in Aerospace Medicine undergoes training in the T-6 Texan II aircraft with an instructor pilot during Medical Officer Flight Familiarization Training.

2. Decompression sickness in extreme high altitude aviation

2.1. Current cabin pressure control and mitigation strategies

Due to the altitudes flown by many high performance aircraft, cabin pressurization is important for a number of reasons. These reasons include hypoxia, hyperventilation, extreme temperature changes, as well as expanding trapped gasses and the risk for decompression sickness. Thus the need for protecting the pilot from stressors in the hypobaric environment is imperative.

Two physiologic responses to high altitude, hypoxia and hyperventilation, share similar symptoms and can be confused for one another. This confusion can make it difficult for aerospace medicine professionals as well as aircraft designers to determine the underlying cause of a pilot's symptoms. These symptoms include muscle cramps, paleness, and cold clammy skin. There may also be changes in mental status which can make a pilot's recall of the event difficult.

The interactions between hypoxia and hyperventilation are as follows, with the caveat that hyperventilation can also be brought about by other causes such as heat, air sickness, positive pressure breathing, and psychological stressors such as fear and anxiety. In brief, lower pressures lead to lower partial pressures of oxygen and increase the risk for hypoxia. Hypoxia in turn will increase respiratory rate, thus causing hyperventilation. With the increased respiration rate, blood CO_2 levels fall which in turn change pH. Changes in blood pH and CO_2 levels may lead to many of the symptoms and can negatively impact cerebral blood flow and thus a pilot's ability to process information and make decisions or react to emergencies.

Different strategies are employed to maintain cabin altitude in order to decrease the risks of high altitude and maintain pressures which are more tolerable for humans. These include isobaric, constant differential, and a sealed capsule. Modern airliners utilize an isobaric mode of pressurization, typically after reaching 6000–8000 ft. Any further increase in altitude beyond the predetermined altitude will not result in a corresponding change in cabin pressure. High performance aircraft on the other hand generally employ a constant differential strategy that maintains a constant pressure difference between the atmosphere inside and outside of the cabin. One advantage for military use with the latter system is, by allowing a higher cabin altitude, less catastrophic results may occur from damage incurred during battle, such as a damaged canopy which would lead to a major pressure breach.

Cabin pressure has typically been maintained by diverting high pressure "bleed air" from the aircrafts engines, cooling the air, then instilling it into the cabin. Since air is continually entering the cabin, it also needs to be released via a pressure valve. Thus aircraft cabins are not air tight and a continual supply of fresh air should always be entering the cabin. Unfortunately, flaws in the bleed air system have proven to be fatal. In 2010 an F-22 crashed in Alaska after an overheating engine caused the bleed air environmental control system and the onboard oxygen generating system to shut down [21]. The widow of the pilot filed suit against the major manufactures of the aircraft and eventually settled litigation. Interestingly the lawsuit stated that the system was built "without adequate backup safety measures or proper sensors to warn the pilot if there is a problems" [22]. Of note, the Boeing 787 was designed to maintain cabin pressurization using electrical pumps versus bleed air systems. Whether this approach will be introduced in high performance aircraft remains a question.

2.2. U2 and other airframe exposures

Exposure to high attitude carries with it a significant risk of decompression sickness (DCS). DCS is thought to occur when inert gasses, primarily nitrogen, come out of solution within tissues at low barometric pressure. In aviation, the first reported cases occurred in high altitude balloons in the 1930s. The risk for DCS can be reduced for altitudes of 18,000–43,000 ft by breathing 100% oxygen prior to ascent for short exposure times of 10–30 min. This has the advantage of "washing out" excess nitrogen. Staying on 100% oxygen is required in flight if exposure to these altitudes is continued. Risk factors for DCS include physical activity at altitude, repeated exposures to altitudes greater than 18,000 ft, prior history of DCS, faster rates of ascent, alcohol consumption prior to ascent, persons with higher body fat, and scuba diving prior to flight. There is also some thought that increased age as well as prior long bone injuries put one at risk [23].

DCS is broken down to Type 1 or Type 2. Type 1 is less serious and involves musculoskeletal and skin illness, classically referred to as the "bends" and "creeps" respectively. Type 2 is more serious and involves neurologic and cardiopulmonary disease, the latter which is termed the "chokes." Neurologic symptoms range from dizziness, ringing in the ears, numbness, bladder incontinence, and inability to walk, to seizures, coma, and death [24]. According to research conducted by the Air Force Research Laboratory (AFRL), descent from high altitudes to ground level is an effective treatment for altitude DCS. The majority (95%) of DCS sufferers who were tested at the AFRL were treated with ground level oxygen and saw a rapid decrease in DCS symptoms, while the remaining individuals were given hyperbaric treatment. Descent is an effective treatment method because DCS is caught early through crew monitoring in the controlled environment at the AFRL. During actual operations, it is likely that a higher percent of DCS sufferers would need hyperbaric treatment [25].

It was well known for years within the Flight Surgeon community that some pilots of high altitude aircraft were experiencing signs and symptoms consistent with decompression sickness and these were often underreported. This was particularly true in the Lockheed U2 community. In the past decade, pilot and researchers have been more open and a number of studies have been performed on U2 pilots as well as personnel who work as safety monitors inside altitude chambers. Excellent work by McGuire and colleagues has now been published in a number of studies. These studies report brain changes with repeated exposures to hypobaric normoxia. Specifically U2 pilots and altitude chamber staff have white matter changes which are seen on MRI [26, 27]. These changes have been linked to diffuse axonal injury [28] and those with a higher burden of white matter changes score lower on neurocognitive tests when compared to other pilots [29]. All these changes were linked to hypobaria without hypoxia, thus it seems low pressure itself may be a risk for permanent changes in the brain which can lead to subtle cognitive decline.

Future aircraft may go higher and even skirt the edges of space. Thus careful consideration needs to be given for aircrew protection. U2 pilots are equipped with a pressure suit, however as seen above, neurocognitive changes may already be occurring. One possible explanation may be that most pressure suits do not provide the wearer with a full 1 ATM of pressure, due to the need for a flexible suit, thus the pilot is exposed to hypobaria.

As opposed to chronic repeated exposures to hypobaria, acute exposure to high altitude, such as a rapid decompression, has its own set of problems. During acute exposure aircrew have a limited amount of time to institute measures to save themselves. This is termed "Time of useful consciousness" or TUC for short. Intuitively the higher an aircraft is, the less time is available for a pilot to save himself. By 50,000 ft an aviator only has between 9 and 12 s before they become unconscious (**Table 1**) [30]. Factors such as exercise and smoking will even further decrease that amount of time.

At the altitude of Armstrong's Line, 63,000 ft, pressure is so low that water boils at body temperature (37°C), although due to the strength of skin in practice this typically does not occur at that level. Above that level the process of ebullism may occur, gas bubbles forming within bodily fluids. There have been accidents which have occurred at these altitudes, although not within fighter aircraft. Most recently the crew of the Space Shuttle Columbia died from this phenomenon. Although they were wearing pressure suits, none were able to close and lock their visors prior to incapacitation and some had their gloves off, thus limiting the protection received by the rest of the suit. Surprisingly exposure to these altitudes is survivable if caught and treated quickly enough. In 1966 a spacesuit technician working in a ground based chamber was accidently exposed to the equivalent of 120,000 ft. He is reported to have felt the saliva "boiling" off his tongue as he passed out. He regained consciousness at 14,000 ft as he was repressurized. Amazingly he suffered no neurologic sequelae and did not even require hospitalization. In 1982 another ground based chamber accident exposed an individual to 73,000 ft for what is believed to be 1–3 min. After a 5-h hyperbaric recompression, he survived. More amazingly a 1-year follow-up revealed no neurologic abnormalities [31].

Altitude	Time of useful consciousness
18,000	20–30 min
22,000	10 min
25,000	3–5 min
28,000	2.5–3 min
30,000	1–2 min
35,000	0.5–1 min
40,000	15–20 s
43,000	9–12 s
50,000	9–12 s

Table 1. Time of useful consciousness "TUC" is the amount of time aircrew members have to institute life saving measures before they are incapacitated after acute exposure to the hypobaric conditions of high altitude.

Current fighter aircraft have been reported in the lay press to operate at extreme high altitude, although likely below the level of the Von Karmann line, which is at 47 miles and is the level at which the atmosphere is too thin for aerodynamic surfaces to control the direction of the aircraft. As fighter aircraft go higher and higher, the very real possibility of aircraft operations in the early reaches of space exist. With this in mind, systems which automatically detect cabin or "space suit" pressures may be needed. In the event of a pressure breach, either through accident or combat, there is mere seconds for a pilot to react. The life of the pilot and the aircraft itself may be saved by an "automated" copilot within the aircraft. This would necessitate a computer system taking over should there be a breach in the pressure system and the pilot not responding to an automated computer generated inquiry.

3. Acceleration, G-forces, and countermeasures

3.1. Brief explanation of Gx, Gy, Gz

During flight, acceleration and changes in vectors can cause changes in the amount of gravitational force that is experienced by a pilot. These can be positive (increased force) or negative (decreased force). Pilots feel forces acting on their bodies is in the opposite direction of the actual force vectors. This can be somewhat confusing so convention sets the positive directions of the acceleration forces. Unfortunately, multiple conventions are used which can further add to the confusion [32]. No one convention is better than another. One commonly used convention is the "right hand rule" (**Figure 3**). The pilot holds his right hand and fingers as indicated in the figure and the fingers then point in the positive direction of each force, +Gx in the direction of the pointing finger, +Gz in the direction of the thumb, and +Gy in the direction of the middle finger.

Another way to think about acceleration forces is to think about how the eyes would move in response to the given acceleration [32]. When the pilot is experiencing +Gx it is referred to as "eyeballs in," and −Gx is referred to as "eyeballs out." One of the advantages of this convention is that it leaves little room for error since the experience of the pilot is exactly what is described.

3.2. Human limitations

There are limits to how much acceleration force the human body can tolerate. Tolerance depends on several factors including the magnitude of the acceleration force applied, direction, and duration as well as subject factors including age, weight, height, and blood pressure [33, 34]. Tolerance is somewhat subject to training, and there is wide variability between individuals. In addition, other factors can affect tolerance of G-forces including medical conditions, medications, and use of other substances (such as alcohol).

Despite the high number of variables that contribute to tolerance, one of the most important factors remains the direction of the acceleration force. Each axis has its own specific limitations in the positive and negative directions. For example, humans can tolerate >10 G in the +Gx direction while only about 2–3 G in the −Gz direction. This is due to the fact that there are

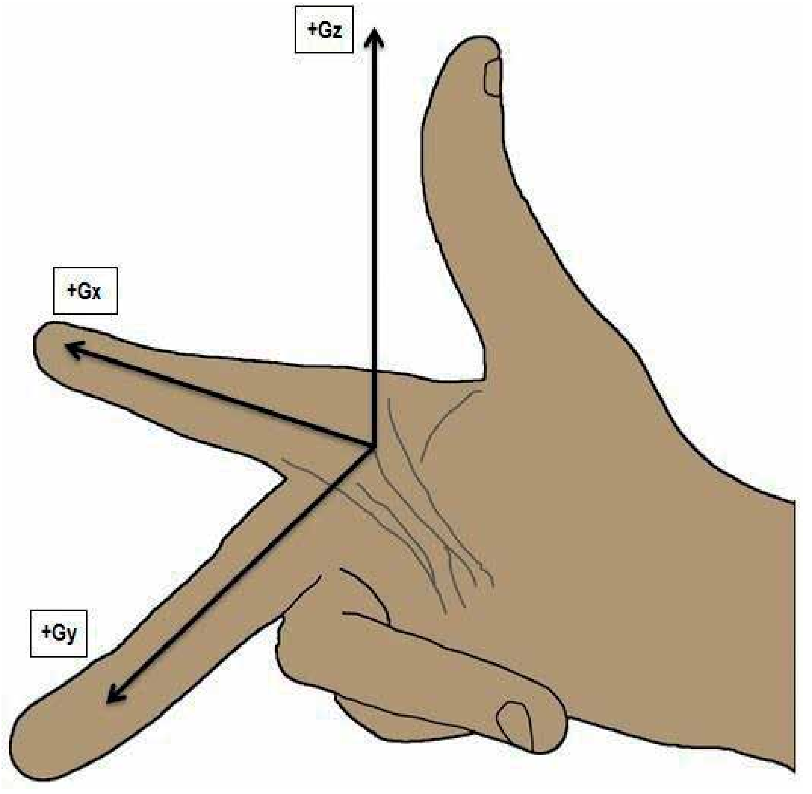

Figure 3. The right-hand rule. This figure demonstrates the "right hand rule" convention of G-force direction. The pilot holds his right hand and fingers as indicated in the figure and the fingers then point in the positive direction of each force, +Gx in the direction of the pointing finger, +Gz in the direction of the thumb, and +Gy in the direction of the middle finger. As an example, when a pilot experiences +Gx (which is pushing forward) the sensation felt is that of being pushed into the seatback (drawing acknowledgement Iaswarya Ganapathira, D.O.).

physiologic compensatory mechanisms to increase blood flow to the brain but none to prevent excess blood flow.

There are also different terms used to describe various aspects of G-force intolerance. "Gray-out" describes when vision loses hue and vision appears to be more gray. Tunnel vision describes the progressive loss of peripheral vision. "Blackout" is the complete loss of vision while still maintaining consciousness. "A-LOC" stands for "Almost Loss of Consciousness" and "G-LOC" describes a G-force induced loss of consciousness. "Red-out" describes the reddening of vision from negative G-forces which drive the lower eyelid into the field of vision.

3.3. Current countermeasures

Excessive G-forces may result in a sufficient reduction in blood flow to the brain such that G-LOC ensues. G-LOC can be and have been catastrophic and countermeasures have been developed to try and prevent G-LOC.

Physiologic countermeasures include physical training to improve overall fitness, cardiovascular function, positive pressure breathing for protection against G, and the anti-G straining maneuver [35]. These measures employ physical techniques to improve G tolerance. They can be helpful but have limitations as well.

Mechanical countermeasures revolve around the anti-G suit, positive pressure breathing (PPB), and (theoretically) cockpit design. During World War 2, Dr. Earl Wood was working as part of a laboratory team located at the Mayo Clinic charged with finding ways to improve G-force tolerance of pilots (**Figure 4**). Their work led to the development of the anti-G suit. The conventional "suit" is worn like trousers and, with the aid of a weighted valve, inflates when G force is above 2G. This compresses the lower extremities and abdomen using air bladders promoting return of blood back to the heart and head (**Figure 5**). Newer versions of the anti-G suit add higher G-force protection [36]. PPB works by assisting pilots to maintain oxygenation when G forces and constricting chest garments work to restrict chest movement and lung expansion. Wood et al. recommended changes in cockpit design to maximize G tolerance, recommending prone position as the best solution. An attempt to improve G tolerance by canting the seat backward was done in the F-16, and while appearing logical, was not supported by centrifuge testing. All recent high performance jets now place the pilot upright in the cockpit [37].

As more advanced aircraft have been created which test the boundaries of human tolerance, there has been ongoing interest in developing more advanced anti-G systems. One of these is the Advanced Technology Anti-G Suit which confers effortless protection up to +9 Gz and consistent protection up to +12 Gz with additional straining [38].

A new challenge for pilots in fifth generation aircraft is multi-axis acceleration wherein thrust vectors may be variable allowing increased aircraft maneuverability. G forces in these aircraft are likely to be multi-axis versus simple Gz or Gx forces. Effects on pilots remain investigational, with research ongoing in specially constructed centrifuge facilities [39].

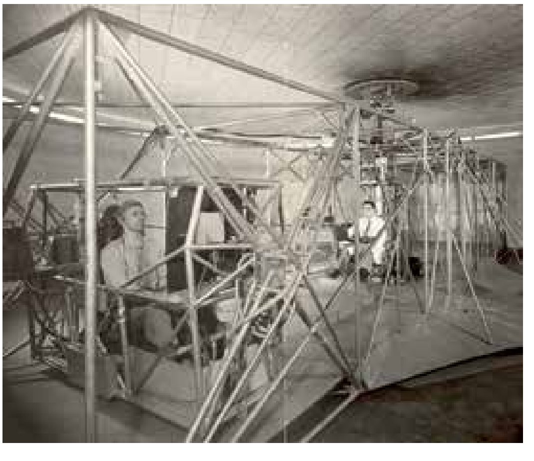

Figure 4. Dr. Earl Wood (on the right, wearing a white lab coat) is working in the Mayo Clinic centrifuge laboratory to help develop the G-suit.

http://dx.doi.org/10.5772/intechopen.75982

Figure 5. Dr. Earl Wood is standing next to a display case exhibiting the G-suit he helped develop.

4. Acceleration atelectasis

4.1. Alveolar collapse under acceleration and increased oxygenation concentrations

Acceleration atelectasis is an old condition which has become new again. In healthy lung tissue, the smallest unit in the lung is the alveoli. These tiny sac-like structures are delicate and as described by John West in west's lung zones, blood flow through each region of the lung is influenced by gravity. Typically at the end of expiration the pressure in the alveoli is within 2 mmHg of atmospheric pressure. Current thinking of the pathophysiology of acceleration atelectasis is, under conditions of high G forces and high increased fraction of inhaled oxygen, alveolar collapse occurs in the dependent regions of the lung. This collapse can cause chest pain, shortness of breath, and cough [40].

Tacker and colleagues found that atelectasis, alveolar collapse, can be exacerbated by three conditions: the use of 100% oxygen, +Gz, and even by the anti-G suit itself. In their study Tacker exposed 12 subjects to aerial combat maneuvers under a range of forces spanning from 4.5 to 9 G. They found that above 5 G up to 50% of the pulmonary airways were in some way distorted and even closed. This distortion of the alveoli led to a reduction of up to 20% of the vital capacity, the greatest volume of air which can be exhaled after taking the largest possible breath, in the research subjects. The G-suit itself may further exacerbate the problem by elevating the diaphragm, thus decreasing vital capacity through extrinsic compression of pulmonary space [40].

The use of high inspired oxygen percentages requires explanation. Prolonged high levels of oxygen have long been shown to be detrimental to ICU patients or those undergoing anesthesia, likely due to another condition known as absorption atelectasis. Absorption atelectasis reflects the fact that the human respiratory system is so efficient at absorbing oxygen that it can be taken up more rapidly across the alveolar-capillary membrane than what can be delivered to the alveoli during normal pressure respiration [40, 41]. When the United States Air Force developed the On Board Oxygen Generation System (OBOGS), Haswell and colleagues found a significant reduction in vital capacity at inspired oxygen concentrations above 70%. Haswell noted "Given the unpleasant nature of the respiratory symptoms and the absence of knowledge about the effects of repeated development of acceleration atelectasis, limiting oxygen concentration … seems worthy of consideration" [42].

This reduced vital capacity could be alleviated by a cough, deep breath, or anti-G straining maneuver. Both Tacker and Haswell found the reduction in vital capacity could be relieved by positive pressure breathing at 30 mmHg. It is worth noting that standard patient ventilator practices in modern intensive care units limit the use of inspiratory pressures to "plateau pressures" less than 30 mmHg [40, 42]. As discussed later in this chapter, there is a need for continued research into this "old" concept of acceleration atelectasis.

5. Musculoskeletal injury and impact of life support systems and aircrew flight equipment

5.1. Neck injuries

Neck pain has been reported in up to 97% of all pilots [43]. Unfortunately the incidence varies tremendously as does its association with the type of airframe. A systematic review and meta-analysis of 20 articles conducted by Shiri and colleagues found no difference in the prevalence of neck pain, cervical disc degeneration, low back pain, or lumbar disc degeneration when they compared fighter pilots to helicopter or transport/cargo pilots. In the subset of high-performance pilots, they did however find that those who were exposed to higher G-forces were at a higher risk of neck pain, as were those that spent time looking over their shoulder in the "check-six" position [44].

There is disagreement regarding whether different models of high performance aircraft cause more neck pain. Some reports indicate as little as 18.9% prevalence of neck pain in F-16 pilots [45], while Verde and colleagues found an incidence of 48.6% in a small group of 35 F-16 pilots. This group had a much higher incidence than Eurofighter Typhoon pilots who only had a reported incidence of 5.7% in age matched controls. Verde speculated that the increased neck pain was secondary to the semi-recumbent seat position of the F-16 [46].

In F-15s, Chumbley et al. found a unique subset of neck pain and speculated it was due to cockpit layout. Similar to work done by Shiri, Chumbley found differences which may be attributed to the "check six" position. As part of their work which involved treating neck pain, Chumbley checked cervical range of motion and found rightward going cervical rotation improved after traction sessions. They speculated that F-15 pilots preferentially turned to the left due to cockpit layout, as the throttle is on the left side and slightly behind the stick which is placed center. In terms of treatment, Chumbley found that neck pain was statistically alleviated, when compared to controls, after cervical traction was applied to pilots after flying. The amount of cervical traction applied was roughly 10% of the pilot's body weight [47].

In their literature review Chumbley and colleagues list proposed etiologies of neck pain experienced by high performance "fighter" pilots. These include high +Gz, rotation of the neck under +Gz (check-six position), fatigue, frequency of endurance training and physical exercise, and prolonged flexed posturing. From an equipment point of view, increasing the weight on the helmet may also place a pilot at risk. This is seen with the addition of night vision goggles as well as with the use of the Joint Helmet Mounted Cueing System (JHMCS). Countermeasures for the neck pain which have included strengthening and stretching exercises, spinal manipulation, and physical therapy have demonstrated mixed results, with spinal manipulation showing some promise [47].

5.2. Ejection seat injuries

In the early part of aviation history, pilots who found themselves in damaged or malfunctioning airframes had no real options to avoid impending death. Later, use of parachutes became common (though in WW 1 some services opted not to provide parachutes as they were worried pilots might leave their aircraft too readily) The challenge these pilots faced was how to escape the cockpit safely, either climbing or falling out when the situation would allow. In the jet age, one of the greatest advances in aircraft safety has been the ejection seat. Ejection seats are powered by rockets to expel the occupant from the cabin and away from the failing aircraft. Since time is of the essence in these situations, the rocket-propelled seat will violently eject the occupant. One common ejection seat, the ACES II, will reach 9-12G during the process which is significantly lower than other seats which could reach more than 18G [48].

Ejections seats, which were designed to save lives, have indeed accomplished that task. One manufacturer, Martin-Baker, keeps a tally of the pilots who have survived because of their ejection seats. In early 2017, their count was over 7500 lives saved because of their ejection seats [49]. However the use of ejection seats comes with the risk for potential bodily harm. Although injury is much more desirable than the alternative, efforts are still needed to focus on the prevention of injury to the extent that is possible.

One study looked at USAF injuries related to the use of ejection seats from 1981 to 1995. It was noted that injuries typically occurred in the head, neck, cervical spine, thorax, thoracolumbar spine, ribs, pelvis, and the upper and lower extremities. Injury rates were noted to be between 2 and 25%. Moreover, fatality was noted to occur in 0–11% [50]. Injuries can range from minor back strain that resolves on its own to as severe as a leg broken in 5 places. Continued work is needed in this area to preserve life and minimize injury.

5.3. Back injuries due to G-forces

Neck pain, as detailed above, and associated injuries are very common in aviation. Although the neck is the most susceptible area of the spine, G force-related injuries can occur along any aspect of the spinal column. Even in the controlled environment of centrifuge training, it is possible to sustain injury to the spinal column. One study assessed 991 subjects who were undergoing high G training in the centrifuge and found that 2.3% of them suffered from an acute spinal injury [51]. In at least one case, the G-force from centrifuge training (which reaches up to +9Gx) was enough to cause a fracture in the lower spine in an otherwise healthy 32-year-old Flight Surgeon [52].

The addition of the highly stressful flight combat environment and more powerful aircraft increases the risk of injury. When the Japanese Air Self Defense Force introduced the F-15 Eagle into their fleet, there was a significant increase in musculoskeletal injuries related to the spine with 90% of surveyed pilots reporting pain [53]. There is some ongoing debate in the literature regarding how important these types of injuries may be and what impact they might have on the long-term health of subjects. One systematic review, which included 20 individual studies evaluating spine injury in pilots, found no statistically significant difference in back pain between pilots and non-flying personnel [44]. One possible interpretation of these conflicting pieces of information would be that ejection seats are indeed getting safer, and we are seeing improvement in back injuries. We would hope to see similar improvements in other areas as well.

6. Environmental factors

6.1. Noise

Measured in decibels (dB), sound is an auditory sensation in response to acoustic stimuli. Subjectively, any undesired sound is considered noise. Since the advent of heavier-than-air flying machines, both sound and noise remain inherent elements of manned aircraft operations, and modern high performance aircraft operations are no exception. While the majority of unwanted sound is generated by the power plant, several other sources of operationally innate noises include vibrations and sounds secondary to weapons system deployment. Regardless of the source, sound and noise exposures that exceed permissible exposure limits, as published by the Occupational Safety and Health Administration and the National Institute for Occupational Safety and Health, have the potential to result in injury.

Effects of noise on overall health have been studied. Deleterious effects have been seen in hearing, ringing in the ears, cognitive performance, and possibly even hypertension [54–57]. Although engineering can potentially mitigate much of external noises, there remains a need to relay critical information to the aircrew in the form of voice communication. This will place limits on the amount of noise mitigation that can be engineered into the system.

It is also important to distinguish between sound and noise exposures that aircrew experience while operating within a closed cockpit/flight deck versus the external environment experienced when approaching their aircraft while other aircraft operations are ongoing. As an example, the F-35A Lightning II is a fifth-generation fighter which has a measured aircraft ground noise level of 145 dB when the throttle is set to “Military Power” and 149 dB when set to “Afterburner” [58]. Obviously, the relative attenuation of the closed cockpit environment serves as an effective adjunct to triple hearing protection utilizing traditional earplugs in conjunction with the physical protection of a helmet and the acoustic protection of active noise-canceling technology. However, with the threshold of pain occurring around 120–

140 dB [59], it is reasonable to conclude that sound and noise considerations will remain critical in aircraft design and deployment as long as humans intend to work in or around them.

6.2. Vibration

Another factor that aircrew deal with is the vibrational forces created by the powerful machines at their command. One study looked at the effect of vibration on the ability to perform complex tasks and found that certain vibration patterns reduced cognitive performance [60]. Another study found that excess vibration can cause temporary hearing loss and impaired vision [61]. Another group studied vibrational effects and found that it reduced motion control [62]. In addition, airborne vibrations were found to cause symptoms of nausea, coughing, headache, and fatigue [63]. One of the most reported effects is that of back pain. It appears to affect rotary-wing aircrew more than fixed-wing aircrew as the former experience much more vibrational forces than the latter. Long term these effects may lead to chronic problems [64, 65]. Any of these adverse health effects could jeopardize safety and warrant continued efforts at mitigation.

6.3. Thermal stress

Another potential physiologic stressor to pilots is thermal stress. Humans are most comfortable in ambient temperatures ranging between 15 and 30°C [66]. There is the potential for cockpit temperatures to rise significantly above this comfortable range. Reports from pilots in the 1960s state that on hot days sitting on the steaming runway, temperatures in the cockpit climbed to nearly 60°C [67]. Even in 2015, it is still possible for cockpit temperatures to exceed 45°C. Sweating can unfortunately exacerbate the problem by increasing cockpit humidity and creating a greenhouse effect. The latest cooling systems try to adjust for humidity as well [68]. Additionally, systems malfunction and a pilot can become stuck inside the cockpit with the canopy down as occurred in an F-22 in 2006. The F-22 canopy system failed and was unable to be fixed or opened manually. Over the next 5 h, crews worked to cut off the canopy from the aircraft, during which cockpit temperatures rose throughout the extraction [69].

Thermal stress has significant implications aside from simple discomfort. Pilots report increased fatigue levels and decreased G-force tolerance under high thermal stress [70]. This can negatively impact performance and pose significant risk. Although efforts have been made to minimize the impact of thermal stress and improvements have been made, there remains ongoing concern in this area.

6.4. Toxins/fumes

Since the early days of aviation, toxins have impacted the health of the both the aviator and the ground crew. Perhaps the most well-known of these is the reports of castor oil's effects on WW1 pilots. Although difficult to verify, castor oil *may* have been the cause of significant diarrhea in combat pilots. It is believed to have been thrown off by the engine and subsequently inhaled or ingested by the pilot sitting directly behind the engine [71].

One WW1 era toxin which has been confirmed is tetrachloroethane. For the ground crew, and those building WW1 aircraft, tetrachloroethane was found to cause significant adverse health effects, including death. It was used ubiquitously by all major combatants during the conflict as the varnish, also known as "dope," to cover the fabric of the plane's wings. Unfortunately reports after the war linked this toxin to at least 70 illnesses and 12 deaths. Many of the symptoms appear to have been hepatic/liver failure with transmission of the toxin through both inhalation and transdermal routes [72–75].

Although not next generation fighter type aircraft, there has been work within the commercial airline sector on this topic. In modern commercial aircraft, multiple volatile liquids exist in the various systems of an aircraft. Because air is circulated around the engine to be heated and pressurized, it is possible for cabin air to become contaminated with various fumes. There have been multiple reports from aircrew and passengers alike complaining of this occurrence. Symptoms associated with contaminated air include fatigue, dizziness, and anxiety [76]. More concerning is the increased rates of cancers, cataracts, and motor neuron diseases that may be associated with exposures, although at doses higher than would be expected in cabin air contamination events [77]. Despite the numerous concerns, investigations into cabin air quality of civilian airliners have repeatedly shown that the air quality on commercial flights is very good and there is no consistent exposure that should affect the general public. As Bagshaw, referencing cabin air quality, concludes in his article, "Aviation medical professionals throughout the world continue to monitor the scientific evidence and remain receptive to objective peer-reviewed evidence" [78].

In military aircraft, hydrazine is a specific example of a toxin which is of medical concern. Present in some current 4th generation fighters, such as the General Dynamics F-16 "Fighting Falcon," it is used to power the emergency power unit (EPU) and is added to other rocket and jet fuels. Routes of exposure include inhalation, ingestions, or even absorption through the skin and eyes. Animal studies have shown liver damage and the potential for cancer formation [79, 80]. Exposure in humans can cause skin burns, dizziness, lethargy, vomiting, contact dermatitis, and conjunctivitis. Long term exposure has been reported in one case to lead to pulmonary edema, intestinal hemorrhage, liver necrosis, and death [81]. Due to the continued need for this potentially deadly material, the United States Air Force has instituted a multidisciplinary approach to dealing with this hazard. From the medical side, a surveillance program looking at labs such as baseline liver function is conducted on those potentially exposed. Furthermore the workers themselves are educated in minimizing exposure, safe handling when necessary, as well as the correct response to an accidental spill [82].

6.5. Radiation exposure: both natural and manmade

Radiation exposure is an area of ongoing concern. Typically our atmosphere protects us from most harmful waves from our sun or other sources of such as cosmic radiation. While operating at high altitude, there is less atmosphere to protect the aircrew and the job of protection falls to the windshield and skin of the aircraft, which may not be as adequate as hoped. One study estimated that pilots who fly for 56 min at 30,000 ft are exposed to the same amount of UV-A radiation as someone sitting in a tanning bed for 20 min [83]. However, as in other areas this is controversial. For example, one study found no measurable increase in UVA/UVB/UVC radiation in flights at cruising altitude. Interestingly, UVA levels inside the cabins were actually lower than on the ground based upon the collected data [84]. Pilots have been shown to be at increased risk of other cancers including brain cancer and Hodgkin's disease [85]. However again, there is controversy regarding if cosmic radiation is solely responsible for this increased risk of cancer [86]. Another complicating factor is that sometimes there appears to be an increased risk of developing a cancer with no associated increase in the risk of death [87]. This raises questions of how clinically significant an increase in risk might be, whether a risk even exists, and whether it is important to address or not.

Design of aircraft cannot fully eliminate the exposure to higher levels of cosmic radiation during flight. Flight practices have changed allowing pilots to retire at a later age, thereby allowing a higher lifetime exposure. As such, we must continue to monitor the impact this has on pilot health and find ways to mitigate any adverse effects.

7. Current issues and controversies

7.1. Hypoxic-like incidents in modern jet fighters

As described above acceleration atelectasis is a pulmonary condition which was well known and described in the literature by the generation of Aerospace physicians active during the 1950s and 1960s. This "corporate knowledge" seems to have faded. A literature review conducted in 2017 on this topic in a major data base revealed only 15 relevant articles. Of these one article was speculative, one was historical, three were review articles, thus leaving only 10 articles. Furthermore these articles began in 1963 and ended with the last basic research article written by Tacker in 1987. Not included in this search was excellent work performed by Dr. J. Ernsting which was published in the 1960s. His research recommended up to 40% nitrogen for cabin altitude levels of 25,000 ft [88].

This older research has been revisited due to respiratory complaints reported in new fifth and some older fourth generation fighters. Most notably pilots of the United States Air Force's F-22 Raptor, a fifth generation stealth fighter, began to experience "hypoxia-like" symptoms in 2008. Due to the rising number of incidents and the subsequent fatal crash of an F-22 in November 2010, the F-22 fleet was subsequently grounded twice in 2011 [89]. After considerable effort to investigate possible causes, the problem was thought to be fixed after researchers came to believe the cause was effects of the upper body pressure vests on pilots' G-suits and narrow oxygen hoses [90, 91]. While the F-22 fleet was returned to flying, unfortunately problems have continued with "hypoxia-like" symptoms now seen in other aircraft. This has led to the grounding of both the newer F-35 Joint Strike Fighter as well as the United States Navy's T-45 jet trainer, an older aircraft [92, 93]. Problems have also been cited with the U.S. Navy's F-18 Super Hornet and the RAF Tornado, both of which use the OBOGS to supply oxygen to pilots.

Although the root cause of these symptoms was initially felt by some, including the United States Air Force Scientific Advisory Board, to be due to hypoxia, some experts have suggested an alternative explanation including acceleration atelectasis. Indeed some of the symptoms reported by pilots, (cough, shortness of breath, chest pain) are very reminiscent of acceleration atelectasis [94, 95]. Other possible explanations put forth by renowned pulmonary researcher John West include reduced cerebral blood flow due to high +Gz, hyperventilation, CO2 retention from increased work of breathing, decompression sickness, or even toxic fumes [94]. Regardless of the cause, both West and the USAF Scientific Advisory Board (SAB) have called for in-flight monitoring and warning systems.

7.2. Studying cognition in hypoxia

Loss of cabin pressure can occur quickly in rapid depressurizations or, more insidiously and dangerously, with gradual or slow depressurizations. United States military aircrews are taught to learn their individual symptoms by experiencing them first hand in hypobaric "altitude" chambers. When aircrew experience these symptoms, they are trained to react by going on 100% oxygen ("gang load" their regulators) to ensure their oxygen equipment is working correctly and when in doubt, to transfer to stored oxygen ("pulling the green apple"), descend to less than 10,000 ft, and communicate with the ground by declaring an in-flight emergency.

Due to the number of decompression sickness (DCS) incidents seen during such training, many military and civilian groups are now transitioning away from hypobaric hypoxia training in the altitude chamber toward normobaric hypoxia training which uses mixed gas to allow aircrew to experience hypoxic symptoms. While initially safer (fewer DCS events), this approach may lead to the potential that the symptoms experienced by the pilot in training may be different if those symptoms are due to hyperventilation during low pressure as opposed to hypoxia.

Additionally the concept of time of useful consciousness "TUC" is a somewhat crude and individually variable measure to describe the neurocognitive function of an aircrew exposed to high altitude. Researchers at Mayo Clinic are currently working on ways to detect subtle degradation due to hypoxia using other physiologic parameters, such as eye tracking, transcranial Doppler, ECG R-R' variability, EEG, etc. [96] (**Figure 6**). After laboratory data are analyzed, future work will be needed to incorporate these findings into an aircraft in order to best support and alert a pilot to the possibility of slow cognitive decline way before TUC becomes an issue.

7.3. Studying cognition in high workload

Pilot workload in flying high performance aircraft has increased largely due to accelerating informational flows. Cockpits, while seemingly simpler in appearance, present multiple and layered details on the flying environment, navigational elements, mission specific data, and systems integration awareness items. Military pilots often are in contact with multiple ground, space, and aviation related resources. Warning systems often overlap or produce simultaneous alarms. Net-centric warfare allows for vast quantities of information to be readily available at the finger-tips of modern airmen. There may be a time in the near future when this information

Figure 6. Ongoing experiments at Mayo Clinic evaluating the physiologic responses which may be early signs of cognitive degradation during exposure to normobaric hypoxia.

is employed in such a way that a pilot in a manned aircraft would control a "squadron" of unmanned/drone aircraft. The primary processing center for these information flows is the pilot's brain. In this setting it would be very advantageous to know the mental state of the pilot in terms of cognitive overload. Thus if one pilot was showing signs of cognitive decline, from any source whether it is due to overload or a physiologic even such as hypoxia, control of unmanned resources could automatically be passed to another manned system, or mitigation algorithms could assist the pilot to reduce overload or stressors.

There are a number of physiologic measures which have been shown to reveal a subject's current cognitive load. These may prove useful if studied to define envelopes wherein performance predictions may be calculated and applied. While incapacitation is critical to detect, it would be better to detect degradation in the early phases to avoid incapacitation. Many of the monitoring and mitigation approaches have limitations which need to be understood if employed.

Relatively recent advances in eye tracking have linked subjects' cognitive loads to pupil diameter in a variety of tasks such as sports and driving [97, 98]. Not only has pupil diameter shown to be a useful measurement, but so too does the amount of eye movement and even blink rates [99]. Because the eye muscles are the most sensitive muscle to oxygen depletion, eye tracking may also be a good indicator of hypoxia [100]. Limitations of eye tracking may include difficulty detecting pupils during G-forces that may pull eyelids down thus obscuring the pupils. Also, due to the continual movement of a pilots head, eye tracking may be better performed by a device which moves with head motions. This would suggest a likely location for an eye tracker to be on/in a pilot's helmet [101–105].

Aside from eye tracking, heart rate variability has been demonstrated by some to also correlate with physiologic reserve and potential cognitive stress. Each peak on an EKG is called the "R" wave. By measuring the distance between successive "R" waves, it has been found that the R to R interval continually changes. In fact there is more variability in young healthy individuals than those who are older and sicker. The latter have a more "fixed" interval with less variation. This decrease in variability has also been seen during increased cognitive load [106]. Further work would need to see if this can be practically performed regularly in flight.

Cognitive function measuring devices have included measurements of ocular saccades (rapid eye movements which change the point of eye fixation from one point to the next), EEG monitors, pupil size, and even eye blink velocity [103]. Practical use of these devices has been limited in the cockpit due to the technical issues such as difficulty of applying electrodes in the first case, bulkiness and reliability of devices and difficulty positioning sensors due to space limitations or changes in signaling under acceleration forces. Much more study is needed in this field but it is clear that in-flight monitoring will be an element in future manned flight.

8. Conclusion and the future of manned flight

An in-flight monitoring and warning system may be one way to safely keep "pilots in the cockpit." One theoretical concept would be to monitor various physiologic parameters of the pilot. If physiologic parameters were found to fall outside of normal references ranges, one could conceive that an auto-pilot would be activated and either takeover flying the aircraft completely or "ask" the pilot if it could assist. This could occur until the pilot was able to regain control, or it may need to "safely" eject the pilot and self-land the aircraft.

This may seem to be very futuristic, but similar technologies already exist. Although not directly measuring the pilot's physiology, newer block F-16s have begun to incorporate an auto-ground collision avoidance system (Auto-GCAS) as of 2014. This system compares the predicted flight path against the known terrain and institutes an automatic recovery if the two are predicted to touch. In an aircraft known to have increased risk for G-LOC, especially in new pilots, this system has already been credited with saving the lives of four pilots and their aircraft as of 2016. Future work is aimed at creating an Automatic Integrated Collision Avoidance System, which will also help prevent mid-air collisions [107].

Actual monitoring of a pilot's movement has been in place in combat aircraft for years via infrared beams. The Army's AH-64 Apache helicopter uses infrared sensors on either side of the pilot/gunner to detect movement of the pilot's head. This system is called the Integrated Helmet and Display Sight System, better known as IHADSS. It allows a computer to slew the aircraft's gun to the pilot's monocle such that wherever the pilot/gunner is looking, the gun is pointed [108]. With a monocle already in place, one could also imagine an eye tracker looking back at the pilot to monitor the pilot's cognitive load and gradually assist in taking the workload off the pilot. It could do this by taking over critical systems of the aircraft, such as flying to avoid collision. Additionally it may even actively change displays in the cockpit in a manner which would help redirect the pilot's attention.

There are experimental research aircraft which currently employ some of these physiologic monitoring devices. At the University of Iowa's Operator Performance Laboratory, two Delfin L-29 jet aircraft are equipped with eye tracking devices as well as ECG monitors. Lead by Dr. Thomas Schnell, researchers there have developed software termed Cognitive Avionics Tool Set (CATS). This software imports on board data from physiologic sensors of the pilot in order to quantify human cognitive workload. Data analyzed include ECG, EEG, and eye tracking to name a few. Using CATS, operators on the ground can increase or decrease training scenarios based on how "overwhelmed" a subject is [109]. Further experimentation may be required to determine if cognitive decline due to hypoxia would also be detected by this system.

Currently the Royal Air Force (RAF) at the RAF Center of Aviation Medicine (CAM) also has jet aircraft with human physiologic monitoring capabilities. These aircraft are specially modified BAE Hawk T1 Mk1 aircraft, a platform similar to the U.S. Navy's T-45 Goshawk training aircraft. As a tandem aircraft, these jets are suited for research as the safety pilot-in-command operates the vehicle from the front seat while research subjects ride in the aft seat. Unfortunately, RAF CAM and its specially modified aircraft is scheduled to close by 2020 [110].

With all that has been discovered to date, there is also much more to be learned. By understanding current problems faced by pilots of 5th generation aircraft improved monitoring can take place. Monitoring can increase understanding of physiologic changes which occur as we push aircraft design into areas never before experienced by humans. By coupling monitors to automated systems which can "take over" when a pilot becomes incapacitated, human endurance can continue to be pushed to the limits in a safe manner.

Acknowledgements

The authors would like to thank Ms. Janice Duncan for help in compiling the manuscript and Iaswarya Ganapathira, D.O. for her illustrating skills.

This manuscript was funded in part by the Department of Defense, Mayo Clinic, and Dr. Paul Magelli.

Conflict of interest

The authors have no conflict of interests to declare.

Author details

Douglas Summerfield[1], David Raslau[2], Bruce Johnson[3,4] and Lawrence Steinkraus[5]*

*Address all correspondence to: steinkraus.lawrence@mayo.edu

1 Critical Care and Aerospace Medicine, Mercy Medical Center, Mason City, IA, United States

2 Aerospace and Internal Medicine, Rochester, MN, United States

3 Human Integrative and Environmental Physiology Laboratory, Mayo Clinic, Rochester, MN, United States

4 Cardiovascular Diseases, Preventive, Occupational, and Aerospace Medicine, Mayo Clinic, Rochester, MN, United States

5 Division of Preventive, Occupational, and Aerospace Medicine, Mayo Clinic, Rochester, MN, United States

References

[1] Welcome to the Aerospace Medical Association [Internet]. Available from: https://www.asma.org/for-the-public [Accessed: Oct 1, 2017]

[2] De Acosta J. Natural and Moral History of the East and West Indies 1604. Whitefish, Montana: Kessinger Publishing; 2003

[3] Hack M, Vesel Z, Gariboldi L, Renshaw S, Ihara S, Fazlıoğlu İ, et al. Torricelli, Evangelista. Biographical Encyclopedia of Astronomers. New York, NY: Springer; 2007. pp. 1146-1147. DOI: 10.1007/978-0-387-30400-7_1390

[4] Acott C. A brief history of diving and decompression illness. South Pacific Underwater Medicine Society. 1999;**29**(2):98-109

[5] Davis JR, Johnson R, Stepanek J, Fogarty JA. Fundamentals of Aerospace Medicine. Philadelphia, Pennsylvania: Lippincott Williams & Wilkins; 2008. p. 2

[6] The First Solo Flight: Jean-François Pilâtre de Rozier and the Marquis d'Arlandes [Internet]. 2009 Air & Space Magazine. Available from: https://www.airspacemag.com/daily-planet/the-first-solo-flight-53893576/ [Accessed: Oct 1, 2017]

[7] Davis J. Fundamentals of Aerospace Medicine. Philadelphia, Pennsylvania: Lippincott Williams & Wilkins; 2002

[8] Bert P. Barometric Pressure: Researches in Experimental Physiology. Columbus, OH: College Book Company; 1943

[9] Sept. 17, 1908: First Airplane Passenger Death [Internet]. Available from: https://www.wired.com/2010/09/0917selfridge-first-us-air-fatality/ [Accessed: Oct 2, 2017]

[10] Loening G. Takeoff into Greatness: How American Aviation Grew So Big So Fast. New York: Putnam; 1968

[11] Jones D. Flying and dying in WWI: British aircrew losses and the origins of US military aviation medicine. Aviation, Space, and Environmental Medicine. 2008;**79**(2):139-146

[12] Davis H. Generals in Khaki. Raleigh, North Carolina: Pentland Press Inc.; 1998

[13] Elshatory Y, Siatkowski R. Wiley Post, around the world with no stereopsis. Survey of Ophthalmology. 2014;**59**(3):365-372. DOI: 10.1016/j.survophthal.2013.08.001

[14] Miller R. Like a Thunderbolt: The Lafayette Escadrille and the Advent of American Pursuit in World War I. Washington, D.C.: Air Force History and Museums Program; 2007

[15] Morgan R, Powers R. The Man Who Flew the Memphis Belle: Memoir of a WWII Bomber Pilot. New York: Penguin; 2001

[16] Yeager C, Janos L. Yeager: An Autobiography. New York: Bantam Books; 1986

[17] Mader T, Koch D, Manuel K, Gibson C, Effenhauser R, Musgrave S. Stability of vision during space flight in an astronaut with bilateral intraocular lenses. American Journal of Ophthalmology. 1999;**127**(3):341-343

[18] Skaggs V, Norris A. Aerospace Medical Certification Statistical Handbook. Oklahoma City, Oklahoma: FAA Civil Aerospace Medical Institute, Administration FA; 2014. 2014 December 2015. Report No.: DOT/FAA/AM-15/22

[19] Aviation Medical Examiner (AME) Training Federal Aviation Administration [Internet]. Available from: https://www.faa.gov/other_visit/aviation_industry/designees_delegations/designee_types/ame/ametraining/ [Accessed: Oct 1, 2017]

[20] Residency Programs and Related Courses [Internet]. Available from: https://www.asma.org/about-asma/careers/aerospace-medicine/residency-programs-related-courses [Accessed: Oct 13, 2017]

[21] Forces PA. Aircraft Accident Investigation: F-22A T/N 06-4125 JOINT BASE ELMENDORF-RICHARDSON ALASKA 16 NOVEMBER 2010. In: Force USA, editor

[22] Settlement Reached in Haney F-22 Crash Lawsuit [Internet]. 2012. Available from: https://www.flightglobal.com/news/articles/settlement-reached-in-haney-f-22-crash-lawsuit-375445/ [Accessed: Oct 1, 2017]

[23] Brown J, Antunano M. Altitude-Induced Decompression Sickness. Okalahoma City, Oklahoma: Federal Aviation Administration, Civil Aerospace Medical Institute Aeromedical Education Division. AM-400-95/2; 1995

[24] Signs and Symptoms of DCS [Internet]. Divers Alert Network. Available from: https://www.diversalertnetwork.org/health/decompression/Signs-and-symptoms-of-DCS [Accessed: Oct 1, 2017]

[25] Krause K, Pilmanis A. The effectiveness of ground level oxygen treatment for altitude decompression sickness in human research subjects. Aviation, Space, and Environmental Medicine. 2000;**71**(2):115-118

[26] McGuire S, Sherman P, Profenna L, Grogan P, Sladky J, Brown A, et al. White matter hyperintensities on MRI in high-altitude U-2 pilots. Neurology. 2013;**81**(8):729-735. DOI: 10.1212/WNL.0b013e3182a1ab12

[27] McGuire S, Sherman P, Wijtenburg S, Rowland L, Grogan P, Sladky J, et al. White matter hyperintensities and hypobaric exposure. Annals of Neurology. 2014;**76**(5):719-726. DOI: 10.1002/ana.24264

[28] McGuire S, Boone G, Sherman P, Tate D, Wood J, Patel B, et al. White matter integrity in high-altitude pilots exposed to hypobaria. Aerospace Medicine and Human Performance. 2016;**87**(12):983-988. DOI: 10.3357/AMHP.4585.2016

[29] McGuire S, Tate D, Wood J, Sladky J, McDonald K, Sherman P, et al. Lower neurocognitive function in U-2 pilots: Relationship to white matter hyperintensities. Neurology. 2014; **83**(7):638-645. DOI: 10.1212/WNL.0000000000000694

[30] Federal Aviation Administration. Introduction to Aviation Physiology. [Internet]. p. 3-3. Available from: https://www.faa.gov/pilots/training/airman_education/media/IntroAviationPhys.pdf [Accessed: Oct 23, 2017]

[31] National Aeronautics and Space Administration. Loss of Signal: Aeromedical Lessons Learned from the STS-107 Columbia Space Shuttle Mishap [Internet]. 2014. Available from: https://www.asma.org/asma/media/asma/Travel-Publications/NASA%20Shuttle/SP-2014-616.pdf [Accessed: Oct 22, 2017]

[32] Gillingham K, Wolfe J. Spatial Orientation in Flight. Texas: USAF School of Aerospace Medicine. Brooks Air Force Base; 1986. pp. 11-12

[33] Voge V. Comparison of several G-tolerance measuring methods at various seatback angles. Aviation, Space, and Environmental Medicine. 1978;**49**(2):377-383

[34] Burton R. Mathematical models for predicting G-duration tolerances. Aviation, Space, and Environmental Medicine. 2000;**71**(10):981-990

[35] Protection Against the 'G' [Internet]. Aviation Medicine: Aerospace Medicine. Available from: http://www.avmed.in/2012/06/protection-against-the-g/ [Accessed: Oct 1, 2017]

[36] Wood E. Development of anti-G suits and their limitations. Aviation, Space, and Environmental Medicine. 1987;**58**(7):699-706

[37] Wood E, Code C, Baldes E. Partial supination versus Gz protection. Aviation, Space, and Environmental Medicine. 1990;**61**(9):850-858

[38] Burns J, Ivan D, Stern C, Patterson J, Johnson P, Drew W, et al. Protection to +12 Gz. Aviation, Space, and Environmental Medicine. 2001;**72**(5):413-421

[39] Albery W. Acceleration in other axes affects +Gz tolerance: Dynamic centrifuge simulation of agile flight. Aviation, Space, and Environmental Medicine. 2004;**75**(1):1-6

[40] Tacker W Jr, Balldin U, Burton R, Glaister D, Gillingham K, Mercer J. Induction and prevention of acceleration atelectasis. Aviation, Space, and Environmental Medicine. 1987;**58**(1):69-75

[41] O'Brien J. Absorption atelectasis: Incidence and clinical implications. American Association of Nurse Anesthetists. 2013;**81**(3):205

[42] Haswell M, Tacker W Jr, Balldin U, Burton R. Influence of inspired oxygen concentration on acceleration atelectasis. Aviation, Space, and Environmental Medicine. 1986;**57**(5):432-437

[43] Lange B, Torp-Svendsen J, Toft P. Neck pain among fighter pilots after the introduction of the JHMCS helmet and NVG in their environment. Aviation, Space, and Environmental Medicine. 2011;**82**(5):559-563

[44] Shiri R, Frilander H, Sainio M, Karvala K, Sovelius R, Vehmas T, et al. Cervical and lumbar pain and radiological degeneration among fighter pilots: A systematic review and meta-analysis. Occupational and Environmental Medicine. 2015;**72**(2):145-150. DOI: 10.1136/oemed-2014-102268

[45] De Loose V, Van den Oord M, Burnotte F, Van Tiggelen D, Stevens V, Cagnie B, et al. Individual, work, and flight-related issues in F-16 pilots reporting neck pain. Aviation, Space, and Environmental Medicine. 2008;**79**(8):779-783

[46] Verde P, Trivelloni P, Angelino G, Morgagni F, Tomao E. Neck pain in F-16 vs. typhoon fighter pilots. Aerospace Medicine and Human Performance. 2015;**86**(4):402-406. DOI: 10.3357/AMHP.4063.2015

[47] Chumbley E, O'Hair N, Stolfi A, Lienesch C, McEachen J, Wright B. Home cervical traction to reduce neck pain in fighter pilots. Aerospace Medicine and Human Performance. 2016;**87**(12):1010-1015. DOI: 10.3357/AMHP.4625.2016

[48] Four Ways Upgraded Ejection Seat Modifications Can Keep Our Pilots Safe [Internet]. The Washington Post. 2009. Available from: http://www.washingtonpost.com/sf/brand-connect/wp/enterprise/four-ways-upgraded-ejection-seat-modifications-can-keep-our-pilots-safe/ [Accessed: Oct 1, 2017]

[49] Ejection Seat Market Is Changing Pace [Internet]. 2017. Available from: http://aviationweek.com/air-combat-safety/ejection-seat-market-changing-pace [Accessed: Oct 12, 2017]

[50] Collins R, McCarthy G, Kaleps I, Knox F. Review of major injuries and fatalities in USAF ejections, 1981-1995. Biomedical Sciences Instrumentation. 1997;**33**:350-353

[51] Kang K-W, Shin YH, Kang S. Acute spinal injury after centrifuge training in asymptomatic fighter pilots. Aerospace Medicine and Human Performance. 2015;**86**(4):386-391. DOI: 10.3357/AMHP.4062.2015

[52] Puderbaugh M. A report of transverse process fractures secondary to the centrifuge in a healthy aviator. Aerospace Medicine and Human Performance. 2016;**87**(7):655-658. DOI: 10.3357/AMHP.4541.2016

[53] Kikukawa A, Tachibana S, Yagura S. G-related musculoskeletal spine symptoms in Japan Air Self Defense Force F-15 pilots. Aviation, Space, and Environmental Medicine. 1995; **66**(3):269-272

[54] Lindgren T, Wieslander G, Dammström B, Norbäck D. Tinnitus among airline pilots: Prevalence and effects of age, flight experience, and other noise. Aviation, Space, and Environmental Medicine. 2009;**80**(2):112-116

[55] Elmenhorst E, Elmenhorst D, Wenzel J, Quehl J, Mueller U, Maass H, et al. Effects of nocturnal aircraft noise on cognitive performance in the following morning: Dose–response relationships in laboratory and field. International Archives of Occupational and Environmental Health. 2010;**83**(7):743-751. DOI: 10.1007/s00420-010-0515-5

[56] Rhee M, Kim H, Roh S, Kim H, Kwon H. The effects of chronic exposure to aircraft noise on the prevalence of hypertension. Hypertension Research. 2008;**31**(4):641-647. DOI: 10.1291/hypres.31.641

[57] Rajguru R. Military aircrew and noise-induced hearing loss: Prevention and management. Aviation, Space, and Environmental Medicine. 2013;**84**(12):1268-1276

[58] Department of Defense Office F-JP. F-35 Noise Measurement Executive Summary. [Internet] 2014. Available from: http://www.jsf.mil/news/docs/20141031_F-35_Noise_Executive_Summary.pdf [Accessed: Oct 13, 2017]

[59] Newman E. Speech and hearing. In: Gray D, editor. American Institute of Physics Handbook. 3rd ed. New York: McGraw-Hill Book Co., Inc; 1957. pp. 3-155

[60] Harris C, Shoenberger R. Combined effects of broadband noise and complex waveform vibration on cognitive performance. Aviation, Space, and Environmental Medicine. 1980; **51**(1):1-5

[61] Griffin M. A comparison of standardized methods for predicting the hazards of whole-body vibration and repeated shocks. Journal of Sound and Vibration. 1998;**215**(4):883-914

[62] El Falou W, Duchêne J, Grabisch M, Hewson D, Langeron Y, Lino F. Evaluation of driver discomfort during long-duration car driving. Applied Ergonomics. 2003;**34**(3):249-255

[63] Smith S. Characterizing the effects of airborne vibration on human body vibration response. Aviation, Space, and Environmental Medicine. 2002;**73**(1):36-45

[64] Bongers P, Hulshof C, DIjkstra L, Boshuizen H, Groenhout H, Valken E. Back pain and exposure to whole body vibration in helicopter pilots. Ergonomics. 1990;**33**(8):1007-1026

[65] Gaydos S. Low back pain: Considerations for rotary-wing aircrew. Aviation, Space, and Environmental Medicine. 2012;**83**(9):879-889

[66] Orlady W, Orlady M. Human Factors in Multi-Crew Flight Operations. Aldershot, England: Ashgate; 1999

[67] Door R. Air Combat: A History of Fighter Pilots. New York, NY: The Berkley Publishing Group; 2006

[68] Shetty J, Lawson C, Shahneh A. Simulation for temperature control of a military aircraft cockpit to avoid pilot's thermal stress. CEAS Aeronautical Journal. 2015;**6**(2):319-333

[69] Robinson TSgt 1st MXG/MXQ. Department of Defense Langley Air Force Base Briefing: F-22 03-041 Stuck Canopy [Internet]. 2006. Available from: http://www.spaceref.com/news/viewsr.html?pid=20396 [Accessed: Oct 1, 2017]

[70] Nunneley S, Flick C. Heat stress in the A-10 cockpit: Flights over desert. Aviation, Space, and Environmental Medicine. 1981;**52**(9):513-516

[71] Lee A. Open Cockpit. London, UK: Grub Street; 2012

[72] Centers for Disease Control and Prevention Criteria for a Recommended Standard: Occupational Exposure to 1,1,2,2-Tetrachloroethane [Internet]. 1976. The National Institute for Occupational Safety and Health. Available from: https://www.cdc.gov/niosh/nioshtic-2/00068146.html [Accessed: Oct 1, 2017]

[73] Heffter K. Industrial poisoning by tetrachloroethane. Vierteljahresschr Gerichtl Med Oeff Sanitaetswes. 1914;**48**:109-114

[74] Willcox W, Spilsbury B, Legge T. An outbreak of toxic jaundice of a new type amongst aeroplane workers—Its clinical and toxicological aspect. Transactions of the Medical Society of London. 1915;**38**:129-156

[75] Browning E. Toxicity and Metabolism of Industrial Solvents. 1st ed. New York: Elsevier; 1965

[76] Harrison V, RS M. An emerging concern: Toxic fumes in airplane cabins. Cortex. 2016;**74**: 297-302. DOI: 10.1016/j.cortex.2015.11.014

[77] Nicholas J, Butler G, Lackland D, Tessier G, Mohr L Jr, Hoel D. Health among commercial airline pilots. Aviation, Space, and Environmental Medicine. 2001;**72**(9):821-826

[78] Bagshaw M. Health Effects of Contaminants in Aircraft Cabin Air: Summary Report v2.7. [Internet]. 2014. Available from: https://www.asma.org/asma/media/asma/Travel-Publications/Air-contamination-health-effects-report-v2-7-Apr2014.pdf [Accessed: Oct 1, 2017]

[79] Hussain S, Frazier J. Cellular toxicity of hydrazine in primary rat hepatocytes. Toxicological Sciences. 2002;**69**(2):424-432

[80] Latendresse J, Marit G, Vernot E, Haun C, Flemming C. Oncogenic potential of inhaled hydrazine in the nose of rats and hamsters after 1 or 10 1-hr exposures. Toxicological Sciences. 1995;**27**(1):33-48

[81] National Institute for Occupational Safety and Health Guideline for Hydrazine: Potential Human Carcinogen [Internet]. 1988. Available from: https://www.cdc.gov/niosh/docs/81-123/pdfs/0329.pdf [Accessed: Oct 1, 2017]

[82] Christensen W. Industrial hygiene and the F-16 air combat fighter. Aviation, Space, and Environmental Medicine. 1981;**52**(3):147-149

[83] Sanlorenzo M, Wehner M, Linos E, Kornak J, Kainz W, Posch C, et al. The risk of melanoma in airline pilots and cabin crew: A meta-analysis. JAMA Dermatology. 2015; **151**(1):51-58. DOI: 10.1001/jamadermatol.2014.1077

[84] Cadilhac P, Bouton M, Cantegril M, Cardines C, Gisquet A, Kaufman N, et al. In-flight ultraviolet radiation on commercial airplanes. Aerospace Medicine and Human Performance. 2017;**88**(10):947-951. DOI: 10.3357/AMHP.4852.2017

[85] Band P, Spinelli J, Ng V, Moody J, Gallagher R. Mortality and cancer incidence in a cohort of commercial airline pilots. Aviation, Space, and Environmental Medicine. 1990;**61**(4): 299-302

[86] Di Trolio R, Di Lorenzo G, Fumo B, Ascierto P. Cosmic radiation and cancer: Is there a link? Future Oncology. 2015;**11**(7):1123-1135. DOI: 10.2217/fon.15.29

[87] Raslau D, Dabrh A, Moain A, Summerfield D, Wang Z, Steinkraus L, et al. Prostate cancer in pilots. Aerospace Medicine and Human Performance. 2016;**87**(6):565-570. DOI: 10.3357/AMHP.4453.2016

[88] Ernsting J. The ideal relationship between inspired oxygen concentration and cabin altitude. Aerospace Medicine. 1963;**34**:991

[89] United States Airforce Scientific Advisory Board: Aircraft Oxygen Generation SAB-TR-11-04 [Internet]. 2012. Available from: http://www.airforcemag.com/DocumentFile/Documents/2012/AFSAB_Oxygen_020112.pdf [Accessed: Oct 1, 2017]

[90] Bumiller E. Oxygen Problems on F-22 Elude the Air Force's Fixes. The New York Times. July 2, 2012

[91] Ferran L. F-22 Raptor, America's Most Expensive Fighter, Grounded Again After Oxygen Scare [Internet]. 2011. Available from: http://abcnews.go.com/Blotter/22-raptor-grounded-oxygen-scare/story?id=14802706 [Accessed: Oct 1, 2017]

[92] Fox News. US Navy grounds T-45 training fleet following Fox News Report [Internet]. 2017. Available from: http://www.foxnews.com/politics/2017/04/05/us-navy-grounds-t-45-training-jet-fleet-following-fox-news-report.html [Accessed: Oct 1, 2017]

[93] CNN. F-35 fighters grounded indefinitely over oxygen issues [Internet]. 2017. Available from: http://www.cnn.com/2017/06/12/politics/f-35-grounded-indefinitely-oxygen-problems/index.html [Accessed: Oct 1, 2017]

[94] West J. A strategy for in-flight measurements of physiology of pilots of high-performance fighter aircraft. Journal of Applied Physiology. 2013;**115**(1):145-149. DOI: 10.1152/japplphysiol.00094.2013

[95] Flottman LCJ. Acceleration Atelectasis in the F-22 [Internet]. 2013. Chicago, IL: Aerospace Medicine Conference. Available from: http://asmameeting.org/asma2013_mp/pdfs/asma2013_present_510.pdf [Accessed: Oct 1, 2017]

[96] McEachen J, Issa A, Marck J, Steinkraus L, Johnson B. Real-time effects of normobaric, transient near-anoxia on performance. Aerospace Medicine and Human Performance. 2015;**86**(2):76-81. DOI: 10.3357/AMHP.4041.2015

[97] Hosseini S, Bruno J, Baker J, Gundran A, Harbott L, Gerdes J, et al. Neural, physiological, and behavioral correlates of visuomotor cognitive load. Scientific Reports. 2017;**7**(1): e8866. DOI: 10.1038/s41598-017-07897-z

[98] Alnæs D, Sneve M, Espeseth T, Endestad T, van de Pavert S, Laeng B. Pupil size signals mental effort deployed during multiple object tracking and predicts brain activity in the dorsal attention network and the locus coeruleus. Journal of Vision. 2014;**14**(4):1-1

[99] Stepanek J, Pradhan G, Cocco D, Smith B, Bartlett J, Studer M, et al. Acute hypoxic hypoxia and isocapnic hypoxia effects on oculometric features. Aviation, Space, and Environmental Medicine. 2014;**85**(7):700-707

[100] Van Liere E, Stickney J. Hypoxia. Chicago and London: The University of Chicago Press; 1963

[101] Marshall S. Identifying cognitive state from eye metrics. Aviation, Space, and Environmental Medicine. 2007;**78**(5):B165-B175

[102] Albery W. Multisensory cueing for enhancing orientation information during flight. Aviation, Space, and Environmental Medicine. 2007;**78**(5):B186-B190

[103] Thomas M, Russo M. Neurocognitive monitors: Toward the prevention of cognitive performance decrements and catastrophic failures in the operational environment. Aviation, Space, and Environmental Medicine. 2007;**78**(5):B144-B152

[104] Tsai Y, Viirre E, Strychacz C, Chase B, Jung T. Task performance and eye activity: Predicting behavior relating to cognitive workload. Aviation, Space, and Environmental Medicine. 2007;**78**(5):B176-B185

[105] Connolly D. Spatial contrast sensitivity at twilight: Luminance, monocularity, and oxygenation. Aviation, Space, and Environmental Medicine. 2010;**81**(5):475-483

[106] Ernst G. Heart-rate variability—More than heart beats? Frontiers in Public Health. 2017; **5**:240. DOI: 10.3389/fpubh.2017.00240

[107] Auto-GCAS Saves Unconscious F-16 Pilot-Declassified USAF Footage [Internet]. 2016. Aviation Week & Space Technology. Available from: http://aviationweek.com/air-combat-safety/auto-gcas-saves-unconscious-f-16-pilot-declassified-usaf-footage [Accessed: Oct 2, 2017]

[108] Chait R, Lyons J, Long D. Critical Technology Events in the Development of the Apache Helicopter: Project *Hindsight* Revisited. Washington, DC: Center for Technology and National Security Policy; 2006. 27 p

[109] Cognitive Avionics Toll Set (CATS) Software [Internet]. Available from: https://hfdata.opl.uiowa.edu/opl/?q=cats [Accessed: Oct 1, 2017]

[110] BBC News. Ministry of Defence to sell 13 sites for 17,000 homes [Internet]. 2016. Available from: http://www.bbc.com/news/uk-37287613 [Accessed: Oct 23, 2017]

Section 2

Design

Chapter 4

Aircraft Gas-Turbine Engine with Coolant Injection for Effective Thrust Augmentation as Controlled Object

Alexandru Nicolae Tudosie

Additional information is available at the end of the chapter

http://dx.doi.org/10.5772/intechopen.76856

Abstract

This chapter deals with some intensive methods regarding aircraft gas-turbine-engine performance enhancement, which are suitable alternatives for the most common temporarily thrust increasing method—the afterburning. Coolant injection method, into the compressor or into the combustor, realizes the desired thrust increase for a short period, when the flight conditions or other aircraft necessities require this. Both methods were studied from aircraft engine's point of view, considering it as controlled object. New engine's mathematical model was built up, following the thermo- and gas-dynamics changes and some quality studies were performed, based on engine's time behavior simulations; some control options and schemes were also studied. Quantitative studies were based on the model of an existing turbo-engine; mathematical model's coefficients are both experimentally determined (in the Aerospace Engineering Division labs) as well as estimated based on graphic-analytic methods. This approach and the presented methods could be applied to any other turbo-jet engine and used even in the stage of pre-design of a new engine, to estimate its stability and quality.

Keywords: gas turbine, control, cooling, injection, volatile, engine, compressor, combustor, fuel, thrust augmentation, step response

1. Introduction

Aircraft engine's performance enhancement is one of nowadays most studied issues. Since conventional methods (in terms of temperature and/or overall pressure ratio growth) have failed due to lack of suitable materials, some alternative methods have been sought. Among these, a few methods for temporarily engine thrust increase were designed and tested, such as the coolant injection (into the compressor or into the combustor), which is one of the most

IntechOpen

© 2018 The Author(s). Licensee IntechOpen. This chapter is distributed under the terms of the Creative Commons Attribution License (http://creativecommons.org/licenses/by/3.0), which permits unrestricted use, distribution, and reproduction in any medium, provided the original work is properly cited.

effective, viable and reliable alternatives to the already classical afterburning. In fact, nowadays most efficient thrust augmentation method is the afterburning, but it is also the most expensive because of its significantly increased fuel consumption; moreover, in case of afterburning implementation, it is compulsory for the engine to have an afterburning chamber with variable area exhaust nozzle, heat insulation and noise dampers, as well as a fuel injection equipment with suitable control system(s), which implies important design and manufacturing issues and, consequently, additional costs.

In order to maximize the gas-turbine engine's thrust, especially of a turbojet, it is necessary that the energy of the hot gases evacuated through the exhaust nozzle is as high as possible [1, 2]. As far as the available energy of the hot gases leaving engine's combustion chamber is divided between the turbine and the exhaust nozzle, there are two methods to increase the nozzle fraction: (1) additional injection of fuel behind the turbine and burning it in a special combustion chamber, above-mentioned method called "afterburning" (which, obviously, is an extensive method); (2) the reduction of turbine power for the nozzle's benefit, by reducing the power required for the compressor, in fact reducing the air compression evolution mechanical work (which is an intensive method).

The second method may have two ways to be accomplished by (1) reducing compressor's specific mechanical work, but keeping the same pressure ratio value, or (2) reducing the compressor air mass flow rate, but keeping the same burned gases mass flow rate, as presented in [1].

The first way involves the conversion of the adiabatic air compression evolution into a polytropic one, by cooling the air flow through the engine's compressor. As long as for an aircraft engine, it is quite impossible to use an external air cooler (because of its prohibited dimension and volume), the only effective cooling method is the volatile coolant injection into the air flow, which realizes the heat extraction during its mixing with the air and vaporization.

The second way involves the injection of a coolant into the rear part of the engine's combustor, which, in order to keep constant the turbine's burned gases mass flow rate, leads to a decrease of the compressor's air mass flow rate and simultaneously, for a constant rotational speed, to the compressor's final pressure increase and to the compression mechanical work decrease.

Both the abovementioned ways are meant to increase the enthalpy drop of engine's exhaust nozzle, by reducing gases enthalpy drop into the turbine, as a consequence of a reduced necessity of mechanical work of the engine's compressor. Thus, the methods for temporarily engine thrust augmentation are based on both previously described operating modes.

2. Gas-turbine jet engine mathematical model

Equations which describe jet engine's operation are: the motion equation of the spool compressor and turbine rotor, characteristics chart(s) of the compressor and of the turbine, the heat balance equation of engine's combustor and, eventually, the mass flow rate equation, as presented in [3–5].

http://dx.doi.org/10.5772/intechopen.76856

- Rotor motion equation [4]:

$$\frac{\pi J}{30}\frac{\mathrm{d}n}{\mathrm{d}t} = \mathrm{M_T} - \mathrm{M_C}, \tag{1}$$

- Compressor characteristic [2]:

$$\frac{i_2^*}{i_1^*} = \frac{T_2^*}{T_1^*} = 1 + \frac{\left(\pi_c^*\right)^{\frac{\chi-1}{\chi}} - 1}{\eta_C}, \tag{2}$$

- Turbine characteristic [2]:

$$\frac{i_4^*}{i_3^*} = \frac{T_4^*}{T_3^*} = 1 - \frac{\left(\delta_T^*\right)^{\frac{\chi_g-1}{\chi_g}} - 1}{\eta_T^*\left(\delta_T^*\right)^{\frac{\chi_g-1}{\chi_g}}}, \tag{3}$$

- Combustor equation [1, 6]:

$$\dot{m}_a c_{p_a} T_2^* + \dot{m}_c(i_c + \zeta_{CA} P_C) = \dot{m}_g c_{p_g} T_3^*, \tag{4}$$

- Mass flow rate equation [1, 2, 4]:

$$\dot{m}_g = \dot{m}_a - \dot{m}_{pr} + \dot{m}_c, \tag{5}$$

where J is turbo-compressor rotor inertia moment, $n-$ engine (rotational) speed, $\mathrm{M_C}, \mathrm{M_T}-$ compressor and turbine torques, T_1^*, T_2^*- total temperature in front/behind the compressor, T_3^*- combustor total temperature (in front of the turbine), T_4^*- total temperature behind the turbine, π_c^*- compressor pressure ratio, δ_T^*- turbine pressure ratio, χ, χ_g- adiabatic exponents (for air and burned gases), η_C, η_T^*- compressor and turbine efficiency, $c_{p_g}, c_{p_a}-$ specific isobar heat of burned gases and air (assumed as equal), $\zeta_{CA}-$ burning process' perfection coefficient, P_c- fuel's chemical energy, $\dot{m}_g-$ burned gases mass flow rate, $\dot{m}_a-$ air mass flow rate, $\dot{m}_{pr}-$ bleed air mass flow rate (extracted from the compressor for aircraft's and/or engine's necessities), $\dot{m}_c-$ injected fuel mass flow rate, A_{5-} nozzle's effective exhaust area.

All of them are nonlinear equations, which makes them extremely difficult to be used for study. In fact, in abovementioned equations, all parameters X are multivariable ($X = X(u_i)$, $i = \overline{1, N}$), such as $\dot{m}_a = \dot{m}_a\left(n, p_2^*\right)$, $\dot{m}_g = \dot{m}_g\left(A_5, p_4^*, T_4^*\right)$, $\mathrm{M_C} = \mathrm{M_C}\left(\dot{m}_a, n, \pi_c^*\right)$, $\mathrm{M_T} = \mathrm{M_T}\left(\dot{m}_g, n, T_3^*, \delta_T^*\right)$, … and so on. Consequently, one has to linearize them (around a steady state regime or operation point, using the finite difference method) and bring them to a dimensionless form (by suitable dividing), then apply the Laplace transformation (with null initial conditions) in order to obtain the useful form of the mathematical model and the possibility of the transfer function describing, as it was done in [3, 5]. So, any parameter noted as X, may be mathematically described as follows:

$$X = X_0 + \frac{\Delta X}{1!} + \frac{(\Delta X)^2}{2!} + \ldots + \frac{(\Delta X)^n}{n!}, \tag{6}$$

where X_0 is the value of X for a steady state regime (assumed as completely determined), ΔX is the static error (or the linear deviation). Assuming a small value of ΔX, terms containing $(\Delta X)^r, r \geq 2$, should be neglected. Consequently, the above-presented equation system has a new form, becoming a linear one. Moreover, dividing favorable $\frac{\Delta X}{X_0}$, the above mathematical model can be transformed into a dimensionless-one. In order to obtain the dimensionless linearized mathematical model, one has to apply the Laplace transformation.

For the first model's equation, Eq. (1), one observe that turbine and compressor torques may be expressed as.

$$\mathrm{M}_T = \mathrm{M}_{T_0} + \Delta\mathrm{M}_T, \mathrm{M}_C = \mathrm{M}_{C_0} + \Delta\mathrm{M}_C, \tag{7}$$

while

$$\Delta\mathrm{M}_T = \left(\frac{\partial \mathrm{M}_T}{\partial T_3^*}\right)_0 \Delta T_3^* + \left(\frac{\partial \mathrm{M}_T}{\partial n}\right)_0 \Delta n + \left(\frac{\partial \mathrm{M}_T}{\partial \delta_T^*}\right)_0 \Delta\delta_T^* + \left(\frac{\partial \mathrm{M}_T}{\partial \dot{m}_g}\right)_0 \Delta\dot{m}_g, \tag{8}$$

and

$$\Delta\mathrm{M}_C = \left(\frac{\partial \mathrm{M}_C}{\partial n}\right)_0 \Delta n + \left(\frac{\partial \mathrm{M}_C}{\partial \pi_c^*}\right)_0 \Delta\pi_c^* + \left(\frac{\partial \mathrm{M}_T}{\partial \dot{m}_a}\right)_0 \Delta\dot{m}_a, \tag{9}$$

where $0-$ index refers to the steady-state regime. Meanwhile, compressor and turbine pressure ratios are expressed as $\pi_c^* = \frac{p_2^*}{p_1^*}$, $\delta_T^* = \frac{p_3^*}{p_4^*}$ and $p_3^* = \sigma_{CA}^* p_2^*$, so, for constant flight regimes (when $p_1^* = \text{const.}$) their linear deviation become.

$$\Delta\pi_c^* = \left(\frac{\partial \pi_c^*}{\partial p_2^*}\right)_0 \Delta p_2^* = \frac{\Delta p_2^*}{p_{1_0}^*}, \Delta\delta_T^* = \left(\frac{\partial \delta_T^*}{\partial p_3^*}\right)_0 \Delta p_3^* + \left(\frac{\partial \delta_T^*}{\partial p_4^*}\right)_0 \Delta p_4^* = \frac{\Delta p_3^*}{p_{4_0}^*} - \frac{\delta_{T_0}^*}{p_{4_0}^*}\Delta p_4^*, p_{3_0}^* = \sigma_{CA}^* p_{2_0}^*, \tag{10}$$

Substituting in Eq. (1) M_T and M_C with their expressions (Eqs. (8) and (9)), then eliminating the terms corresponding to the steady-state regime (identically satisfied), one obtains

$$\frac{\pi J n_0}{30\mathrm{M}_{C_0}} \frac{\mathrm{d}}{\mathrm{d}t}\left(\frac{\Delta n}{n_0}\right) + \frac{n_0}{\mathrm{M}_{C_0}}\left[\left(\frac{\partial \mathrm{M}_C}{\partial n}\right)_0 - \left(\frac{\partial \mathrm{M}_T}{\partial n}\right)_0 + \left(\frac{\partial \mathrm{M}_C}{\partial \dot{m}_a}\right)_0 \left(\frac{\partial \dot{m}_a}{\partial n}\right)_0\right]\frac{\Delta n}{n_0} = \frac{T_{3_0}^*}{\mathrm{M}_{T_0}}\left[\left(\frac{\partial \mathrm{M}_T}{\partial T_3^*}\right)_0 + \left(\frac{\partial \mathrm{M}_T}{\partial \dot{m}_g}\right)_0 \left(\frac{\partial \dot{m}_g}{\partial T_3^*}\right)_0\right]\cdot$$
$$\cdot\frac{\Delta T_3^*}{T_{3_0}^*} + \frac{p_{2_0}^*}{\mathrm{M}_{T_0}}\left[\sigma_{CA}^*\left(\frac{\partial \mathrm{M}_T}{\partial \dot{m}_g}\right)_0 \left(\frac{\partial \dot{m}_g}{\partial p_3^*}\right)_0 + \frac{\sigma_{CA}^*}{p_{4_0}^*}\left(\frac{\partial \mathrm{M}_T}{\partial \delta_T^*}\right)_0 - \frac{1}{p_{1_0}^*}\left(\frac{\partial \mathrm{M}_C}{\partial \dot{m}_a}\right)_0 \left(\frac{\partial \dot{m}_a}{\partial \pi_c^*}\right)_0 - \frac{1}{p_{1_0}^*}\left(\frac{\partial \mathrm{M}_C}{\partial \pi_c^*}\right)_0\right]\frac{\Delta p_2^*}{p_{2_0}^*} -$$
$$- \frac{\delta_{T_0}^*}{\mathrm{M}_{T_0}}\left(\frac{\partial \mathrm{M}_T}{\partial \delta_T^*}\right)_0 \frac{\Delta p_4^*}{p_{4_0}^*}, \tag{11}$$

then, after applying the Laplace transformation (for null initial conditions), the equation becomes

$$(T_1 s + \rho_1)\overline{n} - k_{1T3}\overline{T}_3^* - k_{1p2}\overline{p}_2^* + k_{1p4}\overline{p}_4^* = 0, \tag{12}$$

where $T_1 = \frac{\pi J n_0}{30 \mathrm{M}_{C_0}}$, $\rho_1 = \frac{n_0}{\mathrm{M}_{C_0}}\left[\left(\frac{\partial \mathrm{M}_C}{\partial n}\right)_0 - \left(\frac{\partial \mathrm{M}_T}{\partial n}\right)_0 + \left(\frac{\partial \mathrm{M}_C}{\partial \dot{m}_a}\right)_0 \left(\frac{\partial \dot{m}_a}{\partial n}\right)_0\right]$, $k_{1p4} = \frac{\delta_{T_0}^*}{\mathrm{M}_{T_0}}\left(\frac{\partial \mathrm{M}_T}{\partial \delta_T^*}\right)_0$, $k_{1T3} = \frac{T_{3_0}^*}{\mathrm{M}_{T_0}}$ $\left[\left(\frac{\partial \mathrm{M}_T}{\partial T_3^*}\right)_0 + \left(\frac{\partial \mathrm{M}_T}{\partial \dot{m}_g}\right)_0 \left(\frac{\partial \dot{m}_g}{\partial T_3^*}\right)_0\right]$, $k_{1p2} = \frac{p_{2_0}^*}{\mathrm{M}_{T_0}}\left[\sigma_{CA}^*\left(\frac{\partial \mathrm{M}_T}{\partial \dot{m}_g}\right)_0 \left(\frac{\partial \partial \dot{m}_g}{\partial p_3^*}\right)_0 + \frac{\sigma_{CA}^*}{p_{4_0}^*}\left(\frac{\partial \mathrm{M}_T}{\partial \delta_T^*}\right)_0 - \frac{1}{p_{1_0}^*}\left(\frac{\partial \mathrm{M}_C}{\partial \dot{m}_a}\right)_0 \left(\frac{\partial \dot{m}_a}{\partial \pi_c^*}\right)_0 - \frac{1}{p_{1_0}^*} \left(\frac{\partial \mathrm{M}_C}{\partial \pi_c^*}\right)_0\right]$,

s – derivative operator, $\overline{X}(s)$–the Laplace transformation image of the dimensionless formal parameter $\frac{\Delta X}{X_0}$, or, as simplified notation

$$\overline{X}\left(\overline{X} = \overline{n}, \overline{T}_3^*, \ldots\right). \tag{13}$$

By doing the same for the other equations, one obtains their dimensionless linearized new forms, depending on the same parameters $\left(\overline{n}, \overline{T}_3^*, \overline{T}_4^*, \overline{p}_2^*, \overline{p}_4^*\right)$, as follows:

$$k_{2n}\overline{n} - k_{2T3}\overline{T}_3^* - k_{2p2}\overline{p}_2^* = 0, \tag{14}$$

$$-\overline{T}_3^* + \overline{T}_4^* - k_{3p2}\overline{p}_2^* - k_{3p4}\overline{p}_4^* = 0, \tag{15}$$

$$k_{4T3}\overline{T}_3^* + k_{4T4}\overline{T}_4^* - k_{4p2}\overline{p}_2^* - k_{4p4}\overline{p}_4^* = k_{4A}\overline{A}_5, \tag{16}$$

$$k_{5n}\overline{n} + k_{5T3}\overline{T}_3^* + k_{5p2}\overline{p}_2^* = k_{5c}\overline{\dot{m}}_c. \tag{17}$$

The above presented coefficients can be experimentally determined, or graphic-analytical estimated, based on engine's characteristics chart, as done in [3].

As presented in [5], engine's mathematical model built-up with Eqs. (12) and (14) to (17), may be expressed as an unique matrix eq. $[A]\times(u) = (b)$:

$$\begin{bmatrix} T_1 s + \rho_1 & -k_{1T3} & 0 & -k_{1p2} & k_{1p4} \\ k_{2n} & -k_{2T3} & 0 & k_{2p2} & 0 \\ 0 & -1 & 1 & -k_{3p2} & -k_{3p4} \\ 0 & k_{4T3} & k_{4T4} & k_{4p2} & k_{4p4} \\ k_{5n} & k_{5T3} & 0 & k_{5p2} & 0 \end{bmatrix} \times \begin{pmatrix} \overline{n} \\ \overline{T}_3^* \\ \overline{T}_4^* \\ \overline{p}_2^* \\ \overline{p}_4^* \end{pmatrix} = \begin{pmatrix} 0 \\ 0 \\ 0 \\ k_{4A}\overline{A}_5 \\ k_{5c}\overline{\dot{m}}_c \end{pmatrix}. \tag{18}$$

Moreover, using the Cramer method, one can solve the equation and obtain the expressions of all the output parameters in vector (u). As an example, for engine's speed $\overline{n}$ parameter expression, it results in $\overline{n} = \frac{\det(A_n)}{\det(A)}$, or $\det(A)\overline{n} = \det(A_n)$, where $\det(A)$ is $[A]-$ matrix determinant, while $\det(A_n)$ is the determinant of the matrix obtained by replacing the first $[A]-$ matrix column with the input vector (b). Eventually, one obtains, formally, $(a_1 s + a_0)\overline{n} = f_0\overline{\dot{m}}_c + g_0\overline{A}_5$, or else

$$(\tau_m s + 1)\overline{n} = k_c\overline{\dot{m}}_c + k_A\overline{A}_5, \tag{19}$$

where the involved coefficients (a_1, a_0, f_0, g_0) and (τ_m, k_c, k_A) are used with their expressions determined in [5], depending on the values of $T_1, \rho_1, k_{1T3}, \ldots k_{5p2}, k_{4A}, k_{5c}$. If one considers the aircraft flight regime too (airspeed V and altitude H), Eq. (19) must be completed by a term containing both elements V and H, which is the pressure p_1^* (as determined in [3, 5]):

$$(\tau_m s + 1)\overline{n} = k_c\overline{\dot{m}}_c + k_A\overline{A}_5 - k_{HV}\overline{p}_1^*. \tag{20}$$

Together with the main output $\overline{n}$, secondary outputs may be obtained in the same way:

- Combustor temperature:

$$(\tau_m s + 1)\overline{T}_3^* = (l_{Tc}s + l_T)\overline{\dot{m}}_c + l_A\overline{A}_5 - k_{THV}\overline{p}_1^*, \tag{21}$$

- Engine thrust:

$$(\tau_m s + 1)\overline{F} = (l_{Fc}s + l_c)\overline{\dot{m}}_c + (l_{FA}s + l_A)\overline{A}_5 - k_{Fp}\overline{p}_1^*. \tag{22}$$

If the engine operates at low altitude and speed (such as during the take-off procedure), flight regime has no influence, as well as the exhaust nozzle area (which must be totally open), so $\overline{p}_1^* = 0$ and $\overline{A}_5 = 0$.

3. Coolant injection into gas-turbine engine's compressor

The first described thrust augmentation method consists of the injection of a special cooling fluid (distilled water, methanol, ammonia or mixtures), identified as *coolant*, into engine's axial compressor, in its front part. In order to achieve its task—the heat extraction by vaporization—it is compulsory that the coolant injectors are positioned in the front of the compressor to assure enough room for coolant-air mixing and coolant vaporization. If the coolant is a combustible fluid (such as methanol), not a neutral fluid (such as water), after its vaporization, it can participate into the burning evolution in the engine's combustor, which may reduce the fuel consumption increase due to the coolant injection [1].

Thrust augmentation is significant for an engine operating at uncommon atmospheric conditions (such as high temperatures, more than 30°C, low pressure and humidity), because injected coolant's vaporization is facilitated [1]. Method's disadvantages consist of icing hazard (air intake's and compressor's blades icing, or the suction of ice lumps into the compressor), as well as the necessity of on-board coolant carrying; injection running time is the one who limits the coolant necessary mass to be boarded, so aircraft's coolant injection system design and optimization must take into account aircraft's take-off payload, as well as aircraft mission and take-off atmospheric conditions.

In fact, the temporary thrust augmentation by this coolant injection method may be assimilated to an over-boost method for classic engines; this method is suitable for low or medium power jet-engines, as well as for turboprops (where the afterburning is impossible to be adapted).

3.1. Thermodynamic and gas-dynamic phenomena

The air compression evolution into the engine's compressor is an irreversible adiabatic (of adiabatic exponent $\chi = 1.4$), characterized by increasing air temperature (enthalpy), as depicted in **Figure 1**. The injected coolant vaporizing extracts a significant fraction of the produced compression heat; consequently, the compressed air becomes cooler, its mass flow rate grows, while its volume flow rate is kept constant. The extraction of a fraction of the compression heat (q_i in **Figure 1**) converts the air compression evolution into a polytropic-one (of a_i exponent, smaller than χ) and determines a significant decrease of the compression mechanical work; meanwhile, compressor's total pressure ratio changes, from π_c^* to $\pi_{c_i}^*$, as well as the compressor's working line on its universal characteristics (which moves much closer to the surge line).

The injected coolant may extract the heat $Q_i = \dot{m}_l r_f$, where r_f is coolant's latent heat of vaporization, $\dot{m}_l -$ the injected coolant flow rate, which means that, for $\dot{m}_a$ the air flow rate through the compressor and for $\xi_l -$ the injection fraction, one obtains for q_i

$$q_i = \frac{Q_i}{\dot{m}_a} = \frac{\dot{m}_l}{\dot{m}_a} r_f = \xi_l \cdot r_f. \tag{23}$$

Mechanical work's value should be the same for both evolutions (the adiabatic old one, as well as for the polytropic new one), so

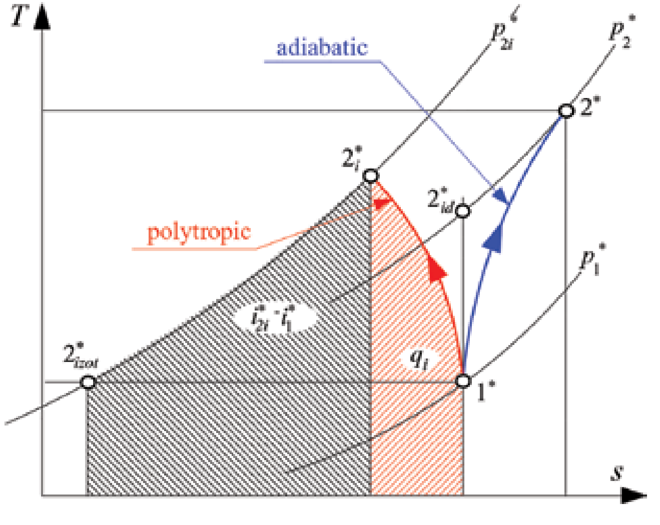

Figure 1. Air compression evolution with and without coolant injection.

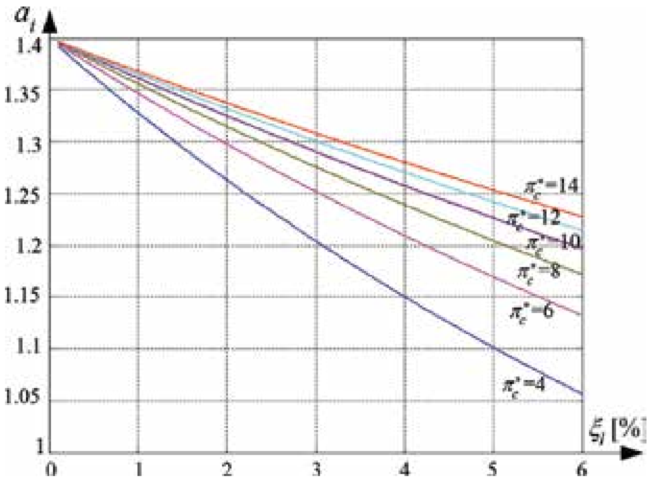

Figure 2. Polytropic exponent versus coolant injection fraction.

$$i_1^*\frac{a_i}{a_i-1}\left[\left(\pi_{c_i}^*\right)^{\frac{a_i-1}{a_i}}-1\right]=i_1^*\left[\frac{\left(\pi_c^*\right)^{\frac{\chi-1}{\chi}}-1}{\eta_c}\right]-q_i=i_1^*\left[\frac{\left(\pi_c^*\right)^{\frac{\chi-1}{\chi}}-1}{\eta_c}\right]-\xi_l r_f, \tag{24}$$

where i_1^* is air's specific enthalpy in the front of the compressor, η_c- compressor's efficiency. This equation gives the connection between ξ_l and a_i, as shown in **Figure 2**. The bigger the coolant fluid flow rate $\dot{m}_l$ and its fraction ξ_l are, the lower the polytropic exponent is; its value tends to 1, which means that the limit evolution is the isothermic-one, extremely difficult to be achieved. Withal, the bigger compressor's total pressure ratio is, the bigger a_i value becomes.

The new value of the compressors total pressure ratio becomes

$$\pi_{c_i}^*=\left\{1+\frac{a_i-1}{a_i}\frac{\chi}{\chi-1}\left[\frac{\left(\pi_c^*\right)^{\frac{\chi-1}{\chi}}-1}{\eta_C}\right]\right\}^{\frac{a_i}{a_i-1}}. \tag{25}$$

In terms of the engine's working fluid mass flow rate, modifications also appear. For the basic engine, burned gases mass flow rate through the exhaust nozzle $\dot{m}_g$ is given by

$$\dot{m}_g=\dot{m}_a-\dot{m}_{pr}+\dot{m}_c, \tag{26}$$

As stated in [1, 2], the bleed air mass flow rate $\dot{m}_{pr}$ and the fuel mass flow rate $\dot{m}_c$ have near the same values, which lead to the conclusion that $\dot{m}_g \approx \dot{m}_a$. Therefore, if the coolant injection system is active, the burned gases flow rate $\dot{m}_{g_i}$ becomes

$$\dot{m}_{gi}=\dot{m}_{a_i}+\dot{m}_l, \tag{27}$$

where $\dot{m}_{a_i}$ is the compressor air mass flow rate amount when the coolant injection is active.

As long as nowadays gas-turbine-engines have critical flow in their turbines [1, 2, 8], their flow parameters should remain constant, even with coolant injection into the compressor. So, the condition $\frac{\dot{m}_g\sqrt{T_3^*}}{p_3^*} = idem$ for the turbine flow leads to

$$\frac{\dot{m}_g\sqrt{T_3^*}}{p_3^*} = \frac{\dot{m}_a\sqrt{T_3^*}}{\sigma_{CA}^* p_2^*} = \frac{\dot{m}_{a_i}\sqrt{T_3^*}}{\sigma_{CA}^* p_{2_i}^*}, \tag{28}$$

where p_3^*- burned gas pressure before the turbine (proportional to p_2^*- the air pressure after the compressor, $p_3^* = \sigma_{CA}^* p_2^*$), σ_{CA}^*- combustor's total pressure ratio, $p_2^* i-$ the air pressure after the compressor when the coolant injection is active.

Consequently, the new value for the compressor's air flow rate becomes

$$\dot{m}_{a_i} = \dot{m}_a \frac{\pi_{c_i}^*}{\pi_c^*}, \tag{29}$$

which, obviously, modifies the value of $\dot{m}_{g_i}$ given by Eq. (27).

3.2. Gas-turbine-engine with coolant injection into its compressor mathematical model

Coolant injection, as presented in previous section, has a significant influence above engine's behavior and, consequently, above its mathematical model form, as well as on its coefficients expressions and values.

First, the mass flow rate equation is modified because of the presence of $\dot{m}_l$; second, according to the coolant nature (combustible fluid or neutral fluid), the combustor's equation may, or may not, be also modified.

In terms of the mass flow equation, Eq. (27) may be written (according to [1, 9] and [10]) as

$$\dot{m}_{g_i}\left(p_3^*, T_3^*\right) = \dot{m}_{a_i}\left(p_2^*, n\right) + \dot{m}_l, \tag{30}$$

or, using the finite difference method for linearization, as

$$\left(\frac{\partial \dot{m}_{g_i}}{\partial p_3^*}\right)_0 \Delta p_3^* + \left(\frac{\partial \dot{m}_{g_i}}{\partial T_3^*}\right)_0 \Delta T_3^* = \left(\frac{\partial \dot{m}_{a_i}}{\partial p_2^*}\right)_0 \Delta p_2^* + \left(\frac{\partial \dot{m}_{a_i}}{\partial n}\right)_0 \Delta n + \Delta \dot{m}_l. \tag{31}$$

The above-determined equation, after some suitable amplifying and terms grouping, may be brought to a dimensionless form, then Laplace transformed, as described in [10], giving

$$\frac{p_{2_0}^*}{\left(\dot{m}_{a_i}\right)_0}\left[\left(\frac{\partial \dot{m}_{g_i}}{\partial p_2^*}\right)_0 \sigma_{CA}^* - \left(\frac{\partial \dot{m}_{a_i}}{\partial p_2^*}\right)_0\right]\frac{\Delta p_2^*}{p_{2_0}^*} + \frac{T_{3_0}^*}{\left(\dot{m}_{a_i}\right)_0}\left(\frac{\partial \dot{m}_{g_i}}{\partial T_3^*}\right)_0 \frac{\Delta T_3^*}{T_{3_0}^*} - \frac{n_0}{\left(\dot{m}_{a_i}\right)_0}\left(\frac{\partial \dot{m}_{a_i}}{\partial n}\right)_0 \frac{\Delta n}{n_0} = \xi_l \frac{\Delta \dot{m}_l}{\left(\dot{m}_l\right)_0}, \tag{32}$$

equivalent to

$$k_{2n}^{/}\overline{n} - k_{2T3}^{/}\overline{T_3^*} + k_{2p2}^{/}\overline{p_2^*} = \xi_l \overline{\dot{m}_l}, \tag{33}$$

which is a new form for the second equation of the mathematical model, so the new coefficients in Eq. (33) left member should replace the old ones in the second line of the system matrix $[A]$. Withal, the input vector (b) should be completed on its second line by $\xi_l \overline{\dot{m}_l}$, the right member in Eq. (33).

In terms of the combustor equation, it shall be modified due to the supplementary presence of the coolant fluid's energy [10, 11], as follows

$$\dot{m}_{g_i} c_{p_g} T_3^* - \dot{m}_{a_i} c_{p_a} T_2^* = \dot{m}_c \zeta_{CA} P_c + \dot{m}_l \zeta_{CA} P_l, \tag{34}$$

where P_l—chemical energy of the injected fluid (if combustible), and T_2^*—air temperature behind the compressor, which may be expressed with respect to p_2^* as follows

$$\overline{T_2^*} = \frac{p_{2_0}^*}{T_{2_0}^*}\left(\frac{\partial T_2^*}{\partial \pi_c^*}\right)_0 \left(\frac{\partial \pi_c^*}{\partial p_2^*}\right)_0 \overline{p_2^*}, \tag{35}$$

while the term $\dot{m}_{a_i}$ shall be expressed from the compressor's characteristic with respect to its rotational speed n and to the pressure behind the compressor p_2^* [2, 8, 10].

Both cases, for neutral, respectively for combustible coolant, were studied in [10], the fifth equation of the mathematical model being modified according to each situation, as shown below.

3.2.1. Neutral coolant injection

When the injected coolant is a neutral fluid$(P_l = 0)$, the term $\dot{m}_l \zeta_{CA} P_l$ becomes null. Consequently, considering Eq. (35) and applying the same above described method (as in [4, 10]), Eq. (34) becomes

$$\begin{aligned}&\frac{c_p\left(T_{3_0}^* - T_{2_0}^*\right)n_0}{\dot{m}_{c_0}\zeta_{CA}P_c}\left(\frac{\partial \dot{m}_a}{\partial n}\right)_0 \overline{n} + \frac{c_p(\dot{m}_{a_0} - \dot{m}_{l_0})T_{3_0}^*}{\dot{m}_{c_0}\zeta_{CA}P_c}\overline{T_3^*} \\ &+ \left[\frac{c_p\left(T_{3_0}^* - T_{2_0}^*\right)p_{2_0}^*}{\dot{m}_{c_0}\zeta_{CA}P_c}\left(\frac{\partial \dot{m}_a}{\partial p_2^*}\right)_0 - \frac{c_p(\dot{m}_{a_0} - \dot{m}_{l_0})}{\dot{m}_{c_0}\zeta_{CA}P_c}p_{2_0}^*\left(\frac{\partial T_2^*}{\partial \pi_c^*}\right)_0\left(\frac{\partial \pi_c^*}{\partial p_2^*}\right)_0\right]\overline{p_2^*} = \overline{\dot{m}_c} - \frac{\dot{m}_{l_0}}{\dot{m}_{c_0}\zeta_{CA}P_c}\overline{\dot{m}_l}\end{aligned} \tag{36}$$

The coefficient $\frac{\dot{m}_{l_0}}{\dot{m}_{c_0}\zeta_{CA}P_c}$ of $\overline{\dot{m}_l}$ in the above-determined equation has a very small value (10^4 times less than any other coefficient), so it may be neglected, which simplifies equation's final form

$$k_{5n}\overline{n} + k_{5T3}^{/}\overline{T_3^*} + k_{5p2}^{/}\overline{p_2^*} = \overline{\dot{m}_c}, \tag{37}$$

so the fifth line in matrix $[A]$ of Eq. (18) must be rewritten. Consequently, one obtains a new form of engine's mathematical model, as follows:

$$\begin{bmatrix} T_1 s+\rho_1 & -k_{1T3} & 0 & -k_{1p2} & k_{1p4} \\ k^{/}_{2n} & -k^{/}_{2T3} & 0 & k^{/}_{2p2} & 0 \\ 0 & -1 & 1 & -k_{3p2} & -k_{3p4} \\ 0 & k_{4T3} & k_{4T4} & k_{4p2} & k_{4p4} \\ k^{/}_{5n} & k^{/}_{5T3} & 0 & k^{/}_{5p2} & 0 \end{bmatrix} \times \begin{pmatrix} \overline{n} \\ \overline{T}^*_3 \\ \overline{T}^*_4 \\ \overline{p}^*_2 \\ \overline{p}^*_4 \end{pmatrix} = \begin{pmatrix} 0 \\ \xi_l \overline{\dot{m}_l} \\ 0 \\ 0 \\ k^{/}_{5c}\overline{\dot{m}}_c \end{pmatrix}, \tag{38}$$

which gives for the main output parameter, by Cramer-method solving, an equation similar to Eq. (19)

$$(\tau_{m1}s+1)\cdot \overline{n} = k_{c1}\overline{\dot{m}_c} - k_l\overline{\dot{m}_l}. \tag{39}$$

3.2.2. Combustible fluid injection

When the coolant is a combustible fluid, Eq. (34) shall be reconsidered and rewritten; consequently, its right member becomes

$$\left(1-\frac{P_l}{P_c}\frac{\dot{m}_{l_0}}{\dot{m}_{c_0}}\right)\overline{\dot{m}_c} - \frac{\dot{m}_{l_0}c_p\left(T^*_{3_0}-T^*_{2_0}\right)}{\dot{m}_{c_0}\zeta_{CA}P_c}\overline{\dot{m}_l} = k^{/}_{5c}\overline{\dot{m}_c} - k^{/}_{5l}\overline{\dot{m}_l}, \tag{40}$$

so, the fifth equation of the model shall have a new form, similar to Eq. (37), but considering the coolant heat effect too:

$$k_{5n}\overline{n} + k^{/}_{5T3}\overline{T^*_3} + k^{/}_{5p2}\overline{p^*_2} = k^{/}_{5c}\overline{\dot{m}_c} - k^{/}_{5l}\overline{\dot{m}_l}. \tag{41}$$

In order to eliminate the term containing the coolant injection flow rate parameter and simplify the input vector's form, one has to multiply the second model's equation by $\frac{k^{/}_{5l}}{\xi_l}$ and to add it to Eq. (40). It results, for the last equation of the model, a simplified form

$$\left(k^{/}_{2n}\frac{k^{/}_{5l}}{\xi_l}+k_{5n}\right)\overline{n} + \left(k^{/}_{2T3}\frac{k^{/}_{5l}}{\xi_l}+k_{5T3}\right)\overline{T^*_3} + \left(k^{/}_{2p2}\frac{k^{/}_{5l}}{\xi_l}+k_{5p2}\right)\overline{p^*_2} = k^{/}_{5c}\overline{\dot{m}_c} \tag{42}$$

and, consequently, the new form of the main matrix $[A_2]$ of engine's mathematical model becomes

$$A_2 = \begin{bmatrix} T_1 s+\rho_1 & -k_{1T3} & 0 & -k_{1p2} & k_{1p4} \\ k^{/}_{2n} & -k^{/}_{2T3} & 0 & k^{/}_{2p2} & 0 \\ 0 & -1 & 1 & -k_{3p2} & -k_{3p4} \\ 0 & k_{4T3} & k_{4T4} & k_{4p2} & k_{4p4} \\ k^{/}_{2n}\frac{k^{/}_{5l}}{\xi_l}+k_{5n} & k^{/}_{2T3}\frac{k^{/}_{5l}}{\xi_l}+k_{5T3} & 0 & k^{/}_{2p2}\frac{k^{/}_{5l}}{\xi_l}+k_{5p2} & 0 \end{bmatrix}, \tag{43}$$

while the vectors (u) and (b) remain the same as in Eq. (38).

3.3. About system's quality

The gas-turbine-engine with coolant injection into its compressor as controlled object, according to its above-determined mathematical model and as **Figure 3** shows, it is a first-order system; it has two inputs (the fuel mass flow rate $\overline{\dot{m}_c}$ and the coolant mass flow rate $\overline{\dot{m}_l}$), but multiple outputs (such as engine's rotation speed $\overline{n}$, combustor's temperature $\overline{T_3^*}$, engine's thrust $\overline{F}$, etc.); obviously, only one output is the main one (in this case $\overline{n}$), the others being secondary outputs.

System's quality evaluation consists of the study of system's time behavior, in fact the study of system's step response(s); system's input(s) is (are) replaced by step functions (Heaviside), and the outputs are evaluated from their behavior point of view, knowing how the system responds to sudden input(s) and gathering information on system's stability, as well as on its ability to reach one stationary state when starting from another [4, 7, 11].

A quantitative study was performed and described in [10], based on an existing VK-1A-type engine (jet-engine with constant geometry exhaust nozzle), excluding its built-in control systems (such as rotation speed controller or combustor's temperature limiter), in order to evaluate only the basic engine as possible controlled object.

One has chosen for study as outputs: the main output – engine's speed parameter $\overline{n}$, as well as two secondary, but very important, outputs – combustor temperature's parameter $\overline{T_3^*}$ and engine's thrust parameter $\overline{F}$. Outputs' quantitative expressions (determined in [10]) are:

a. engine with neutral coolant injection (distilled water):

$$\overline{n}(\mathrm{s}) = \frac{1.283\,\overline{\dot{m}_c}(\mathrm{s}) - 0.092\overline{\dot{m}_l}(\mathrm{s})}{1.6348\,\mathrm{s} + 4.5158}, \tag{44}$$

$$\overline{T_3^*}(\mathrm{s}) = \frac{(1.474\,\mathrm{s} + 2.748)\overline{\dot{m}_c}(\mathrm{s}) - (0.047\,\mathrm{s} + 0.034)\overline{\dot{m}_l}(\mathrm{s})}{1.6348\,\mathrm{s} + 4.5158}, \tag{45}$$

$$\overline{F}(\mathrm{s}) = \frac{(1.385\,\mathrm{s} + 4.516)\overline{\dot{m}_c}(\mathrm{s}) - (0.089\,\mathrm{s} + 0.315)\overline{\dot{m}_l}(\mathrm{s})}{1.6348\,\mathrm{s} + 4.5158}; \tag{46}$$

b. engine with combustible coolant injection (methanol):

$$\overline{n}(\mathrm{s}) = \frac{1.43\,\overline{\dot{m}_c}(\mathrm{s}) - 0.184\overline{\dot{m}_l}(\mathrm{s})}{2.161\,\mathrm{s} + 4.7973}, \tag{47}$$

$$\overline{T_3^*}(\mathrm{s}) = \frac{(1.816\,\mathrm{s} + 2.467)\overline{\dot{m}_c}(\mathrm{s}) - (0.053\,\mathrm{s} + 0.047)\overline{\dot{m}_l}(\mathrm{s})}{2.161\,\mathrm{s} + 4.7973}, \tag{48}$$

$$\overline{F}(\mathrm{s}) = \frac{(1.584\,\mathrm{s} + 6.317)\overline{\dot{m}_c}(\mathrm{s}) - (0.113\,\mathrm{s} + 0.803)\overline{\dot{m}_l}(\mathrm{s})}{2.161\,\mathrm{s} + 4.7973}. \tag{49}$$

Engine outputs' time behavior is graphically represented in **Figures 4–6**, for the basic engine (blue lines), as well as for the engine with coolant injection (green lines for neutral coolant, red lines for combustible coolant). All the obtained curves are proving that the studied system is a stable-one, with asymptotic stabilization and static errors.

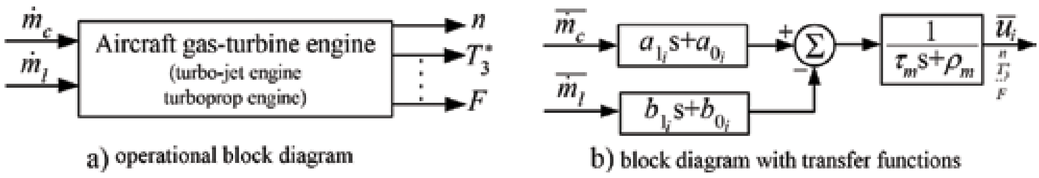

Figure 3. Formal description of a gas-turbine-engine with coolant injection.

In terms of engine's time constant value, whatever the method was, it remains nearly the same, settling time values being kept around (2.5–3.0) s, similar to the basic engine.

As **Figure 4** shows, whatever the nature of the coolant is, the speed parameter behavior is little influenced, the deviation from basic engine's curve being very small; the biggest value is obtained for combustible coolant (obviously, because its supplementary contribution to the burning process and supplementary heat transfer).

Figure 5 shows temperature parameters' initial overshoots, followed by asymptotic settlings. When the coolant is neutral, one can observe a significant growth of the $\overline{T}_3^*-$ parameter's value, as a consequence of air mass flow rate increase, which requires a supplementary fuel injection, in order to avoid temperature and thrust decrease. When the coolant is a combustible fluid, because of its own heat input, the supplementary fuel injection is smaller and, consequently, one obtains a smaller temperature increase, even if the initial overshoot is comparable to the first case.

In terms of thrust parameter's behavior, as **Figure 6** shows, after a sudden initial increase, the curves have similar asymptotic aspects. Most significant thrust increase is obtained when the coolant is a combustible-one because of engine's specific thrust increase (due to the additional heat input), as well as because of air mass flow rate increase, while thrust increase for neutral coolant injection is moderate.

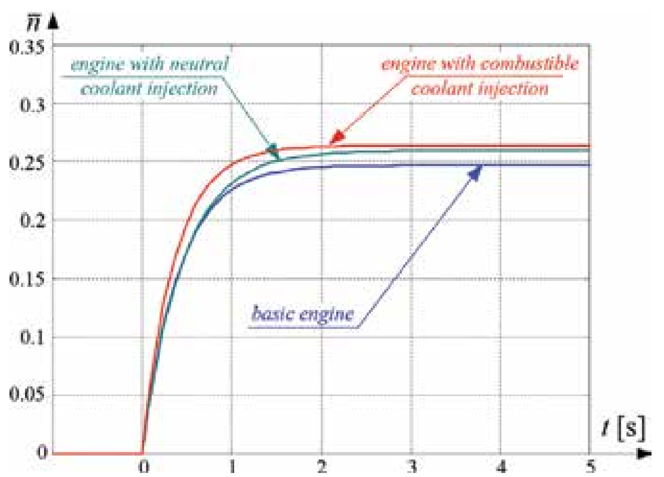

Figure 4. Comparative step response of engine rotational speed parameters.

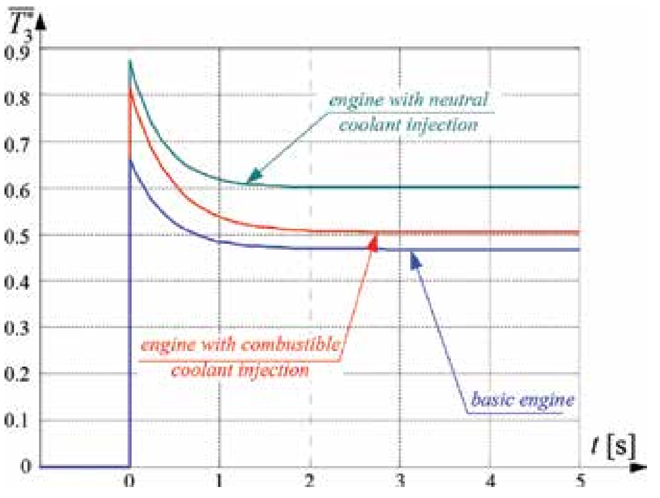

Figure 5. Comparative step response of engine combustor temperature parameters.

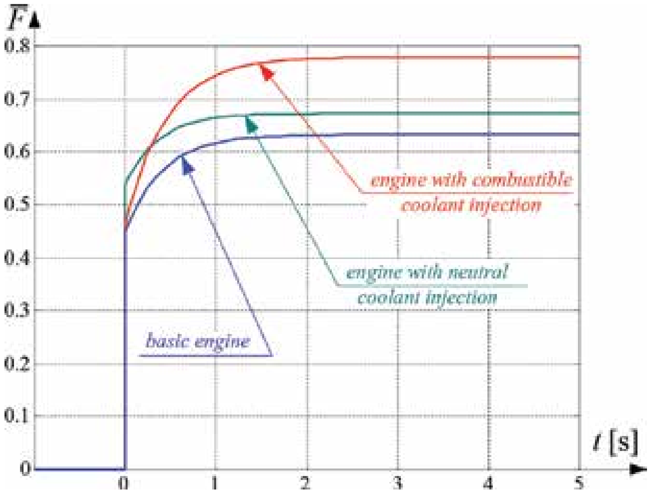

Figure 6. Comparative step response of engine thrust parameters.

3.4. Jet engine with coolant injection controller

The coolant injection into the compressor is done by means of a pump, which may be electrically driven (by a DC motor, supplied by the aircraft electric system), or it may be connected to the engine's gearbox and, consequently, driven by engine shaft [10, 12, 14]. As long as an electric driven pump has a constant rotation speed, both its mass flow rate and its injection pressure are constant, while engine shaft-driven pump's speed is equal (or proportional) to engine's speed n, thus its flow rate behavior is also proportional to n, which introduces another feedback into the engine's control system, as shown in **Figure 7**. In fact, in order to assure an

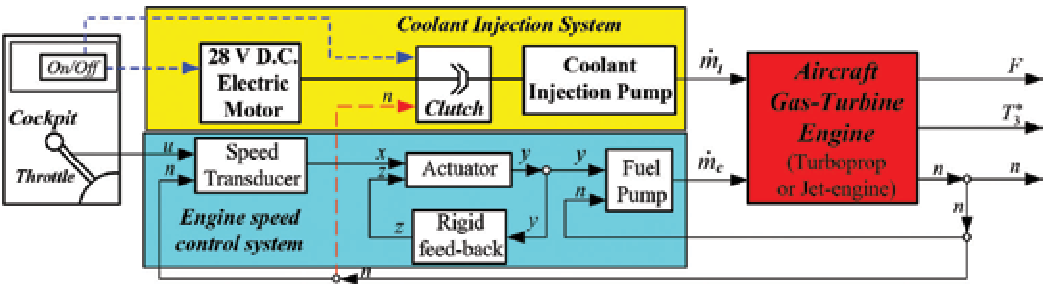

Figure 7. Gas-turbine-engine with coolant injection formal block-diagram.

appropriate engine operation, not only the fuel mass flow rate, but also the coolant mass flow rate must be controlled; this one must be correlated to the compressor provided air mass flow rate. Engine shaft-driven pump assures such a correlation, much better than the electric driven pump (as presented in [12]). Thus, gearbox-driven pump speed follows engine's speed, so the coolant mass flow rate grows smoothly (as engine's speed does); in terms of temperature and thrust parameters, they also show similar behavior to basic engine's parameters. Independent driven injection pump (by an electric DC motor) is a more convenient solution (sometimes easier to manufacture and less expensive); although it does not affect engine's stability, it worsens its time behavior, as stated in [12].

However, some engine manufacturers (based on operational, economic and efficiency reasons) prefer to implement a coolant injection controller (CIC) consisting of an electric driven pump, assisted by a coolant flow rate controller (which correlates the coolant flow rate to the air flow rate, following the compressor's total pressure ratio). Such an embedded system, presented and studied in [14], consists of a gas-turbine-engine, its speed controller (ESCS - based on its fuel mass flow rate control) and the coolant injection controller (CIC – built up with a dosage valve, an actuator and a pressure ratio transducer), as formally depicted in **Figure 8**.

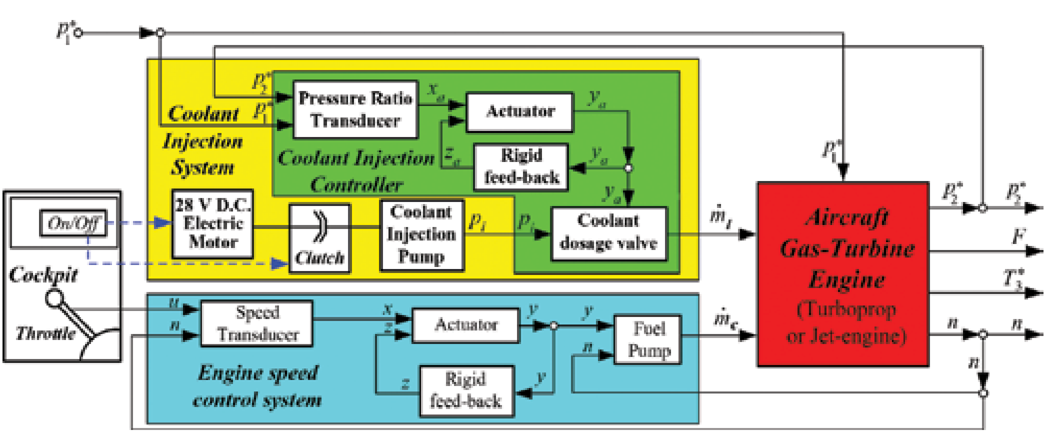

Figure 8. Gas-turbine-engine with speed control system and coolant injection controller.

Embedded system's mathematical model has the following equations:

a. ESCS model (as determined in [4, 13]):

- Fuel pump:

$$\overline{\dot{m}_c} = k_{pn}\overline{n} + k_{py}\overline{y}, \tag{50}$$

- Throttle:

$$\overline{u} = k_{u\alpha}\overline{\alpha}, \tag{51}$$

- Speed transducer:

$$\overline{x} = k_u\overline{u} - k_{es}\overline{n}, \tag{52}$$

- Actuator:

$$\tau_s \mathrm{s}\overline{y} = \overline{x} - \overline{z}, \tag{53}$$

- Rigid feedback

$$\overline{z} = \rho_s\overline{y}, \tag{54}$$

b. CIC model (similar to the one studied in [15]):

- Pressure ratio transducer:

$$\overline{x}_a = k_{px}\left(\overline{p}_1^* - \overline{p}_R\right), \tag{55}$$

$$k_{2R}\overline{p}_2^* - k_{xR}(\tau_{ax}\mathrm{s} + 1)\overline{x}_a = (\tau_R\mathrm{s} + 1)\overline{p}_R, \tag{56}$$

- Actuator:

$$\tau_{sl}\mathrm{s}\overline{y}_a = \overline{x}_a - \overline{z}_a, \tag{57}$$

- Rigid feedback

$$\overline{z}_a = \rho_l\overline{y}_a, \tag{58}$$

- Dosage valve:

$$\overline{\dot{m}_l} = k_{ly}\overline{y}_a. \tag{59}$$

c. jet engine (with operational coolant injection) main output parameter equation, determined in previous subsections, together with engine's secondary output parameter $\overline{p}_2^*$ equation (which is used as CIC main input, as Eq. (56) shows):

http://dx.doi.org/10.5772/intechopen.76856

$$(\tau_{m1}s+1)\cdot\overline{n} = k_{c1}\overline{\dot{m}_c} - k_l\overline{\dot{m}_l} - k_{HV}\overline{p_1^*}, \tag{60}$$

$$(\tau_{m1}s+1)\cdot\overline{p_2^*} = \left(l_{p2c}s+l_{p2}\right)\overline{\dot{m}_c} - \left(l_{p2l}s+l_{l2}\right)\overline{\dot{m}_l}, \tag{61}$$

where the new term $k_{HV}\overline{p_1^*}$ should introduce the effect of flight regime (airspeed and altitude).

Based on above-presented equations, one has built-up embedded controller block diagram with transfer functions, depicted in **Figure 9**; the diagram in **Figure 9a** corresponds to the case when the coolant injection pump is driven by engine's shaft, while the diagram in **Figure 9b**—to the electrically driven pump case (formally depicted in **Figure 8**). One may observe that both embedded control systems have as unique input the engine's power lever angle parameter $\overline{\alpha}$. In fact, engine's power lever (throttle) is the only way for the pilot to command the engine, so the throttle should "control the controllers."

As long as the coolant injection operates only for take-off and at very low flight altitudes, one may consider that p_1^* has a negligible variation; consequently, $\overline{p_1^*} = 0$, while the terms giving the flight regime's influence ($k_{HV}\overline{p_1^*}$ in Eq. (50) and $k_{px}\overline{p_1^*}$ in Eq. (56)) may be neglected.

A quantitative study was performed and described in [14], based on a VK-1A-type jet engine and on some studies concerning the involved controllers, developed in [4, 9, 11, 13]. The quantitative expression of the embedded system mathematical model is given by the equations:

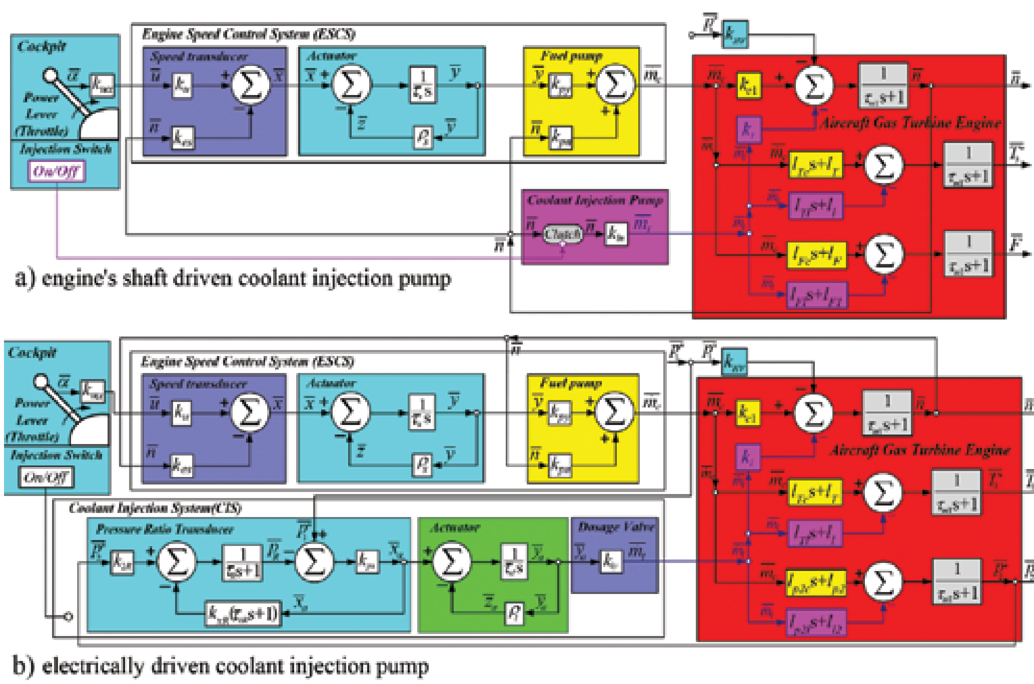

Figure 9. Embedded control systems block diagrams with transfer functions.

$$\overline{n}(s) = \frac{1.283\,\overline{\dot{m}_c}(s) - 0.092\overline{\dot{m}_l}(s)}{1.6348\,s + 4.5158}, \tag{62}$$

$$\overline{p_2^*}(s) = \frac{(0.3425\,s + 2.6718)\overline{\dot{m}_c}(s) - (0.0672\,s + 0.9211)\overline{\dot{m}_l(s)}}{1.6348\,s + 4.5158}, \tag{63}$$

$$\overline{T_3^*}(s) = \frac{(1.474\,s + 2.748)\overline{\dot{m}_c}(s) - (0.047\,s + 0.034)\overline{\dot{m}_l}(s)}{1.6348\,s + 4.5158}, \tag{64}$$

$$\overline{F}(s) = \frac{(1.385\,s + 4.516)\overline{\dot{m}_c}(s) - (0.089\,s + 0.315)\overline{\dot{m}_l}(s)}{1.6348\,s + 4.5158}, \tag{65}$$

$$\overline{x}(s) = 0.317\overline{\alpha}(s) - 0.439\overline{n}, \tag{66}$$

$$\overline{y}(s) = \frac{1}{1.81 \cdot s + 5.306}\overline{x}(s), \tag{67}$$

$$\overline{\dot{m}_c}(s) = 0.5\overline{n}(s) + 0.5\overline{y}(s), \tag{68}$$

$$\overline{x}_a(s) = \frac{0.346}{0.8101 \cdot s + 3.1221}\overline{p_2^*}(s), \tag{69}$$

$$\overline{y}_a(s) = \frac{1}{1.364 \cdot s + 4.617}\overline{x}_a(s), \tag{70}$$

$$\overline{\dot{m}_l}(s) = 0.615\overline{y}_a(s). \tag{71}$$

Simulation was performed based on these equations and on the block diagrams with transfer functions in **Figure 9**, considering as single input the power lever angle (PLA) or the throttle angle

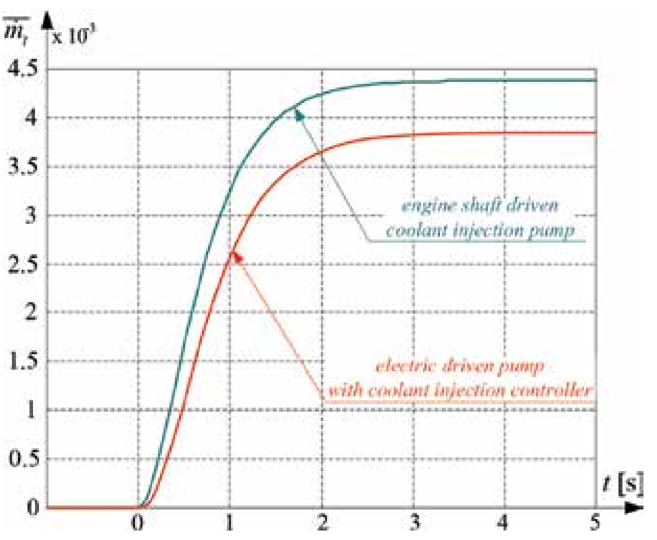

Figure 10. Coolant flow rate parameter step response.

http://dx.doi.org/10.5772/intechopen.76856

parameter $\overline{\alpha}$, while as main output - engine's speed parameter $\overline{n}$; secondary outputs were also considered, such as coolant flow rate parameter $\overline{\dot{m}_l}$, combustor temperature parameter $\overline{T}_3^*$ and total thrust parameter $\overline{F}$. Embedded system step response is graphically presented in **Figures 10–13** for both of abovementioned pump driving options (red lines – electric-driven pump with CIS, green lines – engine shaft-driven pump). In terms of coolant flow rate, as shown in Figure, one has obtained for the electric-driven pump with CIS a suitable behavior, very similar to the engine shaft-driven pump, with smaller static error (around 0.38%), but with a little bigger settling time (around 3.2 s). Comparing to the basic engine, speed parameter has a different behavior (see **Figure 11**); for engine's shaft-driven injection pump one can observe a similar speed parameter

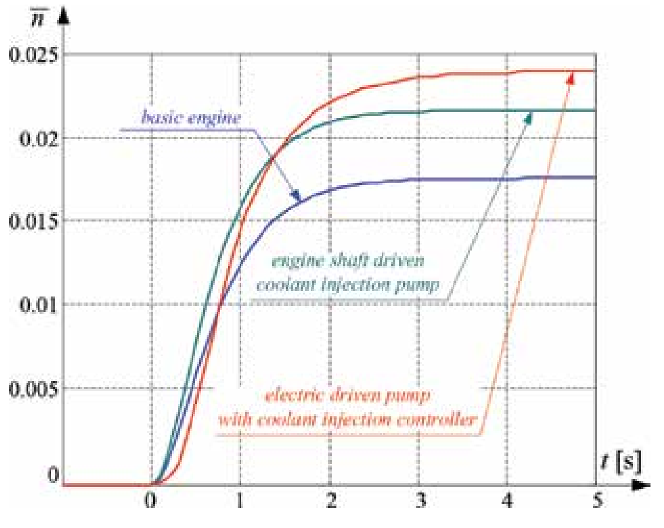

Figure 11. Comparative step response of engine speed parameters.

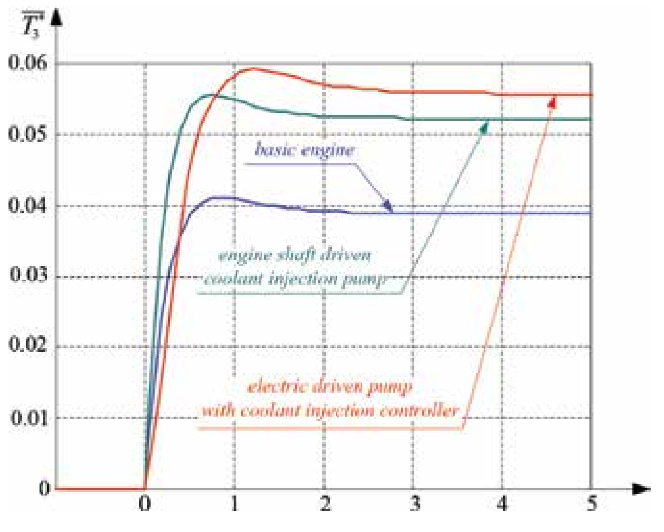

Figure 12. Comparative step response of engine combustor temperature parameters.

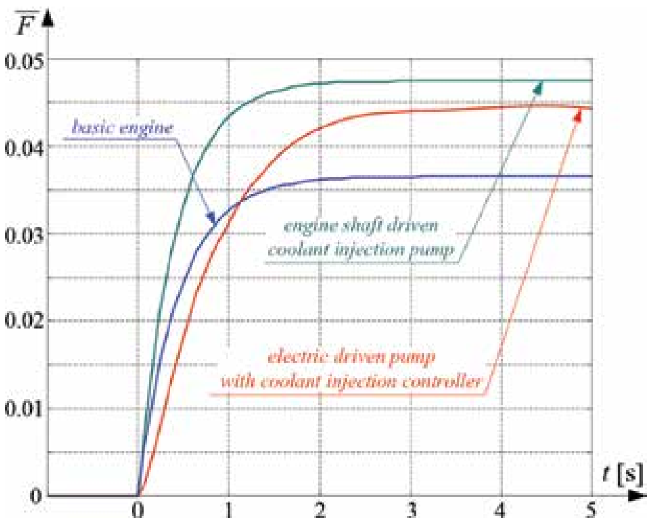

Figure 13. Comparative step response of engine thrust parameters.

behavior, but with bigger static error (2.1% than 1.7%), while for an electric driven-pump assisted by a flow rate controller (with respect to engine's compressor pressure ratio) the static error grows up to 2.35%. Settling times are also growing, from 2.5 to 3.5 s. Engine thrust parameter has a similar behavior (see **Figure 13**), following the engine speed; these are the reasons why the presence of a CIS is mandatory when an electric-driven pump is used.

Combustor temperature parameter's behavior curves show asymptotic stabilization for all studied cases (**Figure 12**), but they all have small initial overshoots; settling time has the same values as for engine speed parameter, but static errors are bigger.

3.5. Engine performance enhancement

Engine thrust expression shows that it depends on working fluid mass flow rate and velocity [1]:

$$F = \dot{m}_g C_5 - \dot{m}_a V = \dot{m}_a \left(\xi_g C_5 - V\right), \tag{72}$$

where C_5- exhaust gases velocity, $V-$ airspeed, ξ_g- gases mass fraction. Consequently, when the coolant injection is active, the terms $\dot{m}_g$ and C_5 grow, as shown in [1]: working fluid flow rate grows because of the coolant injection, while exhaust gases velocity grows because of nozzles enthalpy drop increase, as a consequence of turbine's enthalpy drop decrease. As long as the coolant injection is used only during the aircraft take-off maneuver, for short time periods, at low flight speeds and altitudes, the $V-$ term becomes very small, thus negligible, so, when the coolant injection is active, it results

$$F_i = \dot{m}_{a_i} \xi_g C_{5i} = \dot{m}_{a_i} F_{sp_i} = \dot{m}_a \frac{\pi^*_{c_i}}{\pi^*_c} F_{sp_i}, \tag{73}$$

where the $i-$ index refers to the parameters of the engine with coolant injection.

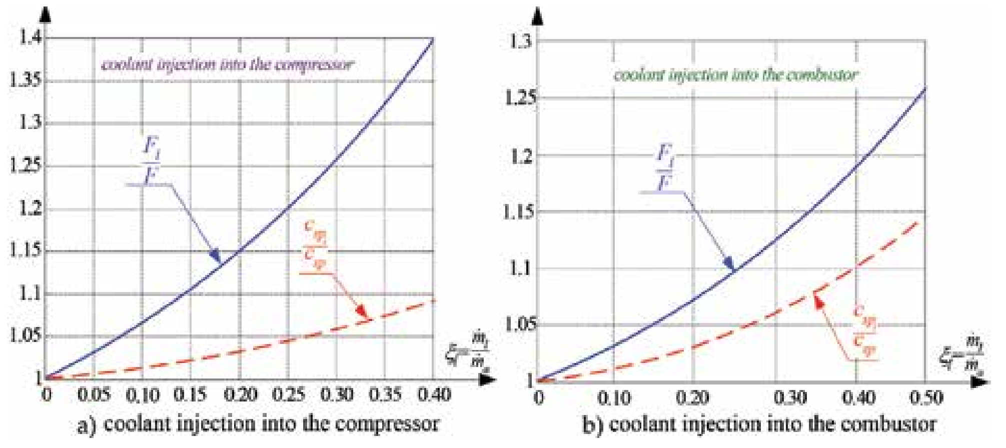

Figure 14. Gas-turbine-engine performance enhancement with respect to coolant fraction.

Figure 14a [1] presents engine's performance (thrust and specific fuel consumption) versus the coolant flow rate fraction, for a neutral injection coolant (such as distilled water). It is worth noting that, even for small injection fractions $\left(\xi_l = \frac{\dot{m}_l}{\dot{m}_a} \leq 0.04\right)$, engine's thrust increases up to 40%, while the specific fuel consumption has a moderate increase (less than 8%), which makes this method a successful one. Fuel consumption grows because of T_2^*- temperature decrease, which forces engine's fuel control system to take action to restore combustor's T_3^*- temperature and compensate the loss by additional fuel injection.

Combustible coolant injection (e.g., methanol, water–methanol mixture or other combustible fluids mixture) also generates T_2^*- temperature's decreases, but engine's fuel control system has to compensate less fuel than for neutral coolant injection, because of the coolant burning, which brings its own heat into the engine's combustor.

4. Coolant injection into gas-turbine jet-engine's combustor

Coolant injection into the combustor is the other thrust augmentation method; it is accomplished by an injection system positioned in the rear part of the burner can, near its wall (as shown in **Figure 15**). It assures a burner's wall supplementary cooling, and it facilitates the mixing of the vaporized coolant into the burned gases. If the compressor's air mass flow rate exceeds the combustor's necessary (as a consequence of the coolant injection), in order to prevent compressor's stall or surge, as well as an unstable engine operation, the combustor may have an air flow rate by-pass duct (see **Figure 15**), to evacuate the air excess [16].

In most of the practical situations, the injected coolant is distilled (pure) water, which means a neutral fluid, the injection of a combustible fluid being unnecessary, even prohibited [1, 15].

Both the mass flow and the exhaust nozzle burned gases' velocity increase cause thrust augmentation, but only up to 25%, for a coolant flow rate fraction of 5% (see **Figure 14b** [1]),

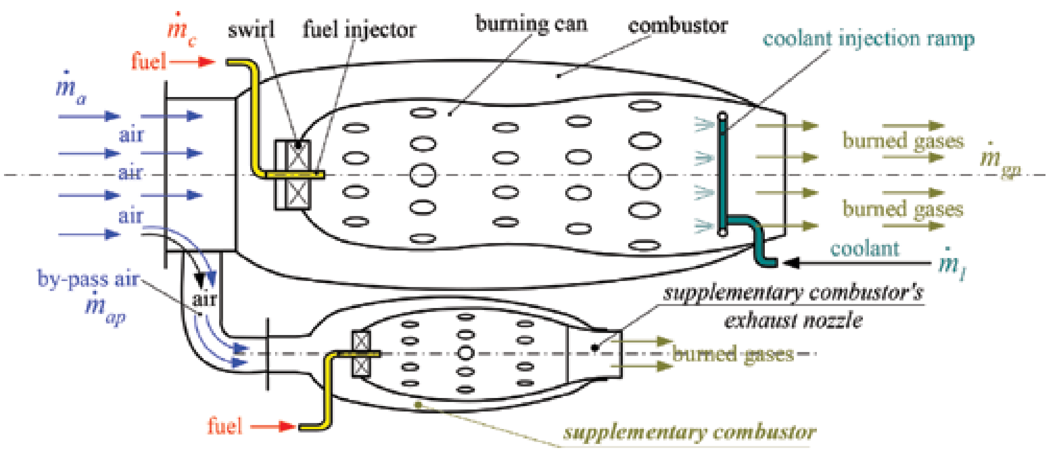

Figure 15. Gas-turbine-engine combustor with coolant injection system, air bypass and supplementary combustor.

while the specific fuel consumption grows moderately, up to 15%, which is an acceptable value considering the thrust increase advantage [1, 15]. One can observe that, comparing to the previous described injection method, this one offers less performance enhancements; however, it offers some other advantages such as constructive simplicity, icing occurring hazard elimination, as well as less blades' corrosion hazard. Method's major disadvantage [1] consists of the fact that an uncontrolled coolant injection could obstruct the burning duct, and consequently, it could impede burning deployment or even extinguish the combustor's flame.

4.1. Thermodynamic and gas-dynamic phenomena

As long as the flow in the turbine of the engine is a critical one, the flow parameter should remain constant, as Eq. (28) states; that means that, for a constant engine operation regime, the hot gases flow rate through engine's turbine must remain constant, no matter if the coolant injection operates or not. Consequently, the greater the coolant mass flow rate $\dot{m}_l$ is, the smaller the compressor air flow $\dot{m}_a$ rate must be and the gases mass flow rate must keep its value; meanwhile, it leads to an important pressure increase (both p_2^* and p_3^*) and engine's regime becomes closer to the stall limit, which is an undesirable phenomenon. Therefore, the burned gases mass flow rate equation should be

$$\dot{m}_g = \dot{m}_{ai} - m_{pr} + \dot{m}_l + \dot{m}_c, \tag{74}$$

where $\dot{m}_{ai}$ is the new compressor air mass flow rate value, smaller than the initial value $\dot{m}_a$.

In order to avoid unstable regimes and to keep the flow rate balance, even when the coolant injection system operates, one has to extract the surplus air mass flow rate $\dot{m}_{ap}$ and to by-pass it before the engine's combustor; thus, the mass flow rate equation becomes

$$\dot{m}_{gi} = \dot{m}_a - m_{pr} - \dot{m}_{ap} + \dot{m}_l + \dot{m}_c \equiv \dot{m}_g. \tag{75}$$

This surplus air mass flow rate should not be a loss for the engine; it may be used into another external, independent, supplementary combustor; it has its own exhaust nozzle and it is supplied with fuel by an additional fuel system. One has obtained a supplementary propulsion system (a complementary thrust augmentation method), which offers its own thrust, added to the basic engine's thrust.

4.2. Engine's mathematical model and quality study

One may observe that, comparing to the basic engine's model, the equations which change are the same as for the previous described method, meaning that both mass flow rate equation and combustor's equation are to be modified. Therefore, formally, mathematical model's equations are the same in subSection 3.2.1, but the coefficients' values should be calculated considering the new values of the air flow rate, injection fraction, temperature(s) and pressure (s), as presented in [16].

A quantitative study was performed and described in [16], based on a VK-1A-type jet engine, but a completion of the study, concerning the possibility of the supplementary combustor adding (with its own fuel control system), was performed and presented in [15].

One has studied the common case of a neutral coolant (distilled water) injection into the rear part of the engine's combustor [16], which gave as results for outputs as follows:

$$\overline{n}(\mathrm{s}) = \frac{1.411\,\overline{\dot{m}_c}(\mathrm{s}) - 0.167\overline{\dot{m}_I}(\mathrm{s})}{2.3761\,\mathrm{s} + 4.817}, \tag{76}$$

$$\overline{T_3^*}(\mathrm{s}) = \frac{(1.8732\,\mathrm{s} + 2.847)\overline{\dot{m}_c}(\mathrm{s}) - (0.0823\,\mathrm{s} + 0.0764)\overline{\dot{m}_I}(\mathrm{s})}{2.3761\,\mathrm{s} + 4.817}, \tag{77}$$

$$\overline{F}(\mathrm{s}) = \frac{(1.583\,\mathrm{s} + 5.167)\overline{\dot{m}_c}(\mathrm{s}) - (0.0834\,\mathrm{s} + 0.4725)\overline{\dot{m}_I}(\mathrm{s})}{2.3761\,\mathrm{s} + 4.817}. \tag{78}$$

Engine step responses are depicted in **Figures 16–18**; one has realized a comparison between the basic engine behavior (as described in [5]) and the engine with thrust augmentation systems, as described by the Eqs. (44)–(46), respectively by the Eqs. (76)–(78).

No matter the coolant injection method, engine's speed parameter is less influenced, as the small $n-$ parameter increases as shown in **Figure 16**. Coolant injection into the combustor brings less speed changes than coolant injection into the compressor, but with a little longer settling time (about 0.5 s); that means that, comparing to the basic engine, it has become a little bit slower. From the response time point of view, coolant injection into the compressor makes the engine a little, but insignificant, faster.

In terms of temperature's parameter behavior (see **Figure 17**), it is noteworthy that, no matter the coolant injection method, it has the same trend as for the basic engine, but bigger initial overshoots, following the initial supplementary fuel injection, meant to restore combustor's T_3^*- temperature.

Engine's thrust parameter behavior (see **Figure 18**) has moderate increases, no matter the injection method. A cause should be the coolant nature, a neutral coolant could not assure additional heat into engine's combustor, thus the thrust augmentation is realized only by the

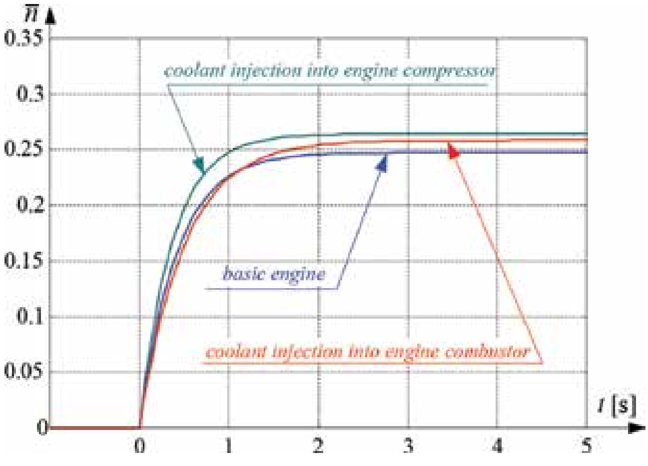

Figure 16. Comparative step response of engine speed parameters.

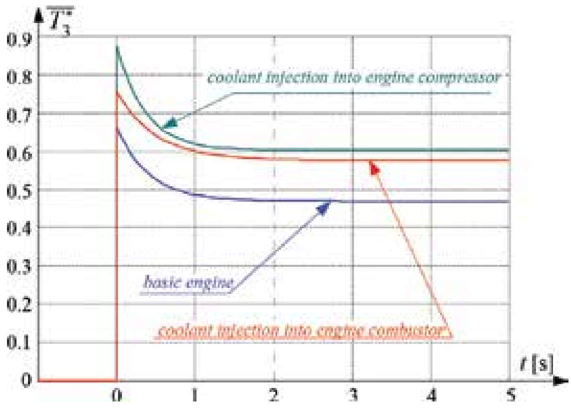

Figure 17. Comparative step response of engine combustor temperature parameters.

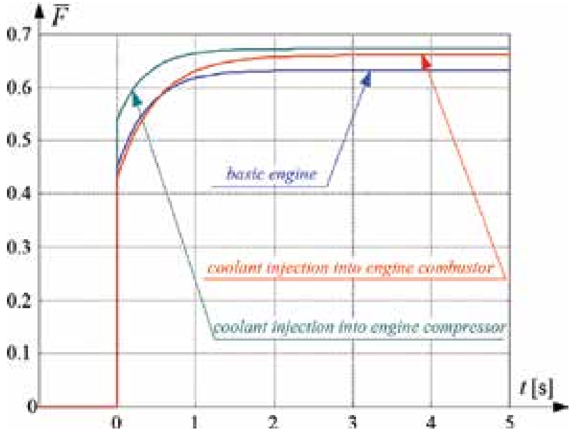

Figure 18. Comparative step response of engine thrust parameters.

http://dx.doi.org/10.5772/intechopen.76856

airflow and gases velocity increases. Coolant injection into the compressor assures a more rapid thrust increase, while growing percentage is near the same for both described injection methods.

5. Conclusions

Between the nowadays issues of aircraft engine design and manufacturing, thrust augmentation, along with operational safety, are some of the most important ones; if the classic over-boost method by afterburning is impossible or too expensive to be adapted (e.g., for turboprops or twin-jet turbofans), coolant injection method(s) shall be used, for temporarily thrust increase. As a result, when the coolant injection system is operational, engine performance temporarily improves, which means a spectacular thrust increase (from 25–40%) and moderate specific fuel consumption increase (8% up to 15%), depending on the used injection method [1].

Comparing to the afterburning, which assures spectacular thrust augmentation (up to 65% for single jets, up to 100% for twin jets) but also significant specific fuel consumption increases (from 50% up to 110%) [1, 2, 4], coolant injection is a less expensive augmentation method, even only from the fuel consumption point of view, offering acceptable performance enhancement and less design and constructive issues. In fact, the afterburning is the choice for supersonic aircraft engines; today it is widespread among combat aircraft engines (for supersonic fighters) and practically misses from transport aircraft, no supersonic jetliner being actually in service. Moreover, supersonic aircraft engines uses the afterburning at low regimes even for cruise flights, which makes of it another propulsion system, with its own controller, but using the same fuel and the working fluid provided by the basic jet engine. Obviously, afterburning's implementation involves significant design effort and manufacturing expenses, so its usage is entitled by the specific necessity of the engine, according to aircraft destination(s) and mission(s).

Coolant injection remains a suitable alternative, meant to equip gas-turbine engines without afterburning adapting possibilities, but who need temporarily thrust increasing, especially for take-off, when total thrust is affected by excessive atmospheric conditions, or/and aircraft's payload has high values, close to its maximum limit. Injection system design, manufacturing and implementation is significantly less expensive than for the afterburning; however, the coolant is, obviously, a different fluid than the fuel, which should be stored in a special tank; consequently, aircraft or/and engine architecture must change and, because of coolant stored additional mass, aircraft fuel storage capacity must diminish, which reduces aircraft maximum flight range. These are reasons for optimization studies, concerning the coolant injection mass flow rate, injection strategy and duration and storage tank's capacity.

One has studied aircraft jet engine with coolant injection as a controlled object, from system's theory point of view, identifying its input(s) and output(s), as well as some control architectures implementation possibilities. Both coolant injection methods' implementation involves thermo- and gas-dynamics engine changes, concerning the air and burned gases mass flow rate, as well as the heat exchange balance. Consequently, engine's model as controlled object changes too, as well as its stability and quality. One has highlighted the mathematical model modifications of the engine with coolant injection, starting from basic engine's model, then describing engine’s control schemes by block diagram with transfer functions; based on it, some simulations were performed and comparative studies of stability and quality were realized.

Studies have proven that small-to-moderate used injection fraction values and suitable control methods and architectures keep the engine as a stable system; static errors have grown, as well as settling times, but still remaining in the acceptable rank of values. Based on the emphasized engine’s changes, embedded engine control systems may be designed and optimized, even during the early design stages (pre-design).

Coolant injection into the compressor, in spite of its icing hazard and other disadvantages, if assisted by a properly designed pump and controller, is an excellent thrust increase method for take-off (especially for turboprops), better rated than coolant injection into the combustor (considered suitable for turbojets and higher altitudes flights) [1, 2].

Studies were performed for a single-spool single-jet engine at sea-level atmospheric conditions and take-off air speed, but can be extended for other engine-types (two-spool, twin jets, turbofans) or for other altitudes and cruise speeds.

Author details

Alexandru Nicolae Tudosie

Address all correspondence to: atudosie@elth.ucv.ro

Department of Electrical, Power Systems and Aerospace Engineering, University of Craiova, Romania

References

[1] Pimsner V. Air-Breathing Jet Engines. Processes and Characteristics. Bucharest: Didactic and Pedagogic Publishing; 1983. 387 p

[2] Mattingly JD. Elements of Gas Turbine Propulsion. New York: McGraw-Hill; 1996. 867 p

[3] Stoicescu M, Rotaru C. Turbo-Jet Engines. Characteristics and Control Methods. Bucharest: Military Technical Academy Inprint; 1999. 314 p

[4] Hill PG, Peterson C. Mechanics and Thermodynamics of Propulsion. New York: Addison - Wesley Publications; 1993. 524 p

[5] Tudosie AN. Aerospace Propulsion Systems Automation. University of Craiova Inprint; 2005. 290 p

[6] Rotaru C, Andres-Mihăilă M, Matei PG. An extended combustion model for the aircraft turbojet engine. International Journal of Turbo & Jet Engines. 2014;**31**(3):229-237. DOI: 10.1515/tjj-2013-0048

[7] Jaw LC, Mattingly JD. Aircraft Engine Controls. Design, System Analysis and Health Monitoring. AIAA; 2009. p. 361

[8] Berbente C, Constantinescu NV. Gases dynamics. Vol. I, II. Politehnica University in Bucharest Inprint. 1985:436

[9] Rotaru C, Edu IR, Andres-Mihaila M, Matei P. Applications of multivariable control techniques to aircraft gas turbine engines. Review of Air Force Academy. 2014;**2**(26):45-50

[10] Tudosie AN. Mathematical model for a jet engine with cooling fluid injection into its compressor. In: Proceedings of International Conference of Scientific Papers (AFASES 2014), volume I; 22–24 May 2014; Brasov; 2014. pp. 265-272

[11] Rotaru C, Sprințu I. State Variable Modeling of the Integrated Engine and Aircraft Dynamics. In: 10th International Conference on Mathematical Problems in Engineering, Aerospace and Sciences (ICNPAA 2014), Vol. 1637; 2014. pp. 889-898. DOI: 10.1063/1.4904661

[12] Tudosie AN. Speed Control System For A Jet-Engine With Fluid Injection Into Its Compressor. Proceedings of the 12th International Conference on Applied and Theoretical Electricity (ICATE 2014); 23-25 Oct. 2014; Craiova. IEEE; 2015. pp. 1-6

[13] Tudosie AN. Aircraft gas-turbine Engine's control based on the fuel injection control. In: Max Mulder, editor. Aeronautics and Astronautics. Croatia: Intech Open Access Publisher, 2011. pp. 305-330

[14] Tudosie AN. Aircraft Engine With Coolant Injection Into Its Compressor And Flow Rate Controller As Controlled Object. Proceedings of the 13th International Conference on Applied and Theoretical Electricity (ICATE 2016); 6–8 Oct 2016; Craiova. IEEE; 2016. pp. 1-6. DOI: 10.1109/ICATE.2016.7754686

[15] Tudosie AN. Supplementary Fuel Control System For A Jet-Engine With Fluid Injection Into Its Combustor. Proceedings of the 12th International Conference on Applied and Theoretical Electricity (ICATE 2014); 23-25 Oct. 2014; Craiova. IEEE; 2015. pp. 1-6

[16] Tudosie AN. Mathematical model for a jet engine with cooling fluid injection into its combustor. In: Proceedings of International Conference of Scientific Papers (AFASES 2014), volume I; 22–24 May 2014; Brasov, 2014. pp. 273-280

Chapter 5

Stator-Rotor Interaction in Axial Turbine: Flow Physics and Design Perspective

Paolo Gaetani

Additional information is available at the end of the chapter

http://dx.doi.org/10.5772/intechopen.76009

Abstract

The stator-rotor interaction is an important issue in turbomachinery design when the highest performances are targeted. Different characters mark the interaction process in high-pressure or low-pressure turbines depending both on the blade height and on the Reynolds number. For small blade heights, being the stator secondary flows more important, a more complex interaction is found with respect to the high blades, where the stator blade wake dominates. In low-pressure turbines, the stator wake promotes the transition to turbulent boundary layer, allowing for an efficient application of ultra-high lift blades. First, a detailed discussion of the flow physics is proposed for high- and low-pressure turbines. Some off-design conditions are also commented. Then, a design perspective is given by discussing the effect of the axial gap between the stator and the rotor and by commenting the effects of three-dimensional design on the interaction.

Keywords: stator-rotor interaction, axial turbines, wake-wake interaction, vortex-blade interaction, high-pressure stages

1. Introduction

The design of high efficiency axial flow turbine stages has to face many challenging problems, and one of these is connected to the interaction between the stationary and the rotating rows of the machine. In high-pressure gas turbines, additional issues related to the combustor-turbine interaction take laces leading to further complexity in the design process.

The overall context for the design space is, in fact, an unsteady and three-dimensional flow field, where the Mach and the Reynolds numbers vary along the machine. High-pressure stages typically operate in high-subsonic or transonic regimes and are normally affected by

IntechOpen

© 2018 The Author(s). Licensee IntechOpen. This chapter is distributed under the terms of the Creative Commons Attribution License (http://creativecommons.org/licenses/by/3.0), which permits unrestricted use, distribution, and reproduction in any medium, provided the original work is properly cited.

shock-induced separation on the rotor crown and unsteady stator rear loading [1]. Moreover, the high-loading, combined to the low aspect ratio of the first stage blading, drives the generation of wide swirling structures, whose mixing contributes significantly to the loss budget [2]. These secondary flows also affect the flow angle distribution and momentum redistribution inside the blade channel and their accurate prediction is fundamental for the designer of the gas turbine cooling system [3].

All of these flow structures affect the blade cascade where they are generated and the adjacent ones in the so-called stator-rotor interaction process. To make clear such a complex flow feature, all of them will be recalled and schematised according to what are available in the open literature.

The primary flow structures involved in the interaction process are the wake and the secondary flows. Many research studies have been proposed in the open literature discussing the wake and the secondary flow evolution and their parametric dependence on the typical turbomachinery parameters (among others, [4–9]).

The interaction process has been addressed in the last 20 years by many authors both for the high-pressure stages and for the low-pressure ones. Differences between high- and low-pressure stages arise for the dependence of the boundary layer and its transition on the Reynolds number.

When the high-pressure stages are of concern, the interaction takes place mainly in terms of shock wave, wake and secondary flows, leading to the so-called wake-blade and vortex-blade interaction. Thanks to the high Reynolds number and high inlet turbulence levels [10], the blade boundary layer state is less influenced by the incoming viscous structures (among others [11–21]). It has to be taken into account that also the inlet boundary layer properties may cause some pressure fluctuation on the cascade loading, as discussed in [22].

Low-pressure stages, on the contrary, are very sensitive to Reynolds number effects. The wakes coming from the upstream cascade periodically act as a trigger for the boundary layer transition from laminar to turbulent conditions. Such periodic transition, possibly re-laminarization, is beneficial in preventing the boundary layer separation and this allows for higher loading. In this context, ultra-high lift blade can be proficiently applied either to reduce the aero-engine weight or to power the fan (among others [25–28]).

All these issues have been addressed both experimentally and by proper CFD simulations; experiments require high promptness instrumentation like FRAPP (among others [29–32]) or LDV and PIV. Simulation, as well, requires high performance codes and schemes able to face the sliding of rotors with respect to the stationary components.

In order to gain a general perspective and to quote the importance of the interaction on the cascade aerodynamics, the reduced frequency concept has been introduced. It refers to the ratio between the time scale of the unsteadiness (typically: Ss/U, where Ss is the stator pitch and U is the rotor peripheral speed) and the one related to the transport of the mass flow across the device (i.e. b/Vax where b = axial chord and Vax = the mean axial velocity component). The reduced frequency definition then is: $f = (b\ U)/(S_s\ Vax)$. When $f << 1$, the process can

http://dx.doi.org/10.5772/intechopen.76009

be considered as steady and its time variation related to U can be approximated as a sequence of steady state. When $f >> 1$, the process is dominated by the unsteadiness. Finally, when $f \approx 1$, the unsteady and quasisteady processes have the same order of magnitude and importance. In many cases, turbomachinery work is in the range of $f \approx 1$ while for example the combustor-1° stage interaction lies in the quasisteady conditions [33].

In the present contribution, the focus is given mainly to the gas turbines geometries and operating conditions, even though the same mechanism can be applied to steam stages. As already introduced by the title, the core of this contribution is devoted to the general discussion of the flow physics, rather than on the quantification and on the detailed description of the specific issues: this way, in author's opinion, once the general aspects are acknowledged, the detailed issues - as discussed in papers here referenced - can be properly understood.

Finally, the discussion will be on a single stage, constituted by a stator and a rotor, taken as a representative for the whole machine. In the case of multistage turbomachines, the flow field discharge by the rotor will affect, with the same mechanics described in the following, the subsequent stator. Additionally, there could be some "clocking" features between stators and rotors that may alter the single stage performance.

Experimental results have been taken by means of a steady five holes probe and fast response aerodynamic pressure probe (FRAPP) on the high-pressure axial turbine located at the laboratory of fluid-machinery (LFM) of the Politecnico di Milano. More information on the rig and measurement techniques is reported in [14, 15, 29, 31]. It is important to stress that the FRAPP is applied in a stationary frame and gives the phase resolved total and static pressure (and hence the Mach number) and the flow angle; then, by assuming a negligible effect of the temperature fluctuations, the relative Mach number and, by this, the relative total pressure are calculated.

CFD results have been obtained on the same HP turbine geometry by means of fluent code.

2. Stator-rotor interaction in axial stages

The stator-rotor interaction features different characters if occurred in high-pressure or low-pressure stages.

In low-pressure stages, thanks to the high blade height, the main interaction element is the wake in a general low-Reynolds environment.

On the contrary, high-pressure stages are typically characterised by small blade heights, due to the high mean density and by a stream with high Mach and Reynolds numbers and high mean temperatures.

As in all stages, the wake generated by the stator impinges on the rotor blades being an important source of interaction, but—due to the specific features of HP stages–other sources of interaction are present.

The small blade height has the primary impact of powering the effects of the secondary and clearance flows; in fact, they cannot be considered as negligible and modifies the potential flow pattern for a large amount of the blade span. From the stator-rotor interaction perspective, this feature makes the problem much more complex as an additional source of interaction takes place.

A common feature of the different kind of secondary flows is to be connected to loss cores, as found for wakes. However, secondary flows are also vortical structures and hence characterised by vorticity whose sense of rotation is different among the different vortices. Therefore, in the analysis of the interaction mechanism, this last feature has to be properly taken into account.

Mach number typically modulates the intensity and position of the swirling cores [7] and, if supersonic, sets the shock wave pattern discharged by the cascades.

The Reynolds number, typically high and for this the flow can be regarded as turbulent, mainly sets the interaction between the incoming structures and the rotor blades boundary layers.

As mentioned earlier, to aid the reader in the comprehension, the different kinds of interaction are discussed separately.

2.1. Stator wake-rotor blade interaction

The stator wake can be regarded either as a velocity defect or a loss filament.

According to the first approach, the velocity triangle composition shows a very different direction and magnitude for the relative velocity. **Figure 1** shows the triangles for the free stream and for the wake flow; it is evident how the relative velocity of the wake flow (W_W) heads towards the blade suction side, featuring also a negative incidence on the rotor blade.

According to the second approach, the wake has no streamwise vorticity associated to it, being the only vorticity present related to the Von Karman street, whose axis is parallel to the blade span. Once the wake interacts with the downstream rotor blade, it is bowed and then chopped by the rotor leading edge. Later on, it is transported inside the rotor channel, being smeared and showing two separate legs: one close to the suction side and one to the pressure side. Globally, the wake is pushed towards the rotor suction side by the cross-passage pressure field and, possibly, its suction side leg may interact with the blade boundary layer, this feature depends mainly on the rotor loading.

Figure 2 shows the wake in terms of entropy filament, as computed by CFD in 2D – 1 × 1 case. Downstream of the rotor blade, the wake typically appears as a distinct loss core close to the rotor wake or as a part of the rotor wake; this option is strictly dependent also on the axial position downstream of the rotor where the analysis is done. For this reason, in some papers [12, 13, 15–18] this mechanism is acknowledged as "wake-wake" interaction.

Being the rotor blade different in number with respect to the stator one, different rotor channels experience the interaction in different time even though the basic mechanism does not differ.

http://dx.doi.org/10.5772/intechopen.76009

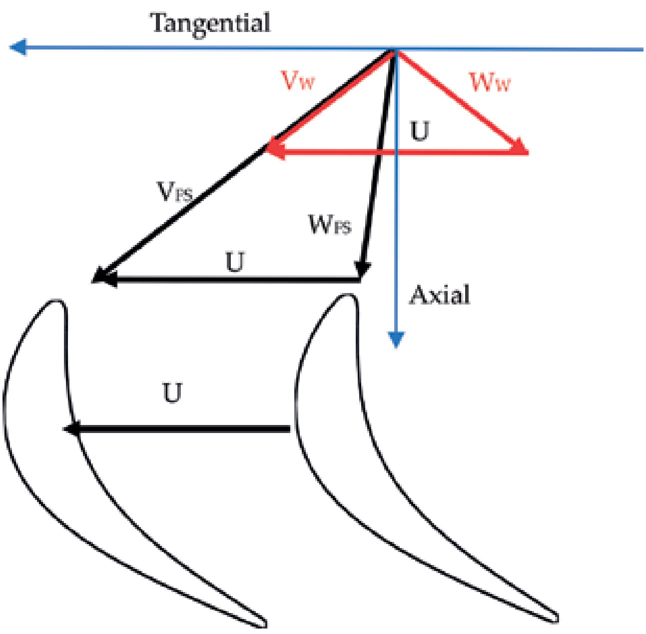

Figure 1. Velocity triangles for the free stream (subscript FS) and the wake (subscript W) flows. V = absolute velocity, W = relative velocity, U = peripheral velocity.

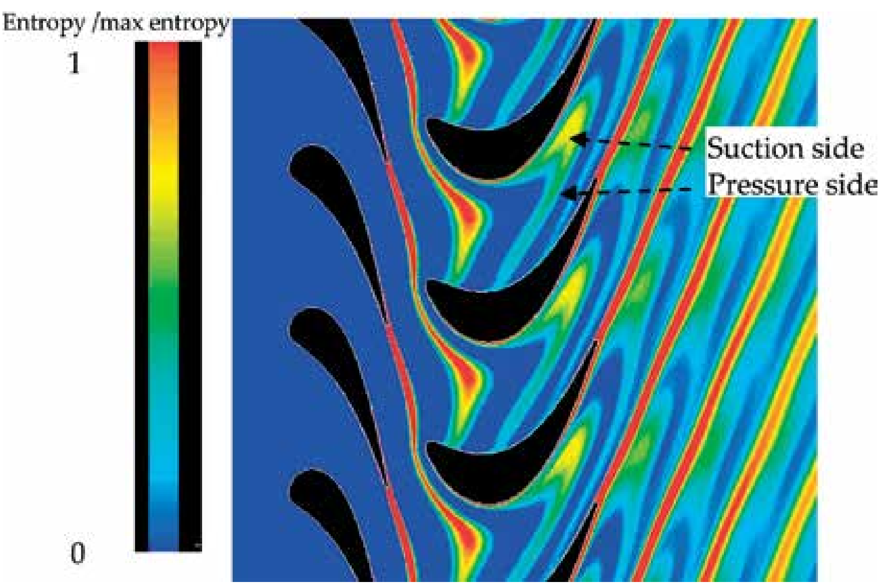

Figure 2. Pattern of entropy evolution (bowing, chopping and transport) of the stator wake in the rotor channel, as foreseen by CFD.

The rate of the interaction depends on the stator wake intensity, that is, on the stator loading, on the blade trailing edge thickness, on the axial stator-rotor gap, on the Reynolds numbers and, for cooled blade, on the kind of cooling applied.

In case of low pressure turbines, where typically the Reynolds number is low, as for the aero-engine cases, the wake – wake interaction is in fact the only effective mechanism. Its importance grows as the Reynolds number decreases and specifically, the incoming wakes, once interacting with the suction side boundary layer, promotes the laminar to turbulent transition. Such a transition, on one hand increases losses but on the other hand increases the boundary layer capability to face adverse pressure gradient and for this delaying the boundary layer separation and hence the blade stall. Thanks to this mechanism, aero-engines low-pressure stages have seen an increase of loading and for this a reduction of weight, either for a reduction of solidity or overall number of rows [25, 26].

It has to be recalled that this mechanism constitutes an aerodynamic forcing on the rotor blade whose frequency depends on the stator blade passing frequency that is in the rotating frame of reference the frequency which the rotor sees the stator wake passing ahead.

2.2. Stator secondary flows-rotor blade interaction

The basic mechanism for this kind of interaction is the same of the wake-blade one, the vortical filament is bowed, chopped and hence transported in the rotor channel. Notwithstanding such similarity, two main differences can be acknowledged. The vortical structure has its own streamwise vorticity in terms of magnitude and sense of rotation and for this a different interaction and impact with the rotor can be expected depending on the entering position in the rotor channel. Moreover, the vortex entering in the rotor channel is a flow structure specifically localised along the blade span and pitch, whereas the wake is distributed along the span.

It has to be recalled, without aiming at being exhaustive, that different swirling structures can be acknowledged downstream of the stator, as depicted in **Figure 3** and discussed in [6]. The main ones are the passage vortices, located symmetrically at tip and hub, activated by the pressure gradient across the passage and hence directed from the pressure side to the suction side. These vortices have a wide extension but typically low intensities (i.e. vorticities). At the same time, the presence of the inlet boundary layer activates also the horseshoe vortices, two legs per endwall. Coupled to each passage vortex, the shed vortex can be found, activated by the interaction between the passage vortex and the low momentum fluid belonging to the blade wake. The two passage vortices have opposite sense of rotation. The two horseshoe vortex legs have opposite sense of rotation between them and the pressure side leg is co-rotating to the corresponding passage vortex.

Passage and horseshoe vortices start their growing at the stator leading edge and continue it along the stator channel, possibly merging among them or smearing depending on the stator loading and on the inlet boundary layer thickness.

The shed vortex, being activated by the viscous transport, starts growing at the stator trailing edge at the expense of the passage vortex swirling energy, reaches its highest intensity in about half chord and then weakens due to the viscous stress that smoothens the velocity gradients. Its sense of rotation is opposite to the one of the corresponding passage vortex.

http://dx.doi.org/10.5772/intechopen.76009

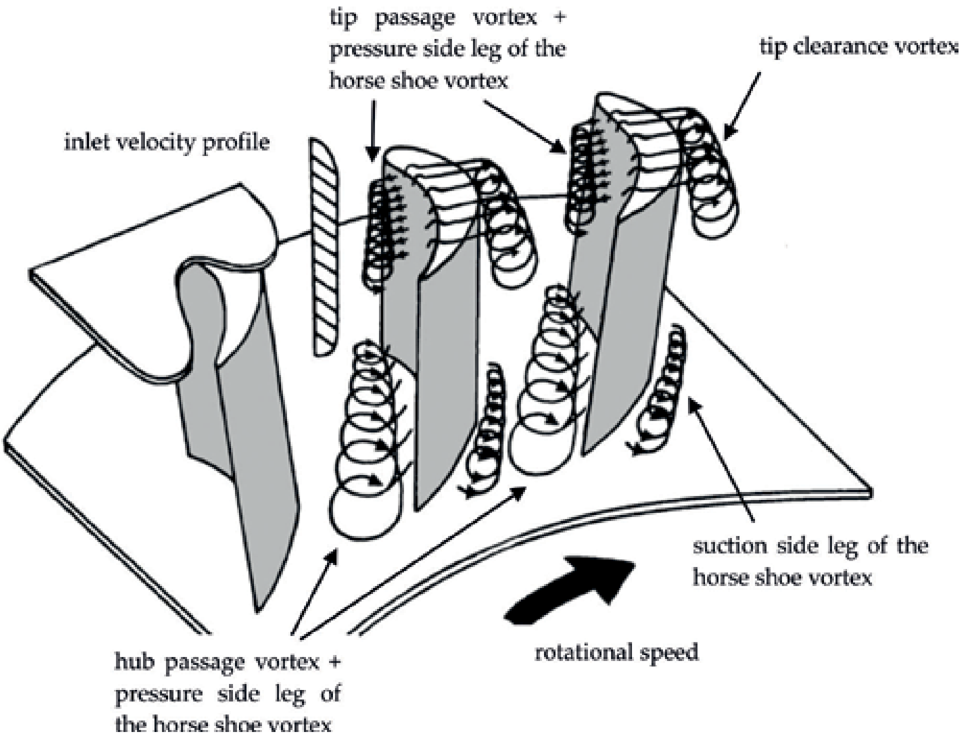

Figure 3. Simplified schematic of the secondary flows system downstream of a rotor.

Tip clearance vortex may be present depending on the sealing geometries of the stator and of the rotor. Typically, it is located at the hub in stators while it is at the tip in rotors, this latter case being much more important and frequent. Its sense of rotation is opposite to the passage vortex, being directed from the pressure side towards the suction side across the blade.

It is important to underline that all these swirling flows are present both in stators and in rotors, but with opposite sense of rotation as a consequence of the different cross pressure gradient versus in the two channels.

The secondary flow magnitude and position, besides the difference related to the tip clearance, is different between the hub and the tip. In fact, the radial equilibrium, that onsets due to the tangential component downstream of the stator, makes the static pressure at the tip higher than at the hub and for this a higher Mach number at the hub. The effect of the Mach number is well known and primarily documented by Perdichizzi [7]. Moreover, the pressure gradient acts to diffuse and to shift centripetally the vortical structures at the tip and to confine close to the endwall the hub ones.

Possible incidence angles to the stator additionally modulate the secondary flows. Positive incidence angle strengthens secondary flows, as well as lower solidities, as a consequence of the higher blade loading. Among others, a global review is reported in [8].

The flow entering the rotor is then highly three dimensional and complex, as depicted in **Figure 4**. In the case presented in **Figure 4**, by the total pressure loss coefficient and the vorticity, the passage vortices, the shed vortices and a corner vortex can be acknowledged. The Mach number map is also proposed to show the reduction due to the viscous effects of the wake and vortices and the modulation by the potential field.

To get the rotor perspective, unsteady measurements performed in the stator-rotor axial gap are reported in **Figure 5**. Such measurements, taken by FRAPP, have been plotted by applying a phase-averaging technique and a phase-lag reconstruction. The rotor pitch being smaller than the stator one, the stator wake in some instant occupies more than half of the rotor pitch, as clearly evidenced by the total pressure loss map (**Figure 5a**). The condition of constant inlet total pressure both in the absolute and in the relative frame is, so far, an unrealistic condition; **Figure 5b** shows the periodic nonuniformities throughout the relative total pressure coefficient ($C_{PT,R}$).

To aid the reader comprehension, it is first introduced that, given such complex and stator dependent flow, in this chapter, only the basic flow physics is described; in fact, the scope is to provide tools for the fluid dynamic understanding rather than a unique explanation.

As introduced at the beginning of this paragraph, the basis of the interaction between the vortex filament and the rotor blade field can be considered as not really different with respect

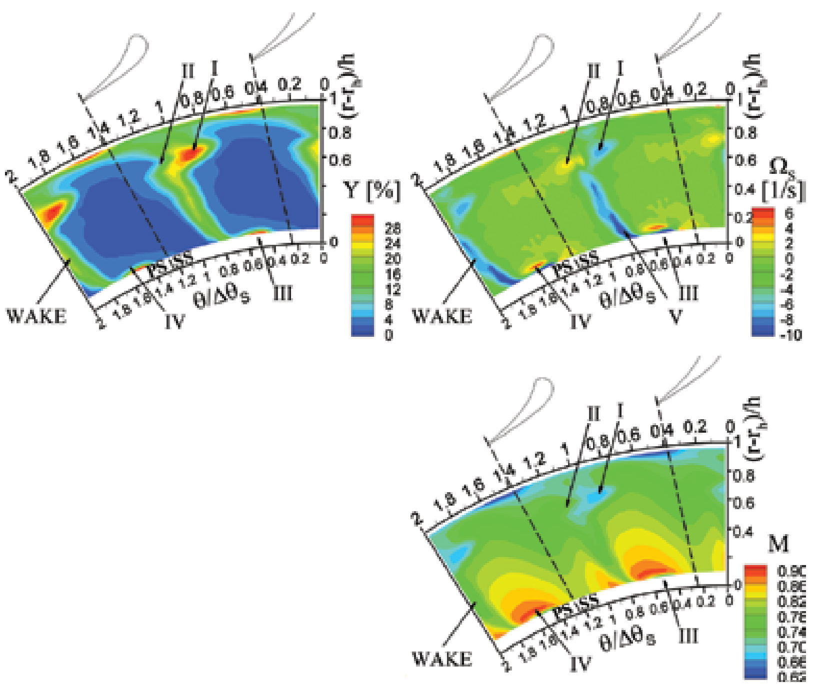

Figure 4. Total presure loss (Y%), streamwise vorticity (Ω_s) and absolute Mach number (M) downstream of the stator. Experiments at the Fluidmachinery Lab. at Politecnico di Milano (Italy).

http://dx.doi.org/10.5772/intechopen.76009

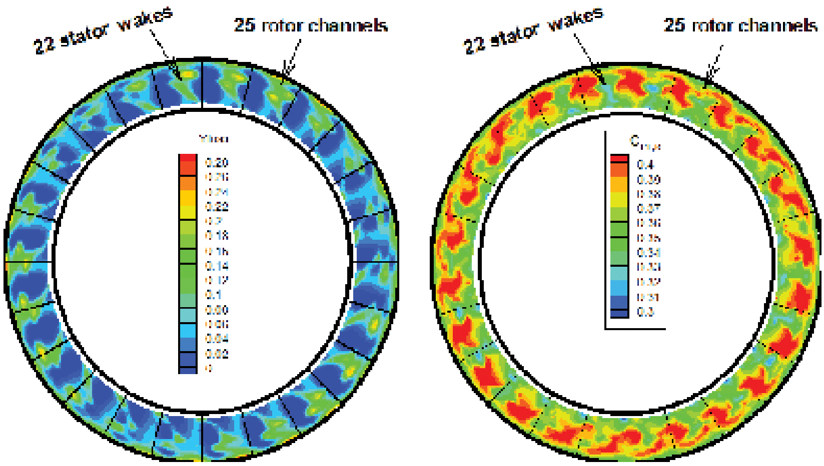

Figure 5. Rotor inlet flow field in the rotating frame of reference. Frame (a) Yloss = total pressure loss. Frame (b) $C_{PT,R}$: relative total pressure coefficient. Experiments at the Fluidmachinery Lab. at Politecnico di Milano (Italy).

to the wake one. The huge difference consists of the streamwise vorticity that characterises the vortical filament. Reader can refer to [11–13, 15–18, 20, 21] for this topic.

Once the swirling filament is bended in the rotor channel, the pressure side leg sense of rotation changes while the suction side leg preserves the original one (**Figure 6**). Moreover, being the suction side leg accelerated by the overspeed on the rotor section side, its vorticity increases; on the contrary, the pressure side leg decreases and it is smeared out along its transport.

Once the vortical structures enter the rotor channel, they interact both with the passage pressure field and with the rising vortical structure of the rotor itself. So far, the stator tip passage vortices, being opposite to the rotor one, tend to weaken it (and the same occurs for the hub ones). On the contrary, the stator shed vortex, being co-rotating with the rotor passage one will strengthen it.

Swirling flows structure entering in the rotor close to the endwalls will have stronger effects on the rotor secondary flows generations; on the contrary, the ones entering far from endwalls will interact in the downstream portion of the channel.

Moreover, the pressure side legs, as their sense of rotation is opposite with respect the original one, will undergo the opposite interaction features.

As the stator vortical structures enter the rotor periodically, with a frequency in the rotor frame equal to the stator blade passing one, the interaction process takes places periodically and this generates a pulsation of the rotor field.

Before discussing in detail the different time frames, it is straightforward to consider first the mean flow (**Figure 7a** and **b**): the $C_{PT,R}$ coefficient is in fact the total pressure in the relative frame and this evidence the loss cores generated in the rotor and in the stator. The wide low $C_{PT,R}$ region is mainly due to the rotor wake with some strengthening and enlargement due to the rotor secondary vortices (tip clearance and tip/hub passage vortex). The vortical

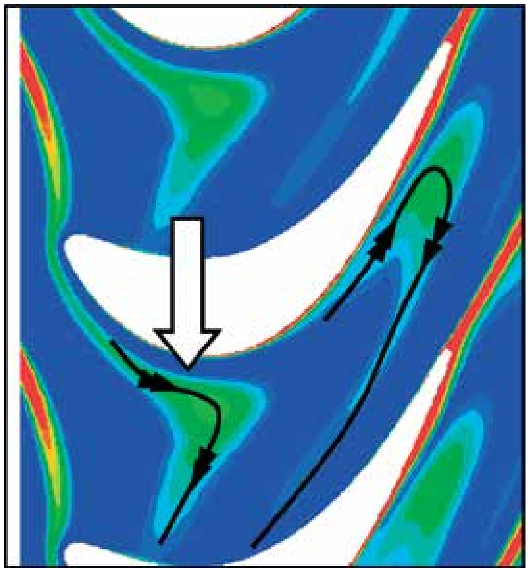

Figure 6. Skematics of the stator vortical structure transport in the rotor passage.

structures can be acknowledged by making use of the Rankine vortex model [34] applied to the deviation angle map and reported in **Figure 7b**. The clearance flow experiences a positive deviation angle as it is less deflected by the blade than the main flow. At the same time, the cross flow activated at the hub by the transversal pressure gradient, generates higher flow deflection and for this a negative deviation angle is found.

However, the time mean flow field differs from the instantaneous one due to the interaction process.

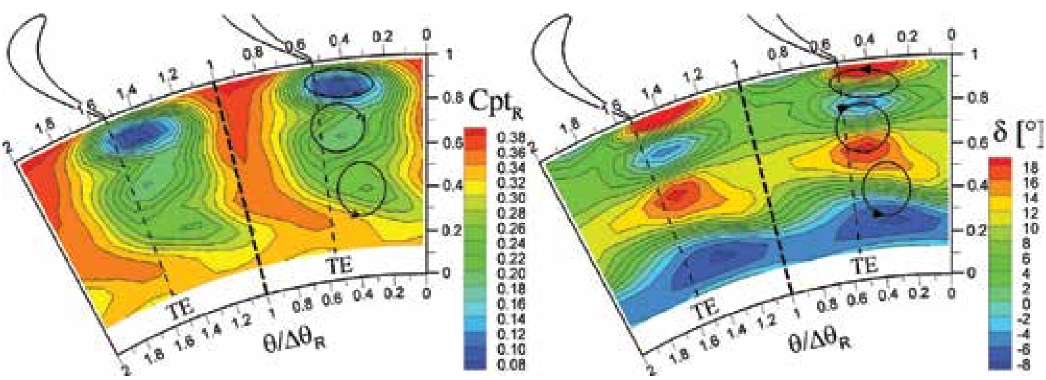

Figure 7. Time mean flow field downstream of the rotor for a subsonic operating condition (expansion ratio 1.4, reaction degree at midspan 0.3 and incidence angle close to zero). Frame (a) relative total pressure coefficient ($C_{PT,R}$); frame (b) deviation angle (δ). Experiments at the Fluidmachinery Lab. at Politecnico di Milano (Italy).

Figure 8 shows different time frame of the flow field discharged by the rotor. The full rotor crown has been calculated by applying a phase leg technique to the experimental results, measured downstream of the rotor for different stator/rotor phases over one stator pitch.

It is clearly shown in **Figure 8** how the 25 channels of the turbine rotor experience different flow conditions, each of them different with respect to the time mean one.

The tip region, being dominated by the tip clearance vortex is weakly sensitive to the periodic flow evolution. On the contrary, the midspan/hub region is strongly periodically pulsating. Being the stator (n° 21) and rotor blades (n° 25) prime numbers and given that the closest periodicity is around one-thirds, the pattern evidences a periodicity every 120°.

By considering the total pressure unresolved unsteadiness, calculated as the standard deviation of the total pressure for each phase and position in the measuring plane [31], the turbulent structure can be acknowledged: for this it will be considered as the turbulence (Tu). Some of them are rotor dependent, like the rotor wake, clearance flows and rotor secondary flows; other structures, on the contrary have a clear periodic evolution with some instant where they do not exist.

Figure 9 reports different instants of the rotor evolution for three quantities: the relative total pressure coefficient, the deviation angle and the unresolved unsteadiness. With respect to the time averaged flow reported in **Figure 7** (for the same operating condition), the relative total

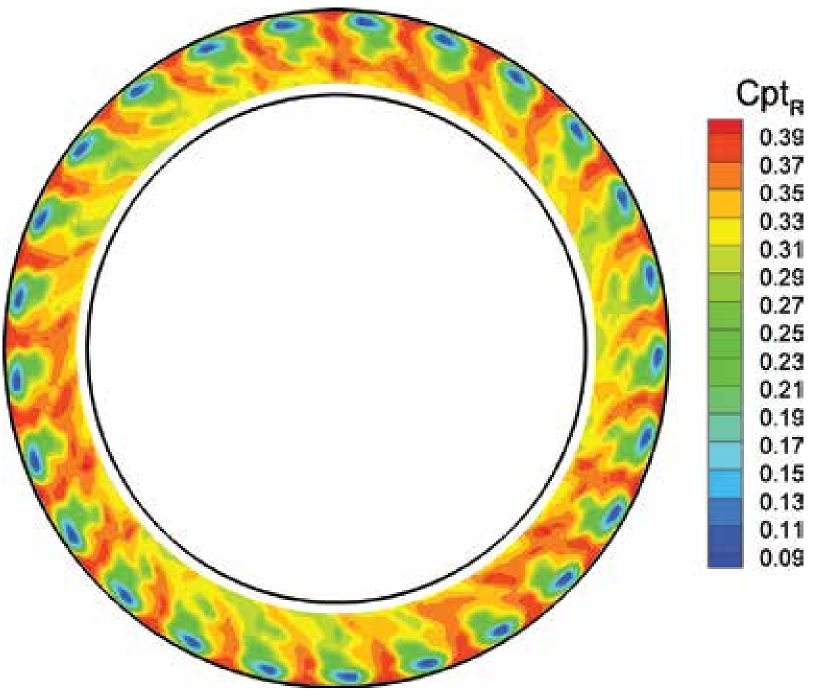

Figure 8. Relative total pressure coefficient on the whole rotor crown. Experiments at the Fluidmachinery Lab. at Politecnico di Milano (Italy).

pressure coefficient shows a fluctuating loss region, with the widest extension at t/BPP = 0.83 and the smallest one at t/BPP = 0.25, mainly in the hub region. For this latter time instant, the deviation angle shows the smallest gradient in the hub region and the unresolved unsteadiness the lowest intensity.

At t/BPP = 0.37, a vortical structure, evidenced by a high deviation angle gradient, appears in the hub region and magnifies up to t/BPP = 0.83 where its intensity is the largest. Unresolved unsteadiness and relative total pressure, mark this structure as a loss core periodically impact-

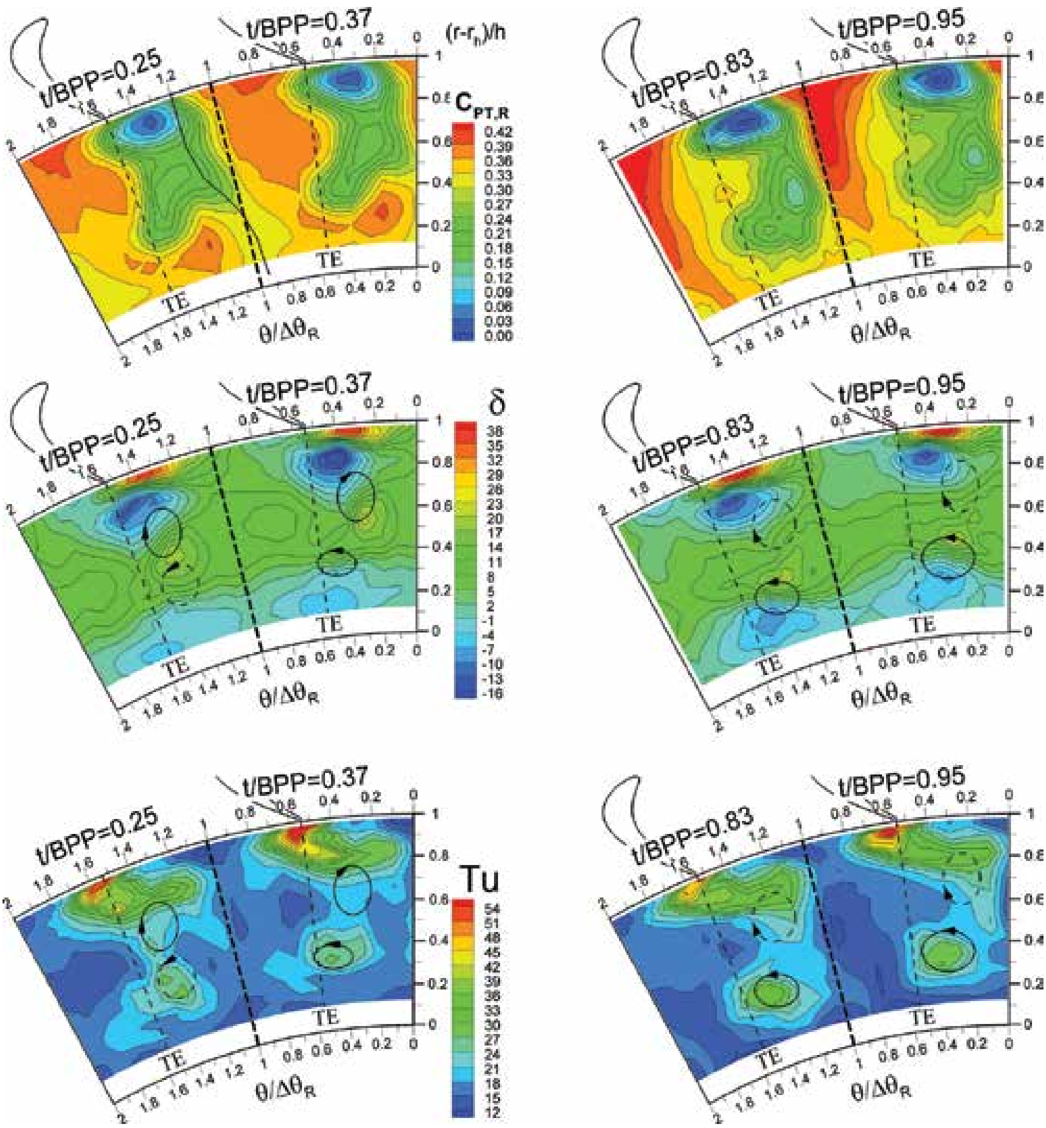

Figure 9. Relative total pressure coefficient ($C_{PT,R}$), deviation angle (δ) and turbulence (Tu) for 4 interaction phases. Experiments at the Fluidmachinery Lab. at Politecnico di Milano (Italy).

ing on the rotor channel. The sense of rotation allows accounting this phenomenon as the impact of the stator hub shed vortex, strong enough at the stator exit, on the rotor hub passage vortex.

The tip region on the contrary experiences an opposite trend with the strongest vortical structure at t/BPP = 0.25, when likely the higher inlet total pressure is found.

The highest turbulent and loss contents are found in the tip clearance region due to the high dissipation related to the clearance flow [17].

The interaction here briefly described is unfortunately for the designer case dependent where, as discussed later one, the axial gap and the loading are important issues.

To get a comprehensive perspective on the importance and on the region where the interaction takes place, the standard deviation among the different time fames is straightforward and reported in **Figure 10**. With reference to the relative total pressure coefficient, the wider fluctuations are, as qualitatively expected by **Figures 8** and **9** in the midspan-hub region. The more sensitive region at midspan is located on the wake suction side border that is the place where the stator wake interacts with the rotor one; in that region, the deviation angle evidences coherently small fluctuations. The tip region is in fact steady as the clearance flow dominates over all other structures. The hub regions, experience both variation on the total pressure coefficient and deviation angle, being the seat of the vortex/wake and vortex/vortex interaction. With reference to the deviation angle map (**Figure 10b**), the deviation angle experiences the highest fluctuation in the interface between the tip and hub passage vortex; moreover, all along the rotor wake, it fluctuates, showing the flow turning to be highly sensitive to the periodic interaction.

Off design conditions: To improve the analysis, different operating conditions are described here, being different for the incidence angle and expansion ratio. The effect of the axial gap will be discussed in the following chapter.

As the interaction depends on the rotor loading, all changes in this parameter will affect the intensity. Specifically, the increase in the rotor loading, by increasing the incidence angle, will

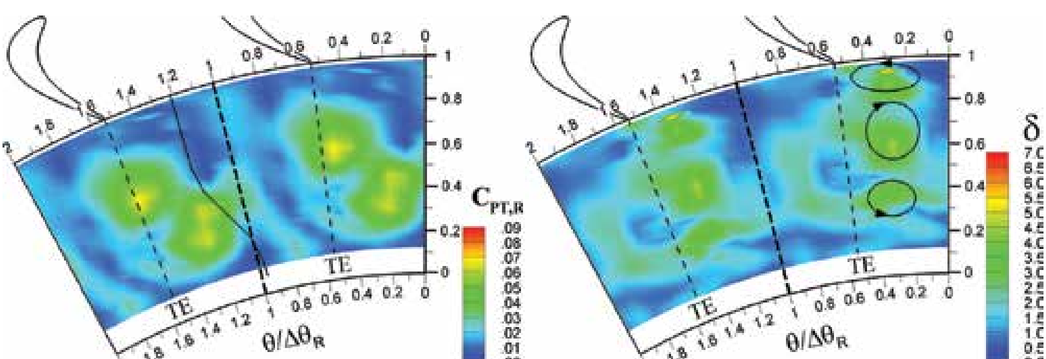

Figure 10. Standard deviation of the Cptr and δ for the different time frames. Experiments at the Fluidmachinery Lab. at Politecnico di Milano (Italy).

strengthen the interaction leaving unchanged the basic mechanism. In fact, when the rotor loading increases, the rotor suction side boundary layer is more prone to instability and the rotor vortical structure more intense, making all of them more sensitive to any variation coming from upstream. **Figure 11**, shows the relative total pressure coefficient and deviation angle standard deviations, calculated among the different time instants, for a negative incidence conditions (**Figure 11a**, incidence at midspan = −10°) and a positive one (**Figure 11b**, incidence at midspan = +10°) [35].

When the overall effect is of concern, the different interaction intensity leaves a trace on the total to total efficiency that can be summarised by stating that the higher the interaction, the lower is the efficiency.

When the fluid-dynamic forcing on the rotor blade is under study, the frequency of the forcing event is the one of the stator passing frequency multiplied by the number of swirling structures found along the pitch.

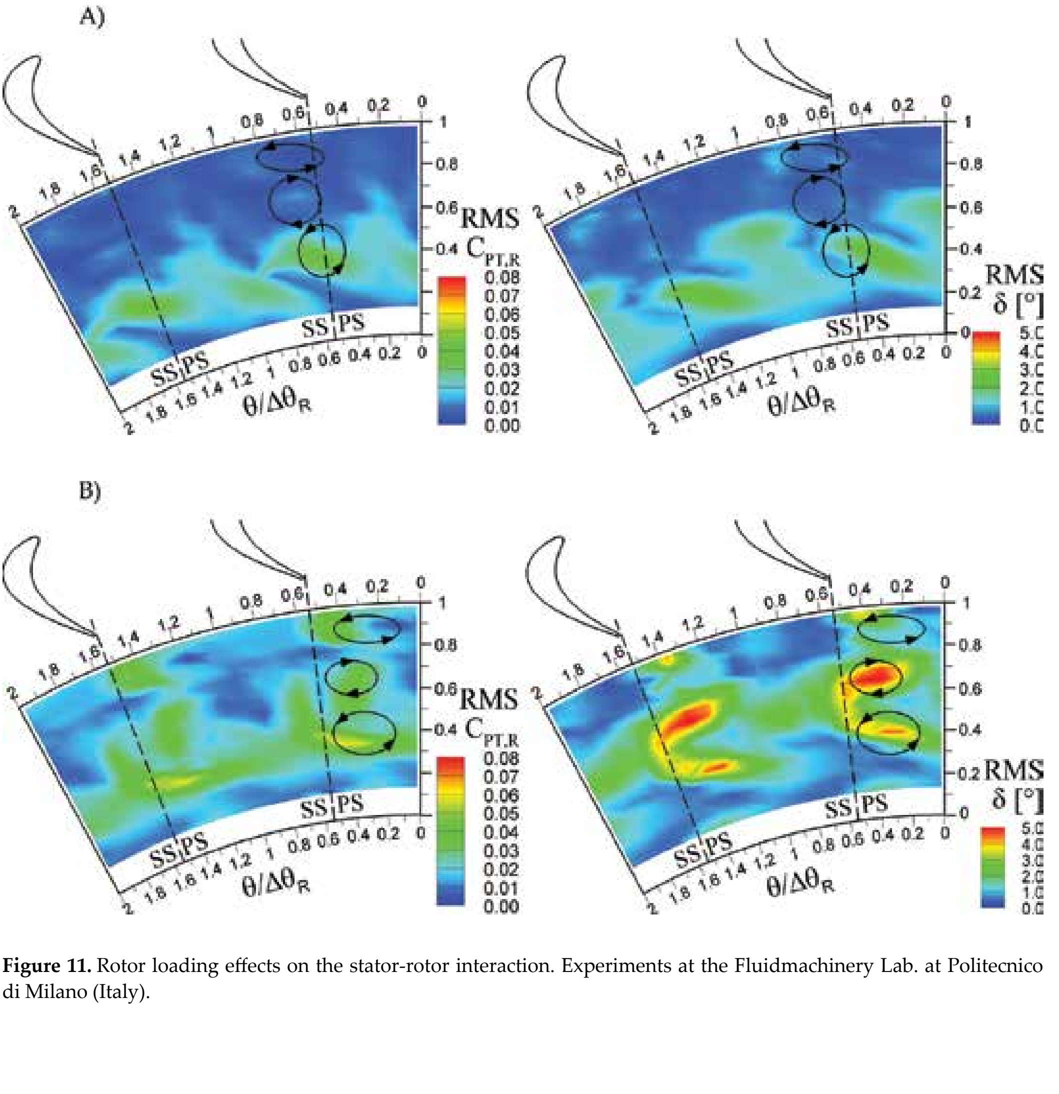

Figure 11. Rotor loading effects on the stator-rotor interaction. Experiments at the Fluidmachinery Lab. at Politecnico di Milano (Italy).

It has to be brought to the attention of the reader that the stator-rotor interaction is fundamental for the analysis of the interconnection frames, as discussed in [23] and of the turbine acoustic behaviour [24].

2.3. Stator shock-rotor blade interaction

The third possible source of interaction is related to the shocks generated at the stator trailing edge that impinge on the rotor leading edge region. Stators in high-pressure stages work often in transonic conditions at least in the hub region. Rarely, they are chocked as in this condition flow rate regulation is limited. The shock system typically has a fish-tail pattern characterised by oblique shocks; the suction side shock is stronger than the pressure side one. The suction side shock propagates downstream and interacts with the following row, while the pressure side one impinges on the adjacent blade, specifically on the suction side, being further reflected downstream.

Across the shock, the flow experiences a steep and opposite pressure gradient that, if applied to the boundary layer, acts to de-stabiles it, leading to separated flow bubbles. Thanks to the high Reynolds number, whose action is to promote the momentum exchange in the boundary layer, the effect is not that critical in high-pressure stages; it has to be recalled that rarely the outlet Mach number exceed 1.5, value where the entropy rise due to shock starts to be important.

As the stator shock sweep the rotor leading edge region, unsteadiness in the static pressure is found and for this in the boundary layer evolution; luckily, this happens where the boundary layer momentum deficit is close to be the smallest at the very beginning of the boundary layer evolution. As reported by [1, 36–38], the rotor trailing edge region is slightly affected, at least in term of static pressure and for this the boundary layer and the rotor wake are expected to be almost steady. The highest interaction is found in the leading edge/suction side region as clearly reported in **Figure 12**; the shock sweeping on the rotor leading edge first interact with the suction side of the blade (approx. in the location of measuring point n° 6, in **Figure 12**) and then reached

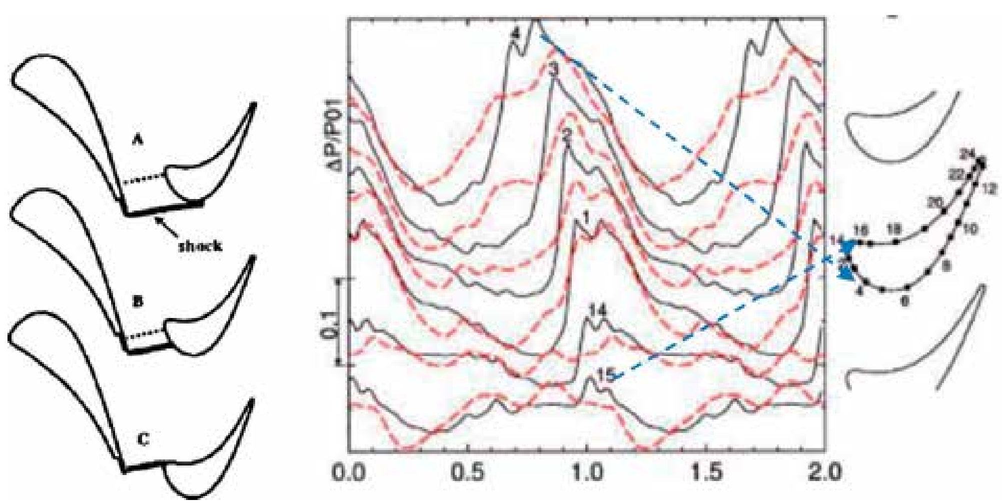

Figure 12. Vane shock-rotor interaction in axial turbine blades. Red: computation, black: experiments. Adapted from [1].

the leading edge (measuring point n° 2). The pressure side is less affected by the interaction being overshadowed by the leading edge. It is clear how the blade shape, in terms of camber/stagger angles and front/rear loading as well, it is a key parameter for this class of interaction.

The magnitude of the stator shock impinging on the rotor is strictly dependent on the axial gap; the wider it is, the weaker is the shock effect, being the shock decay rather fast.

From a mechanical perspective, the forcing induced by the stator shock on the rotor is at the stator passing frequency multiplied by the number of shocks impinging on the rotor per each stator passage, even though typically only one is important.

Other interesting studies on the interaction in transonic turbine are [39–40], where different conditions and geometries are discussed.

3. Design perspective

In general, there are a huge number of parameters that can be adjusted during the design process. Among the different parameters, some of them will be hereby described to deepen the understanding of the interaction features.

3.1. Axial gap

The axial gap is one of the key parameter for the stage optimisation. In general, the increase of the axial gap promotes the wake and secondary flows mixing and this leads to a more uniform rotor inlet flow field in the absolute frame of reference. However, the mixing increases losses and the overall total pressure level reduces. For low axial gaps, on the contrary, low-mixing takes places but a highly nonuniform flow enters in the rotor, leading to additional losses in the rotor itself. It is clear so far, how the axial gap is a parameter that has to undergo an optimisation process and this is the reason why it has been the focus of a number of research that gave different results, likely depending on the operating condition and stage loading [41].

In the context of the wide experimental campaign on the stator-rotor interaction at Politecnico di Milano, the axial gap has been also addressed and studied. The detailed discussion of the results is reported in [17], while in this context only a brief recall is proposed. Three gaps have been experimentally investigated, equal to 16, 35 and 50% of the stator axial chord. For the lowest gap case, the stator structures like wake and passage vortices are more intense than other cases and this promotes a strong interaction that results in a severe periodic fluctuation in the rotor outlet quantities. On the contrary as the gap increases, the mechanism is mainly driven by the stator shed vorticities that strengthen at the expense of the passage vortices intensities, as described in the previous paragraph. The somehow surprising result is that the lowest interaction rate is for the design case that is a gap of 35% of the stator axial chord, condition where the inlet flow field is the more uniform in terms of relative total pressure and rotor deviation angle, as clearly depicted in **Figure 13**.

For larger gaps, the combination of stator potential field and wake acts to amplify the inlet fluctuation, as reported for the incidence angle in **Figure 14**.

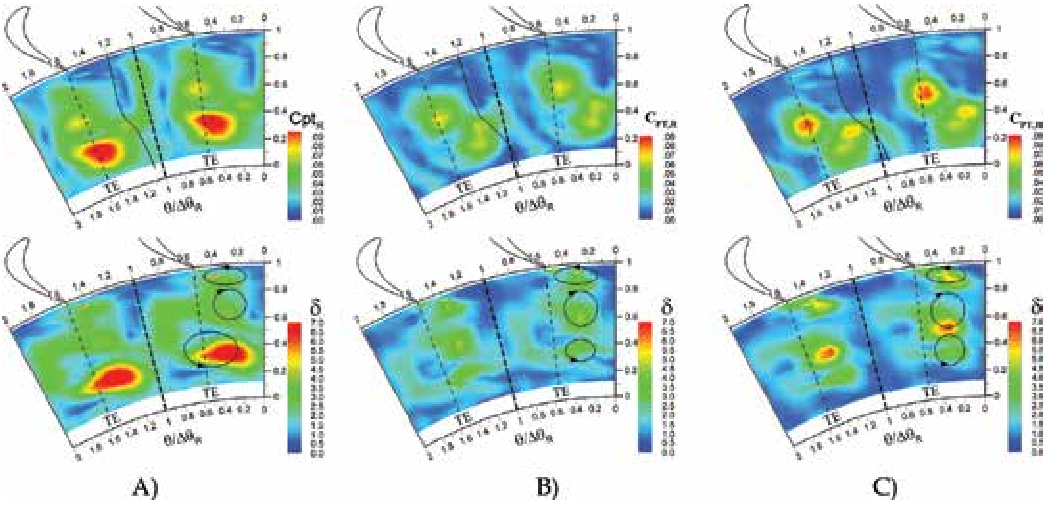

Figure 13. Standard deviation for the different instants of the interaction phases. (A) axial gap: x/bs = 16%; (B) axial gap: x/bs = 35%, nominal; C) axial gap = 50%. Experiments at the Fluidmachinery Lab. at Politecnico di Milano (Italy).

Overall, the stage experiences the maximum efficiency for the design case (**Figure 15**), about 1% higher, showing the potential of this parameter in the optimisation during the design process. According to the open literature, this trend is confirmed by some authors [42–46] but seems not general (as also reported and discussed by [41]), either for a lack of detailed data or for a case dependency in the stator wake-potential field coupling along the axial direction, in the axial gap region.

When the aerodynamic forcing is of concern, the axial gap plays a role as discussed in [47], since the forcing functions, as the wake velocity defect and the secondary flows, are stronger for low axial gaps.

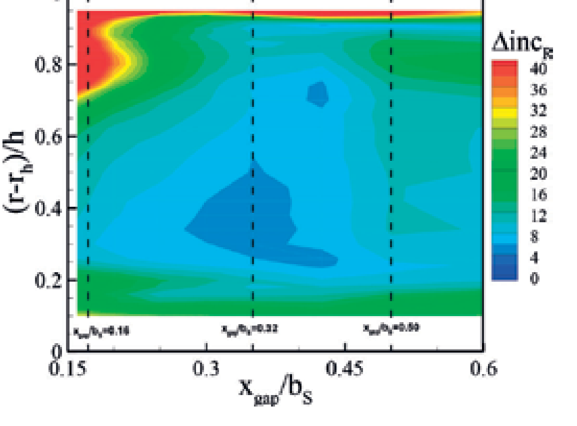

Figure 14. Rotor incidence fluctuations in circumferential direction for the differente axial gaps along the blade span.

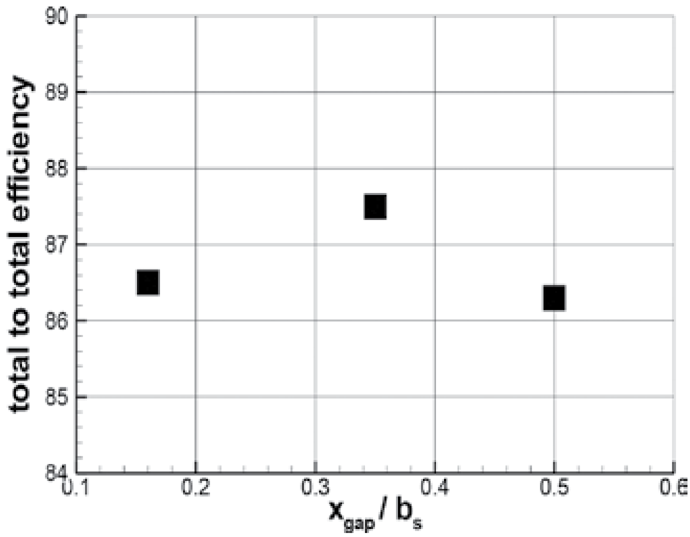

Figure 15. Efficiency trend versus the axial gap. Experiments at the Fluidmachinery Lab. at Politecnico di Milano (Italy).

3.2. Endwall contouring and 3D blade geometries

As discussed in the previous sections, the secondary flows are in the high-pressure turbine stages a leading issue for the cascade interactions. Given this matter of fact, any action devoted to the secondary flow reduction or segregation is straightforward for softening the stator-rotor interaction, aiming moreover to an overall efficiency increase.

Among the possible turbomachinery design methodologies, two of them are here briefly commented: the endwall contouring and the 3D blade design.

The **endwall contouring** consists of a specific endwall shape, at tip/hub or both, aiming at providing lower velocities in the blade portion where the highest loading is applied, that is higher turning. This feature results in a lower local cross-passage pressure gradient and a strong acceleration in the rear part of the blade. The final result is a reduction of the passage vortex in the contoured side of the passage, while the not contoured side experience about the same vortical structures [48–50].

The second possible action is the **3D blade design**. It consists of a design methodology based on a different blade stacking with respect to the conventional radial one, leading to the so-called leaned and/or bowed blades. Typically, the lean given to blades is positive that means a blade stacking inclined towards the pressure side. The bowing is given by applying a symmetrical leaning at tip and hub. These methodologies allow for a "flow control' at the cascade outlet in terms of radial pressure gradient and hence reaction. In case of positive leaning, an additional vorticity is introduced on the channel; specifically, it increases the one related to the passage vortex at the hub and smear the tip one. At the same time, the lean change the blade loading along the span by amplifying the tip one and reducing the hub one: overall such a feature makes the secondary flow at the hub less intense than the case of prismatic blades. **Figure 4** shows the vorticity field downstream of the lean annular cascade, characterised by a positive lean of 10°. When the lean is applied symmetrically at hub and tip, this benefit is gained also at tip. Overall,

http://dx.doi.org/10.5772/intechopen.76009

the final effect in the frame of the stator/rotor interaction process is the reduction of the secondary flows and their segregation at the endwalls. This design methodology leads to an overall benefit even though the single cascade does not improve significantly its performance [51–54].

3.3. Cascades clocking

Cascades clocking refers to the design option related to the proper alignment of blades belonging to different cascades in the same frame of reference (stator/stator or rotor/rotor) in the context of multistage machines. In fact, downstream of each stage the "wake avenue' is found, that is the global effect of the stator wake and secondary flows on the rotor outlet flow field in the time mean context. This concept can be applied also to the rotor wake, when a multistage environment is considered.

To ease the understanding, let us refer to a two stages machine and specifically to the impact of the 1° stator wake avenue on the 2° stator. Depending on the kind of stages and their loading, the impact of the wake avenue can be proficiently used for increasing the following cascade efficiency. In order to clock the two different rows, cascades should have number of blades that are multiple each other and for this the design assumption of prime number have to be abandoned (it can be kept for the stator and rotor of the single stage). So far, the highest efficiency is therefore gained by using the same blade numbers between the two stators (or rotors for rotor-clocking). In LP turbines the clocking is directly linked to the wakes, while in transonic HP turbines the effect is mainly related to the interaction of wakes and secondary flows, that is the total pressure and total temperature fields on the whole, downstream the first stage with the second stator.

According to the early work from [55], the efficiency is achieved when the segments of the first vane wake avenue, released by the rotor, impinge on the leading edge of the second vane. The basic reason for this result is that the low momentum fluid coming from the first stage, collapse in the boundary layer of the second vane and for this do not affect the passage (among others, [56–58]), studied in detail the clocking effects driven by the stator secondary flows in a two stage subsonic and transonic turbines.

According to Schennach et al. [58], the interaction with secondary vortices is highly complex due to the different kind and intensity of the vortical structure itself. When the rotor structures dominate, as can happen in the tip region due to the tip clearance or for the hub secondary vortex, the clocking effect is somehow shadowed. The outer part of the channel, being typically the rotor tip passage vortex highly sensitive to the stator-rotor interaction in the upstream stage, is the place with the highest potential for the clocking. This result makes the proper alignment choice complex for the designer as it is not really general.

In case of transonic stages, the hub region, being the seat of the 1° stator shock wave and hence of the highest stator-rotor modulation, has a high potential for clocking.

As a general conclusion, when the low momentum fluid enters on the 2° stator leading edge or close to the pressure side, the highest efficiency is found. On the contrary, when the low momentum fluid coming from the 1° vane enters close to the 2° vane suction side, the lowest efficiency is found, as a consequence of the destabilising effects on the suction side boundary layer and the lowest expansion ratio there available and for this lowest suction side overspeed and for this blade lift.

Low-pressure turbines behaviour is discussed in detail in [59], where an increase of 0.7% in the efficiency is found by numerical simulations.

As a conclusive comment, the benefit achievable by clocking the cascades can be of the order of 1% in the 2° stator efficiency, being anyway highly depending on the stage features.

Nomenclature

P = pressure

$Y = (P_{T0} - P_{T1})/(P_{T1} - P_1)$: total pressure loss

$\delta = \beta_{blade} - \beta_{fluid}$: deviation angle, angles taken form the axial direction.

β = relative flow angle

$C_{PT,R} = (P_{T,R} - P_{atm})/(P_{t0} - P_{atm})$

Tu = turbulence intensity calculated by the unresolved relative total pressure [28]

V = velocity

Ω_s = streamwise vorticity: $\Omega_s = \frac{(\nabla \times \vec{V}) \cdot \vec{V}}{\|\vec{V}\|}$

Subscript

R = relative

T = total

0 = stator upstream

1 = stator downstream

Author details

Paolo Gaetani

Address all correspondence to: paolo.gaetani@polimi.it

Dipartimento di Energia, Politecnico di Milano, Milano, Italy

References

[1] Denos R, Arts T, Paniagua G, Michelassi V, Martelli F. Investigation of the unsteady rotor aerodynamics in a transonic turbine stage. ASME Journal of Turbomachinery. 2001;**123**(1):81-89

[2] Sieverding CH. Recent progress in the understanding of basic aspects of secondary flows in turbine blade passages. Journal of Engineering for Gas Turbines and Power. 1985;**107**:248-257

[3] Ong J, Miller RJ. Hot streak and vane coolant migration in a downstream rotor. Journal of Turbomachinery. 7 May 2012;**134**(5). Article number 051002

[4] Raj R, Lakshminarayana B. Characterisitcs of the wake behind a scascade of airfoils. Journal of Fluid Mechanics. 1973;**61**(4):707-730

[5] Ravindranah A, Lakshminarayana B. Mean velocity and decay characteristics of the near and far-wake of a compressor rototr blade of moderate loading. ASME Journal of Engineering for Power. 1980;**102**(3):535-548

[6] Langston LS. Secondary flows in axial turbines—A review. 2006. Annals of the New York Academy of Science. https://doi.org/10.1111/j.1749-6632.2001.tb05839.x

[7] Perdichizzi A. Mach number effects on secondary flow development of a turbine cascade. Journal of Turbomachinery. 1990;**112**:643-651. DOI: 10.1115/1.2927705

[8] Dossena V, D'Ippolito G, Pesatori E. Stagger angle and pitch-chord ratio effects on secondary flows downstream of a turbine cascade at several off-design conditions. In: Proceedings of the ASME Turbo Expo. Vienna, Austria: ASME Turbo Expo; 2004;**5**:1429-1437

[9] Boletis E, Sieverding CH, Van Hove W. Effects of a skewed inlet endwall boundary layer on the three-dimensional flow field in an annular turbine cascade. In: AGARD, CP 351; 1983. Paper No. 16

[10] Binder A. Turbulence productions due to secondary vortex cutting in a turbine rotor. ASME Journal of Engineering for Gas Turbines and Power. 1985;**107**:998-1006

[11] Dring RP, Joslyn HD, Hardin LW, Wagner JH. Turbine rotor-stator interaction. ASME Journal of Engineering for Power. 1982;**104**:729-742

[12] Chaluvadi VSP, Kalfas AI, Benieghbal MR, Hodson HP, Denton JD. Blade-row interaction in a high-pressure turbine. AIAA Journal of Propulsion and Power. 2001;**17**:892-901

[13] Pullan G, Denton JD. Numerical simulation of vortex-turbine blade interaction. In: Proceedings of the 5th European Conference on Turbomachinery; March 7-11, 2003; Prague, Czech Republic; 2003

[14] Gaetani P, Persico G, Dossena V, Osnaghi C. Investigation of the flow field in a HP turbine stage for two stator-rotor axial gaps—Part I: 3D time averaged flow field. ASME Journal of Turbomachinery. 2007;**129**:572-579

[15] Gaetani P, Persico G, Dossena V, Osnaghi C. Investigation of the flow field in a HP turbine stage for two stator-rotor axial gaps—Part II: Unsteady flow field. ASME Journal of Turbomachinery. 2007;**129**:580-590

[16] Persico G, Gaetani P, Osnaghi C. Effects of off-design operating conditions on the blade row interaction in a HP turbine stage. In: Proceedings of the ASME Turbo Expo. Montreal, Que, Canada: ASME Turbo Expo; 2007;**6**(PART A):503-517

[17] Gaetani P, Persico G, Osnaghi C. Effects of axial gap on the vane-rotor interaction in a low aspect ratio turbine stage. Journal of Propulsion and Power. 2010;**26**:325-334

[18] Persico G, Gaetani P, Osnaghi C. A parametric study of the blade row interaction in a high pressure turbine stage. Journal of Turbomachinery. 2009;**131**:031006

[19] Herbert GJ, Tiederman WG. Comparison of steady and unsteady secondary flows in a turbine stator cascade. ASME Journal of Turbomachinery. 1990;**112**:625-632

[20] Schlienger J, Kalfas AI, Abhari RS. Vortex-wake-blade interaction in a shrouded axial turbine. ASME Journal of Turbomachinery. 2005;**127**(4):699-707

[21] Pullan G. Secondary flows caused by blade row interaction in a turbine stage. Journal of Turbomachinery. 2006;**128**:484-491

[22] Hu B, Ouyang H, Jin G-Y, Du Z-H. The influence of the circumferential skew on the unsteady pressure fluctuation of surfaces of rear stator blades. Journal of Experiments in Fluid Mechanics. 2013;**27**(1):25-31

[23] Spataro R, Göttlich E, Lengani D, Faustmann C, Heitmeir F. Development of a turning mid turbine frame with embedded design—Part II: Unsteady measurements. Journal of Turbomachinery. 2014;**136**(7):071012/1-8

[24] Knobloch K, Holewa A, Guérin S, Mahmoudi Y, Hynes T, Bake F. Noise transmission characteristics of a high pressure turbine stage. In: 22nd AIAA/CEAS Aeroacoustics Conference; Lyon, France; 2016

[25] Stieger RD, Hodson HP. The unsteady development of a turbulent wake through a downstream low-pressure turbine blade passage. Journal of Turbomachinery. 2005;**127**:388-394

[26] Hodson HP, Howell RJ. The role of transition in high lift low pressure turbines. In: Effects of Aerodynamic Unsteadiness in Axial Turbomachinery, VKI Lecture Series 2005-03. 2005

[27] Lengani D, Simoni D, Pichler R, Sandberg RD, Michelassi V, Bertini F. Identification and quantification of losses in LPT cascade by POD applied to LES data, 2018. International Journal of Heat and Fluid Flow. 2018;**70**:28-40

[28] Lengani D, Simoni D, Ubaldi M, Zunino P, Bertini F, Michelassi V. Accurate estimation of profile losses and analysis of loss generation mechanism in turbine cascade. Journal of Turbomachinery. 2017;**139**:121007/1-9. DOI: 10.1115/1.4037858

[29] Persico G, Gaetani P, Guardone A. Design and analysis of new concept fast-response pressure probes. Measurement Science and Technology. 2005;**16**:1741-1750

[30] Kupferschmied P, Koppel P, Roduner C, Gyarmathy G. On the development and application of the FRAP (fast response aerodynamic probe) system for turbomachines—Part I: The measurement system. ASME Journal of Turbomachinery. 2000;**122**(3):505-516

[31] Persico G, Gaetani P, Paradiso B. Estimation of turbulence by single sensor pressure probes. In: Proceedings of the 19th Symposium of Measuring Techniques in Turbomachinery; 7-8 April 2008; Belgium: Von Karman Institute; 2008

[32] Porreca L, Hollenstein M, Kalfas AI, Abhari RS. Turbulence measurements and analysis in a multistage axial turbine. AIAA Journal of Propulsion and Power. 2007;**23**:227-234

[33] Greitzer EM, Tan CS, Graf MB. Internal Flow-Concepts and Applications. Cambridge University Press; 2004. ISBN: 0-521-34393-3

[34] Kundu PK, Cohen IM, Dowling DR. Fluid Mechanics, 5th ed. Academic Press; 2012. ISBN 978-0-12-382100-3

[35] Gaetani P, Persico G, Spinelli A. Coupled effect of expansion ratio and blade loading on the aerodynamics of a high-pressure gas turbine. Applied Sciences. 2017;**2017**(7):259. DOI: 10.3390/app7030259

[36] Paniagua G, Yasa T, de la Loma A, Castillon L, Coton T. Unsteady strong shocks interaction in a transonic turbine: Experimental and numerical analysis. Journal of Propulsion and Power. 2008;**24**(4):722-731

[37] Miller RJ, Moss RW, Ainsworth RW, Harvey NW. Wake, shock and potential field interactions in a 1.5 stage turbine—Part I: Vane-rotor and rotor-vane interaction. ASME Journal of Turbomachinery. 2003;**125**(1):33-39

[38] Tang E, Leroy G, Philit M, Demolis J. Unsteady analysis of inter-rows stator-rotor spacing effects on a transonic, low-aspect ratio turbine. In: Proceedings of the ASME Turbo Expo 2015; Montreal, Canada; 2015

[39] Rubechini F, Marconcini M, Giovannini M, Bellucci J, Arnone A. Accounting for unsteady interaction in transonic stages. Journal of Engineering for Gas Turbines and Power. 2015;**137**(5):052602/1-9

[40] Gougeon P, Boum GN. Aerodynamic interactions between a high-pressure turbine and the first low-pressure stator. Journal of Turbomachinery. 2014;**136**(7):071010

[41] Gronman A, Biester M, Turunen Saaresti T, Varri AJ, Backmann J, Seume JR. Importance of the vane exit Mach number on the axial clearance related losses. Proceedings of the Institution of Mechanical Engineers, Part A: Journal of Power and Energy. 2016;**230**(2): 175-183

[42] Dejc ME, Trojanovskij BM. Untersuchung und Berechnung Axialer Turbinenstufen. Berlin: VEB Verlag Technik; 1973

[43] Venable BL, Delaney RA, Busby JA, Davis RL, Dorney DJ, Dunn MG, Haldemann CW, Abhari RS. Influence of vane-blade spacing on transonic turbine stage aerodynamics: Part I—Time-averaged data and analysis. ASME Journal of Turbomachinery. 1999;**121**:663-672

[44] Bellucci J, Rubechini F, Arnone A, Arcangeli L, Maceli N, Paradiso B, Gatti G. Numerical and experimental investigation of axial gap variation in high-pressure steam turbine stages. Journal of Engineering for Gas Turbines and Power. 2017;**139**(5):052603/1-9

[45] Restemeier M, Jeschke P, Guendogdu Y, Gier J. Numerical and experimental analysis of the effect of variable blade row spacing in a subsonic axial turbine. Journal of Turbomachinery. 2012;**135**(2):021031

[46] Chen Y, Zhong Z, Li J, Zhou W, Zhong G, Sun Q, Ping Y, Wang S. Effect of stage axial distances on the aerodynamic performance of three-stage axial turbine using experimental measurements and numerical simulations. In: Proceedings of the ASME Turbo Expo; Charlotte, United States; 2017

[47] Jiang JP, Li JW, Cai GB, Wang J. Effects of axial gap on aerodynamic force and response of shrouded and unshrouded blade. Science China Technological Sciences. 2017;**60**(4):491-500

[48] Dossena V, Perdichizzi A, Savini M. The influence of Endwall contouring on the performance of a turbine nozzle guide vane. Journal of Turbomachinery. 1999;**121**:200-208

[49] Kopper FC, Milano R, Vanco M. Experimental investigation of endwall profiling in a turbine blade cascade. AIAA Journal. 1981;**19**(8):1033-1040

[50] Moustapha SH, Williamson RG. Effect of two Endwall contours on the performance of an annular nozzle cascade. AIAA Journal. 1986;**84**(9):1524-1530

[51] Denton JD, Xu L. The exploitation of three dimensional flow in turbomachinery design. IMechE Journal of Mechanical Engineering Science. 1999;**213**:125-137

[52] D'Ippolito G, Dossena V, Mora A. The influence of blade lean on straight and annular turbine cascade flow field. In: Proceedings of the ASME Turbo Expo. Berlin, Germany: ASME Turbo Expo; 2008;**6**(PART B):11

[53] Harrison S. The influence of the blade lean on turbine losses. Journal Turbomach. 1992;**114**(1):184-190. DOI: 10.1115/1.2927982

[54] Havakechian S, Greim R. Aerodynamic design of 50 percent reaction steam turbine. Journal of Mechanical Engineering Science. 1999;**213**:1-25

[55] Huber FW, Johnson PD, Sharma OP, Staubach JB, Gaddis SW. Performance improvement through indexing of turbine airfoils: Part 1—Experimental investigation. ASME Journal of Turbomachinery. 1996;**118**:630-635

[56] Haldeman CW, Dunn MG, Barter JW, Green BR, Bergholz RF. Experimental investigation of vane clocking in a one and one-half stage high pressure turbine. Journal of Turbomachinery. 2005;**127**(3):512-521

[57] Behr T, Kalfas AI, Abhari RS. Stator-clocking effects on the unsteady interaction of secondary flows in 1.5 stage unshrouded turbine. Proceedings of the Institution of Mechanical Engineers, Part A: Journal of Power and Energy. 2007;**221**:779-792

[58] Schennach O, Woisetschläger J, Paradiso B, Persico G, Gaetani P. Three dimensional clocking effects in a one and a half stage transonic turbine. Journal of Turbomachinery. 2010;**132**(1):011019. 1-10. Inglese

[59] Arnone A, Marconcini M, Pacciani R, Schipani C, Spano E. Numerical investigation of airfoil clocking in a three-stage low-pressure turbine. Journal of Turbomachinery. 2002;**124**:61-68

Chapter 6

Hierarchical Progressive Optimization for Aerodynamic/Stealth Conceptual Design Based on Generalized Parametric Modelling and Sensitivity Analysis

Fang Chen and Hong Liu

Additional information is available at the end of the chapter

http://dx.doi.org/10.5772/intechopen.73282

Abstract

A hierarchical progressive optimization approach is proposed for multidisciplinary optimal design by integrating with generalized parametric modeling and sensitivity analysis. The framework includes the following: (1) to set up a generalized parametric model for the geometric parameters of flight vehicles with different levels, (2) to reduce the number of design parameters using sensitivity analysis method and (3) to use the gradual optimization design method to solve the problem of integrated aerodynamic-stealth optimization design. The results from the application on the configuration optimization of an aircraft demonstrate that the hierarchical progressive optimization increases the fitness of the optimization design by 51.1% and improves the conceptual design efficiency.

Keywords: aircraft design, hierarchical progressive optimization, generalized parameters, sensitivity analysis, multidisciplinary optimization

1. Introduction

Stealth is a significant development trend of weaponry in the future. Because the requirements of aerodynamics/stealth conceptual design are often contradictory, in order to obtain aircraft configuration with good aerodynamic/stealth performance, it is necessary to conduct the studies on multidisciplinary optimization of aerodynamics and stealth.

With the development of computing technology, the integration of high fidelity numerical simulation and multidisciplinary optimization (MDO) has become common for the conceptual

IntechOpen

© 2018 The Author(s). Licensee IntechOpen. This chapter is distributed under the terms of the Creative Commons Attribution License (http://creativecommons.org/licenses/by/3.0), which permits unrestricted use, distribution, and reproduction in any medium, provided the original work is properly cited.

design of aircraft configuration [1]. However, the researches mostly rely on the empirical approach to realize the multidisciplinary concept design.

In view of practical engineering application, there is an inevitable trend to integrate CAD modeling into multidisciplinary optimization design framework. This parametric modeling necessarily involves more parameters for the optimization of aerodynamics and stealth than those only for aerodynamics design. The resultant extra-optimization design due to the additional parameters would reduce the optimization efficiency. Sensitivity analysis is, therefore, necessary to classify the generalized parameters. Moreover, in comparison to the conventional optimization method, MDO requires available treatment to the coupling of aerodynamics and stealth.

The present study aims to conduct rapid conceptual design for aerodynamics/stealth optimization of a four-tailed aircraft configuration. Firstly, parametric modeling method is proposed to describe aerodynamic/stealth multidisciplinary characteristics. Secondly, hierarchical progressive optimization process integrated with sensitivity analysis is proposed to achieve rapid conceptual design. Finally, the methods are applied to rapid optimization for conceptual design of aerodynamic/stealth of an aircraft. Therefore, this hierarchical progressive optimization approach integrated generalized parametric modeling and sensitivity analysis is expected to simplify the optimization and improve the design efficiency, which has the following advantages:

(1) Combined with the progressive process of CAD modeling, it can extract the parameters to describe both aerodynamics and stealth and then provide generalized parameters for hierarchical progressive design.

(2) By classifying the generalized parameters with sensitivity analysis, it can not only reduce the complexity and workload of the optimization but also guide the optimization based on the parametric sensitivity information.

2. Hierarchical progressive optimization

The main idea of MDO is to integrate the knowledge of different disciplines in complex design systems, to fully consider the interaction and coupling between the disciplines, to organize the design of the whole system with effective design and optimization strategies, to reduce the design cycle by realizing modular parallel design of different disciplines, to exploit design potential by considering interdisciplinary coupling and to select and evaluate the optimization design by systematic integrated analysis.

As shown in **Figure 1**, traditional optimization design is the case, where N = 1. This approach features simple process and relatively low optimization efficiency. In order to improve the efficiency of MDO design, hierarchical progressive optimization (shown in **Figure 1**) is proposed for engineering practice.

The hierarchical progressive optimization is capable of dividing the enormous design space into several subspaces; each dramatically reduces the number of optimization parameters and

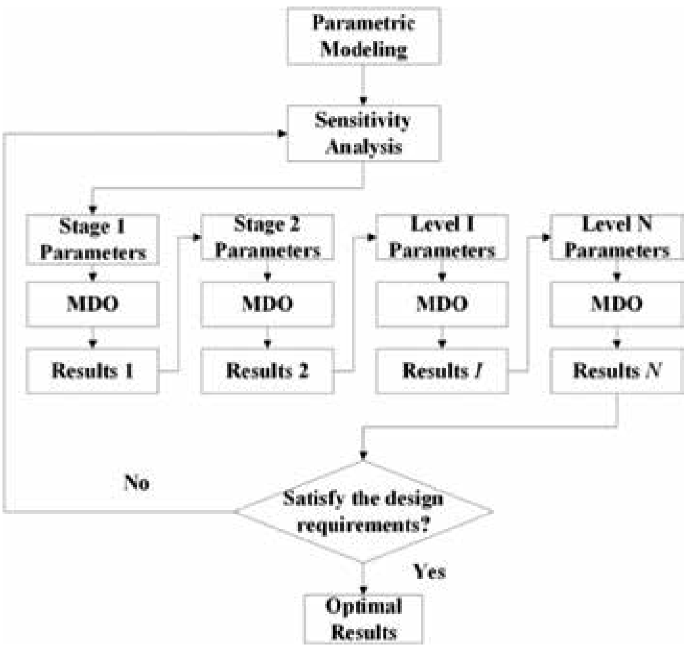

Figure 1. The schematic diagram of hierarchical progressive optimization.

constraint conditions, which significantly reduce the complexity of optimization. The optimal solution of the design can be obtained by iteration among the subspace. In order to exert this design superiority, it is crucial to construct a suitable optimization design system to adapt to the hierarchical progressive optimization design framework.

2.1. Differential evolution (DE) method

A differential evolution (DE) algorithm is a stochastic heuristic search algorithm to simulate the biological population evolution in nature of "survival of the fittest" principle. It was proposed by Storn and Price [2] to improve the genetic algorithm. Due to its simplicity, ease of use, robustness and powerful global search capability, differential evolution has been successfully applied in many fields.

The basic idea is to generate a random initial population in the beginning, to sum up with vector weighted of any two and third individuals according to specific rules to generate new individuals. By comparing this new individual fitness and a predetermined individual, the better individual will be survived. Through the continuous iteration of retaining the excellent individuals and eliminating the inferior individuals, the search process is directed to approximate the optimal solution.

The differential evolution algorithm has the characteristics of memorizing optimal solution of individual and sharing information within the population, and its essence is a greedy genetic algorithm with real coding based on the idea of preserving optimality. Compared with the traditional optimization method, it has the following main features:

1. It starts to search from a group, i.e., multiple points rather than a point, which can avoid the defects of retention at local optimum and thus has high probability to find the global optimal solutions.
2. The evolutionary rule is based on adaptive information and without any other additional auxiliary information (such as requiring the function to be derivable or continuous), which greatly extends its application range and inherits the advantages of genetic algorithm.
3. It has inherent parallelism, which makes it very suitable for massively parallel distributed processing and therefore reducing the time cost.
4. Using probability transfer rules to search, this is the improvement of the genetic algorithm, to ensure that it quickly finds the optimal solutions.

Differential evolution algorithm is an evolutionary algorithm based on real coding, which is similar to other evolutionary algorithms in structure. It consists of three basic operations: mutation, crossover and selection.

Let suppose that $X_i(t)$ is the ith individual in the population t, then

$$X_i^t = \left(X_{i1}^t, X_{i2}^t, \cdots, X_{in}^t\right), \quad i = 1, 2, \cdots, M; t = 1, 2, \cdots, t_{\max} \tag{1}$$

where n is the chromosome number of the individual (i.e., the number of variables in the vector), M is the population number and $t_{\max}$ is the maximum number of evolution.

The detailed description of the basic strategies [2] is as follows:

1. Initial population:

   In an n-dimensional space, M individuals that satisfy constraint conditions are randomly generated:

$$X_{ij}^0 = rand_{ij}\ (0, 1)\left(X_{ij}^U - X_{ij}^L\right) + X_{ij}^L, \quad i = 1, 2, \ldots, M; j = 1, 2, \ldots, n \tag{2}$$

   where X_j^U and X_j^L are the upper and lower bounds of j chromosome, respectively; $\text{rand}_{ij}(0, 1)$ is a random decimal between [0, 1].

2. Mutation:

   The most basic variant of differential evolution algorithm is the parent difference vector; each vector pair includes two different individuals in the parent (generation t) population. The difference vector is defined as

$$D_{r1,2} = X_{r1}^t - X_{r2}^t \tag{3}$$

   r1 and *r2* represent the index numbers of two different individuals in a population. The differential vectors are added to another randomly selected vector to generate the variation vectors. For each objective vector X_i^t, mutation manipulation is used as

$$v_i^{t+1} = X_{r3}^t + F*\left(X_{r1}^t - X_{r2}^t\right) \tag{4}$$

$r1, r2, r3 \in \{1, 2, \dots, NP\}$ is an integer different from each other, and $r1, r2, r3$ is different from the current objective vector index i, so the number of population $NP \geq 4$. F is a scaling factor with a range of [0, 2] to control the differential vector scaling.

3. Crossover:

The crossover operation is used to crossover the objective vector individuals X_i^t in the population with the mutation vector v_i^{t+1} to generate the test individuals u_i^{t+1}. In order to ensure the evolution of the individuals, at least one of v_i^{t+1} is contributed to u_i^{t+1} by random selection, while for others, a crossover probability factor CR can be used to decide which one of v_i^{t+1} or X_i^t is contributed to u_i^{t+1}. The equation of crossover operation is

$$u_{ij}^{t+1} = \begin{cases} v_{ij}^{t+1}, randl_{ij} \leq CR\text{或}j = rand(i) \\ x_{ij}^{t}, randl_{ij} > CR\text{或}j \neq rand(i) \end{cases} \tag{5}$$

where $randl_{ij} \in [0, 1]$ is the random number in uniform distribution, j represents the jth variable (gene), and CR is the crossover probability constant with the range of [0, 1], and the length is predetermined. $\mathrm{rand}(i) \in [1, 2, \dots, n]$ is the index of dimension variables for random selection to ensure that at least one-dimension variable is contributed by the variation vector. Otherwise, the test vector may be the same as the objective vector and cannot generate new individuals.

4. Selection:

DE uses the greedy search strategy to compete the test individuals u_i^{t+1} generated by mutation and crossover operations with X_i^t, and the fitness u_i^{t+1} is chosen as the offspring only when it is better; otherwise, X_i^t will be directly used as the offspring. For example, the equation of operation for minimization optimization is chosen as

$$X_i^{t+1} = \begin{cases} u_i^{t+1}, f\left(u_i^{t+1}\right) < f\left(X_i^t\right) \\ X_i^t, f\left(u_i^{t+1}\right) \geq f\left(X_i^t\right) \end{cases} \tag{6}$$

Execute the above four operations repeatedly until the maximum number of evolution $t_{\max}$ is reached.

2.2. Optimization strategy

The mathematical model of the multi-objective optimization problem (MOP) [3] widely used and accepted in multi-objective optimization is defined as follows:

$$\begin{aligned} &\min \quad y = f(x) = \left(f_1(x), f_2(x), \cdots, f_k(x)\right) \\ &s.t. \quad e(x) = \left(e_1(x), e_2(x), \cdots, e_m(x)\right) \leq 0 \\ &where \quad x = (x_1, x_2, \cdots, x_n) \in X \\ &\qquad\quad y = \left(y_1, y_2, \cdots, y_k\right) \in Y \end{aligned} \tag{7}$$

The model consists of n parameters (decision variables), K objective functions and m constraints. The objective function and constraints are the functions of decision variables. Among them, x represents the decision vector, y represents the objective vector, X represents the decision space formed by the decision vector x, and Y represents the objective space formed by the objective function y, and the constraint condition determines the feasible range of the decision vector.

Modern aircraft not only has high aerodynamic performance but also requires good stealth performance. At present, reducing radar cross section (RCS) is the most important part of stealth technology. Aircraft design must take into account both the high aerodynamic efficiency and low RCS requirements in the configuration design. However, the requirements of the two are often contradictory.

Through an auto-adjusting weighted object (AWO) optimization method [3], the multi-objective optimization problem is transformed into the optimization strategy of the single objective problem, which can effectively solve the design requirements of such contradictions.

Its advantage is that in the process of optimization, certain adjustments can be done to improve the objective function for each subject according to the rate of information. It can avoid the suppression of the further optimization of other objective functions due to the extremely quick changes of some objective function and therefore obtain an effective solution with relatively synchronous optimization for all the subject object functions.

AWO is used as follows:

$$\Delta Obj_i = \frac{Obj_i - R_e Obj_i}{\left|R_e Obj_i\right|} \ (\mathrm{i} = 1, 2 \ldots, \mathrm{n}) \tag{8}$$

$$Globj_i = \sum_{i=1}^{n} C_i Obj_i, \ \sum_{i=1}^{n} C_i = 1 \tag{9}$$

where R_eObj_i is the objective reference value, Obj_i is the single subject fitness, $Globj_i$ is the comprehensive performance (fitness), and C_i is the weighted coefficient. For any i, if $\Delta Obj_i \leq \delta_0$, then accept the optimal solution and change the objective reference, or if $R_e Obj_i = Obj_i$, then give up the optimal solution. δ_0 is the control value of objective optimization, which generally takes $\delta_0 \leq 0.1$. If the optimal solution is accepted, the weighted coefficient is adjusted:

$$\begin{aligned} C_{better} &= C_{better} - \delta_c \\ C_{worse} &= C_{worse} + \delta_c \end{aligned} \tag{10}$$

where δ_c is the adjustment step size of the weighted coefficient, which is set as $\delta_c = 0.1 \times 0.9$ L, and L is the optimized step number. C_{better} is the weighted coefficient to optimize the better objective, and C_{worse} is the weighted coefficient to optimize the worse objective.

Most optimization problems contain some constraints, which divide the decision space into two parts: feasible and infeasible. The task of constrained multi-objective optimization is transformed into finding the Pareto optimal solution in the feasible region of the decision space. The penalty function method [4] is used to deal with the fitness function with the constrained problem, and the individuals beyond the constraint are discarded.

Penalty function method is the most commonly used method for solving constrained optimization problems. By calculating the constraint offset of the solution, the objective function is punished, and the constrained problem is transformed into an unconstrained optimization problem. Before computing the constraint offset, the constraint function is normalized as $e_j(x) \leq 0, j = 1, 2, \cdots, M$ so that the offset of the constraint function j is defined as the form of the following vector:

$$w_j(x) = \begin{cases} |e_j(x)|, & \textit{if } e_j(x) > 0 \\ 0, & \textit{otherwise} \end{cases} \tag{11}$$

The sum of the offset of the vector x on each constraint function is called the total offset:

$$\Omega(x) = \sum_{j=1}^{M} w_j(x) \tag{12}$$

For the minimization problem, the objective function value of the solution vector x will be modified as follows:

$$F_m(x) = f_m(x) + R_m\Omega(x), m = 1, 2, \cdots, K \tag{13}$$

where $f_m(x)$ is the function value of the individual i under the unconstrained condition on the m objective and R_m is the penalty function coefficient, which is used to balance the differences caused by the different dimensions of each objective. From the above definition, we can see that when $\Omega(x)$= 0, x is a feasible solution. When x is an infeasible solution, the farther away from the feasible domain, the greater the value of the objective function, the more penalties. After obtaining the objective function value after penalty, the unconstrained multi-objective optimization method can be used to solve the Pareto optimal solution. For example, for m constraints:

$$\varphi_j(x) \geq C_j, j = 1, \ldots, m \tag{14}$$

$$P_j = \begin{cases} 0, & \varphi_j < C_j \\ 1, & \varphi_j \geq C_j \end{cases} \tag{15}$$

The fitness is adjusted to be $Y_i = Globj_i \prod_{i=1}^{n} P_j$, where $Globj_i$ is the global performance (fitness).

3. Generalized parametric modeling

Parameters are both the objects for multidisciplinary design and the manifestation of the design results. Single disciplinary parametric modeling tends to ignore the requirements of multidisciplinary optimization as well as the requirements of other disciplines. However, the multidisciplinary parametric modeling is expected to not only integrate with various disciplines but also meet the requirements of practical optimization. Therefore, aerodynamics/stealth multidisciplinary optimization urges the construction of a parametric system that can meet the requirements of both aerodynamics and stealth discipline as well as to adapt to practical optimization design.

3.1. Generalize parameter

Generalized parameters are proposed to assist the increasingly complicated multidisciplinary design process of aircraft. They are necessary to reflect the discipline characteristics such as aerodynamics and stealth more than their appearance of the aspect of configuration. The whole generalized parametric system is divided into four dimensions, namely, design phase, component, discipline and design. It is constructed for aerodynamics/stealth optimization by classifying the design phases based on the progressive features of CAD modeling and analyzing the component characteristics of the major components (fuselage, wing, etc.).

3.2. Parametric modeling

Parametric modeling is the direct source of design parameters in multidisciplinary optimization design and the prerequisite of analysis and optimization design. Based on the integrated consideration of different requirements of aerodynamics and stealth on modeling parameters, the following modeling parameters of three levels is extracted in accordance with the hierarchy and progressive of CAD modeling:

(1) Twenty-seven general profile parameters: These parameters are used to describe the main profile of the fuselage cross section, shape characteristics, as well as installation angle and dihedral angle of wings and tails. The fuselage parameters include deviation angle of the head longitudinal line, head length, length of the head transition section, length of the intermediate section, tail length, the magnification ratio of fuselage cross section, and the magnification ratio of the tail cross section. The wing parameters include aspect ratio, root chord length, sweepback angle, taper, installation angle, and dihedral angle. Among them, some parameters of angle are introduced in view of stealth, as is shown in **Figure 2**; the height of head cross section is controlled by the upward deflection angle of head longitudinal line $\angle AOE$ and the downward

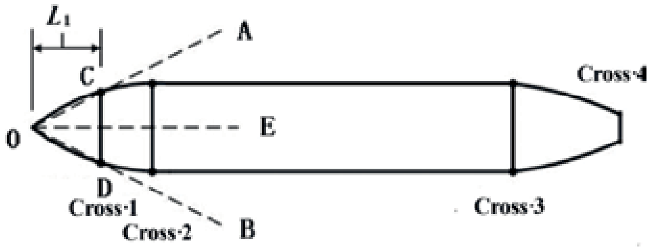

Figure 2. Geometric parameters of fuselage sections.

deflection angle of head longitudinal line $\angle BOE$ and head length $L1$. The parametric relation is indicated by Eq. 16:

$$\overline{|CD|} = \overline{|L_1|} \cdot (tg\,\angle AOE + \ tg\,\angle BOE) \tag{16}$$

(2) Twenty major control parameters of cross sections: As shown in **Figure 2**, the fuselage is controlled by four control cross sections along the axis. The major control parameters refer to the line segment ratios, angles, etc. of the main edges of the control cross sections. As shown in **Figure 3**, the position of the edge endpoint F is determined by the line segment ratio between BF and BC, while that of G is determined by the endpoint F and $\angle CFG$.

(3) Eighty-four profile modifying parameters of cross sections: Based on the specific edge positions of the cross sections that have been obtained, the conics are applied to modify the cross section edges. The conic control endpoints are obtained by distributing the line segment ratios on each edge; then the conics are constructed between the endpoints to obtain the specific profile of the cross sections. For example, points ①~⑥ in **Figure 3** are controlled by line segment ratios. By altering the position of control points and shape parameters of the conics, the cross sections can be expressed as various shapes, such as a circle, polygon and so on, which can meet the requirements of stealth on cross section shapes as the CAD examples shown in **Figure 4**.

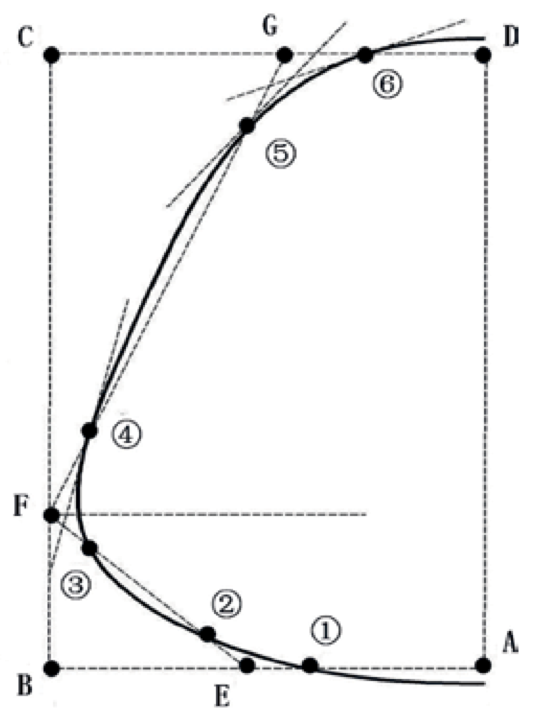

Figure 3. Geometric parameters of cross sections.

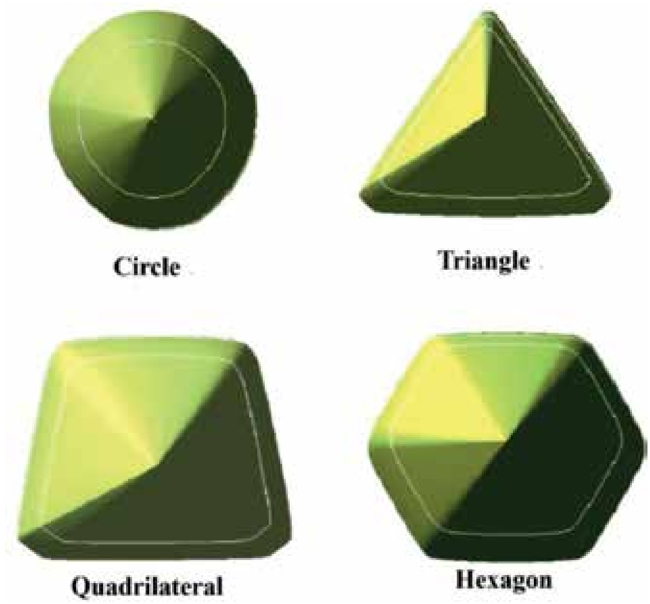

Figure 4. Several shapes of body sections.

In general, the width and height of each cross section can be altered through general profile parameters. Then, the edge position of the cross sections can be changed by adjusting the major control parameters of the cross section. Finally, extra padding is done at the head, fuselage transition section, fuselage and tail through interpolation. This parametric modeling method features clear with progressive modeling and hierarchical parameter, which is highly applicable for hierarchical progressive optimization.

3.3. Generalized parameter system

Based on the characteristics of the design phase, components and disciplines, the generalized parameter system with a total number of 131 including 3-level modeling parameters is listed in **Table 1**. In order to adapt to hierarchical progressive optimization, the sensitivity analysis is applied to classify the design parameters.

Design phase	Parameters	Numbers	Components	Disciplines
Layout	Layout parameters	6	Fuselage and wing	Aerodynamics/stealth
Component	Profile parameters	27	Fuselage and wing	Aerodynamics/stealth
Component	Control parameters	20	Fuselage	Aerodynamics/stealth
Component	Modification parameters	84	Fuselage	Stealth

Table 1. Design parameters.

4. Sensitivity analysis

Sensitivity is the derivative information of system parameters versus design parameters, and it reflects the variation trend and degree. The sensitivity analysis [5] can determine the affecting magnitude of system design parameters on the objective function and guide the process of optimization design. N points in the design range are uniformly distributed, and then the sensitivity is analyzed by central difference scheme, as shown in Eq. 17:

$$\frac{dF}{dX} = \frac{1}{N}\sum_{i=1}^{N}\left|\frac{F(X_i+\Delta X_i)-F(X_i-\Delta X_i)}{2\Delta X_i} + O\left((\Delta X_i)^2\right)\right| \approx \frac{1}{N}\sum_{i=1}^{N}\left|\frac{F(X_i+\Delta X_i)-F(X_i-\Delta X_i)}{2\Delta X_i}\right| \tag{17}$$

In consistent with the hierarchy features of generalized parameters, the two-round sensitivity analysis method is proposed in **Figure 5**. In the first round, the individual sensitivity analysis for aerodynamics and stealth is first carried out, respectively, by finite difference method for hierarchical parameters in order to classify the generalized parameters. Then, in the second round, sensitivity analysis is carried out based on the optimal fitness to obtain three levels of design parameters. According to the sensitivity analysis results in practical operation, the criterion for sensitivity analysis of individual disciplinary and optimal fitness is set as the sensitivity of the parameters is larger than 1. The relatively independent sensitive analysis of hierarchical parameters can reserve the progressive of parametric modeling, and the resultant three-level parameters will be more suitable for hierarchical progressive optimization and get better optimization efficiency.

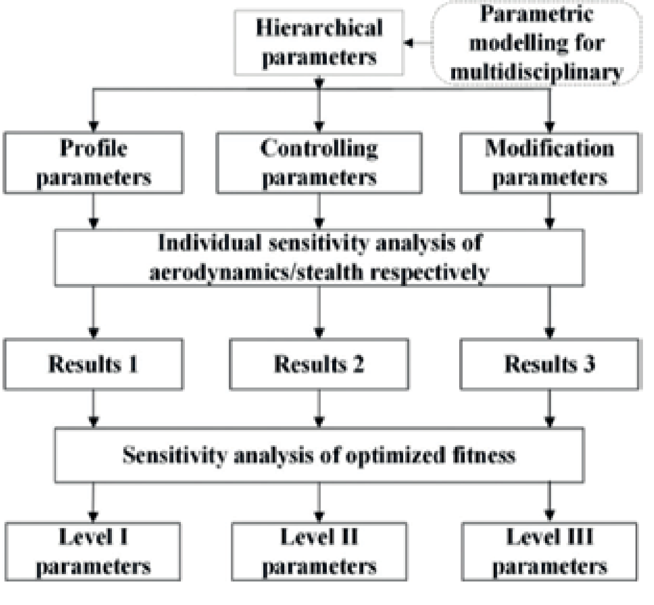

Figure 5. Hierarchical progressive optimization based on sensitivity analysis.

5. Analysis and discussion

5.1. Optimization descriptions

The aerodynamic/stealth optimization design is conducted for four-tailed layout aircraft, which can be described as follows:

1. Calculation conditions: flight height of 5 km, Mach number of 0.7, radar microwave frequency of 6.0 GHz and threat angle of 0~120°.
2. Constraint conditions: radar cross section (RCS) in the opposite direction no more than 0.01 and the cross section area of fuselage no more than 0.5 m^2.
3. Objective function: the maximum lift-to-drag ratio with the weight of 0.5, minimum RCS in the forward direction with the weight of 0.5 and minimum RCS in side direction with the weight of 0.5.
4. Original design parameters: 131 modeling parameters.

As shown in **Figure 1**, the optimization process is started with parametric modeling for several disciplines and the corresponding computational grid. The two-round sensitivity analysis is then conducted to classify the hierarchical generalized parameters. The MDO is implemented by differential evolution method [6] and hierarchical progressive optimization. According to the preliminary test of multimodal function with the same number of design parameters, the control parameters are set for differential evolution method as the initial population is double of the number of design parameters, the number of optimization generations of each stage is 30, the scaling factor is 0.6, and crossover factor is 0.5.

5.2. Optimization results

The sensitivity analysis results are shown in **Table 2**. After two rounds of sensitivity analysis, the number of first-level design parameters is reduced by 39.9%, the number of second-level design parameters is reduced by 30%, the number of third-level design parameters is reduced by 80.9%, and the number of all design parameters is reduced by 64.4%.

The normalized optimization process is shown in **Figure 6**. It indicates that the hierarchical progressive approach with two-round sensitivity analysis has great advantages with better optimization efficiency according to the variations of fitness versus the evolution generations.

Parameter level	Numbers	First round	Second round	Variation
Level I	28	21	17	39.90%
Level II	20	16	14	30%
Level III	84	36	16	80.90%

Table 2. The variations in the number of design parameters.

Table 3 is the statistical table of optimization adaptive value. As for the initial fitness of 59.818, the optimization results show that hierarchical progressive optimization with two-round sensitivity analysis increases the adaptive value by 51.1%. The objective function in two-round sensitivity analysis is shown in **Table 4**. It can be seen that the lift-to-drag ratio is increased by 38.5%, RCS in the forward direction is reduced by 52.03%, and RCS in side direction is reduced by 62.8%. **Figure 7** shows the aircraft configuration before and after the optimization. The

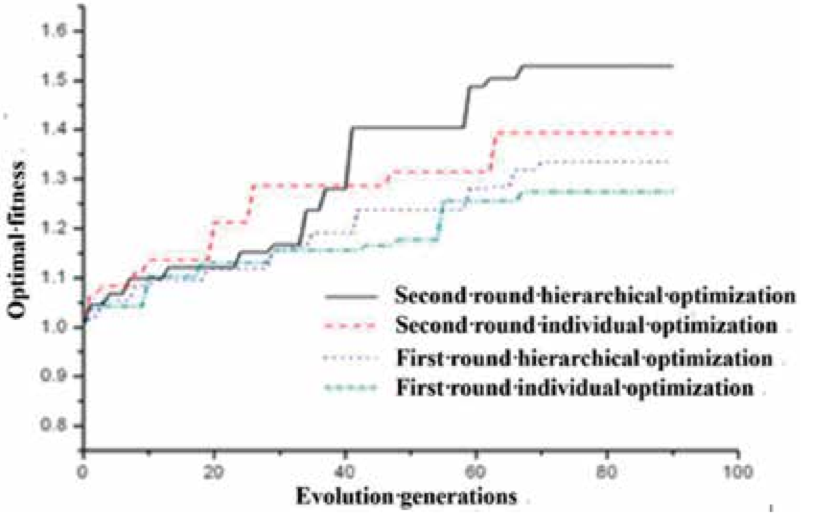

Figure 6. The variation of optimal fitness versus evolution generations.

Optimization process	Optimal fitness	Variation
Second round hierarchical optimization	90.385	51.1%
Second round individual optimization	83.41	39.44%
First round hierarchical optimization	79.91	33.59%
First round individual optimization	76.186	27.36%

Table 3. The variation of optimal fitness.

Optimal objects	Initial value	First round optimization	Second round optimization	Second round optimization	Variation
Lift-to-drag ratio	4.21	4.98	5.32	5.83	+38.5%
RCS in forward direction	0.0123	0.0086	0.0072	0.0059	−52.03%
RCS in side direction	1.6786	1.2658	0.8963	0.6237	−62.8%

Table 4. The variation of optimal objects.

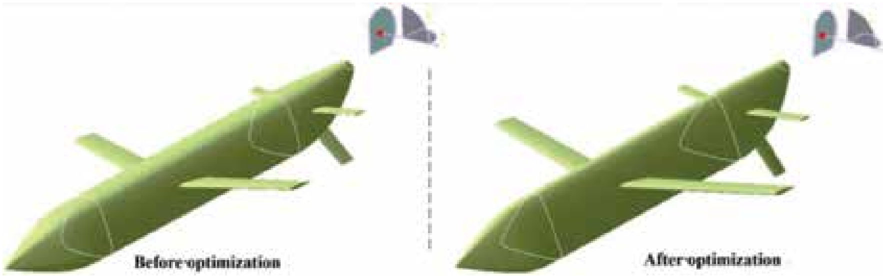

Figure 7. The variation of aircraft shape.

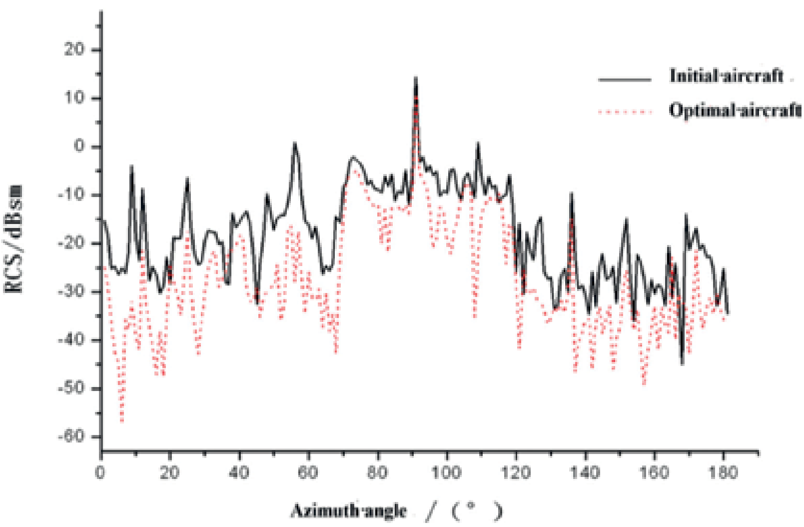

Figure 8. The variation of RCS value.

cross section of fuselage is significantly altered from quasi-quadrangle to quasi-triangle, which meets the requirements of stealth, while the aspect ratio and area of the wing are both increased. RCS in the opposite direction is 0.0055, and the fuselage cross section is 0.396 m^2. **Figure 8** shows the comparison between RCS before and after optimization. The RCS value is significantly reduced, which means the stealth performance is better after optimization.

6. Conclusions

The optimization results indicate that hierarchical progressive optimization based on generalized parametric modeling and sensitivity analysis demonstrates high optimization efficiency and excellent optimization results. Within the prerequisite of optimization constraints, the lift-to-drag ratio is increased by 38.5% and RCS decreases by more than 50%, which achieve the goal of multidisciplinary optimization design.

http://dx.doi.org/10.5772/intechopen.73282

Acknowledgements

This study was supported by the National Natural Science Foundation of China (nos. 11672183, 91641129 and 91441205).

Author details

Fang Chen* and Hong Liu

*Address all correspondence to: fangchen@sjtu.edu.cn

Shanghai Jiao Tong University, Shanghai, China

References

[1] Piperni P. Preliminary aerostructural optimization of a large business jet. Journal of Aircraft. 2007;**44**(5):1422-1438

[2] Storn R, Price K. Differential Evolution, a Simple and Efficient Adaptive Scheme for Global Optimization over Continuous Spaces. Berkley: Technical Report International Computer Science Institute; 1995

[3] Zhu ZQ, Li HM, Li J. Discussion of bi-disciplinary (aerodynamics/electromagnetic) bi-objective optimization. Science in China (Series E). 2000;**30**(3):208-215

[4] Yu RX, Zhu ZQ. Computation of the biobjective/bidisciplinary numerical optimization. Acta Aeronautica and Astronautica Sinica. 2002;**23**(4):330-333

[5] Pierret S, Van den Braembussche RA. Turbomachinery blade design using a Navier-stokes solver and artificial neural network. Journal of Turbomachinery. 1999;**121**:326-332

[6] Chi YC, Fang J, Cai GB. Hybrid optimization algorithm based on differential evolution and particle swarm optimization. Computer Engineering and Design. 2009;**30**(12):2963-2965

Section 3

Manufacturing

Additive Manufacturing of Polymer Matrix Composites

Evren Yasa and Kıvılcım Ersoy

Additional information is available at the end of the chapter

http://dx.doi.org/10.5772/intechopen.75628

Abstract

Due to the developments and the interest of leading aerospace companies, additive manufacturing (AM) has become a highly discussed topic in the last decades. This is mainly due to its capability of producing parts with high geometrical complexity, short manufacturing lead times, and suitability for customization as well as for low-volume production. As is the case with aircraft fuselage body where weight reduction while keeping the demanding mechanical properties is of uttermost importance, modern technology applications sometimes need materials with unusual combinations of properties that cannot be solely provided by metals, polymers, or ceramics. In this case, composite materials combining two or more materials allow having the preferred properties in one material. Thus, AM of composites is becoming more and more important for critical applications. Fiber reinforcement can significantly enhance the properties of resins/polymeric matrix materials. Although continuous fiber composites even present higher mechanical performance, the manufacturing methods for chopped fibers are more commercially available. This chapter reviews the studies in the field involving many aspects spanning from design, process technology, and applications to available equipment.

Keywords: additive manufacturing, polymer matrix composites, layered manufacturing, carbon fiber-reinforced polymers, rapid manufacturing

1. Introduction

Due to the developments and the interest of leading aerospace companies, AM, also known as 3D printing, became a highly discussed topic in the last decades. Due to its capability of producing parts with a high geometrical complexity and short manufacturing lead times, AM has been utilized more especially in aerospace and motorsports. Revenues from the production of end use parts, as a proportion of total AM production, have risen from under 4% in 2003 to 34.7% in 2013 [1]. The first step of applying AM technology was historically producing

IntechOpen

© 2018 The Author(s). Licensee IntechOpen. This chapter is distributed under the terms of the Creative Commons Attribution License (http://creativecommons.org/licenses/by/3.0), which permits unrestricted use, distribution, and reproduction in any medium, provided the original work is properly cited.

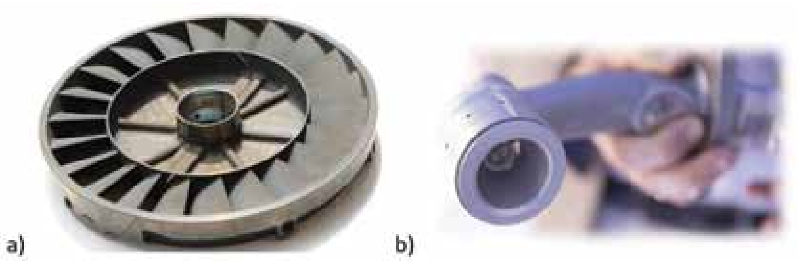

Figure 1. (a) Safran obtains the first certification for a 3D-printed gas turbine engine major part in the auxiliary power unit (APU) from Hastelloy X: conventionally machined by Inconel casting, the 3D-printed part is now 35% lighter and is now comprised of only four versus eight components prior to the new manufacturing technique [3]. (b) GE LEAP engine fuel nozzle: the 3D-printed nozzle combined all 20 parts into a single unit, but it also weighed 25% less [4].

plastic prototypes using various AM processes such as fused deposition modeling (FDM), stereolithography (SLA), and other processes. Producing complex net-shaped materials including metals, ceramics, and composites as functional parts later became available [2]. Today, polymers and metals are considered as commercially available materials for AM processes (see **Figure 1**). Meanwhile, ceramics and composites are rather considered still under research and development. **Table 1** shows various properties of AM processes including the state of

State of the starting material	Process	Material preparation	Layer creation method	Typical materials	Applications
Filament	FDM	Melted in nozzle	Continuous extrusion and deposition	Thermoplastics, waxes	Prototypes, casting patterns
	Robocasting	Paste in nozzle	Continuous extrusion	Ceramic paste	Functional parts
Liquid	SLA	Resin in a vat	Laser scanning	UV curable resin, ceramic suspension	Prototypes, casting patterns
	MJM	Polymer in jet	Ink-jet printing	Acrylic plastic, wax	Prototypes, casting patterns
Powder	SLS	Powder in bed	Laser scanning	Thermoplastics, waxes, metal powder, ceramic powder	Prototypes, casting patterns
	SLM	Powder in bed	Laser scanning	Metal	Tooling, functional parts
	EBM	Powder in bed	E-Beam scanning	Metal	Tooling, functional parts
	3DP	Powder in bed	Drop-on-demand binder printing	Polymer, metal, ceramic, and other materials	Prototypes, casting shells, tooling
Solid sheet	LOM	Laser cutting	Feeding and binding of sheets with adhesives	Paper, plastic, metal	Prototypes, casting models

Table 1. Analysis of the state of starting material working principle for AM processes [5].

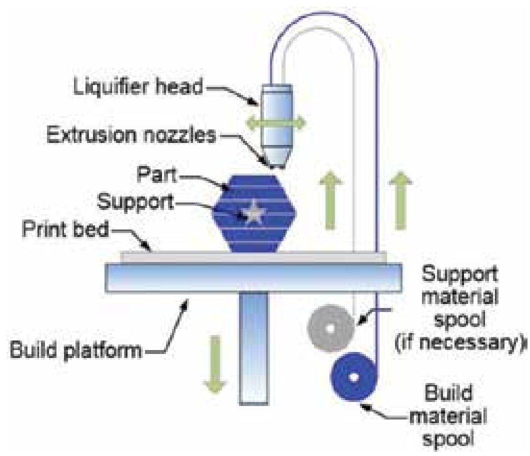

Figure 2. Schematic of fused deposition modeling [7].

starting material, material preparation, layer creation method, typical materials, as well as applications [5]. As is the case with aircraft fuselage body where weight reduction while keeping the demanding mechanical properties is of uttermost importance, modern technology applications sometimes need materials with unusual combinations of properties which cannot be solely provided by metals, polymers, or ceramics. In this case, composite materials combining two or more materials allow us to have the preferred properties in one material [2].

Fused deposition modeling (FDM) (see **Figure 2**) is one of the AM technologies and a widely used method for fabricating thermoplastic parts with advantages of low cost, minimal waste, and ease of material change [7]. In order to improve the mechanical properties of pure thermoplastic materials, one of the methods is to reinforce plastic matrix by different materials like carbon fibers to produce CFRPs (carbon fiber-reinforced polymers) composites which can be directly used as functional end parts. FDM is an advantageous process for producing polymer matrix composites because of the possibility to use multiple nozzles with loading of different materials. Moreover, being low-cost and high-speed, simplicity makes FDM a suitable process for composite manufacturing. One drawback of the FDM process for producing PMCs is that the input material has to be in filament form to enable the extrusion. Additionally, the usable matrix material is limited to thermoplastic materials due to needed melt viscosity (high enough for structural rigidity and low enough for extrusion) [6].

2. AM composites: literature review

Producing CFRPs (carbon fiber-reinforced polymers) by AM is quite a new research topic, and therefore there are a very limited number of studies that can be found in the literature as the summary in **Table 2** presents. Zhong et al. have studied the processability of glass fiber-reinforced ABS matrix composites with three different glass contents used as feedstock filaments in FDM leading to the result that the reinforcement could improve the tensile strength and surface rigidity at the expense of flexibility and handleability [8]. These limits were overcome

	Reinforced by	Matrix material	Investigated properties	Limitations
Zhong et al. [8]	Glass fibers	ABS	Tensile strength and surface rigidity	Flexibility and handleability
Gray et al. [9]	Thermotropic liquid crystalline polymer	Polypropylene	Tensile strength	Poor adhesion and delamination
Shofner et al. [10]	Vapor-grown carbon fibers	ABS	Tensile strength and tensile modulus	Interlayer and intralayer fusion; change behavior from ductile to brittle
Tekinalp et al. [11]	Carbon fiber	ABS	Tensile strength and tensile modulus	Porosity, weak interfacial adhesion between the fibers and the matrix, and fiber breakage
Ning et al. [7]	Carbon fiber	ABS	Tensile strength, Young's modulus, flexural properties	Decrease in toughness, yield strength, and ductility; increase of porosity with an increased level of carbon fiber
Love et al. [12]	Carbon fiber	ABS	Strength, stiffness, thermal properties, and distortion and geometric tolerances	—

Table 2. A summary of studies in FDM of chopped fibers.

by adding a small amount of plasticizer and compatibilizer. Gray et al. reinforced polypropylene with thermotropic liquid crystalline polymer fibers and provided a significantly increased tensile strength, whereas they encountered some problems of poor adhesion and delamination [9]. Shofner et al. studied reinforcing ABS matrix with vapor-grown carbon fibers at nanoscale. Although the tensile properties were improved, the amount of improvement depended on built parameters as well as the degree of interlayer and intralayer fusion [10]. Tekinalp et al. [11] have studied carbon fiber-reinforced ABS polymers in order to evaluate the potential for load-bearing components leading to the result that composites with highly dispersed and highly oriented carbon fibers can be printed by FDM process (see **Figure 3**) [11]. Ning et al. have provided a more comprehensive study on the effect of fiber content on mechanical properties. Carbon fiber content varying between 0 and 15% was studied on tensile and flexural properties of carbon fiber-reinforced ABS plastics. Some limitations such as decrease in toughness and ductility as well as encountered porosity were identified [7]. Love et al. have addressed reinforcement of ABS material with carbon fibers regarding the thermal deformations and leading geometrical tolerances in addition to strength and stiffness achieved (see **Figure 4**). They have concluded that carbon fiber additions can significantly reduce the distortion and warping of the material during processing allowing large-scale, out-of-the-oven, high deposition rate manufacturing [12].

The effect of fiber content on the mechanical properties is also another interesting research topic. Tekinalp et al. [11] have investigated the fiber loading on the tensile strength and modulus as shown in **Figure 5**. Some interesting results were obtained in this study. The results

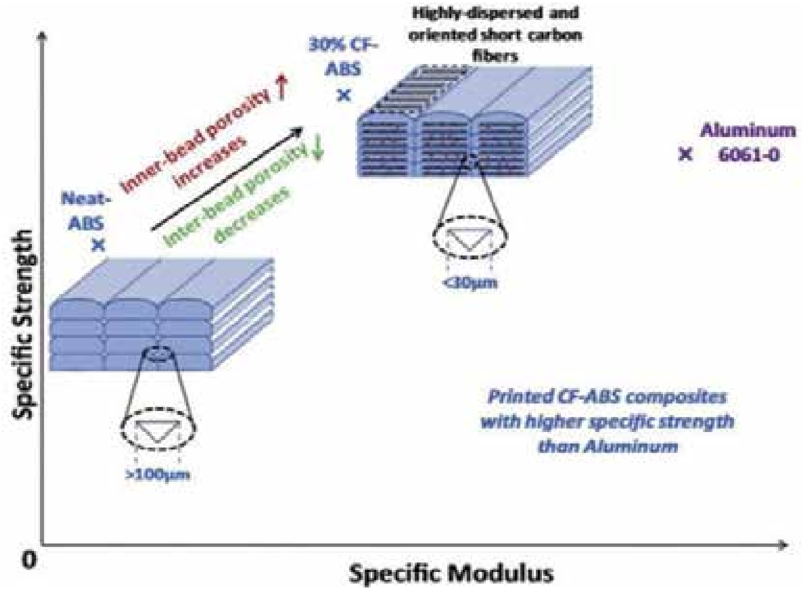

Figure 3. Schematic presentation of 3D-printed fiber-reinforced composite by fused deposition modeling [11].

Figure 4. Tensile test specimens produced along z-axis and deformation coupons showing the difference between carbon fiber-reinforced ABS and no reinforcement part in terms of deformation [12].

leading to the fact that modification/optimization of the mixing process to minimize fiber breakage and modification of the FDM process to minimize inner-pore formation may result in a much more optimized process are summarized as follows [11]:

- An increase in fiber length and fiber orientation improves the tensile properties, whereas an increase in void fraction reduces the strength of a composite by both creating stress concentration points and lowering the fiber-matrix interface and bonding.
- Tensile strength increases with increasing fiber content in both CM and FDM processes.
- The ABS samples with 0% fiber loading prepared by the FDM process have higher tensile strength, while the standard deviations in tensile strength measurements for the FDM samples were significantly lower than those for the CM samples.

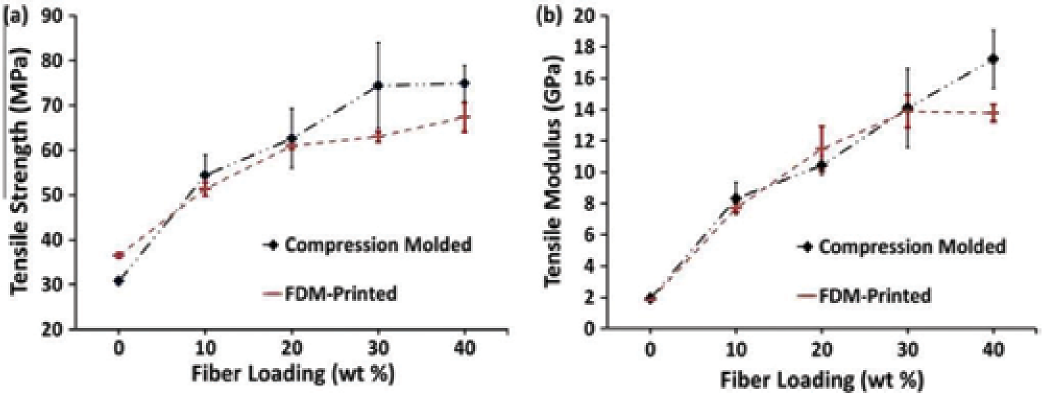

Figure 5. Effect of fiber loading on tensile strength and modulus in comparison to compression molded specimens [11].

- The FDM process increases the orientation of the polymer molecules in addition to improving fiber dispersion and uniformity since the parts are manufactured in a layer-wise and line-wise manner.
- The FDM samples can compensate the negative effect of porosity/weak fiber bonding by the strongly enhanced fiber and thus still reach strength values close to CM samples.
- For both processes, the tensile strength increase with the increase of the fiber content becomes less obvious at higher fiber loadings. This can be attributed to the decrease in average fiber length with increasing fiber content.
- At 40 wt% fiber loading, the modulus value of the CM composites is increased by nearly an order of magnitude. However, the FDM samples could not be fully fabricated due to the repeated nozzle clogging at this high fiber loading. These samples could only be printed to a few layers of thickness. This thickness difference possibly caused the difference in moduli between the FDM and CM specimens [11].

However, the optimum fiber loading obtained in [11] is not in line with the results of Ning et al. [7] due to differences in the material in terms of fiber distribution and interfacial bonding strength which leads to the conclusion that a basic standard for design and processing needs to be established as is the case with many other AM processes. Ning et al. concluded that the best performance of the produced parts was obtained with 5% fiber loading and higher loading of fiber reduced the performance. The studies found in the literature have tested up to 40 wt%, and the composites with higher loading could not be produced due to nozzle clogging issues. In addition, it is difficult to make filaments with such high fiber content due to the loss of toughness. As a solution to improve feedstock processability, plasticizers are added as already mentioned [8]. To eliminate the voids impairing the mechanical properties of FDM parts, a novel solution was found by [13]. Thermally expandable microspheres are added to the matrix, and a thermal treatment is combined with FDM. The results show that tensile and compressive strength of treated specimens increase 25.4 and 52.2%, respectively, in comparison to the untreated ones when 2 wt% microspheres are added [13].

http://dx.doi.org/10.5772/intechopen.75628

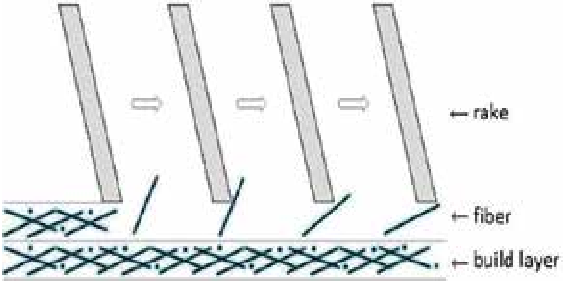

Figure 6. Illustration of the rake spreading a powder layer in the build chamber [14].

Fused deposition modeling is not the only method to produce polymer matrix composites by additive manufacturing. Selective laser sintering, a powder-bed AM technology, is also investigated in this field. Jansson and Pejryd have characterized carbon fiber-reinforced polyamide manufactured by this technology using the CarbonMide® (CF/PA12) material provided by EOS [14]. The material in its raw form is a powder consisting of polyamide spherical particles and carbon fibers of diameter 10 μm and length 100–200 μm. However, porosity is a significant problem as is the case with other studies [15–17]. The study given in [14] also has confirmed that porosity was concentrated in between the layers produced weakening the material in the direction normal to the layered structure. They also obtained different mechanical properties along different build directions mainly due to fiber orientation and porosity. They also concluded that the fiber orientation is linked to the powder rake mechanisms (see **Figure 6**). Some sample products produced by CarbonMide® material are demonstrated in **Figure 7**.

More recently, studies on embedding continuous fiber in the plastic materials are realized mainly using fused deposition modeling (FDM) for different applications [20–27]. Yao et al. have investigated embedding carbon fiber tows which provided a tensile strength increase of 70% and flexural strength increase of 18.7% compared to non-reinforced specimens. As seen in **Figure 8**, an artificial hand printed by FDM with embedded carbon fibers is manufactured

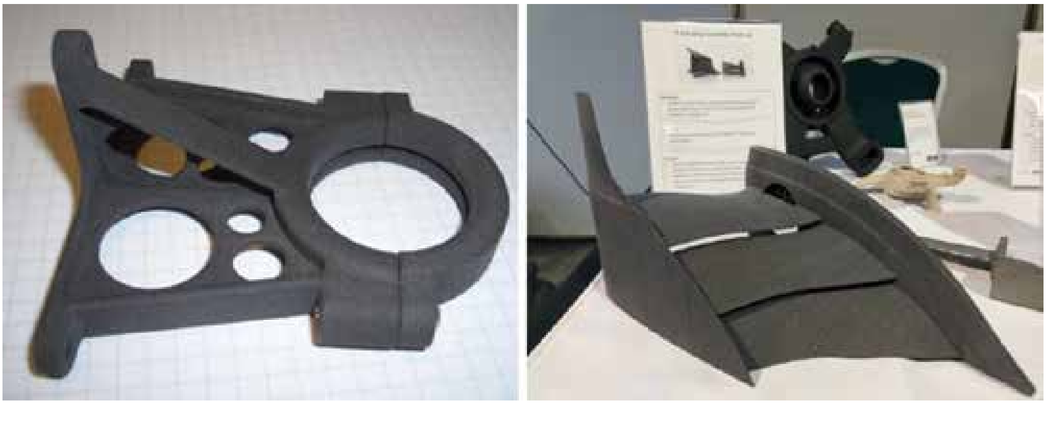

Figure 7. Sample products produced from CarbonMide® material [18, 19].

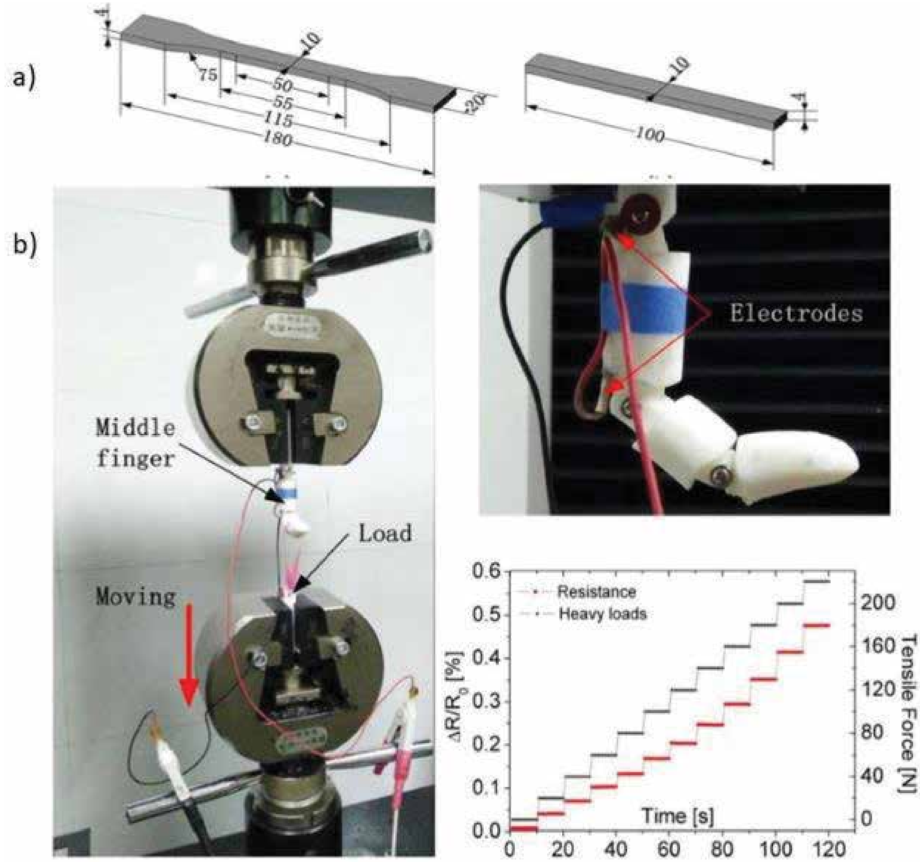

Figure 8. (a) Test specimen geometries per ISO 527-4:1997 for tensile and ISO 14125:1998 for flexural tests and (b) demonstration part [20].

as a demonstration part [20]. Dickson et al. have utilized a Mark One 3D printer in order to reinforce glass, carbon, and Kevlar fibers into nylon material (see **Figure 9**). For each of the printed composites relative to that obtained for the nylon samples with no reinforcement, up

Figure 9. Schematic description of the process (left) and produced specimens with different types of reinforcement fibers (right) [21].

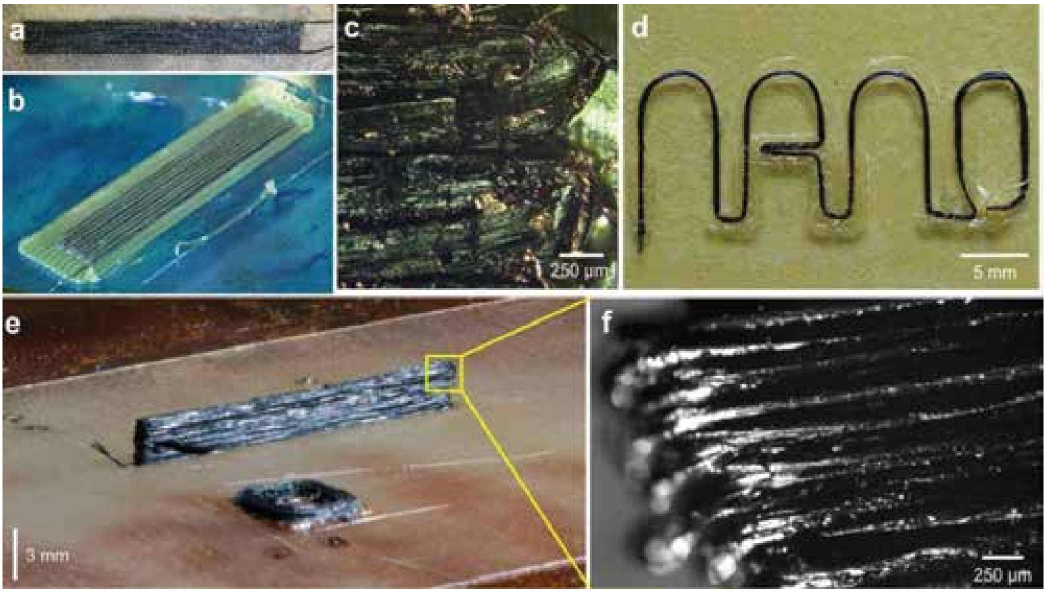

Figure 10. Samples produced: (a) Uniaxial CNT yarn filament layer (b) embedded electrical signal (c) at higher magnification (d) Letters nAno printed (e) printed thin walls (f) at higher magnification [22].

to a 6.3- and 5-fold enhancement in the tensile and flexural strengths were obtained, respectively, and the fiber type superior to others was observed to be carbon fiber [21]. Some studies did not only look into material but also equipment development as is the case with [22].

Gardner et al. have investigated reinforcing ULTEM® material with carbon nano-yarn filaments leading to better tensile and electrical conductivity properties (see **Figure 10**) [22]. Rather than FDM or selective laser sintering, some new techniques are proposed by some researchers. For example, Parandoush et al. proposed a novel method for AM of fiber composites by using prepreg composite. A laser is used to heat successive layers of prepreg tapes, and a compaction roller is utilized to bond these layers (see **Figure 11**) [23]. Moreover, Tian et al. also proposed a new methodology for continuous fiber reinforcement in AM (see **Figure 12** for

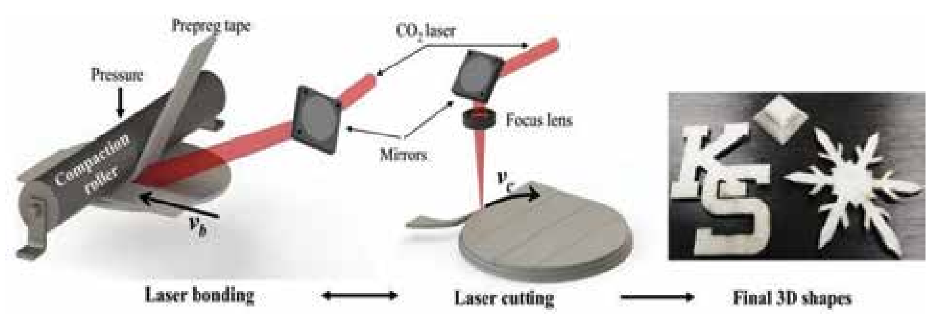

Figure 11. Schematic demonstration of the process [23].

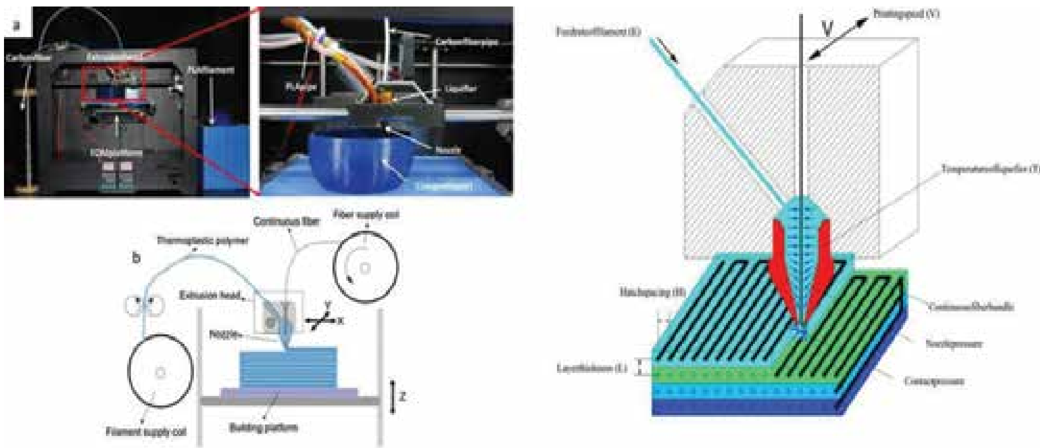

Figure 12. (a) Equipment for 3D printing for CFR PLA composites (b) Schematic printing process [24].

schematic demonstration of the process). In their study, the influence of process parameters on the interfaces and performance of printed composites have been investigated. With the optimized parameters, a fiber content of about 27% could achieve the maximum flexural strength of 335 MPa and flexural modulus of 30 GPa [24].

A similar technology is presented by Matsuzaki in [25], while another study conducted by Matsuzaki et al. [26] reports a very significant mechanical improvement by reinforcing continuous carbon fibers by FDM. Their results show that the tensile modulus and strength of 3D-printed continuous carbon fiber-reinforced PLA composites are 19.5 ± 2.08 GPa and 185.2 ± 24.6 MPa, respectively, which are 599 and 435% of the tensile modulus and strength

	Reinforced by	**Matrix material**	**Investigated properties**	**Limitations**
Yao et al. [20]	Carbon fiber	Epoxy resin + polyamide	Flexural and tensile properties, weight reduction	Adhesion between fibers and matrix and carbon fiber placement
Dickson et al. [21]	Carbon, glass, and Kevlar fiber	Nylon	Tensile and flexural properties	Weak bonding and porosity
Gardner et al. [22]	Carbon nanotube yarn	ULTEM®	Tensile strength, specific modulus, and electrical conductivity	Cutting mechanism
Parandoush et al. [23]	Continuous glass fiber	Polypropylene	Tensile and flexural properties	Adhesion
Tian et al. [24]	Carbon fiber	PLA (polylactic acid)	Flexural strength and modulus	None reported
Matsuzaki et al. [25, 26]	Carbon fiber	PLA (polylactic acid)	Tensile modulus and strength	Irregularity and discontinuity of fiber

Table 3. A summary of studies in FDM of continuous fibers.

of the pure PLA specimens. This mechanical improvement is much larger compared to that of short fiber-reinforced PLA composites [25]. **Table 3** gives a summary of studies involving continuous fiber reinforcement by FDM technology.

3. AM equipment for processing composites

The commercial machines available in the market for producing composite materials by AM are limited as given in **Table 4**. As seen, only MarkForged equipment (Mark X and Mark Two) can build composites with continuous fibers. Some examples of parts produced on a Mark Two machine are demonstrated in **Figure 13**. It is crucial to note that the MarkForged company producing Mark series for 3D printing of continuous fiber-reinforced plastics holds a patent for this technology [27]. The fiber replacement in Eiger software, which is compatible with MarkForged equipment, can be done in different ways as shown in **Figure 14**. Concentric fill strategy involves following the outer profile of the part and fitting a single strand of fiber inward in rings from that boundary. The other option is isotropic fill where the whole layer is covered with a single strand where the angle of filling can be changed from in 45° changes. Moreover, a combination of two fill options is also possible.

Another company working on commercializing continuous fiber-reinforced polymers is based in Russia and entitled as Anisoprint [30]. Their equipment named as Composer is shown in **Figure 15** with sample products. However, the technology is not yet fully commercialized, and thus sufficiently detailed information cannot be found in open literature about the technology.

The other machines available in the market for producing composites give the only option of using chopped fiber (generally of about 20–35%) in combination with a plastic matrix. For example, Roboze offers a material called Carbon PA including 20% chopped carbon fiber in nylon combining chemical resistance of nylon and mechanical properties of carbon fiber. Some examples of products manufactured on Roboze are shown in **Figure 16**. Some companies like GE are also investigating this technology, as entitled "fused filament fabrication (FFF)" for lightweight structures from other materials like PEEK [31, 32]. Processing high-temperature materials like PEEK and PEI are advantages of Roboze One+400 compared to Roboze One (see **Table 4**).

Stratasys also offers equipment for processing a composite material FDM Nylon 12CF. The material comprises of a blend of Nylon 12 resin and chopped carbon fiber, at a loading of 35% by weight. Some sample parts are shown in **Figure 17** [33]. Some mechanical properties of Nylon 12CF and Carbon PA are given in **Table 5** to give a general understanding. However, they are not comparable due to the fact that the tested specimens are produced along different axes.

At the moment, the easiest method to reinforce carbon fiber in the AM is considered to be the use of a filament which typically combines chopped fiber with a thermoplastic polymer for FDM processes which are simple and cheap as described above [34]. The manufacturers of the filaments are various. It can be either a machine vendor, as is the case with MarkForged

MarkForged Mark X	MarkForged Mark Two	Stratasys Fortus 450	Roboze ONE	Roboze One + 400
	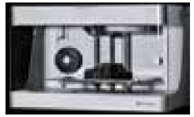			
50 μm resolution	100 μm resolution	Minimum layer thickness 0.127 mm	Not specified	25 μm resolution
330 x 250 x 200 mm	320 × 132 × 154 mm	406 × 355 × 406 mm	280 × 220 × 200 mm	200 × 200 × 200 mm
Dimensional accuracy online measurement		Parts are produced within an accuracy of ±0.127 mm or ±0.0015 mm/mm whichever is greater	The X and Y motion is provided by helical racks and pinions, enabling positioning precision of 0.025 mm. A C7 ball screw with flexible motor coupling, enabling precision of up to 0.025 mm for z axis	Extruders over 400 C designed for reaching very high temperatures and to print high viscosity materials (patent pending)
Plastic materials: nylon and onyx Fiber materials: carbon, fiberglass, Kevlar, high-strength high-temperature fiberglass CW fiber	Plastic materials: nylon and onyx Fiber materials: carbon, fiberglass, Kevlar, high-strength high-temperature fiberglass CW fiber	No CW fiber-chopped fiber ABS, PC, nylon, ULTEM, nylon 12CF	Carbon PA (20% chopped fiber, no CW), ABS, nylon, ASA	Carbon PA (20% chopped fiber, no CW), ABS, nylon, ASA + PEEK, PEI

Table 4. The commercially available machines for producing composites by AM.

Figure 13. Holder with Kevlar reinforcement (left), head support for go-cart cars with carbon reinforcement (middle), and a structural part made of nylon and carbon fiber (right) [28].

[29], or material supplier. colorFabb, based in the Netherlands, produces XT-CF20 combining polyethylene terephthalate glycol-modified (PETG) copolyester with 20% chopped carbon fiber (see **Figure 18** (left)) [35]. Proto-pasta's Carbon Fiber PLA is a mix of PLA and chopped carbon fiber [36]. 3DXTECH makes a variety of carbon fiber filaments ranging from PLA to ABS, nylon, ULTEM®, and PEEK having different characteristics [37]. A PLA composite may be the easiest to print with, whereas ABS may be a bit stronger. Nylon may be even tougher and more wear resistant. PEEK may be the ultimate choice for functional applications requiring resistance to higher temperatures and chemical attack [34]. Fuel intake runners printed from PEEK filament are demonstrated in **Figure 18** [38]. Although these filaments give superior strength compared to non-reinforced polymers, due to their chopped nature of the carbon fibers, the enhancement is limited. Therefore, Arevo Labs has worked on 6-Axis Composite Part Additive Manufacturing Platform [39]. Arevo Labs has developed filaments with chopped carbon fiber, in addition to continuous carbon fiber filament as well as materials with carbon nanotubes/nanofibers. In order to overcome the problem of delamination with AM of chopped fiber-reinforced polymers, in collaboration with ABB, they have worked on a robotic solution for AM of polymer matrix composites [34]. Instead of stacking 2D layers on top of each other, the robot can deposit material on a 3D surface, which is not limited to XY plane only as demonstrated in **Figure 19** [39].

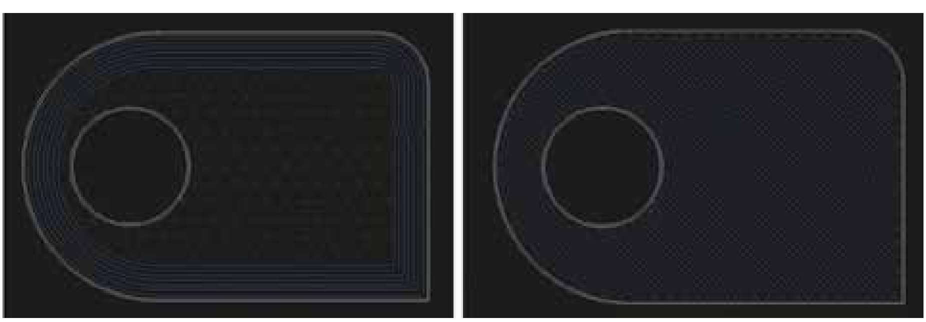

Figure 14. Different infill properties for the reinforcement of fibers [29]: left- concentric fiber replacement and right-isotropic fiber replacement.

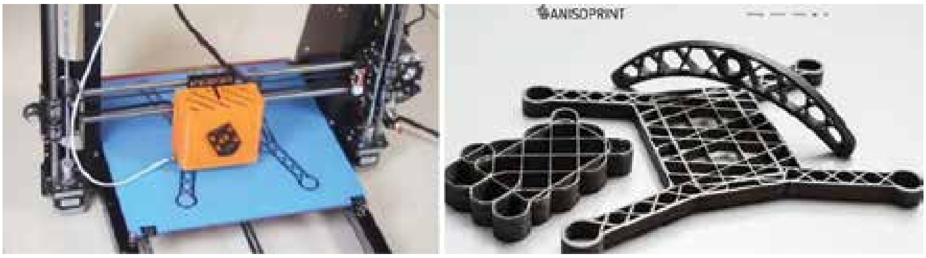

Figure 15. Anisoprint's composer (left) and sample products (right) [30].

Impossible objects' composite-based AM (CBAM) technology may overcome some limitations of AM of composites by combining fiber reinforcement with any number of matrix materials potentially at high speeds and at scalable sizes. In this process, namely, CBAM, a CAD file has been sliced into layers, which are converted into individual bitmaps. Then, for every layer, the printer leaves an aqueous solution into the shape of that bitmap onto a substrate sheet made from a given reinforcement material [40]. The substrate sheet is subsequently poured with the thermoplastic matrix material in powder form, which sticks only to the wet from deposited aqueous solution. The excessive powder is then removed, leaving only the plastic powder adhering to the liquid (see **Figure 20** for process steps). This cycle is repeated with each layer of the part to be produced. After all the substrate sheets are layered on top of each other, they are heated to the melting temperature and compressed to the final height. After the object is then taken out of the oven, the excess un-bonded portions of the reinforcement material are removed. The result is a thermoplastic print reinforced with a wide variety of options ranging from carbon fiber to silk and cotton [40]. **Figure 21** depicts some samples produced by CBAM. While the technology as a whole is very promising in terms of unlimited geometric complexity, every 3D printing process has its limitations when it comes to the exact shapes a system can produce. In CBAM, the geometry is partially determined by the chosen substrate material which brings a restriction on the design. Removing carbon fiber requires sand blasting, creating similar limitations faced by SLS due to the fact that the sand must be able to access the interior of the part to remove excess carbon fiber. This is a limitation regarding internal features. However, a chemical process is

Figure 16. Products from Carbon PA on Roboze equipment [31].

Figure 17. Products made of Nylon 12CF [33].

used to remove other reinforcement materials, such as Kevlar and polyester. In those cases, the geometric complexity is more similar to that possible with FDM, when using soluble supports [40].

Another company on the horizon of developing new composite AM methods is EnvisionTEC with their first and only industrial thermoplastic reinforced woven composite printer, SLCOM (Selective Lamination Composite Object Manufacturing) [42]. SLCOM allows building composite parts using thermoplastic composite fabric sheets from a roll in a layer-wise manner. This technology utilizes a wide range of matrix materials such as PEEK (polyetherketoneketone), PEKK (polyetherketoneketone), PC (polycarbonate), PPS (polyphenylene sulfide), PEI (polyetherimide), PE (polyethylene), and polyamides (Nylon 6, Nylon 11, or Nylon 12), whereas the possible fiber reinforcements include carbon fiber, fiberglass, and aramid fiber along with metal fibers (see **Figure 22**) [42]. The supply roll is fed into the print bed. Later, the thermoplastic within the roll is melted and compressed with a heated roller passing over. At the same time, a mechanism similar to an ink-jet head deposits a waxlike substance and a binding agent to the metal. A carbon blade with an attached ultrasonic emitter cleanly cuts away any area with wax. However, the price tag of 1 M USD makes it an expensive option.

Material	Vendor	Machine model	Build plane	Yield tensile stress (MPa)	Ultimate tensile strength (MPa)	Tensile modulus (MPa)	Tensile elongation at break (%)	Tensile elongation at yield (%)	Melting point (°C)
Nylon 12 CF	Stratasys	Fortus	*XZ*	63.4	75.6	7515	1.9	0.9	233
			ZX	28.8	34.4	2300	1.2	1.1	233
Carbon PA	Roboze	ONE	*XZ*		98.0	7850			178
			XY		94.0	6400			178

Table 5. Comparison of mechanical properties provided by Nylon 12CF produced on a Fortus equipment from Stratasys and by carbon PA produced on a one equipment from Roboze.

Figure 18. 3D-printed car from XT-CF20 material (left) [34]; fuel intake runners 3D printed with Arevo Labs' PEEK filament (right) [38].

Figure 19. Six-axis composite part additive manufacturing platform from Arevo Labs [39].

Another interesting development in the field of AM of composites is BAAM (Big Area Additive Manufacturing) technology [43, 44]. The Oak Ridge National Laboratory has developed this technology, which is a large scale out of the oven extrusion-based 3D printer that enables faster and cheaper fabrication of large parts. Cincinnati Incorporated has commercialized the

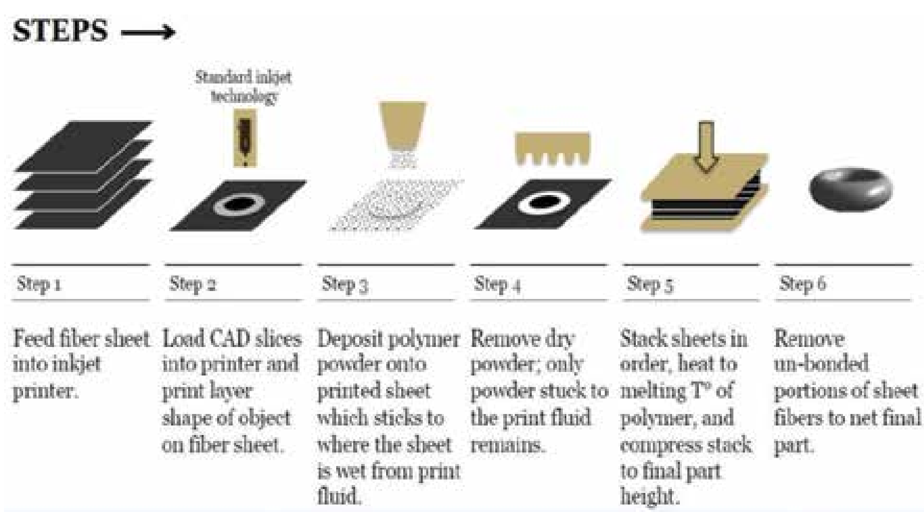

Figure 20. Process steps of CBAM [41].

Figure 21. Sample products produced by Impossible Objects' CBAM technology [34].

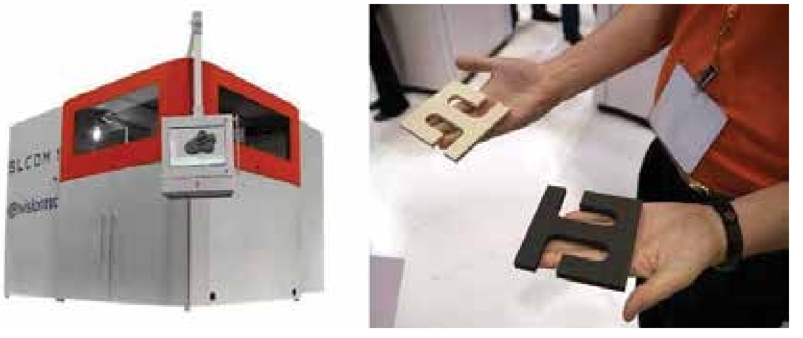

Figure 22. EnvisionTEC's SLCOM process demonstration (left) and sample parts (right) [34, 42].

Figure 23. Large parts produced by BAAM technology [45].

system for ABS, PPS, PEEK, and ULTEM® materials. By adding carbon fiber and glass fiber, it is possible to increase the strength and thermal stability. It is possible to have built volumes up to 6096 × 2286 × 864 mm which allows making huge parts as shown in **Figure 23** [45].

Despite the dominance of polymer matrix composites by carbon fiber, graphene is also considered as an interesting reinforcement material. With a thickness of a single carbon atom, graphene is about 100 times stronger than steel, incredibly lightweight, and electrically and thermally conductive. The difficulty of 3D printing with graphene is the inability to deposit this hydrophobic wonder material from a print head. PLA-based graphene filaments are commercially available from Graphene 3D Lab [46], but no commercial application seems to have created impact other than at laboratory scale [47, 48] in open literature.

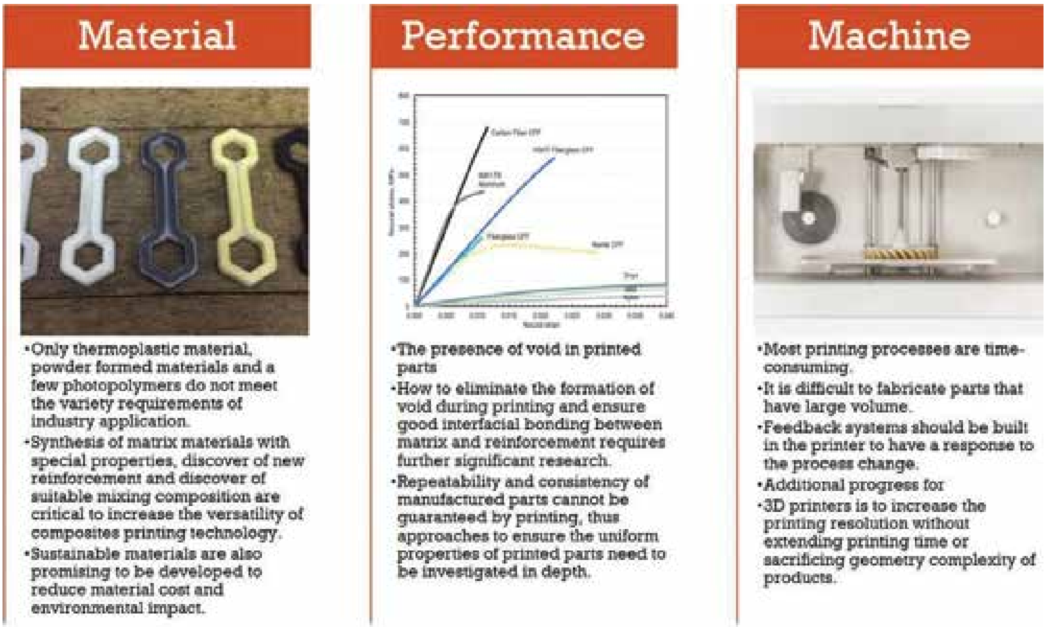

Figure 24. Limitations of the AM of polymer matrix composites similar to other materials in their development phases adapted from [6].

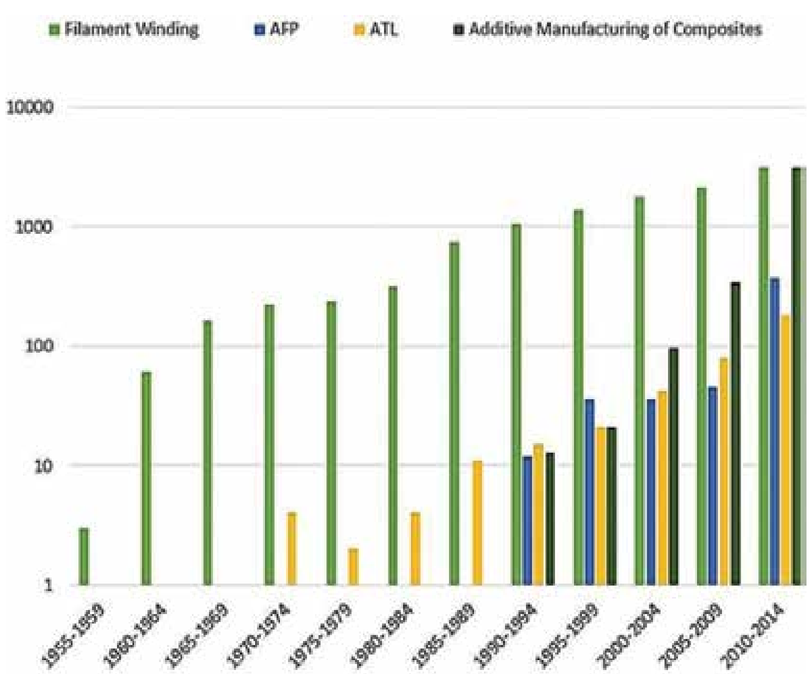

Figure 25. The number of papers considering filament winding, AFP (automated fiber placement), ATL (automated tape layup), and AM (data from Google Scholar) [49].

4. Summary

Although additive manufacturing of polymer matrix composites has gone through a significant improvement in the last years (see the dates of publications in the references list), it is still not widely adopted by various industrial sectors for functional applications. Several limitations that need to be overcome are demonstrated in **Figure 24**. These problems are very similar to other AM techniques, such as direct metal laser sintering, which are more mature and overcome these restrictions for a wider infusion into industry. As seen in **Figure 25**, the interest of the industry and academia in AM for producing polymer matrix composites has been growing significantly, and this seems to continue exponentially in the coming years.

Author details

Evren Yasa[1]* and Kıvılcım Ersoy[2]

*Address all correspondence to: eyasa@ogu.edu.tr

1 Eskişehir Osmangazi University, Eskisehir, Turkey

2 FNSS Defence Systems, Ankara, Turkey

References

[1] Wohlers T, editor. Wohlers Report 2017. USA: Wohlers Associates, Inc.; 2017. 341 p

[2] Hegab HA. Design for additive manufacturing of composite materials and potential alloys: A review. Manufacturing Review. 2016;**3**(Special Issue - Additive Manufacturing Materials & Devices):1-17. DOI: 10.1051/mfreview/2016010

[3] Safran. Safran obtains the first certification for a 3D-printed gas turbine engine major part [Internet]. June 17, 2017. Available from: https://www.safran-group.com/media/safran-obtains-first-certification-3d-printed-gas-turbine-engine-major-part-20170619?sthash.WpWGoxIy.mjjo [Accessed: September 11, 2017]

[4] GE Reports. An epiphany of disruption: GE additive chief explains how 3D printing will upend manufacturing [Internet]. June 21, 2017. Available from: http://www.gereports.com/epiphany-disruption-ge-additive-chief-explains-3d-printing-will-upend-manufacturing/ [Accessed: September 11, 2017]

[5] Kruth J-P. Material incress manufacturing by rapid prototyping techniques. CIRP Annals. 1991;**40**(2):603-614. DOI: 10.1016/S0007-8506(07)61136-6

[6] Wang X, Jiang M, Zhou Z, Gou J, Hui D. 3D printing of polymer matrix composites: A review and prospective. Composites Part B Engineering. 2017;**110**:442-458. DOI: 10.1016/j.compositesb.2016.11.034

[7] Ning F, Cong W, Qui J, Wei J, Wang S. Additive manufacturing of carbon fiber reinforced thermoplastic composites using fused deposition modeling. Composites Part B. 2015;**80**: 369-378. DOI: 10.1016/j.compositesb.2015.06.013

[8] Zhong W, Li F, Zhang Z, Song L, Li Z. Short fiber reinforced composites for fused deposition modeling, materials science and engineering. Materials Science and Engineering. 2001;**A301**(2):125-130. DOI: 10.1016/S0921-5093(00)01810-4

[9] Gray RW, Baird DG, Bohn JH. Effects of processing conditions on short TLCP fiber reinforced FDM parts. Rapid Prototyping Journal. 1998;**4**(1):14-25. DOI: 10.1108/13552549810197514

[10] Shofner ML, Lozano K, Rodrigues-Maciaz FJ, Barrera EV. Nanofiber-reinforced polymers prepared by fused deposition Modeling. Journal of Applied Polymer Science. 2003;**89**(11):3081-3090. DOI: 10.1002/app.12496

[11] Tekinalp HL, Kunc V, Velez-Garcia GM, Duty CE, Love LJ, Naskar AK, Blue CA, Ozcan S. Highly oriented carbon fiber-polymer composites via additive manufacturing. Composites Science and Technology. 2014;**105**:144-150. DOI: 10.1016/j.compscitech.2014.10.009

[12] Love LJ, Kunc V, Rios O, Duty CE, Elliott AM, Post BK, Smith RJ, Blue CA. The importance of carbon fiber to polymer additive manufacturing. Journal of Materials Research. 2014;**29**(17):1893-1898. DOI: 10.1557/jmr.2014.212

[13] Wang J, Xie H, Weng Z, Senthil T, Wu L. A novel approach to improve mechanical properties of parts fabricated by fused deposition modeling. Materials & Design. 2016;**105**:152-159. DOI: 10.1016/j.matdes.2016.05.078

[14] Jansson A, Pejryd L. Characterisation of carbon fibre-reinforced polyamide manufactured by selective laser sintering. Additive Manufacturing. 2016;**9**:7-13. DOI: 10.1016/j.addma.2015.12.003

[15] Van Hooreweder B, Moens D, Boonen R, Kruth J-P, Sas P. On the difference in material structure and fatigue properties of nylon specimens produced by injection molding and selective laser sintering. Polymer Testing. 2013;**32**(5):972-981. DOI: 10.1016/j.polymertesting.2013.04.014

[16] Van Hooreweder B, Kruth J-P. High cycle fatigue properties of selective laser sintered parts in polyamide 12. CIRP Annals - Manufacturing. 2014;**63**:241-244. DOI: 10.1016/j.cirp.2014.03.060

[17] Shahzad K, Deckers J, Zhang Z, Kruth J-P, Vleugels J. Additive manufacturing of zirconia parts by indirect selective laser sintering. Journal of the European Ceramic Society. 2014;**34**(1):81-89. DOI: 10.1016/j.jeurceramsoc.2013.07.023

[18] 3D Printing Industry. Williams racing F1 team uses 3D printing for new car development [Internet]. March 6, 2017. Available from: https://3dprintingindustry.com/news/williams-racing-f1-team-uses-3d-printing-new-car-development-107183/ [Accessed: September 11, 2017]

[19] Muhonen J. Laser sintering—AM solutions from EOS to meet changing market demands and opening up future possibilities. In: PLASTIC FANTASTIC; May 29, 2013; Fredericia, Denmark. 2013

[20] Yao X, Luan C, Zhang D, Lan L, Fu J. Evaluation of carbon fiber-embedded 3D printed structures for strengthening and structural-health monitoring. Materials and Design. 2017;**114**:424-432. DOI: 10.1016/j.matdes.2016.10.078

[21] Dickson AN, Barry JN, McDonnel KA, Dowling DP. Fabrication of continuous carbon, glass and Kevlar fibre reinforced polymer composites using additive manufacturing. Additive Manufacturing. 2014;**16**:146-152. DOI: 10.1016/j.addma.2017.06.004

[22] Gardner JM, Sauit G, Kim JW, Cano RJ, Wincheski RA, Stelter SJ, Grimsley BW, Working DC, Siochi EJ. 3-D printing of multifunctional carbon nanotube yarn reinforced components. Additive Manufacturing. 2016;**12**:38-44. DOI: 10.1016/j.addma.2016.06.008

[23] Perandoush P, Tucker L, Zhou C, Lin D. Laser assisted additive manufacturing of continuous fiber reinforced thermoplastic composites. Materials and Design. 2017;**131**:186-195. DOI: 10.1016/j.matdes.2017.06.013

[24] Tian X, Liu T, Yang C, Wang Q, Li D. Interface and performance of 3D printed continuous carbon fiber reinforced PLA composites. Composites Part: A. 2016;**88**:198-205. DOI: 10.1016/j.compositesa.2016.05.032

[25] Japan Society for Composite Materials. 3D printer using continuous carbon fiber composite materials [Internet]. Available from: http://www.jscm.gr.jp/3Dprinting/images/introduction_CFRP3Dprinter.pdf [Accessed: September 11, 2017]

[26] Matsuzaki R, Ueda M, Namiki M, Jeong T-K, Asahara H, Horiguchi K, Nakamura T, Todoroki A, Hirano Y. Three-dimensional printing of continuous-fiber composites by in-nozzle impregnation. Scientific Reports. 2016;**6**(23058):1-7. DOI: 10.1038/srep23058

[27] Mark GT, Gozdz AS. US 20150108677 A1 Patent [Internet]. April 23, 2015. Available from: https://www.google.com/patents/US20150108677

[28] Mark Two 3-B Yazıcı Genel Tanıtım ve Uygulama Sunumu obtained from Altar Teknoloji

[29] Develop3D. Markforged Mark Two: Part 1 [Internet]. Available from: https://markforged.com/pdfs/Markforged-D3D.pdf

[30] ANISOPRINT. ANISOPRINT connects the world of 3d printing with the world of high performance fiber reinforced plastics [Internet]. 2016. Available from: http://anisoprint.ru/en/ [Accessed: September 11, 2017]

[31] Lavi G. Breaking the boundaries of techno-polymers AM. In: Formnext 2016; 15.11.2016; Frankfurt, Germany; 2016

[32] Molitch-Hou M. GE Global Research Turns to Roboze for R&D 3D Printing [Internet]. February 2, 2017. Available from: http://www.engineering.com/3DPrinting/3DPrintingArticles/ArticleID/14234/GE-Global-Research-Turns-to-Roboze-for-RD-3D-Printing.aspx [Accessed: September 11, 2017]

[33] Stratasys. FDM Nylon 12CF: Data Sheet [Internet]. 2017. Available from: http://www.stratasys.com/-/media/files/nylon-12cf/mss_fdm_nylon12cf_0517a_web.pdf [Accessed: September 11, 2017]

[34] Engineering.com. Best 3D Printer Materials: Carbon Fiber Edition [Internet]. August 23, 2016. Available from: http://www.engineering.com/3DPrinting/3DPrintingArticles/ArticleID/12957/Best-3D-Printer-Materials-Carbon-Fiber-Edition.aspx [Accessed: October 21, 2017]

[35] colorFabb. XT-CF20 [Internet]. Available from: http://colorfabb.com/xt-cf20 [Accessed: September 11, 2017]

[36] Proto-Pasta. Carbon Fiber PLA [Internet]. 2017. Available from: https://www.proto-pasta.com/pages/carbon-fiber-pla [Accessed: September 11, 2017]

[37] CARBONX™ CARBON FIBER FILAMENT [Internet]. 2017. Available from: https://www.3dxtech.com/carbonx-carbon-fiber-filament/ [Accessed: September 11, 2017]

[38] Engineering.com. Printing 3D Carbon Fiber Parts with Robotic Arm [Internet]. March 24, 2016. Available from: http://www.engineering.com/3DPrinting/3DPrintingArticles/ArticleID/11744/Printing-3D-Carbon-Fiber-Parts-with-Robotic-Arm.aspx [Accessed: October 21, 2017]

[39] 3DPrint.com. Arevo Labs Takes 3D Printing 3D with New 6-Axis Composite Part Additive Manufacturing Platform [Internet]. November 16, 2015. Available from: https://3dprint.com/105787/arevo-labs-6-axis-ram-platform/ [Accessed: September 11, 2017]

[40] Engineering.com. Impossible Objects Brings Impossible Speed and Flexibility to Carbon Fiber 3D Printing [Internet]. July, 27, 2016. Available from: http://www.engineering.com/3DPrinting/3DPrintingArticles/ArticleID/12763/Impossible-Objects-Brings-Impossible-Speed-and-Flexibility-to-Carbon-Fiber-3D-Printing.aspx [Accessed: October 21, 2017]

[41] Impossible Objects. How CBAM Works [Internet]. 2017. Available from: http://impossible-objects.com/technology/ [Accessed: September 11, 2017]

[42] Envisiontec. Large Format 3D Printer For Industrial Composites [Internet]. 2017. Available from: https://envisiontec.com/3d-printers/slcom-1/ [Accessed: September 11, 2017]

[43] Cincinnati. BAAMCI [Internet]. 2017. Available from: https://www.e-ci.com/baam/ [Accessed: September 11, 2017]

[44] Kishore V, Ajinjeru C, Nycz A, Post B, Lindahl J, Kunc V, Duty C. Infrared preheating to improve interlayer strength of big area additive manufacturing (BAAM) components. Additive Manufacturing. 2017;**17**:7-12. DOI: 10.1016/j.addma.2016.11.008

[45] Engineering.com. How Big Area Additive Manufacturing is Enabling Automotive Microfactories [Internet]. June 9, 2016. Available from: http://www.engineering.com/AdvancedManufacturing/ArticleID/12363/How-Big-Area-Additive-Manufacturing-is-Enabling-Automotive-Microfactories.aspx [Accessed: October 21, 2017]

[46] Graphene 3D Lab Inc.. Investor Presentation [Internet]. March 2017. Available from: http://www.graphene3dlab.com/i/pdf/presentation/presentation.pdf [Accessed: September 11, 2017]

[47] Sayers M. Video: Engineers create graphene components using 3D printing [internet]. February 12, 2015. Available from: http://www3.imperial.ac.uk/newsandeventspggrp/imperialcollege/newssummary/news_12-2-2015-8-58-8 [Accessed: September 11, 2017]

[48] Lawrence Livermore National Laboratory. 3D-printed aerogels improve energy storage [Internet]. April 22, 2015. Available from: https://www.llnl.gov/news/3d-printed-aerogels-improve-energy-storage [Accessed: September 11, 2017]

[49] Frketic J, Dickens T, Ramakrishnan S. Automated manufacturing and processing of fiber-reinforced polymer (FRP) composites: An additive review of contemporary and modern techniques for advanced materials manufacturing. Additive Manufacturing. 2017;**14**:69-86. DOI: 10.1016/j.addma.2017.01.003

Edited by Melih Cemal Kuşhan

It is well known that improvements in space and aviation are the leader of today's technology, and the aircraft is the most important product of aviation. Because of this fact, the books on aircraft are always at the center of interest. In most cases, technologies designed for the aerospace industry are rapidly extending into other areas. For example, although composite materials are developed for the aerospace industry, these materials are not often used in aircraft. However, composite materials are utilized significantly in many different sectors, such as automotive, marine and civil engineering. And materials science in aviation, reliability and efficiency in aircraft technology have a major importance in aircraft design.

Published in London, UK
© 2018 IntechOpen
© 77studio / iStock

IntechOpen

ISBN 978-1-83881-454-0